DEVELOPMENT OF REGULATORY T CELLS CAPABLE OF MAINTAINING IMMUNE HOMEOSTASIS

A DISSERTATION

SUBMITTED TO THE FACULTY OF THE GRADUATE SCHOOL

OF THE UNIVERSITY OF MINNESOTA

BY

David Lee Owen

IN PARTIAL FULFILLMENT OF THE REQUIREMENTS

FOR THE DEGREE OF

DOCTOR OF PHILOSOPHY

Michael A. Farrar, Advisor

September 2020

Acknowledgements

I would like to first thank my mentor, Dr. Michael Farrar. Mike has been a fantastic example of the passion, enthusiasm and persistent attitude a scientist must have to succeed. Mike has provided me with a combination of guidance and freedom that allowed me to begin developing my skills as an independent investigator. He has always championed my career and has done whatever possible to promote me throughout my training. I also want to thank my thesis committee, Dr. Yoji Shimizu (chair), Dr. Bruce Blazar, Dr. Scott Dehm, Dr. Kristin Hogquist, and Dr. Daniel Mueller, for contributing their time and effort to supporting my project and progress throughout my thesis. I would also like to thank the other members of the Farrar lab, both past and present, for contributing their time to help me develop the technical skills required in the lab and in theoretical discussion on various projects. The list of collaborators, both inside and outside the University of Minnesota, who contributed to this work is too long to list but I want to express my gratitude for their generosity both of time and resources. Finally, thank you to everyone in the Center for Immunology who create a fun, collaborative and productive environment to develop as a young scientist.

Dedication

I want to dedicate this work to my family who have always supported me in any endeavor I have taken on. First, my parents, James and Kathy, and my brother Daniel who have all given me the utmost support throughout the long process of PhD training. I also want to thank the rest of my extended family who have also remained connected and interested in my thesis work. Finally, I want to thank my wife, Wendy, who I met and married during my thesis training in Minnesota. You have always been supportive and patient with me. Thank you to all my family and friends for their interest, support and love.

Abstract

The adaptive immune response, comprised of both T cells and B cells, is essential to control infections and eliminate transformed cancer cells. The success of the adaptive immune system relies on the ability to discriminate self from non-self-antigens. The thymus is the site of selection for T cells, where self-reactive T cells are eliminated, generating a non-self focused T cell compartment. However, this selection process is leaky and potentially pathogenic cells do escape thymic, or central, tolerance. Thus, a population of suppressor cells termed regulatory T cells (T_{reg} cells) co-evolved in order to keep these self-reactive escapees in check.

T_{reg} cells that develop in the thymus as part of central tolerance induction are a critical population of T cells that are required to maintain immune homeostasis and prevent autoimmunity. Without intervention, mice or humans that lack the ability to generate T_{reg} cells die shortly after birth from widespread autoimmune-mediated tissue destruction. Further, neonatal thymectomy in mice causes the development of an autoimmune wasting phenotype. These observations highlight the importance of thymic T_{reg} cell selection in immune homeostasis.

Thymic T_{reg} cell development occurs via a two-step process. Step one involves developing $CD4^+$ thymocytes receiving strong T cell receptor (TCR) stimulation via engagement of thymic self-antigens, leading to upregulation of CD25, the high affinity subunit of the IL-2 receptor, or FOXP3, the lineage defining transcription factor of T_{reg} cells, generating either $CD25^+$ or $FOXP3^{lo}$ T_{reg} cell progenitors ($T_{reg}P$). Step two is driven by encounters between $T_{reg}P$ cell and intrathymic STAT5 activating cytokines, predominantly IL-2, leading to co-expression of CD25 and FOXP3. These $CD25^+FOXP3^+$ cells represent fully mature T_{reg} cells that disseminate from the thymus to mediate immune tolerance.

While the framework of this two-step development process is understood, many details of each step remain incompletely understood. This thesis addresses several aspects of thymic T_{reg} cell development. First, we identify that T cells are the critical source of IL-2 required to drive T_{reg} differentiation. Second, we provide evidence that $CD25^{+}$ and $FOXP3^{lo}$ T_{reg}P arise via distinct selection programs and contribute functionally distinct TCRs to the mature T_{reg} compartment. Third, using single-cell RNA-sequencing analysis of conventional and T_{reg} lineage thymocytes we provide a more detailed analysis of transcriptional signatures and intermediates of thymic T_{reg} development. Finally, we gathered preliminary data to better understand the heterogeneity and function of recirculating or resident thymic T_{reg} cells. Developing a holistic understanding of T_{reg} development is essential to discern the etiology of immune disorders and properly modulate T_{reg} cells to treat autoimmune disease, infections and cancer.

Table of Contents

List of Tables

List of Figures

Chapter 1: Introduction

*Portions of the introductory text are derived from a review article written by the author[1]

Adaptive immunity evolved as a powerful defense mechanism to eliminate foreign pathogens and eradicate transformed cells. This system relies on two chief capabilities- extensive repertoire diversity and the ability to discriminate "self" versus "non-self" [2]. In T cells, diversity is derived from random rearrangements of the T cell receptor (TCR) alpha and beta loci [3,4]. However, diversity comes at a cost, as some of these rearrangements will generate self-reactive T cells capable of initiating pathogenic immune responses. The thymus acts as a training ground for T cells and plays a role in ensuring a diverse, "non-self" focused, TCR repertoire capable of eliminating pathogens. The process of generating a diverse TCR repertoire also leads to the development of many autoreactive T cells. Many of these autoreactive T cells are eliminated via clonal deletion in the thymus. However, a large proportion of self-reactive T cells do escape clonal deletion and, when left uncontrolled, elicit detrimental autoimmune diseases. While several mechanisms evolved to control autoimmune responses, a specialized subset of $CD4^+$ T cells, termed regulatory T cells (T_{reg}), plays a particularly important role in maintaining immune homeostasis.

Over the past 20 years tremendous progress has been made in the identification and understanding of T_{reg} cells. This relatively small population, ~1% of developing CD4 single positive (CD4SP) thymocytes and ~10-15% of $CD4^+$ T cells in secondary lymphoid organs, is responsible for maintaining immune homeostasis and is crucial for survival [5–10]. T_{reg} cells are an incredibly diverse population with regard to both TCR repertoire and function. T_{reg} cells regulate numerous physiologic processes, including maternal-fetal conflict [11–18], germ cell tolerance [19], stem cell differentiation in the skin [20], muscle repair [21], adipocyte homeostasis and function [22–26], and retinal inflammation [27]. In addition, T_{reg} cells also

regulate effector immune responses in disease states such as germinal center reactions [28,29], inhibit overzealous T cell responses during infection [30–35], enhance effector T cell differentiation and memory formation to pathogens [36–38], inhibit tumor immunity [39,40], and promote tolerance to environmental and commensal antigens [41–43]. The burden of regulating these diverse processes has led the field to propose two broad functional classes of T_{reg} cells defined by their ontogeny- peripheral- (pT_{reg}) and thymic- (tT_{reg}) derived T_{reg} cells. The thesis focuses on tT_{reg} cells.

Why the thymus?

The thymus has been an organ of immense curiosity for immunologists for some time. While initial thymectomy experiments failed to reveal immunological consequences [44], subsequent work revealed a central function in immune responses [45–47]. Work as early as 1962 by Jacques Miller suggested a role in immune tolerance, as day 3 thymectomized (d3Tx) mice succumbed to a wasting disease by 3 months of age [48]. A seminal study in 1969 described that day 3, but not day 7 or later, thymectomized mice developed autoimmunity of the ovary that could be rescued by a thymus transplant [49]. Work by Gershon and Kondo subsequently showed that thymocytes could produce dominant tolerance during immune responses to sheep red blood cells and coined the term “suppressor T cells” [50–52]. Together, this work suggested the existence of a population of thymus-derived suppressive T cells that had delayed kinetics of thymic export.

Although the concept of immune suppression was clearly correct, early models to explain this process proved unsatisfactory. Most notably, it was suggested that “suppressor T cells” could function via a soluble factor encoded in the MHC locus, I-J [53]. However, the I-J locus was eventually found not to encode a unique protein [54]. This led many to reject the concept of a unique population of T cells capable of immune suppression [55]. Despite these

controversies, work in the early 1980's already suggested the presence of a subpopulation of T cells, defined by anti-Lyt-1 (later described as CD5) antibody positivity, that were capable of suppressing autoimmunity in d3Tx mice [56]. A seminal study by Sakaguchi in 1995 discovered that $CD25^+$ T cells were necessary and sufficient for suppressing autoimmune responses. The identification of CD25 as a marker of suppressive T cells was critical to add legitimacy to the field [5]. A follow-up study connected this concept to autoimmunity observed in d3Tx experiments, as d3Tx prevented accumulation of $CD25^+$ cells in the periphery of mice. Transfer of $CD25^+$ cells into d3Tx mice was able to rescue autoimmunity, while transfer of CD25-depleted splenocytes caused autoimmunity in athymic mice, revealing that thymically derived $CD25^+$ T cells were critical controllers of autoimmunity [57]. Groundbreaking studies in humans, suffering from immune dysregulation, polyendocrinopathy, enteropathy, X-linked syndrome (IPEX), and scurfy mice, identified a critical role for the transcription factor FOXP3 in T_{reg} cells[7,8,58]. This led to the generation of a series of reporter mice to track FOXP3 expression in live cells[59–61], enabling functional T_{reg} transfer experiments. Additionally, protocols were developed to detect intracellular FOXP3 by flow cytometry that enabled tracking and quantification of T_{reg} cells in non-reporter mice and humans [62]. The identification of CD25 and FOXP3 as useful markers of T_{reg} cells led to an explosion of studies seeking to understand T_{reg} cell development and function.

Two-step model of thymic T_{reg} cell development

The prevailing paradigm of thymic T_{reg} cell development involves a two-step process [63,64]. Step one is driven by strong TCR stimulation in developing CD4 single positive thymocytes. This causes the upregulation of the high affinity IL-2 receptor, CD25, as well as TNF receptor superfamily (TNFRSF) members GITR, OX40 and TNFR2, thereby generating $CD25^+FOXP3^-$ T_{reg} cell progenitors ($T_{reg}P$). The second step is driven by

cytokine-dependent conversion of $T_{reg}P$ into mature T_{reg} cells via upregulation of FOXP3. These $CD25^{+}FOXP3^{+}$ cells are mature T_{reg} cells that emigrate from the thymus and mediate tolerance. More recent studies have implicated an alternative $T_{reg}P$ cell population, defined by the absence of CD25 and low expression of FOXP3 ($CD25^{-}$ $FOXP3^{lo}$ $T_{reg}P$) [65]; differentiation of these $T_{reg}P$ cells depends on the same two-step process [66]. Here I focus on the mechanisms that drive T_{reg} cell development in the thymus and summarize current evidence on how the thymus shapes the T_{reg} cell repertoire and function to maintain comprehensive immune tolerance.

TCR signals as an instructive cue for thymic T_{reg} cell development

Whether the T_{reg} cell TCR repertoire is enriched in self-reactive TCRs was initially controversial. For example, one group found extensive overlap between TCRs in conventional T cells (T_{conv}) and T_{reg} cells and suggested that T_{reg} cells respond to "non-self" antigens [67]. Likewise, analysis of mice expressing a TCR transgene specific for the foreign antigen pigeon cytochrome C, the AND TCR, observed that inducing antigen expression increased T_{reg} cell proportion but not numbers in the thymus, suggesting that engagement of cognate self-antigen was not driving T_{reg} cell development [68]. Nevertheless, other studies have provided evidence that the T_{reg} cell TCR repertoire is more self-reactive than its conventional counterpart, and that acquisition of agonist TCR stimulation is important in T_{reg} cell development. This view originated from early experiments observing the presence of $CD25^{+}$ cells in the thymus of wildtype mice, but not those expressing a transgenic TCR specific for foreign antigen [69]. This hypothesis was confirmed in later studies showing that TCR transgenics could drive thymic T_{reg} cell development only when the cognate antigen was also expressed in the thymus [70]. Further, TCR sequencing experiments on mice with reduced TCR repertoires observed that T_{reg} TCRs are largely distinct from conventional T cell TCRs [71,72], but overlap with TCRs

expressed by pathogenic self-reactive T cells in *Foxp3*$^{-/-}$ mice [73]. In addition, a series of experiments observed that intraclonal competition for cognate antigen limits T_{reg} cell differentiation [74,75] suggesting that interaction with antigen, presumably self-antigen, is important for T_{reg} cell development. Later work used TCR transgenics with varying affinity for the foreign antigen chicken ovalbumin (OVA) and observed a linear relationship between TCR affinity and T_{reg} cell development [76]. OVA-specific T_{reg} cells develop in RIP-mOVA thymi, where OVA is expressed as a self-antigen, with TCRs spanning a broad 3 log fold response range. While lower affinity TCRs can drive T_{reg} induction, TCR affinity and T_{reg} cell niche size are directly correlated with higher affinity TCRs driving increased numbers of T_{reg} cells [76]. Further, analysis of Nur77-GFP transgenic reporter mice, in which GFP is expressed coordinately with TCR signal strength, observed that T_{reg} cells interact more strongly with self-antigens[77]. Furthermore, lower proportions of TCR transgenic thymocytes in chimeric mice led to increased $CD25^{+}$ cell proportions and higher Nur77-GFP signal, confirming that developing T_{reg} cells compete for self-antigen during lineage commitment. TCR signal strength has also been related to the competency of developing T_{reg}P cells to respond to low levels of intrathymic IL-2, suggesting another mechanism that would bias a T_{reg} cell repertoire towards self-reactivity [66]. More recent studies have shown that intermediate dwell times for TCR-peptide:MHC complexes facilitate T_{reg} differentiation, while shorter dwell times preferentially drive positive selection and longer dwell times lead to clonal deletion [78]. This evidence collectively suggests that T_{reg} cell interaction with thymically presented antigen, at some elevated threshold, is necessary for initiating T_{reg} cell development.

Medullary thymic epithelial cells (mTECs) in T_{reg} cell development

Thymic selection is defined by a cellular dilemma - without the presence of specialized cell subsets, such as pancreatic beta cells, how is the T cell repertoire pruned of reactivity

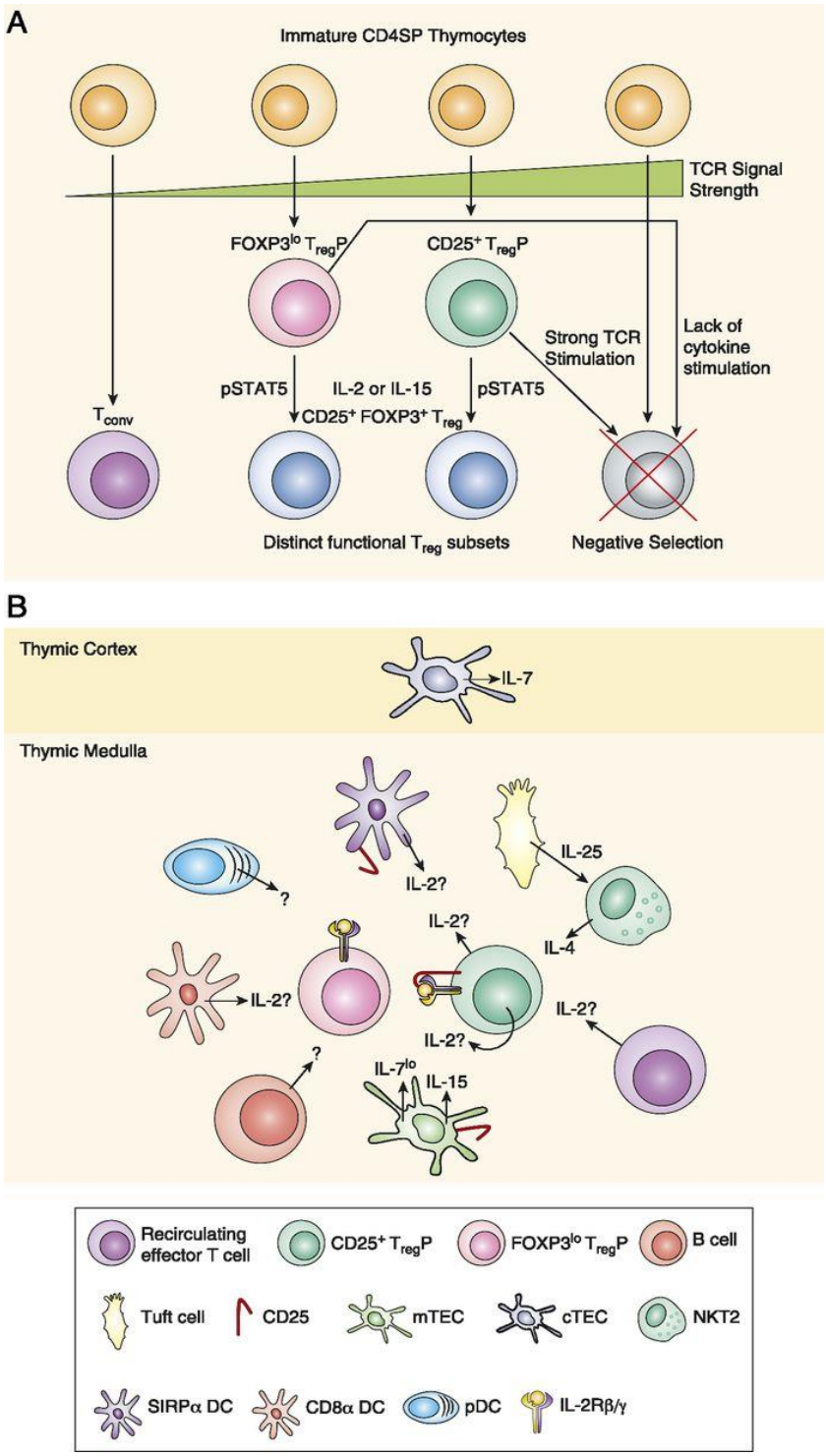

Figure 1.1. Model of thymic T_{reg} cell development. **a)** CD4 single positive thymocytes interact with a range of different affinity for self-antigens presented by thymic antigen-presenting cell (APC) subsets including, SIRPα$^+$ and CD8α$^+$ dendritic cells (DC),

plasmacytoid dendritic cells (pDC), medullary thymic epithelial cells (mTEC), B cells and perhaps macrophages. TCR signal strength initiates fate decisions. Weak TCR signaling is required to develop T_{conv}, while strong TCR stimulation drives clonal deletion. Intermediate TCR signaling drives T_{reg} cell commitment; stronger TCR signals lead to upregulation of CD25 generating a $CD25^+$ $T_{reg}P$ while weaker TCR stimulation causes upregulation of FOXP3 and produces a $FOXP3^{lo}$ $T_{reg}P$. Some $CD25^+$ $T_{reg}P$ still undergo clonal deletion, likely due to the high TCR signal strength experienced by this population and FOXP3 expression in $FOXP3^{lo}$ $T_{reg}P$ drives clonal deletion unless counterbalanced by survival signals mediated by engagement of γC cytokines. When either $T_{reg}P$ bind IL-2, or IL-15, this activates STAT5 and completes the differentiation of mature tT_{reg} cells, defined by dual expression of CD25 and FOXP3. **b)** Cytokine producing cells in T_{reg} cell development. Various cells in the thymus contribute cytokines to the thymic microenvironment. Cortical thymic epithelial cells (cTEC) produce IL-7 which may function as a survival factor for developing thymocytes in the cortex. mTEC have been shown to produce IL-15 as well as low levels of IL-7. mTEC also express CD25 which may function to transpresent IL-2 to developing $T_{reg}P$ or deplete local IL-2 from $T_{reg}P$. DC derived IL-2 may be produced by $CD8\alpha^+$ DC or $SIRP\alpha^+$ DC however, $SIRP\alpha^+$ DC also express CD25 which may modulate local IL-2 availability. It is unknown if pDC produce T_{reg} inducing cytokines. Similarly, it is unknown if thymic B cells contribute any cytokines capable of driving T_{reg} differentiation or serve only as an antigen presenting cell. Tuft cells produce IL-25 which acts on NKT2 cells to produce intrathymic IL-4. IL-4 plays a role in promoting survival and/or differentiation of $FOXP3^{lo}$ $T_{reg}P$. Finally, T cells represent the critical source of IL-2 required to drive T_{reg} cell differentiation, however, it is unclear if the IL-2 is being produced by $CD25^+$ $T_{reg}P$ or a subset of recirculating effector T cells.

to tissue specific antigens (TSA) uniquely encoded by these cells? This led to the hypothesis that these specialized self-antigens were in fact expressed at some low level in the thymus, an idea first corroborated by human data correlating thymic insulin expression and susceptibility to the development of diabetes [79,80]. Subsequent work revealed evidence of broad "promiscuous" gene expression in the thymus and attributed mTEC with the sole ability to produce these TSAs [81]. These studies also correlated expression of the transcriptional modulator Autoimmune Regulator (*Aire*), a gene previously linked to polysymptomatic autoimmunity [82,83], with the presence of TSA expression in mTECs. This supposition was confirmed in a set of ground-breaking experiments, showing AIRE expression was necessary for tissue specific gene expression in mTECs. Mice that lacked thymic expression of these TSAs had increased numbers of autoreactive T cells in peripheral lymphoid organs, which led to multiorgan immune destruction and generation of autoantibodies [84]. Likewise, hen egg lysozyme (HEL) reactive TCR transgenic T cells underwent clonal deletion when HEL was expressed under the control of the rat insulin promoter, an AIRE responsive locus in mTEC. The proportion of $CD25^+$ thymocytes in HEL transgenic mice increased; however, since there was no change in absolute number of these cells, the authors dismissed a role for T_{reg} cell development to these antigens [85]. These observations led to the hypothesis that the main role of AIRE in central tolerance was clonal deletion of tissue specific effector T cells.

While some controversy exists, numerous studies have now defined a role for AIRE-mediated ectopic antigen expression in mTECs in thymic T_{reg} cell development. Early studies in humans patients with Autoimmune Polyendocrinopathy Candidiasis and Ectodermal Dysplasia, a disorder caused by mutations in *AIRE*, documented a loss of T_{reg} cells and alterations in their TCR repertoire [86]. Further, expression of hemagglutinin (HA) via the AIRE promoter in mice led to the development of HA-specific T_{reg} cells, which was

dependent on MHC-II expression on mTECs [87]. However, a follow-up study in *Aire*^{OVA} mice, which express a fusion protein of AIRE and the OVA epitope recognized by the DO11.10 TCR, produced a counterpoint to this hypothesis, as MHC-II knockdown on mTECs caused an increase in OVA-specific T_{reg} cell development [88]. This finding suggested that low levels of high affinity antigens drive tT_{reg} differentiation, while higher expression of these same antigens resulted in clonal deletion. In addition, another study observed AIRE-dependent prostate-reactive T_{reg} cell development in the thymus [89]. Interestingly, analysis of the TCR repertoire of T_{conv} and T_{reg} cells in wildtype and *Aire*$^{-/-}$ mice found that cells normally directed towards the T_{reg} cell lineage were instead found in the T_{conv} lineage in *Aire*$^{-/-}$ mice [90], suggestive of T_{reg} cell agonist selection via AIRE driven antigens. A similar phenomenon is observed in human patients harboring *AIRE* mutations in which TCRs normally found in T_{reg} cells are found in the T_{conv} compartment [91]. In addition to AIRE, the transcription factor FEZF2 also regulates expression of TSA in the thymus. *Fezf2*$^{-/-}$ mice also developed multiorgan autoimmunity, but the spectrum of organs targeted was distinct from *Aire*$^{-/-}$ mice [92]. *Fezf2*$^{-/-}$ mice have fewer T_{reg} cells in the thymus and an altered TCR repertoire, reiterating a role for TSA expression in T_{reg} cell development. These results point to a crucial role for mTEC-derived TSA in central tolerance and T_{reg} cell development.

Recently, a distinct stromal cell involved in initiating type II mucosal immune responses, the Tuft cell, has been identified in the thymus. Tuft cells were found to resemble mTEC and produce IL-25, a major inducer of IL-4 production [93,94]. Tuft cells contribute to the Hassel's corpuscle, a structure in the thymus previously associated with T_{reg} cell generation in humans via licensing thymic dendritic cells (DC) to produce CD80 and CD86 via thymic stromal lymphopoietin (TSLP) stimulation [95]. Interestingly, we observed that mice lacking the transcription factor POU2F3, which is required for Tuft cell development,

have reduced numbers of FOXP3^{lo} T_{reg}P suggesting that Tuft cells can influence T_{reg} cell differentiation [96]. Although the mechanism for this remains unclear, it may be due to IL-25 production or the expression of unique TSAs by Tuft cells such as taste receptors [94].

Dendritic cells in T_{reg} cell development

The thymic DC compartment consists of conventional DC, including SIRPα$^+$ and CD8α$^+$ DC, and plasmacytoid DC (pDC) [97]. Earlier studies suggested that DC favor clonal deletion over T_{reg} cell development [87,98]. However, experiments using MHC-II$^{-/-}$ bone marrow chimeras clearly implicated a role for bone marrow-derived DC in both clonal deletion and T_{reg} cell induction [99]. Other experiments, using *in vitro* models of T_{reg} cell development, also observed efficient T_{reg} generation by conventional DC, and to a lesser extent pDC [99–101]. While the role of DCs in T_{reg} development has become clearer, the antigens they present, required for inducing tolerance, remain blurry. This is due to the paradox that tolerance to AIRE-driven antigens are frequently dependent on DCs [102]. Mechanistic insight to this paradox was revealed in studies documenting antigen transfer from AIRE-expressing mTEC to medullary DC [103,104]. Interestingly, AIRE$^+$ mTEC^{hi} cells produce the chemokine XCL1 that recruits thymic CD8α$^+$ DCs to the medulla, and *Xcl1*$^{-/-}$ mice exhibit defects in T_{reg} generation [105]. CD8α$^+$ DC are the dominant cross-presenting thymic DC subtype; thus, in addition to producing intrathymic antigens [106], AIRE also mediates recruitment of APC populations to the thymic medulla required for efficient T_{reg} cell induction. Subsequent work used TCR sequencing and TCR transgenics derived from TCRs isolated from T_{reg} cells to determine the relative contributions of DCs and mTECs on central tolerance [106]. This study observed that for some antigens, mTEC and DC played non-redundant roles in T_{reg} cell differentiation and clonal deletion. However, for other antigens, mTEC and DC played redundant roles in T_{reg} cell selection due to transfer of antigen from mTEC to DC. Indeed, more recent studies using a prostate reactive TCR

transgenic observed that DC were required to generate T_{reg} cells in the thymus, despite expression of the antigen being AIRE dependent [107]. These experiments highlight the complex interconnections between thymic DC and mTEC necessary for broad induction of antigen-specific thymic T_{reg} cells.

The contribution of SIRPα^{+} DC and pDC in T_{reg} cell polarization is particularly interesting as these represent migratory DC populations, capable of trafficking peripheral antigens to the thymus and inducing T_{reg} cell differentiation [97,108,109]. pDC also survey the gut via a CCR9 dependent mechanism [110], a chemokine receptor also required for pDC thymic localization and induction of central tolerance to peripheral antigens [111]. This could represent a mechanism to transport gut-derived environmental or commensal antigens to the thymus. However, the contribution of endogenous peripheral self- or non-self-antigen trafficking to the thymus in T_{reg} development remains an open question.

B cells in T_{reg} cell development

The presence of non-transformed B cells in the thymus first appreciated more than 30 years ago [112]. Early studies observed that B cell-deficient animals failed to delete Mtv-9, an endogenous superantigen, specific T cells, but reconstitution of these mice with B cells rescued this deletion [113]. Further, *in vitro* studies observed efficient deletion of thymocytes by thymic but not splenic B cells [114]. More recent studies have confirmed a role for thymic B cells in deletional tolerance to self-antigens [115,116]. For example, B cells induce clonal deletion of KRN TCR, a TCR reactive against the autoantigen glucose-6-phosphate isomerase, transgenic T cells [117]. The role of intrathymic B cells in T_{reg} cell development is less clear. The first evidence that thymic B cells affect tT_{reg} cell development came from the observation that B cell activating factor transgenic mice (BAFF-Tg) mice had more T_{reg} cells than wildtype (WT) mice, due to an increase in thymic B cells. However, tT_{reg} cell

development was decreased when thymic B cells were derived from hen egg lysozyme specific transgenic B cells, suggesting that a broad, self-reactive B cell repertoire was required to promote tT_{reg} cell development [118]. Using *in vitro* differentiation models, it was also observed that B cells isolated from the thymus were able to polarize $CD4^+$ thymocytes to the T_{reg} cell lineage in a contact, CD80/86, and MHC-II dependent manner [119]. These experiments suggested that B cells increase the presence of $CD25^+$ $T_{reg}P$ cells but do not facilitate the subsequent conversion of $T_{reg}P$ cells to mature T_{reg} cells.

T cells reactive to B cell encoded proteins (such as immunoglobulin (Ig)) are deleted by thymic B cells [120–122]. There is some evidence that T_{reg} cells may also be generated to BCR antigens [121], although whether this happens in the thymus is unclear. In mouse and humans, activation induced cytidine deaminase (AID)- and CD40L-deficiency results in autoimmunity that correlates with a decrease in the proportion T_{reg} cells [123]. These studies, combined with observations that thymic B cells induce T_{reg} cell development in an MHC-II dependent manner, suggest that thymic B cell-induced T_{reg} cell generation is critical for comprehensive immune homeostasis. Moreover, it was observed that self-antigens drive thymic B cell class-switching, which was required for inducing tolerance to self-antigens and is dependent on AID [124]. A thymic B cell licensing process has also been described wherein interactions with T cell-derived CD40L increases antigen presentation on thymic B cells and induces AIRE expression on these B cells [125]. This raises the possibility that thymic B cells have a parallel function to mTEC in producing TSA. However, it is still unclear what specificities of tT_{reg} cells are dependent on thymic B cells and whether interactions with thymic B cells preferentially promote T_{reg} cell development via $CD25^+$ or $FOXP3^{lo}$ $T_{reg}P$ cells.

Cytokines in thymic T_{reg} cell development

Prior to the identification of CD25 as a marker for T_{reg} cells there were hints that IL-2 receptor signaling was important for immune tolerance. In 1993, *Il2*$^{-/-}$ mice were generated; these mice had increased numbers of activated T cells and developed colitis-like disease [126]. Similar observations were made in *Il2ra*$^{-/-}$ and *Il2rb*$^{-/-}$ mice [127,128]. This was initially puzzling as IL-2 is a known T cell growth factor. Subsequent studies revealed that expression of IL2Rβ specifically in the thymus was sufficient to rescue the autoimmune phenotype observed in *Il2rb*$^{-/-}$ mice, suggesting a role for IL2R signaling during tT_{reg} development [129]. These findings were questioned by studies showing development of CD25^{-}FOXP3^{+} T_{reg} cells in *Il2*$^{-/-}$ mice [130–132] and that transfer of T cells from *Il2*$^{-/-}$ mice could protect against experimental autoimmune encephalomyelitis (EAE) [133]. However, further analysis observed that while *Il2*$^{-/-}$ mice do develop a small population of CD25^{-}FOXP3^{+} T_{reg} cells, *IL2Rβ*$^{-/-}$ have a larger block in T_{reg} cell development [132,134]. Further experiments observed that IL2Rβ binding cytokines, IL-2 and IL-15, were the major inducers of T_{reg} cell development [132], although IL-7 had limited capacity to induce FOXP3 expression[135,136]. These latter findings reconciled previous reports of T_{reg} cell development in *Il2*$^{-/-}$ mice, suggesting that in the absence of IL-2 other cytokines drive T_{reg} development, although not as efficiently as IL-2. Further, *Stat5*$^{-/-}$ T cells are unable to differentiate into T_{reg} cells, while constitutive activation of STAT5 in STAT5b-CA transgenic mice led to a striking increase in T_{reg} cell differentiation [137,138]. Together, these findings confirm the critical role STAT5 plays in T_{reg} cell development.

Other γC cytokines have also been evaluated for their effect on T_{reg} cell development. IL-4 potently inhibits induced T_{reg} cell generation, and IL-4 blockade increased T_{reg} cell differentiation both *in vitro* and *in vivo* [139]. Moreover, IL-4 is unable to induce STAT5 activation in CD25^{+} T_{reg}P cells and *Il4ra*$^{-/-}$ mice show no obvious defect in T_{reg} cell

generation in the thymus [135]. However, more recent work has observed that IL-4 stimulation of FOXP3^{lo} T_{reg}P maintains FOXP3 expression and upregulates CD25. Further, *Itk*$^{-/-}$ mice, which exhibit elevated IL-4 production, exhibited an IL4Rα-dependent increase in FOXP3^{lo} T_{reg}P and mature T_{reg} cells. Consistent with this observation, BALB/c mice also have increased tT_{reg} cell production that is diminished on the *Cd1d*$^{-/-}$ background [96], which eliminates the type 2 invariant natural killer T (NKT2) cells responsible for producing excess IL-4 in BALB/c mice [140,141]. Thus, IL-4 may function as a survival factor, or provide a direct differentiation stimulus, for FOXP3^{lo} T_{reg}P. However, the mechanism by which IL-4 promotes tT_{reg} cell development and the significance of this pathway remain unclear.

The cellular sources of cytokines needed for tT_{reg} development remain incompletely understood. T cells and dendritic cells represent the most likely cellular sources of IL-2 for tT_{reg} differentiation. Recent studies have observed that DC-derived IL-2 was particularly important for inducing T_{reg} cell development in *ex vivo* thymic slice models [142]. These experiments suggested that DCs create a niche for efficient T_{reg} cell development by providing the antigenic stimulation for T_{reg}P cell generation and the cytokine responsible for driving T_{reg} cell maturation. However, more recent work, using *Il2*$^{fl/fl}$ mice crossed to T cell (*Cd4-Cre*), DC (*Cd11c-Cre*) or B cell (*Cd79a-Cre*) specific CRE-recombinases, observed that T cell-derived IL-2 is necessary and sufficient to drive tT_{reg} cell development [143]. Further, autocrine production of IL-2 is not required for conversion of T_{reg}P cells into mature T_{reg} cells. It remains unclear what subset of T cells is producing the intrathymic IL-2 necessary for T_{reg} cell development. FOXP3 blocks *Il2* transcription [144], likely precluding FOXP3^{lo} T_{reg}P as producers of IL-2. However, CD25^{+} T_{reg}P may be competent to produce intrathymic IL-2 as these cells are receiving strong TCR stimulation. Indeed, we have observed *Il2* transcript in CD25^{+} T_{reg}P cells in bulk RNA seq experiments. Further analysis

of our single-cell RNA-seq experiments show *Il2* is predominantly produced by $CD25^+$ $T_{reg}P$ cells undergoing agonist selection. A recent study came to similar conclusions, suggesting that *de novo* developing self-reactive thymocytes, but not mature thymocytes, are a critical source of IL-2 for developing T_{reg} cells [145]. Despite these observations, a number of questions remain open on the requisite sources of IL-2 for T_{reg} cell development. First, while APC and stromal populations appear unlikely to contribute IL-2 for bulk T_{reg} cell differentiation it is unknown if IL-2 produced by these cells is important for certain parts of the T_{reg} cell repertoire. Secondly, it is still not well understood if $CD25^+$ $T_{reg}P$ are the only source of T cell-derived IL-2 or whether mature, recirculating, T cells are also capable of contributing IL-2 for T_{reg} cell differentiation as well. Finally, thymic IL-2 production and availability has still not been evaluated spatially, thus it is unclear if IL-2 is available ubiquitously throughout the thymic medulla or if IL-2 is limited to pockets that are permissive for T_{reg} cell survival and differentiation.

Generation of IL-7 and IL-15 reporter mice has provided initial insight into the cellular players producing these cytokines in the thymus. Using IL-7-GFP knock-in mice, it was observed that IL-7 is present in both the thymic cortex and medulla. However, on a per-cell basis cortical thymic epithelial cells produced more IL-7 than mTECs [146]. The lack of robust IL-7 production in the thymic medulla may explain the negligible effect of IL-7 on T_{reg} development [135]. IL-15-CFP reporter-mice produced the opposite result; IL-15 was preferentially found in the thymic medulla [147]. Interestingly, IL-15 production was highest in $mTEC^{hi}$ cells, the most robust antigen-presenting subset of mTECs defined by high expression of AIRE. More work is required to understand the cellular sources of IL-15 that may be contributing to tT_{reg} cell development.

Transcriptional regulation of in T_{reg} cells

Transcriptional regulation of *Foxp3* and the broader T_{reg} epigenetic signature is essential for proper tT_{reg} cell development. Experiments to reverse engineer the T_{reg} cell transcriptional network surprisingly revealed a highly redundant system [148]. It was revealed that FOXP3 alone was insufficient to drive the stable T_{reg} cell transcriptional landscape. However, FOXP3 plus any one of a quintet of other transcription factors - EOS, IRF4, SATB1, LEF1 or GATA1 - was sufficient to solidify the T_{reg} cell transcriptional signature. Deletion of *Ikzf4* (EOS) or *Lef1* have no effect on T_{reg} development by themselves [149,150], while the effects of IRF4 or GATA1 deletion on T_{reg} development remain unstudied. However, subsequent studies observed a critical role for SATB1 in tT_{reg} cell development. SATB1 deletion at the $CD4^+CD8^+$ thymocyte stage prevented subsequent establishment of T_{reg} cell super-enhancers and caused inefficient *Foxp3* expression during later T_{reg} cell differentiation [151]. Early work suggested that TCR stimulation also facilitates T_{reg} cell epigenetic signatures [152,153]. However, more recent experiments using an *Il2ra* mutant mouse provide evidence that IL-2 signaling is important for initiating the T_{reg} epigenetic signature [154]. Specifically, SATB1 positioning throughout the genome was interrupted in developing T cells in *Il2ra* mutant mice. These results suggest that IL-2 signaling is also important for SATB1 to establish the T_{reg} epigenetic signature. Finally, deletion of the transcription factors Nr4a1-3 almost completely blocks tT_{reg} generation [155,156]. Whether Nr4a family members, or other transcription factors, act in concert with SATB1 to establish a permissive state prior to *Foxp3* upregulation remains an open question.

Several studies have shown a crucial role for NFκB activation in T_{reg} cell development. In particular, c-Rel activation is required for T_{reg} cell development [157–160]. c-Rel, but not NFκB1, activation downstream of CD28 is required for developing T cells to become $CD25^+$ $T_{reg}P$ [158]. However, $FOXP3^{lo}$ $T_{reg}P$ are highly dependent on both c-REL and NFκB1

expression [96]. Moreover, p65 (RELA) deficient thymi also contain decreased amounts of $CD25^+$ $T_{reg}P$ and mature T_{reg} cells [161]. RELA and c-REL play partially redundant roles in maintaining T_{reg} cell transcriptional signature and homeostasis, although deletion of RELA resulted in a more severe autoimmune phenotype than deletion of c-REL [161]. These findings suggest that NFkB family members may also be important in locking in a stable T_{reg} cell phenotype, although the precise function of each NFκB member during tT_{reg} development in establishing the T_{reg} cell transcriptional signature is still uncertain.

A key step in the development of tT_{reg} cells is stable upregulation of *Foxp3*. Much effort has focused on the factors and regulatory elements that control *Foxp3* expression. Several conserved regulatory regions in the Foxp3 locus have been identified. These include the *Foxp3* promoter, three intronic enhancers (*Cns1-3*) [160] and the *Foxp3* pioneer enhancer element *Cns0* [151]. *Cns0* is targeted by the transcriptional regulator SATB1 and acts to poise the *Foxp3* locus for active transcription [151]. Later during T_{reg} cell selection, *Cns3* acts as a pioneer regulatory element in the *Foxp3* locus to drive *de novo Foxp3* expression. This pioneer function is dependent on agonist TCR stimulation- and CD28-induced activation of c-Rel and binding of c-Rel to *Cns3* [159,160]. c-Rel targeting to the *Foxp3* locus arranges an enhanceosome including several other transcription factors important for *Foxp3* expression including RELA, NFAT, SMAD and CREB [162]. *Cns3*$^{-/-}$ T_{reg} cells are biased towards higher self-reactivity suggesting that c-Rel targeting of *Cns3* is required to sensitize the *Foxp3* locus to TCR stimulation [163]. Additionally, *Cns3*$^{-/-}$ thymi are devoid of the less self-reactive $FOXP3^{lo}$ $T_{reg}P$ cell population [96]. These experiments suggest that *Cns3* evolved in part to expand the repertoire of T_{reg} cells. Interestingly, deletion of an *Il2ra* enhancer element CaRE4[164], that has been linked to autoimmune SNPs in humans [165–167], causes a mild block in $CD25^+$ $T_{reg}P$ and mature T_{reg} development [96]. Thus, regulatory regions inside the *Foxp3* locus as well as those outside of *Foxp3* are required for proper

T_{reg} cell development. DNA demethylation of canonical T_{reg} cell genes is not completed until very late in T_{reg} cell development[168]. This paradigm is likely true of other modifications to chromatin accessibility[151]. Future studies will need to identify other enhancer elements critical for tT_{reg} cell development, characterize their upstream regulators and understand when these regulatory elements are being modified. Further, the contribution of these enhancers in generating the mature T_{reg} cell repertoire and transcriptome will be important in order to understand defects related to disease associated human allele variants.

Cellular models of thymic T_{reg} cell development

Studies of early T_{reg} cell ontogeny [59] illustrated that CD25 expression precedes FOXP3 expression and the thymic $CD4^+CD25^+$ compartment is comprised of both $FOXP3^+$ and $FOXP3^-$ cells [169]. This data provided the first hint that $CD4^+CD25^+$ $FOXP3^-$ thymocytes may represent cellular progenitors for mature $CD25^+FOXP3^+$ T_{reg} cells. Subsequent studies illustrated that $CD25^+FOXP3^-$ thymocytes represent the direct cellular progenitors of mature T_{reg} cells [63,64]. These studies provided a "two-step" model of thymic T_{reg} cell differentiation. In step one agonist TCR stimulation generates a $CD25^+$ $T_{reg}P$ cell, while in step two IL-2/STAT5-converts $CD25^+$ $T_{reg}P$ cells into mature T_{reg} cells. Later studies connected these two steps, finding that TCR signal strength correlated with expression of three TNFRSF members, GITR, OX40 and TNFR2, and signaling via these TNFRSF members renders developing $T_{reg}P$ cells more sensitive to IL-2 [66]. Thus, higher TCR self-reactivity imputes a selective advantage for developing $T_{reg}P$ by allowing these cells to compete more effectively for IL-2, thereby biasing the T_{reg} cell repertoire towards self-reactivity.

More recently, an alternative $T_{reg}P$ population was identified, defined by low FOXP3 and lack of detectable CD25 expression ($FOXP3^{lo}$ $T_{reg}P$). Initial reports demonstrated that

FOXP3^{lo} T_{reg}P cells efficiently develop into mature T_{reg} cells either *in vitro* to high dose IL-2 (200 U/mL) or *in vivo* in the periphery of mice. However, this paper also suggested that FOXP3 is normally a pro-apoptotic protein and must be counterbalanced by γC cytokine stimulation, such as IL-2, in order for FOXP3^{lo} T_{reg}P to survive thymic selection [170]. Despite the lack of CD25 expression, FOXP3^{lo} T_{reg}P cells are able to differentiate into mature T_{reg} cells in response to low-dose IL-2 (0.2-1 U/mL) [66,96] or intrathymic transfer [96,171]. Interestingly, in competitive intrathymic transfer experiments, CD25^{+} and FOXP3^{lo} T_{reg}P both differentiated into mature T_{reg} cells at similar efficiencies - it remains unclear how FOXP3^{lo} T_{reg}P are capable of such IL-2 sensitivity while lacking CD25 expression. CD25^{+} T_{reg}P cells experience greater TCR stimulation, as measured by NUR77-GFP signal intensity, than FOXP3^{lo} T_{reg}P during thymic selection [96,171]. The TCR repertoire of these two T_{reg}P cell populations overlap significantly with mature T_{reg} cells but much less so with each other [96]. These observations suggested that these were unique T_{reg}P cell populations selected by distinct interactions with self-antigens and contributed unique TCRs to the mature T_{reg} cell repertoire. Remarkably, T_{reg} cells derived from CD25^{+} T_{reg}P, but not FOXP3^{lo} T_{reg}P, could protect mice from EAE while T_{reg} cells derived from FOXP3^{lo} T_{reg}P were able to consistently suppress colitis. Collectively, these data provide an updated model of thymic T_{reg} cell development in which both CD25^{+} and FOXP3^{lo} T_{reg}P contribute quantitatively equivalently, but qualitatively distinctly, to the mature T_{reg} cell repertoire.

Recirculating or resident T_{reg} cells in thymic homeostasis

The thymic T_{reg} pool is composed of recently differentiated cells but also T_{reg} cells that have been retained following development (resident) or have recirculated to the thymus from the periphery [172–174]. Studies with *Rag2-GFP* mice demonstrate that older GFP-negative T_{reg} cells progressively accumulate in the thymus as mice age and represent the majority of thymic T_{reg} cells by about 8 weeks of age [174,175]. However, the origin of these

T_{reg} cells is debated with some suggesting that they are mostly resident cells that never left the thymus [172] and others proposing that they are primarily recirculating cells [174]. It has been difficult to distinguish between these two populations to determine their relative contributions to the thymic T_{reg} cell pool. Thymus transplantation studies demonstrate that T_{reg} cells migrate from the periphery to the thymus preferentially by comparison to conventional T cells [176]. Additionally, mature RAG2-GFP^{-} T_{reg} cells in the thymus have a similar gene expression profile to splenic T_{reg} cells and their TCR repertoire shows evidence of peripheral modification supporting the possibility that these cells are recirculating [174]. Resident and recirculating T_{reg} cells compete with developing thymic T_{reg} cells for access to IL-2 and limit their differentiation to the T_{reg} cell lineage [142,174]. Cellular phenotypes for "old" contaminating T_{reg} cells have been proposed, including CCR6^{+}CCR7^{-} [176] as well as CD73^{+} [96]; these markers can now be used to exclude "old" T_{reg} cells in studies *de novo* thymic T_{reg} development.

The mechanism by which recirculating T_{reg} cells restrict T_{reg} cell development is unknown and the immunological benefit of this restriction is unclear. It is possible that these older T_{reg} cells compete with thymocytes for antigen, co-stimulatory ligands, cytokines or chemokines, and/or TNFRSF ligands necessary for T_{reg} cell development – all actions that would decrease net T_{reg} cell generation. I hypothesize that recirculating T_{reg} cells may represent a mechanism by which the periphery of an organism communicates the establishment of a T_{reg} cell pool capable of maintaining tolerance. Thus, after dominant tolerance is induced, the thymus can safely loosen selection to allow a broader array of effector T cells to escape. In such a system, T_{reg} mediated peripheral tolerance is favored during the neonatal period when the relative lymphopenia could allow self-reactive effectors to proliferate unregulated and cause pathology. Further, neonates are protected from local infections via passive immunity from maternal antibodies. After this period,

thymic selection can be loosened and favor effector T cell TCR repertoire diversity to combat a broader array of unknown pathogens.

Differentiation of T_{reg} cells throughout ontology

A growing body of literature suggests T_{reg} cell development, and more broadly thymic selection, are not a static process but in fact change throughout the life of an organism. Using a doxycycline inducible model of AIRE expression, an early study suggested that expression of AIRE in neonatal mice is sufficient for tolerance induction while AIRE expression only in adult mice was unable to rescue the early tolerance defect of AIRE deficiency[177]. This study questioned the importance of T_{reg} cells in this process. However, a follow-up study showed that T_{reg} cells generated in a peri-natal window, approximately the first 10 days of life, could rescue the defects in tolerance typical of AIRE deficient mice. Adult T_{reg} cells were largely unable to suppress immune pathologies with the exception of insulitis[178]. Further, T_{reg} cell accumulation in neonatal skin is critical for developing tolerance to commensal microbes[179,180]. Interestingly, $mTEC^{hi}$ cells peak early in life, suggesting that some mechanism exists to decrease mTEC abundance later in ontogeny[181]. Lower $AIRE^{+}$ mTEC abundance would lead to a lower concentration of tissue restricted antigens in the thymus which should result in a more self-reactive effector repertoire. However, neonatal T cells express higher levels of CD5 and NUR77 than adult T cells[182]. This could indicate a difference in selection or could be caused by known intrinsic differences in neonatal versus adult T cell transcriptomes that may lower activation thresholds, such as miR-181a expression[183,184]. These observations point to the critical need to better understand T_{reg} cell differentiation and thymic function throughout ontogeny.

While the above studies have suggested differences in T_{reg} cell capabilities throughout ontogeny, they have suffered from some shortcomings in effectively understanding the differences in the function of T_{reg} cells that develop at different stages of life. Together with another graduate student, Lucy Sjaastad, we developed a novel mouse called *Foxp3*^{iDTR}, that will give insight into these questions. Activation of CRE in the *Foxp3*^{iDTR} mouse will remove a lox-stop-lox cassette and drive a *Foxp3-DTR-GFP* construct (Figure 1.2a). Crossing the *Foxp3*^{iDTR} to *Tcrd*^{CreER} mice, which only express CRE-ER in all immature thymocytes but not mature αβ T cells (Figure 1.2b), will allow for tamoxifen treatment to label waves of thymocytes at different points in ontogeny. T_{reg} cells that develop in a certain time period can then be tracked to see if there are differences in localization or phenotype. Following DT treatment, these cells can be depleted to understand what role T_{reg} cells that develop at different points in ontogeny play in immune homeostasis.

Concluding Remarks

Despite decades of research directed at understanding the development of thymic T_{reg} cells, many questions remain unanswered. While two cellular progenitors have been described that contribute to the mature T_{reg} cell repertoire, the precursors to each of these populations have not been effectively described. Preliminary reports have identified a CD122^{+} GITR^{+}CD25^{-}FOXP3^{-} T_{reg}P cell precursor that can give rise to CD25^{+} T_{reg}P cells via a c-Rel dependent mechanism [185]. However, whether this population also represents the precursors to FOXP3^{lo} T_{reg}P remains unclear. Defining the signals and relevant antigens that commit T_{reg} cell development via either T_{reg}P pathway will be important for understanding the holistic role each T_{reg}P pathway plays in immune tolerance.

Cytokine signaling is clearly required for T_{reg} cell generation. However, more nuanced effects of cytokines on T_{reg} selection remain poorly defined. CD25 can be expressed on

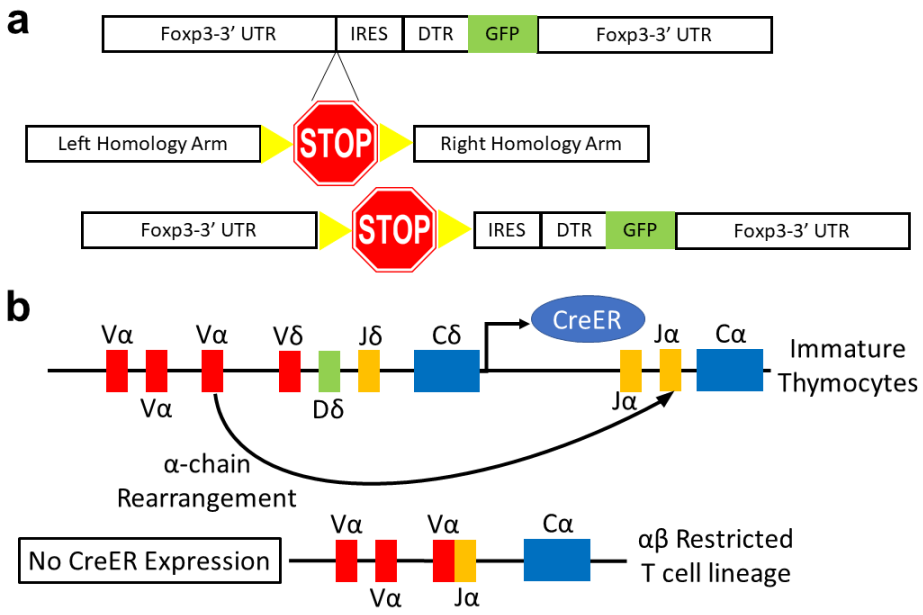

Figure 1.2. Schematic of *Foxp3*^{iDTR} allele generation and *Tcrd*^{CreER} function. **a)** Schematic of the 3' UTR of FOXP3-DTR mice (top), the targeting cassette (middle), and the predicted final locus after appropriate targeting (bottom). CRE expression leads to excision of the STOP cassette and expression of DTR and GFP. **b)** *Tcrd* is active in immature thymocytes leading to expression of CreER in all immature thymocytes. However, following α-chain rearrangement the δ locus is excised, removing the CreER and preventing CreER expression in mature αβ lineage T cells.

thymic DC and mTEC [143]; however, it is unclear if CD25 *trans* presentation[186] occurs in the thymus. Expression of CD25 may either bolster T_{reg} cell development by presenting IL-2 directly to developing T_{reg}P or by inhibiting the diffusion of IL-2. However, CD25 expression on mTEC or thymic DC could also reduce locally available IL-2, thus inhibiting conversion of T_{reg}P to mature T_{reg} cells. The role of IL-4 is also unclear; mice of different background produce distinct amounts of IL-4 [96,140,141], which could influence thymic T_{reg} cell TCR repertoire and possibly susceptibility to different types of autoimmunity. Further, certain subsets of thymic APC produce different cytokines, such as IL-2 from DC [142] and IL-15 from mTEC[147]. Future studies directed at understanding how distinct cytokines affect T_{reg} development will likely produce interesting insight into how cytokine stimulation affects T_{reg} cell repertoires.

Another mystery in T_{reg} cell development is how T_{reg} cells develop that enforce tolerance to transitory states, such as inflammation, puberty, estrous, or distinct metabolic states. Certainly for B cell immune responses there is evidence of thymus induced T_{reg} tolerance to Ig antigens [120–123], and loss of Tuft cells leads to the development of anti-IL-25 antibodies [94]. Further, development of inflammation specific T_{reg} cells has been observed in the thymus[78]. Interestingly, testosterone levels regulate AIRE-mediated TSA production [187], which may explain resistance to various forms of autoimmunity in males. Prepubertal males and females have similar levels of testosterone [188]; thus, any differences imposed by this hormone likely occur after puberty has initiated in humans. The specificities of thymic T_{reg} cells needed to provide tolerance in transitory states is still poorly understood.

Despite years of debate, controversy still exists over the relative role of thymic T_{reg} cells and peripheral T_{reg} (pT_{reg}) cells. The hypothetical requirement for pT_{reg} is at mucosal surfaces [189] where diverse non-genetic self-antigens are being surveyed or during pregnancy where ectopic alloantigens are contributed by the male gamete [190]. Several

studies suggest a role for thymic deletion and T_{reg} cell selection in mucosal tolerance [67,191–193] while other studies argue for the importance of pT_{reg} generation [41,189,194–197]. More recent studies have suggested that some populations of thymic T_{reg} cells are required to polarize T_{conv} to pT_{reg} cells, perhaps relating these disparate findings [194,198]. Likewise, T_{reg} cells derived from thymic FOXP3^{lo} T_{reg}P are able to suppress colitis, suggesting tolerance to commensal organisms can be induced by specific thymic T_{reg} cell subsets [96]. Further experimentation is required to conclusively delineate the unique and overlapping responsibilities of pT_{reg} and thymic T_{reg} in immune tolerance.

Finally, the evolutionary constraints placed on T cell selection in the thymus are immense - exogenous pressure from pathogens places a high priority on TCR diversity, while endogenous pressure from autoimmune hazards requires removal of self-reactive and potentially pathogenic T cells. Thus, T_{reg} cell development represents a mechanism that allows this leaky selection system to persist and focus effector T cell responses on "non-self" antigens. Future studies defining endogenous T_{reg} cell antigenic targets, and the thymic populations required to produce these antigens, will be required to understand the complex processes that govern the selection of a competent repertoire of thymic T_{reg} cells. Further, understanding the role of antigen specificity of T_{reg} cells in homeostatic, inflammatory, or autoimmune contexts will be crucial in linking thymic selection to peripheral homeostasis.

Questions addressed in this thesis

The experiments outlined in this thesis address several unanswered questions about thymic T_{reg} cell differentiation. First, using *Il2*$^{fl/fl}$ mice crossed to T cell, B cell and DC specific CRE expressing mice, *Cd4-Cre, Cd79a-Cre and Cd11c-Cre* respectively, we identify that T cells are the critical source of IL-2 for developing T_{reg} cells. Using bulk RNA-

seq and single cell RNA-seq I found that the dominant IL-2 producing T cells in the thymus are $CD25^+$ $T_{reg}P$ cells receiving strong TCR stimulation. Second, I compared two putative $T_{reg}P$ populations, $CD25^+FOXP3^-$ and $CD25^-FOXP3^{lo}$ $T_{reg}P$, and found that both could develop into mature T_{reg} cells at equivalent rates in the thymus. However, these $T_{reg}P$ cell populations differ in TCR repertoire, transcriptome, self-reactivity and perform distinct functions in immune homeostasis. Third, using single cell RNA-seq I developed a census of the thymic T_{reg} cell developmental pathway and further resolved $CD4^+$ thymocyte maturation. Finally, I will present preliminary data on the phenotype and function of recirculating or resident thymic T_{reg} cells. Combined, the experiments discussed add to a more comprehensive understanding of T_{reg} selection and differentiation as well as the role of T_{reg} cells in governing thymus function.

Chapter 2. Defining the important sources of IL-2 required for regulatory T cell development and homeostasis

*Portions of this chapter are derived from an article written by the author[143]

2.1 Background

Regulatory T (T_{reg}) cells play a critical role in preventing self-reactivity, limiting responses to commensal organisms, and dampening responses to pathogens following clearance of the infectious agents. Previous studies have shown that the cytokine IL-2 is critical for the development of T_{reg} cells in the thymus and for their subsequent homeostasis in peripheral lymphoid tissues. Mice lacking either IL-2 or the IL-2Rα- or β-chains all exhibit profound autoimmunity, although the reason was initially unclear[126–128]. Following the discovery of $CD25^+$ T_{reg} cells by Sakaguchi and colleagues[5], several groups reported that IL-2 is essential in $CD4^+$ $CD25^+$ $FOXP3^+$ T_{reg} cell development or function[9,130–134,138,199]. More recent studies have shown that IL-2 also plays a critical role in the conversion of thymic $CD25^+$ $FOXP3^-$ and $CD25^-FOXP3^{lo}$ T_{reg}P cells into mature T_{reg} cells[63,64,66,200]. Thus, substantial evidence implicates IL-2 as a key cytokine for the development and homeostasis of $FOXP3^+$ T_{reg} cells. A fundamental question is "What cells produce the IL-2 needed for T_{reg} cell development and homeostasis?" One obvious candidate is T cells themselves. Initial studies by Yang-Snyder and Rothenberg[201,202] detected IL-2 production in the thymus and found that this required the presence of T cells. However, developing thymocytes produce much less IL-2 than activated mature T cells. Moreover, the studies by Yang-Snyder and Rothenberg demonstrated that T cells were necessary to detect IL-2 in the thymus but did not demonstrate that the T cells produced the IL-2 themselves. Thus, it is plausible that other cellular sources of IL-2 contribute to T_{reg} cell development. Consistent with this possibility, IL-2 is produced by both B cells and dendritic cells (DCs)

under specific circumstances[203,204]. Because both of these cell subsets are found within the thymic medulla where T_{reg} cell development takes place, each could also be a potential source of IL-2 needed for T_{reg} cell development. Supporting this possibility, Robey and colleagues[142] found that DC-dependent development of T_{reg} cells in thymic slices was reduced by 50% when the DC were derived from *Il2*$^{-/-}$ mice. Thus, there are multiple potential sources of IL-2 that could play an important role in either T_{reg} cell development in the thymus or homeostasis in peripheral lymphoid tissues. To definitively address what sources of IL-2 are required for T_{reg} cell development and homeostasis, we used mice in which the *Il2* gene is flanked by loxP sites[205]. We crossed *Il2*$^{fl/fl}$ mice with *Cd4-Cre*, *Cd79a-Cre*, and *Cd11c-Cre* mice[206–209] to selectively delete IL-2 in T cells, B cells, and DCs, respectively. Furthermore, because IL-15 can partially substitute for IL-2 in T_{reg} cell development, we also crossed these mice onto the *Il15*$^{-/-}$ background. These studies revealed that the only critical source of IL-2 required for T_{reg} cell development in the thymus was T cells. Bulk RNA-seq revealed that CD25^{+} T_{reg}P cells, but not conventional CD4SP, FOXP3^{lo} T_{reg}P or mature T_{reg} cells, produced IL-2 in the thymus. Using single-cell RNA-seq, we found that the major source of T cell derived IL-2 in the thymus is CD25^{+} T_{reg}P cell undergoing agonist selection. Although T cell–derived IL-2 is necessary and sufficient to maintain T_{reg} cells in most peripheral lymphoid tissues, both T cell– and DC-derived IL-2 contributed to T_{reg} cell homeostasis in mesenteric lymph nodes. Thus, multiple cellular sources of IL-2 contribute to mature T_{reg} cell homeostasis.

2.2 Results

Thymic T cells and DCs can produce IL-2

To determine if developing T cells or thymic DCs produce IL-2, we carried out flow cytometry with intracellular staining for IL-2. Upon stimulation with PMA and ionomycin,

both thymocytes and thymic DCs were able to produce IL-2 (Figure 2.1 a,b), although a much smaller fraction of DCs produced IL-2 compared with thymocytes. Staining for IL-2 was specific, as staining was lost in *Cd4-Cre* x *Il2*$^{fl/fl}$ and *Cd11c-Cre* x *Il2*$^{fl/fl}$ mice, respectively (data not shown). Similar results were found when we sorted thymocytes or DCs and assayed for *Il2* mRNA levels by quantitative real-time PCR. In contrast, we failed to detect IL-2 production by mTECs (data not shown). These results suggest that either T cells or DCs could be responsible for producing the IL-2 needed for thymic T_{reg} cell development. A previous study suggested that IL-2 can be trans-presented by CD25 expressed on DCs[186]. To examine whether such trans presentation of IL-2 could occur in the thymus, we stained thymic DCs, mTECs, and splenic DCs for CD25. A large fraction of mTECs as well as thymic, but not splenic, conventional SIRPα^{+} DCs expressed CD25 (Figure 2.1 c,d). Neither mTECs nor thymic DCs expressed the IL-2R β-chain (data not shown). Thus, CD25 expression by mTECs and DCs is not involved in signaling cell-intrinsic responses to IL-2. Rather, this finding suggests that these APCs in the thymus may use CD25 to increase the local concentration of IL-2 available to T_{reg}P cells and thereby facilitate T_{reg} cell development. Alternatively, CD25 expression on APCs could limit the availability of IL-2, similar to T_{reg} cell IL-2 competition limiting effector responses in the periphery[210].

T cell–derived IL-2 is important for T_{reg} cell homeostasis in IL-15–sufficient mice

Given that DCs, B cells, and T cells are the most likely candidates to produce the IL-2 required for T_{reg} cell development and homeostasis, we analyzed *Cd4-Cre*, *Cd11c-Cre*, and *Cd79a-Cre* mice crossed to *Il2*$^{fl/fl}$ mice. None of these mice exhibited statistically significant reductions in thymic T_{reg} cell production, although *Cd4-Cre* mice trended

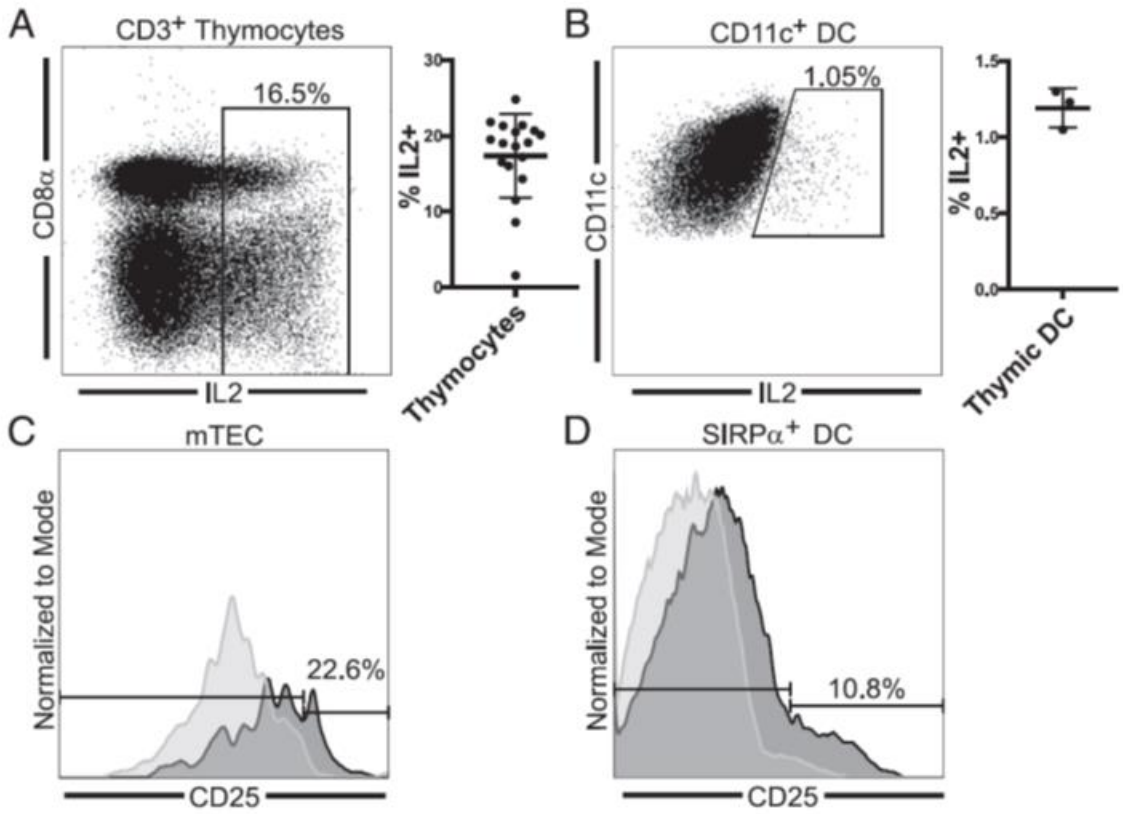

Figure 2.1. Thymocytes and thymic DCs produce IL-2. **a)** Thymocytes were stimulated with PMA/Ionomycin and stained for IL-2 production. Left panel. A representative flow plot showing IL-2 production in thymocytes pre-gated on CD3. Right panel. Quantification of %IL-2+ cells; data represents 7 experiments, n=18 mice. **b)** Thymic DCs were stimulated with PMA/Ionomycin and stained for IL-2 production. Left panel. A representative flow plot showing IL-2 production from thymic DCs. Right panel. Quantification of %IL-2+; data represents 3 experiments, n=3 mice. Bars represent mean plus SEM. **c)** CD25 expression on mTECs (dark grey) compared to isotype staining control (light grey), **d)** Expression of CD25 in thymic (dark grey) or splenic (light grey) SIRPα^{+} DC.

toward lower thymic T_{reg} cell abundance (2.5-fold mean reduction from controls, p = 0.39) (Figure 2.2 a). This is in agreement with previous reports, showing that IL-15 could rescue T_{reg} cell development in IL-2 deficient mice[132,134]. Although thymic T_{reg} cell development was not grossly inhibited, *Cd4-Cre* x *Il2*$^{fl/fl}$ mice, but not *Cd11c-Cre* x *Il2*$^{fl/fl}$ or *Cd79a-Cre* x *Il2*$^{fl/fl}$ mice, exhibited significant reductions in splenic T_{reg} ($CD4^+$ $CD25^+$ $FOXP3^+$) cells (Figure 2.2 b). Moreover, when we stained for CD44 and CD62L in CD4 and CD8 effector T cells, we observed significant increases in activated CD4 and CD8 T cells in *Cd4-Cre* x *Il2*$^{fl/fl}$ mice but no differences in *Cd11c-Cre* x *Il2*$^{fl/fl}$ or *Cd79a-Cre* x $Il2^{fl/fl}$ mice (Figure 2.2 c). This result suggests that the T_{reg} cell compartment in *Cd4-Cre* x $Il2^{fl/fl}$ mice is failing to maintain immune homeostasis, likely because of the defect in T_{reg} cell abundance in the periphery of these mice.

DC- and B cell–derived IL-2 are dispensable for T_{reg} cell development and homeostasis

Previous studies reported that IL-15 can substitute for IL-2 during thymic T_{reg} cell development[132,134]. Thus, to understand the role of DC- and B cell–derived IL-2 in T_{reg} cell differentiation, we crossed *Cd11c-Cre* and *Cd79a-Cre* mice to *Il2*$^{fl/fl}$ x *Il15*$^{-/-}$ mice. We observed that *Il2* deletion in DCs, B cells, or both subsets, had no effect on T_{reg} cell development in the thymus (Figure 2.3 a,b). Furthermore, the spleens of these mice also had no differences in T_{reg} cell abundance (Figure 2.3 c). There was also no increase in the percentage of $CD44^{hi}CD62L^{lo}$ activated $CD8^+$ or $CD4^+$ effector T cells (Figure 2.3 d). This suggests that T_{reg} cells in mice lacking IL-2 from DCs or B cells can maintain immune tolerance and T_{reg} cell homeostasis in the spleen, even in the absence of compensatory IL-15.

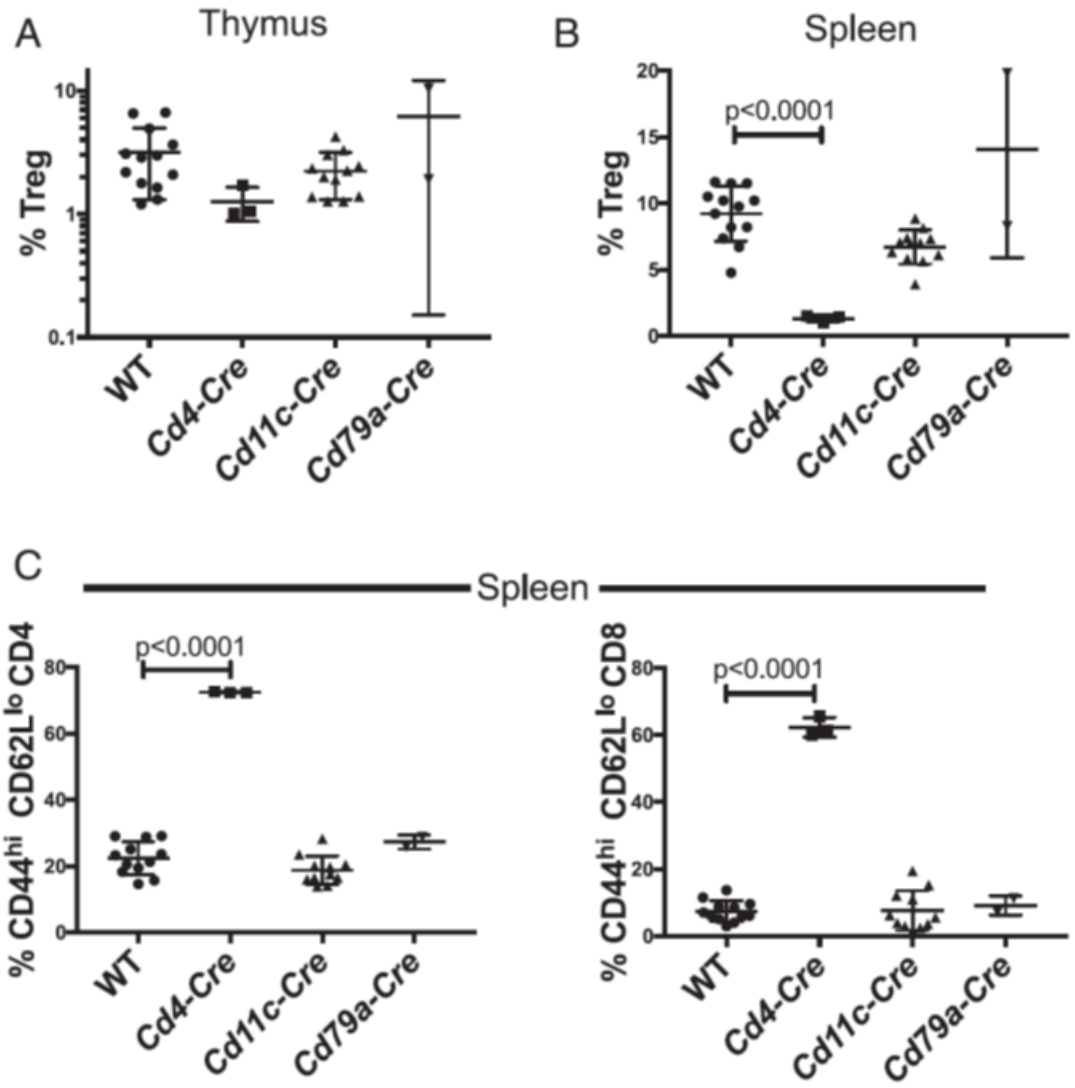

Figure 2.2. T cell-derived IL-2 is important for T_{reg} cell homeostasis in IL-15 sufficient mice. **a)** Quantification of the % ($CD25^{+}FOXP3^{+}$) T_{reg} within CD4+ thymocytes of the indicated CRE+ mice on an $Il2^{FL/FL}$ background. **b)** Quantification of the % T_{reg} ($CD25^{+}FOXP3^{+}$) within splenic CD4+ T cells of the indicated mice **c)** Quantification of the % of activated/effector CD4 (left panel) and CD8 (right panel) T cells in the spleen of the indicated mice. Data is representative of 6 experiments, n=13 mice (Wildtype), 3 experiments, n=3 mice (*Cd4-Cre x* $Il2^{FL/FL}$), 4 experiments, n=12 mice (*Cd11c-Cre x* $Il2^{FL/FL}$), and 1 experiment, n=2 mice (*Cd79a-Cre x* $Il2^{FL/FL}$). Data was analyzed by one-way ANOVA.

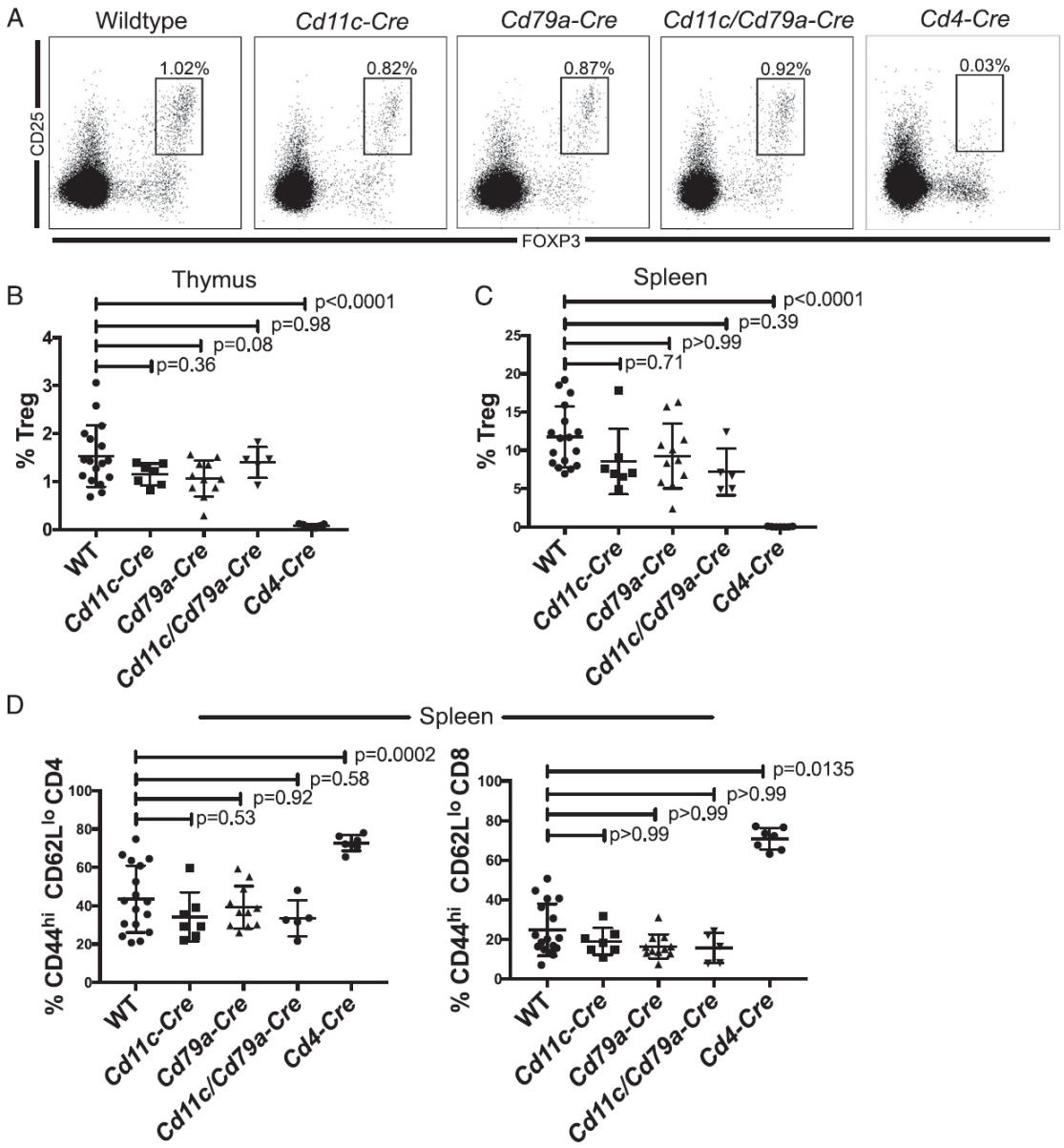

Figure 2.3. Dendritic cell- and B cell-derived IL-2 is dispensable for T_{reg} cell development and homeostasis. **a)** Representative flow plots of CD25 and FOXP3 expression in CD4SP thymocytes of the indicated CRE+ mice on an *Il2*$^{FL/FL}$ *x Il15*$^{-/-}$ background. **b,c)** Quantification of the % (CD25^{+}FOXP3^{+}) T_{reg} within CD4+ T cells in the thymus (B) and spleen (C). **d)** Quantification of the % of activated/effector CD4 (left panel) and CD8 (right panel) T cells in the spleen of the indicated mice. Data is representative of 9 experiments, n=17 mice (Wildtype), 4 experiments, n=7 mice (*Cd11c-Cre*), 6 experiments, n=11 mice

(*Cd79a-Cre*), 4 experiments, n=5 mice (*Cd11c-Cre x CDd79a-Cre*) and 2 experiments, n=7 mice (*Cd4-Cre*). Data was analyzed by one-way ANOVA (b and d) or Kruskal-Wallis tests (c). Wildtype and *Cd4-Cre x Il2*$^{FL/FL}$ *x Il15*$^{-/-}$ data points are identical for Fig. 2.3a,b and Fig. 2.4c,d. Wildtype and *Cd4-Cre x Il2*$^{FL/FL}$ *x Il15*$^{-/-}$ data points are identical for Fig. 2.3c,d and Fig. 2.7a,b.

T cell–derived IL-2 is critical for T_{reg} cell development in the thymus

The most likely sources of IL-2 that could be important for T_{reg} cell development are thymocytes themselves. To test this possibility, we generated *Cd4-Cre* x *Il2*$^{fl/fl}$ x *Il15*$^{-/-}$ mice and analyzed their thymi for T_{reg} cell development. Interestingly, we observed no defect in T_{reg}P cell generation in mice depleted of IL-2 in T cells, DC and/or B cells and IL-15 compared to *Il15*$^{-/-}$ mice (Figure 2.4 a). In contrast, *Il15*$^{-/-}$ mice had reductions in both T_{reg}P cell populations versus wildtype controls (Figure 2.4 b). These results contrast with previous reports that IL-15 is specifically important for FOXP3^{lo} T_{reg}P cell formation and that IL-2 and/or IL-15 is important for FOXP3^{lo} T_{reg}P cell survival[65,211]. However, we observed a striking loss of almost all T_{reg} cells in the thymi of mice lacking IL-2 in T cells in the *Il15*$^{-/-}$ background (Figure 2.4 c,d). This finding demonstrates that T cell–derived IL-2 is necessary for T_{reg} cell development in the thymus. We also wanted to see if deletion of *Il2* in T cells, B cells, and DCs combined would exacerbate the loss of T_{reg} cells observed in *Cd4-Cre* x *Il2*$^{fl/fl}$ x *Il15*$^{-/-}$ mice. We observed no significant differences in T_{reg} cell development when comparing *Cd4-Cre* x *Il2*$^{fl/fl}$ x *Il15*$^{-/-}$ mice with *Cd11c-Cre* x *Cd4-Cre* x *Il2*$^{fl/fl}$ x *Il15*$^{-/-}$, *Cd79a-Cre* x *Cd4-Cre* x *Il2*$^{fl/fl}$ x *Il15*$^{-/-}$, or *Cd79a-Cre* x *Cd11c-Cre* x *Cd4-Cre* x *Il2*$^{fl/fl}$ x *Il15*$^{-/-}$ mice (Figure 2.4 c,d). These results demonstrate that T cell–derived IL-2 is both necessary and sufficient for the conversion of T_{reg}P to mature T_{reg} cells in the thymus.

Autocrine production of IL-2 by T cells is not required for T_{reg} cell development

Given that T_{reg}P cells undergoing agonist selection produce IL-2, a model for T_{reg} cell development could be that developing CD4SP thymocytes that receive a strong TCR stimulus would upregulate IL-2, which would then bind to the IL-2 receptor on that cell and drive T_{reg} cell differentiation. To test this hypothesis, we created bone marrow chimeras in *Rag2*$^{-/-}$ x *Il2*$^{-/-}$ x *Il15*$^{-/-}$ recipients from a 1:1 mixture of wild-type

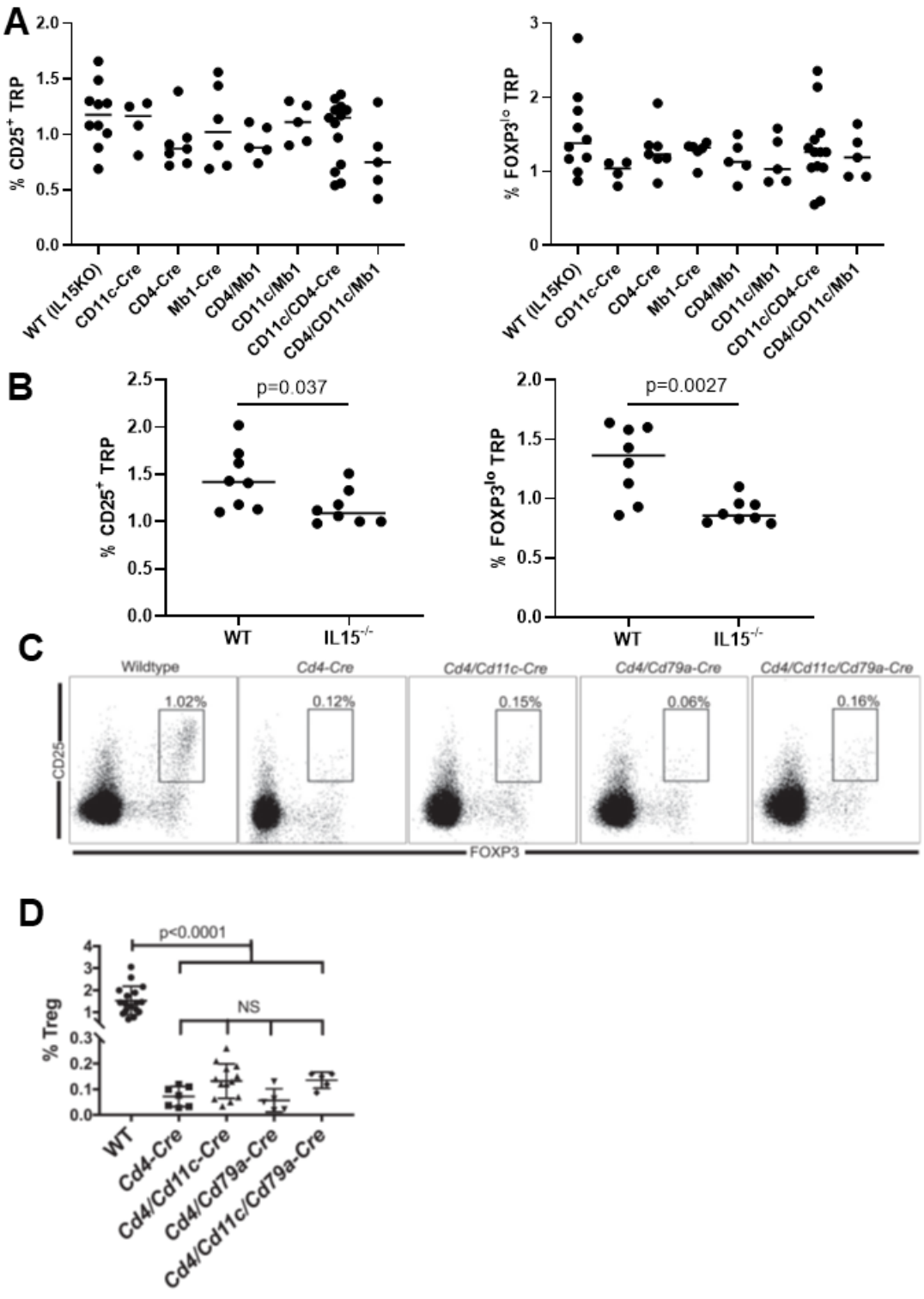

Figure 2.4. T cell-derived IL-2 is critical for thymic T_{reg} differentiation. **a)** % of $CD25^+$ T_{reg}P (left) or $FOXP3^{lo}$ T_{reg}P (right) cells in indicated mice. **c)** Representative flow plots of CD25

and FOXP3 expression in CD4SP thymocytes of the indicated CRE+ mice on an *Il2*$^{FL/FL}$ *x IL*$l5^{-/-}$ background. **d)** Quantification of the % ($CD25^{+}FOXP3^{+}$) T_{reg} within CD4SP thymocytes in the indicated mice strains. **a,** Data is representative of 4 experiments, n=10 mice (Wildtype), 4 experiments, n=4 mice (*Cd11c-Cre*), 2 experiments, n=7 mice (*Cd4-Cre*), 4 experiments, n=6 mice (*Cd79a-Cre*), 2 experiments, n=5 (*Cd4-Cre x CD79a-Cre*), 4 experiments, n=5 mice (*Cd11c-Cre x Cd79a-Cre*), 6 experiments, n=13 mice (*Cd11c-Cre x Cd4-Cre*), and 4 experiments, n=5 mice (*Cd11c-Cre x Cd4-Cre x Cd79a-Cre*). Data was analyzed by Kruskal-Wallis with Dunn's multiple comparisons test. **b,** Data is representative of 3 experiments, n=8 mice (Wildtype) and n=8 mice (*Il15*$^{-/-}$). Data was analyzed by unpaired *t* test. **c,d.** Data is representative of 9 experiments, n=17 mice (Wildtype), 2 experiments, n=7 mice (*Cd4-Cre*), 6 experiments, n=13 mice (*Cd4-Cre x Cd11c-Cre*), 2 experiments, n=5 mice (*Cd4-Cre x Cd79a-Cre*), 4 experiments, n=5 mice (*Cd4-Cre x Cd11c-Cre x Cd79a-Cre*). Data was analyzed by one-way ANOVA. Wildtype and *Cd4-Cre x Il2*$^{FL/FL}$ *x Il15*$^{-/-}$ data points are identical for Fig. 2.3a,b and Fig. 2.4c,d.

(WT) bone marrow with either congenically marked WT or *Cd4-Cre* x *Il2*$^{fl/fl}$ x *Il15*$^{-/-}$ bone marrow. We observed identical development of T_{reg} cells from IL-2– deficient and –sufficient T cells (Figure 2.5 a,b). This demonstrates that autocrine signaling of IL-2 by T cells is dispensable for T_{reg} cell development and that bystander T cell production of IL-2 is sufficient to drive this developmental process.

Identification of the specific thymic T cell population producing IL-2

Paracrine, T cell derived, IL-2 is critical to thymic T_{reg} differentiation. However, we wanted to better understand what population of T cells in the thymus is producing IL-2. To answer this question, we sorted conventional CD4SP, CD25^{+} T_{reg}P, FOXP3^{lo} T_{reg}P and mature T_{reg} cells from thymi and subjected these samples to bulk RNA-sequencing (RNAseq). We found *Il2* expression in CD25^{+} T_{reg}P cells but not any other sorted population (Figure 2.6 a), suggesting CD25^{+} T_{reg}P cells are the likely source of IL-2 required to facilitate thymic T_{reg} development. This observation is in line with CD25^{+} T_{reg}P receiving strong TCR stimulation[96] and FOXP3 repressing *Il2* transcription[212]. We further wanted to understand if we could identify a sub-population of CD25^{+} T_{reg}P cells that are producing IL-2. We performed single cell RNA-seq (scRNAseq) on CD25^{+} T_{reg}P cels as well as conventional CD4SP, FOXP3^{lo} T_{reg}P and mature T_{reg} cells. *Il2* expression could be detected at a low rate in the CD25^{+} T_{reg}P cell population. The *Il2* expression is confined to the most immature CD25^{+} T_{reg}P cells undergoing agonist selection (Figure 2.6 b). Collectively this data suggests that immature CD25^{+} T_{reg}P cells receiving TCR stimulation are the predominant source of IL-2 in the thymus, a finding in agreement with a recent study suggesting that *de novo* developing self-reactive thymocytes are the majority producers of IL-2[145].

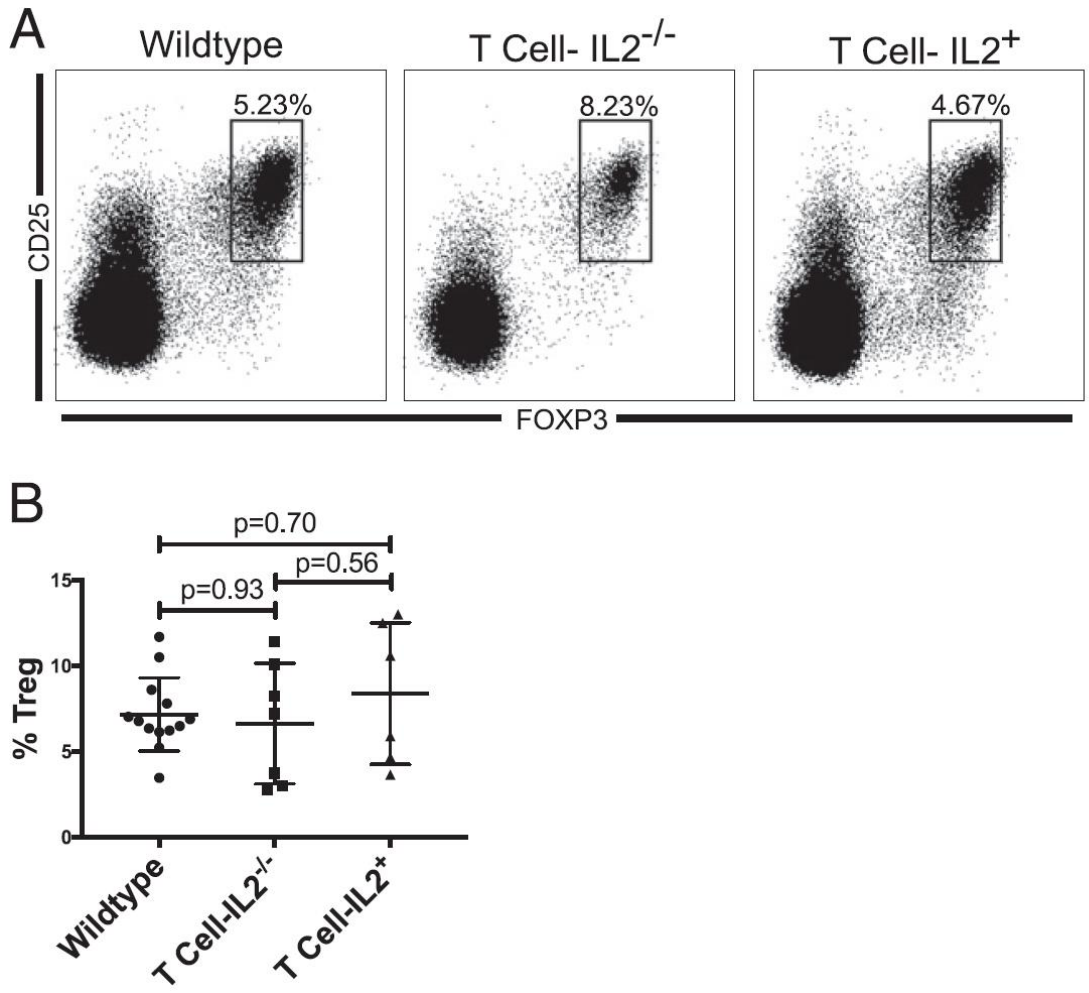

Figure 2.5. Cell intrinsic IL-2 is not required for thymic T_{reg} differentiation. **a)** Representative flow plots of CD25 and FOXP3 expression in the CD4SP thymocytes of the indicated donor origin with chimeric mice. **b)** Quantification of the % ($CD25^+FOXP3^+$) T_{reg} within CD4SP thymocytes from each donor origin. Data is representative of 2 experiments, n= 13 (Wildtype, $CD45.1^+$), 7 T cell- $IL2^{-/-}$ (*Cd4-Cre x* $Il2^{FL/FL}$ *x* $Il15^{-/-}$), 6 T cell- $IL2^+$ (*Cd4-Cre x* $Il2^{FL/+}$ *x* $Il15^{-/-}$ or $Il2^{FL/FL}$ *x* $Il15^{-/-}$). Data was analyzed by one-way ANOVA.

Production of IL-2 by T cells and DCs is required for T_{reg} cell homeostasis in mesenteric lymph nodes

Given that DC- and B cell–derived IL-2 is dispensable for T_{reg} cell homeostasis in the spleen (Figure 2.3 c,d), we wanted to know if T cell–derived IL-2 is responsible for this function. To answer this question, we analyzed T_{reg} cell abundance in the spleen and inguinal and mesenteric lymph nodes of *Cd4-Cre* x *Il2*$^{fl/fl}$ x *Il15*$^{-/-}$, *Cd11c-Cre* x *Cd4-Cre* x *Il2*$^{fl/fl}$ x *Il15*$^{-/-}$, *Cd79a-Cre* x *Cd4-Cre* x *Il2*$^{fl/fl}$ x *Il15*$^{-/-}$, or *Cd79a-Cre* x *Cd11c-Cre* x *Cd4-Cre* x *Il2*$^{fl/fl}$ x *Il15*$^{-/-}$ mice. Deletion of *Il2* in T cells resulted in an ~100-fold reduction in T_{reg} cell proportions in the spleen. No further decrease in T_{reg} cell proportions was observed when combining deletion of *Il2* in T cells with deletion of *Il2* in DCs, B cells, or all three cell subsets (Figure 2.7 a,c). Consistent with these findings, we observed a significant increase in the percentage of activated $CD4^+$ and $CD8^+$ T cells in the spleen of mice with a selective defect in T cell–derived IL-2 (Figure 2.7 b). Similar results were observed in inguinal lymph nodes (data not shown). Deletion of *Il2* in T cells, but not DCs or B cells, also led to a significant decrease in T_{reg} cells in mesenteric lymph nodes. However, deletion of *Il2* in both T cells and DCs led to a further ~10-fold drop in T_{reg} cell abundance in mesenteric lymph nodes (Figure 2.7 c). Deletion of *Il2* in B cells provided no additional decrease in T_{reg} cell abundance under any experimental conditions. Finally, *Il2* deletion in *Cd4-Cre* x *Il2*$^{fl/fl}$ x *Il15*$^{-/-}$, *Cd11c-Cre* x *Cd4-Cre* x *Il2*$^{fl/fl}$ x *Il15*$^{-/-}$, *Cd79a-Cre* x *Cd4-Cre* x *Il2*$^{fl/fl}$ x *Il15*$^{-/-}$, or *Cd79a-Cre* x *Cd11c-Cre* x *Cd4-Cre* x *Il2*$^{fl/fl}$ x *Il15*$^{-/-}$ mice led to increased T cell activation in the mesenteric lymph node, consistent with reduced percentages of T_{reg} cells in all of these mouse strains (Figure 2.7 d). These observations demonstrate the importance of T cell–derived IL-2 in maintaining T_{reg} cell abundance and function in peripheral lymphoid organs but also highlight a role for DCs in contributing to T_{reg} cell homeostasis in mesenteric lymph nodes.

a

Comparison	Gene	logFC	PValue	FDR
CD4SP to CD25+ TRP	Il2	-7.59165	0.003839	0.036358
CD25+ TRP to Foxp3lo TRP	Il2	7.59165	0.003847	0.024417
CD25+ TRP to Mature Treg	Il2	7.59165	0.004857	0.039509

b

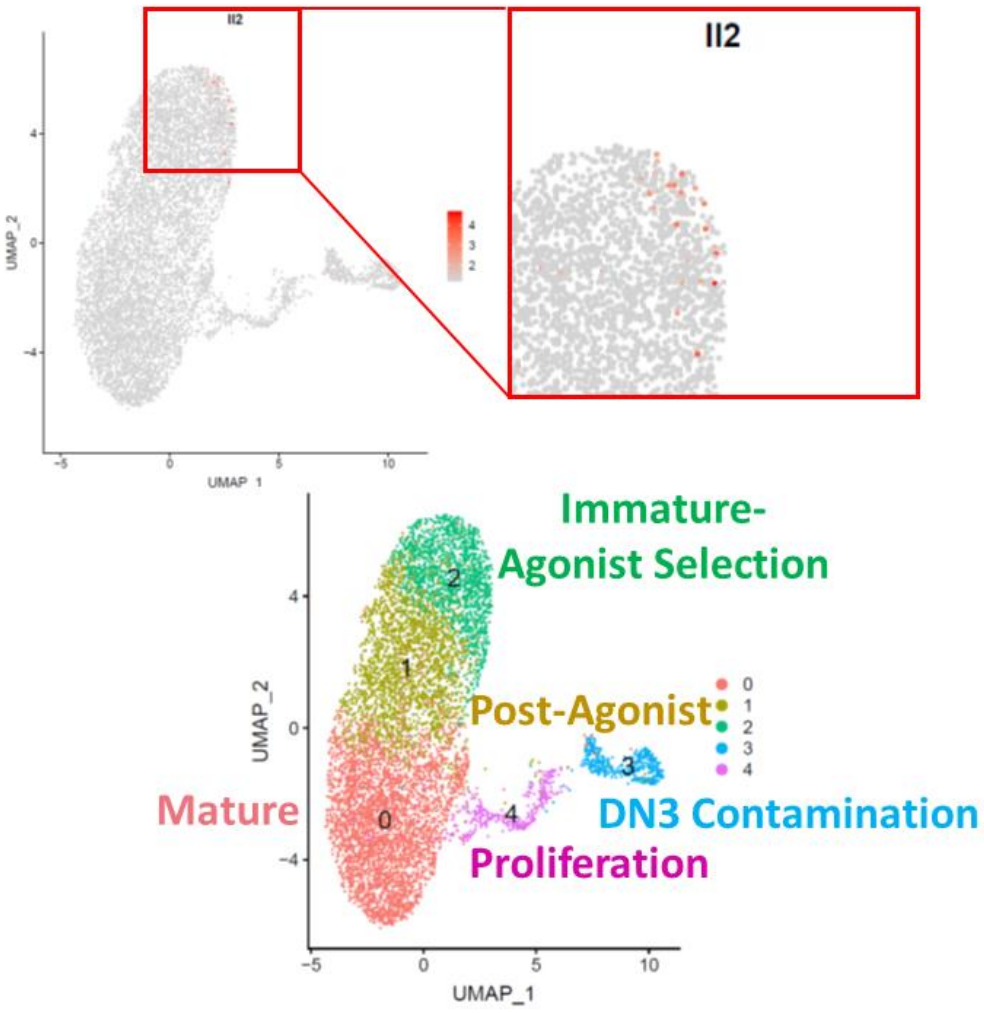

Figure 2.6. CD25^{+} T_{reg}P cells undergoing agonist selection are a major source of T cell derived intrathymic IL-2. **a)** Log fold change of *Il2* in CD25^{+} T_{reg}P vs conventional CD4SP (top), FOXP3^{lo} T_{reg}P (middle), and mature T_{reg} cells (bottom) from bulk RNAseq analysis of CD73^{-} sorted thymic populations. **b)** scRNAseq analysis of CD73^{-}CD25^{+} T_{reg}P cells for *Il2* expression, indicated by red shading in the feature plot, (top) and cluster identities (bottom).

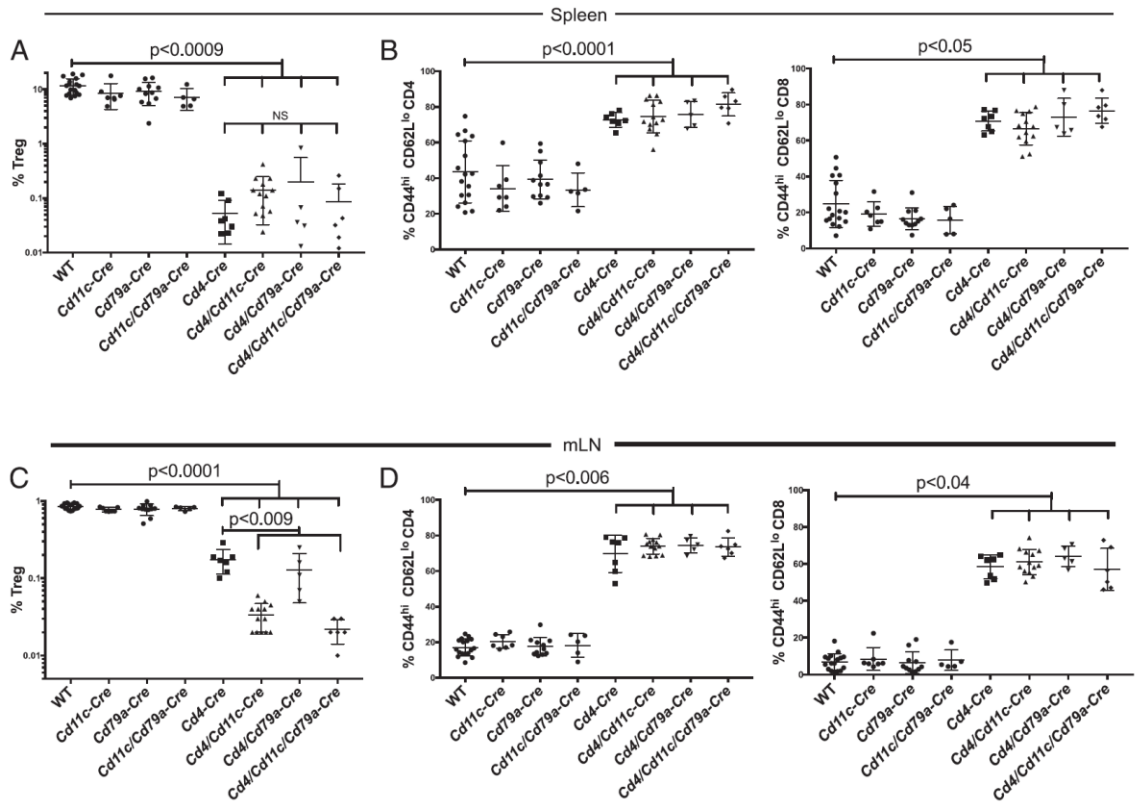

Figure 2.7. T cell-derived IL-2 is critical for T_{reg} cell homeostasis. **a,b)** Quantification of the % ($CD25^{+}FOXP3^{+}$) T_{reg} in the spleen (a) and % of activated/effector CD4 (left panel) or CD8 (right panel) T cells in the spleen (b). **c,d)** Quantification of the % ($CD25^{+}FOXP3^{+}$) T_{reg} cells in mesenteric lymph nodes, log_{10} transformed data, (c) and % of activated/effector CD4 (left panel) or CD8 (right panel) (d). Data is representative of 9 experiments, n=17 mice (Wildtype), 4 experiments, n=7 mice (*Cd11c-Cre*), 6 experiments, n=11 mice (*Cd79a-Cre*), 4 experiments, n=5 mice (*Cd11c-Cre x CDd79a-Cre*), 2 experiments, n=7 mice (*Cd4-Cre*), 6 experiments, n=13 mice (*Cd4-Cre x Cd11c-Cre*), 2 experiments, n=5 mice (*Cd4-Cre x Cd79a-Cre*), 4 experiments, n=6 mice (*Cd4-Cre x Cd11c-Cre x Cd79a-Cre*). Data was analyzed by Kruskal-Wallis (a) and one-way ANOVA (b-d). Wildtype and *Cd4-Cre x* $Il2^{FL/FL}$ *x* $Il15^{-/-}$ data points are identical for Fig. 2.3 c,d and Fig. 2.6 a,b.

T cell–derived IL-2 is important for maintaining resting T_{reg} cells

Resting or central T_{reg} (cT_{reg}) cells are specifically dependent on IL-2 for maintenance[213]. Given this dependence, we quantified the proportion of T_{reg} cells that were phenotypically effector (effector T_{reg} (eT_{reg}); $CD44^{hi}$ $CD62L^{lo}$) or central (cT_{reg}; $CD44^{lo}CD62L^{hi}$) T_{reg} cells in mice lacking IL-2 in DCs, B cells, or T cells. In *Cd11c-Cre* x $Il2^{fl/fl}$ x $Il15^{-/-}$, *Cd79a-Cre* x $Il2^{fl/fl}$ x $Il15^{-/-}$, or *Cd11c-Cre* x *Cd79a-Cre* x $Il2^{fl/fl}$ x $Il15^{-/-}$ mice, which lack IL-2 in B cells, DCs, or both these cell subsets, there was no change in the relative percentages of splenic or mesenteric eT_{reg} and cT_{reg} cells (Figure 2.8 a). In contrast, when IL-2 was lost in the T cell compartment in *Cd4-Cre* x $Il2^{fl/fl}$ x $Il15^{-/-}$ mice, the proportion of T_{reg} cells that were eT_{reg} cells versus cT_{reg} cells is significantly altered, with increased percentages of eT_{reg} cells and decreased percentages of cT_{reg} cells in the spleen and mesenteric lymph node (Figure 2.8 b). These results again highlight an important role for T cell–derived IL-2 in T_{reg} cell phenotype and directly demonstrate that cT_{reg} cells are dependent on T cell–derived IL-2. However, we cannot determine if this phenotypic shift is due to IL-2 availability or the increase in inflammation and effector T cell activation.

2.3 Discussion

The cellular sources of IL-2 important for T_{reg} cell development and homeostasis have been a controversial issue for some time. For example, work from the Germain laboratory using intravital imaging observed clustering of pSTAT5+ T_{reg} cells around activated effector T cells producing IL-2, supporting a role for T cell– derived IL-2 in T_{reg} cell homeostasis or function in peripheral lymphoid organs[214]. Likewise, work by Sakaguchi and colleagues[199] also supported a role for T cell–derived IL-2 in T_{reg} cell homeostasis. Conversely, work from the Robey laboratory showed a dependence on DC-derived IL-2 for optimal T_{reg} cell differentiation in thymic slices[142]. In this study, we

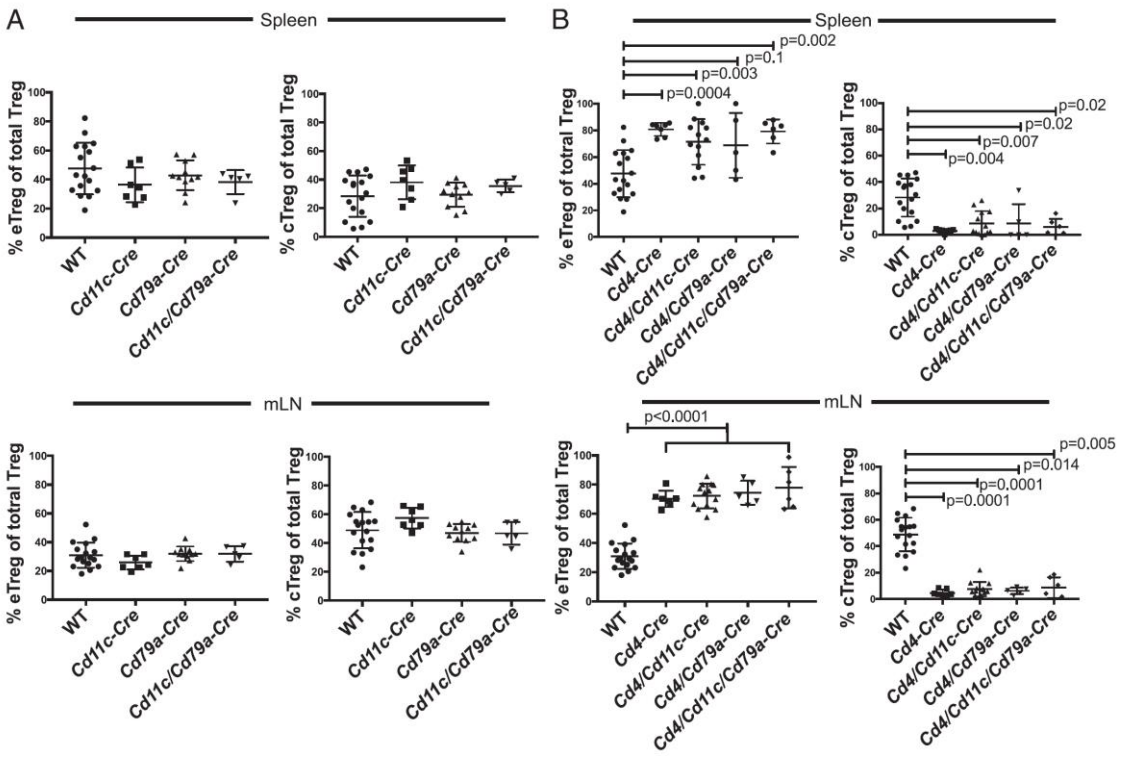

Figure 2.8. T cell-derived IL-2 is important in maintaining resting T_{reg} cells. **a,b)** Quantification of the % of ($CD25^{+}FOXP3^{+}$) T_{reg} cells in the indicated CRE+ mice which are the eT_{reg} (left) or cT_{reg} (right) phenotype in the spleen (top) or mesenteric lymph node (bottom)**.** Data is representative of 9 experiments, n=17 mice (Wildtype), 4 experiments, n=7 mice (*Cd11c-Cre*), 6 experiments, n=11 mice (*Cd79a-Cre*), 4 experiments, n=5 mice (*Cd11c-Cre x CDd79a-Cre*), 2 experiments, n=7 mice (*Cd4-Cre*), 6 experiments, n=13 mice (*Cd4-Cre x Cd11c-Cre*), 2 experiments, n=5 mice (*Cd4-Cre x Cd79a-Cre*), 4 experiments, n=6 mice (*Cd4-Cre x Cd11c-Cre x Cd79a-Cre*). Data was analyzed by one-way ANOVA (a. cT_{reg} spleen, eT_{reg} mLN, cT_{reg} mLN; b. eT_{reg} spleen, eT_{reg} mLN) or Kruskal-Wallis (a. eT_{reg} spleen; b. cT_{reg} spleen, cT_{reg} mLN). Wildtype data points are the same for individual conditions in a and b.

provide direct evidence that production of IL-2 from T cells is critical for T_{reg} cell development, homeostasis, and function in vivo. In the absence of T cell–derived IL-2, there is a significant defect in T_{reg} cell development in the thymus (when IL-15 is absent) and a dramatic reduction in T_{reg} cells in peripheral lymphoid tissues. T_{reg} cell development in the thymus is initiated by relatively strong TCR signals[66,71,77]. Indeed, we found that this signal is perhaps also the driver of IL-2 production, as the source of IL-2 was immature $CD25^+$ $T_{reg}P$ cells receiving strong TCR stimulation signals. It is possible that these cells undergoing agonist selection are the major source of IL-2 required for IL-2–dependent T_{reg} cell development. In agreement with this, a recent study found that self-reactive thymocytes, but not mature T cells, are the major source of IL-2 in the thymus[145]. However, we currently cannot exclude the possibility that recirculating effector T cells produce some IL-2 that contributes to T_{reg} cell development. Despite these observations, our studies with mixed bone marrow chimeras demonstrate that bystander T cell production of IL-2 is sufficient to drive T_{reg} cell differentiation in the thymus. This suggests that nearby activated self-reactive thymocytes produce the IL-2 needed for T_{reg} cell development and autocrine IL-2 signaling is not essential. An intriguing possibility is that this process may be enhanced by the selective expression of CD25 on thymic DCs and mTECs, which may allow for trans-presentation of IL-2 to developing T_{reg} cells or increasing local IL-2 concentrations by reducing IL-2 diffusion. IL-2 trans-presentation is a proposed mechanism for peripheral DC to promote T cell responses but has not yet been described in thymic T_{reg} cell selection[186]. Finally, although DCs and B cells in the thymus are potential sources of IL-2 that could contribute to T_{reg} cell development, we found that they are neither necessary (as T_{reg} cells develop normally in the absence of DC- and B cell–derived IL-2) nor sufficient (as the T_{reg} cell defect is just as severe when IL-2 is deleted in T cells as when it is deleted in all cells). This is consistent with the observation that $CD4^+$ and

$CD8^+$ thymocytes appeared to produce much more IL-2 than stimulated thymic DCs. Thus, the only critical cellular source of IL-2 needed for T_{reg} cell development in the thymus appears to be T cells. Our work also points to a key role for T cell–derived IL-2 on T_{reg} cell homeostasis and function in the spleen and inguinal lymph nodes. In these organs, T cell–derived IL-2 appears to be both necessary and sufficient to maintain normal proportions of T_{reg} cells and their function, as effector T cell activation was only seen in these organs when *Il2* was selectively deleted from T cells. Additional deletion of *Il2* in DCs and/or B cells did not result in a further reduction in T_{reg} cells in these peripheral lymphoid tissues or affect effector T cell activation, demonstrating that DC- and B cell–derived IL-2 does not influence T_{reg} cell homeostasis or function in these organs. In contrast, we saw a somewhat different effect when examining mesenteric lymph nodes. Loss of T cell–derived IL-2 led to a clear reduction in T_{reg} cells and a concomitant induction of effector T cell activation that was further exacerbated by loss of DC derived IL-2 but not by loss of B cell derived IL-2. This suggests that DC production of IL-2 contributes to T_{reg} cell maintenance in this mucosal-associated tissue. Our findings point to a more general role for DC-derived IL-2 at mucosal interfaces in promoting T_{reg} cell homeostasis. Alternatively, our results are also consistent with the possibility that DC-derived IL-2 is specifically required to maintain a unique subset of T_{reg} cells only found at these locations. Consistent with previous reports[213], loss of T cell– derived IL-2 led to an almost total loss of the cT_{reg} cell phenotype, as the majority of remaining T_{reg} cells were eT_{reg} cells. This supports the importance of IL-2 in maintaining cT_{reg} cells, whereas eT_{reg} cells can likely be supported by factors other than IL-2 such as ICOS[213].

Although our work demonstrates a critical dependence on T cell–derived IL-2 for T_{reg} cell development and homeostasis, it is important to note that these studies focused on the thymus and secondary lymphoid organs. Further investigation will be required to

understand if distinct paradigms of IL-2 cellular production and importance exist in unique lymphoid environments, such as the mesenteric lymph node, or in nonlymphoid tissues, like the large and small intestine, where T cells are not as abundant as in lymphoid tissues. Our observations that DC-derived IL-2 contributes to T_{reg} cell homeostasis in the mesenteric lymph node, but not in the spleen or inguinal lymph nodes, is one such example in which different cell types are required to produce IL-2 needed for optimal T_{reg} cell homeostasis in distinct microenvironments. A recent study utilized *Ncr1-Cre* x *Il2*$^{fl/fl}$ mice to knockout *Il2* in ILC3 cells. ILC3 produced IL-2 is required to preserve normal numbers of intestinal T_{reg} cells and reduced production of IL-2 by ILC3 cells is correlated with Crohn's disease[215]. Other cell type–specific knockouts of IL-2 and/or inducible *Il2* deletion will provide insight into the cellular partners of T_{reg} cells required for maintaining immune tolerance in both lymphoid and non-lymphoid tissues.

Chapter 3. Development of regulatory T cells in the thymus from two distinct developmental pathways

*Portions of this chapter are derived from an article written by the author[96]

3.1 Background

Regulatory T cells (T_{reg} cells) play key roles in protecting against autoimmune responses to tissues, preventing inappropriate responses to commensal organisms and dampening effector T cell responses following clearance of pathogens. However, the mechanisms leading to the development of a population of T_{reg} cells that can mediate such diverse functions remain unclear. T_{reg} cells develop through a two-step process in the thymus[63,64]. The first step is driven by strong signals sent through the T cell antigen receptor (TCR), which leads to upregulation of CD25, the key component of the high-affinity receptor for the cytokine IL-2, as well as the tumor necrosis factor (TNF) receptor superfamily members GITR, OX40 and TNFR2, but not to upregulation of the transcription factor FOXP3[63,66]. A second, TCR-independent step involves the conversion of $CD25^+$ T_{reg}P cells into mature $CD25^+FOXP3^+$ T_{reg} cells in a manner dependent on IL-2 and the transcription factor STAT5[63,64,132,137]. A distinct T_{reg} cell progenitor population, characterized by low expression of FOXP3 and lacking detectable expression of CD25, was also described in the thymus[65]. This $FOXP3^{lo}$ T_{reg}P cell shows high expression of GITR and OX40[66] and can differentiate into mature $CD25^+FOXP3^+$ T_{reg} cells following stimulation with IL-2[65]. The relative contributions of these T_{reg}P cell populations to the mature T_{reg} cell pool remain controversial.

Here we demonstrate that $CD25^+$ T_{reg}P cells and $FOXP3^{lo}$ T_{reg}P cells generated mature T_{reg} cells with relatively comparable efficiency both *in vitro* and *in vivo*. The two developmental pathways for T_{reg} cell generation differed in many aspects, including

distinct transcriptomes and TCR repertoires. $CD25^+$ $T_{reg}P$ cells exhibited increased apoptosis, developed into mature T_{reg} cells with faster kinetics and exhibited greater reactivity with self-antigens in the thymus than $FOXP3^{lo}$ $T_{reg}P$ cells. Development of the two T_{reg} cell progenitor subsets is controlled in the thymus by different cytokines, signaling pathways, gene enhancers and stromal cells. Finally, T_{reg} cells derived from $CD25^+$ $T_{reg}P$ cells, but not those derived from $FOXP3^{lo}$ $T_{reg}P$ cells, protected against experimental autoimmune encephalomyelitis (EAE). Our data suggest a model in which two distinct T_{reg} cell progenitor subsets both contribute to generate a broad T_{reg} cell repertoire able to protect against immune responses to self-antigens, limit immune responses to commensal organisms and resolve immune responses to foreign pathogens.

3.2 Results

$CD25^+$ and $FOXP3^{lo}$ $T_{reg}P$ cells differentiate into T_{reg} cells

To determine whether $CD25^+$ $T_{reg}P$ cells and $FOXP3^{lo}$ $T_{reg}P$ cells are both bona fide thymic T_{reg} cell progenitors, we compared their ability to convert into mature T_{reg} cells in response to low doses of IL-2 for 3 days in vitro[216]. Sorted $CD25^+$ $T_{reg}P$ cells and $FOXP3^{lo}$ $T_{reg}P$ cells responded to very low amounts of IL-2 (0.2–1.0 U ml^{-1}) by converting to mature $CD25^+FOXP3^+$ T_{reg} cells (Figure 3.1 a), indicating that although they lack CD25 expression, $FOXP3^{lo}$ $T_{reg}P$ cells, which express the low-affinity IL-2R consisting of the chains IL-2Rβ and IL-2Rγ, are responsive to IL-2. Mature $CD25^+FOXP3^+$ T_{reg} cells exhibited even greater sensitivity to IL-2, as they maintained their phenotype and viability at concentrations of IL-2 (0.04 U ml^{-1}) to which $CD25^+$ $T_{reg}P$ cells and $FOXP3^{lo}$ $T_{reg}P$ cells did not respond (Figure 3.1 a). To confirm these findings *in vivo*, we used ultrasound-guided intrathymic injection[217] to co-transfer sorted, congenically distinct

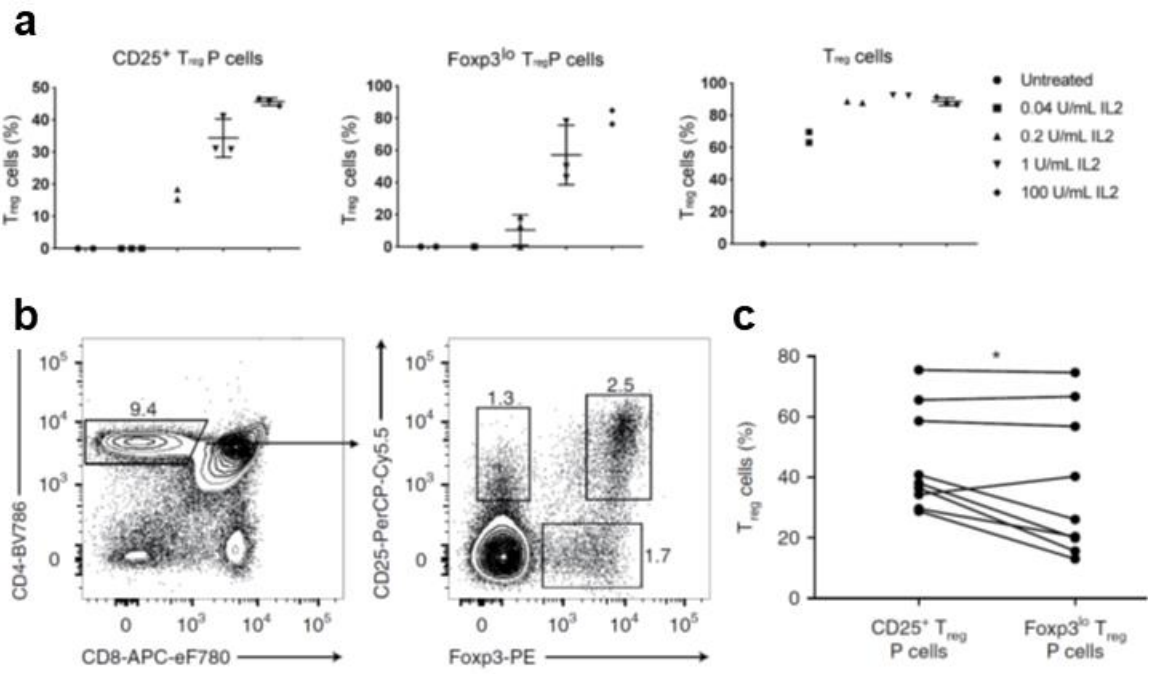

Figure 3.1. Two thymic T_{reg} progenitor cell populations exist. **a)** Sorted T_{reg} cell lineage subsets were stimulated for 3 days in the indicated concentrations of IL-2 and analyzed for the % of cells which converted into (left and middle panel) or remained (right panel) $CD25^+FOXP3^+$ mature T_{reg} cells. Data represents 1 experiment, *n* = 2 ($CD25^+$ T_{reg}P cells- untreated, 0.2 U/ml IL-2; $FOXP3^{lo}$ T_{reg}P cells- untreated, 100 U/ml IL-2; T_{reg} cells- 0.04 U/ml IL-2, 0.2 U/ml IL-2, 1 U/ml IL-2), *n* = 1 ($FOXP3^{lo}$ T_{reg}P cells- 0.04 U/ml IL-2; T_{reg} cells- untreated), *n* = 3 ($CD25^+$ T_{reg}P cells- 0.04 U/ml IL-2, 1 U/ml IL-2, 100 U/ml IL-2; $FOXP3^{lo}$ T_{reg}P cells- 0.2 U/ml IL-2, 1 U/ml IL-2; T_{reg} cells- 100 U/ml IL-2) technical replicates. Bars represent mean ± SD. **b)** Gating scheme used throughout this paper to quantify or isolate $CD25^+FOXP3^-$ and $CD25^-$ $FOXP3^{lo}$ T_{reg}P cell populations. **c)** Quantification of the proportion of sorted, congenically distinct (CD90.2+CD45.2+ or CD90.1+CD45.2+) $CD25^+$ and $FOXP3^{lo}$ T_{reg}P cells, co-injected into the thymus of CD45.1+ mice, that differentiated into $CD25^+FOXP3^+$ T_{reg} cells 6 days post-injection. Each dot represents a single recipient mouse; pairing represents data within the same recipient thymi. Data represent three

independent experiments, n = 9 mice. Data were analyzed by a two-sided paired t-test, *P < 0.05.

(CD90.2$^+$CD45.2$^+$ or CD90.1$^+$CD45.2$^+$) CD25$^+$ or FOXP3^{lo} T_{reg}P cells into the thymus of CD45.1$^+$ mice (Figure 3.1 b). Six days post-injection, CD25$^+$ T_{reg}P cells and FOXP3^{lo} T_{reg}P cells converted into mature CD25$^+$FOXP3$^+$ T_{reg} cells at approximately the same frequency, although CD25$^+$ T_{reg}P cells did so slightly more efficiently (~45% ± 16.9% and 37% ± 23.5%, respectively; Figure 3.1c). Thus, both CD25$^+$ T_{reg}P cells and FOXP3^{lo} T_{reg}P cells contributed to the generation of mature T_{reg} cells with high efficiency both in vitro and in vivo.

CD25$^+$ T_{reg}P cells and FOXP3^{lo} T_{reg}P cells have distinct TCR repertoires

To address whether CD25$^+$ T_{reg}P cells and FOXP3^{lo} T_{reg}P cells represent distinct subsets of cells with different TCR repertoires, or whether the T_{reg} cell developmental pathway chosen reflects only the stochastic expression of CD25 or FOXP3, we used mice expressing a fixed TCliβ *Tcrb* transgene, to reduce TCR diversity by fixing the TCRβ chain, on a *Tcra*$^{+/-}$ heterozygous background, to eliminate dual TCR expressing cells, expressing a *Foxp3*^{RFP} Foxp3–red fluorescent protein reporter[71,218,219]. Using these mice, we carried out high-throughput sequencing of the TCR *Trav14* genes in conventional CD25$^-$FOXP3$^-$ thymocytes, CD25$^+$ T_{reg}P cells, FOXP3^{lo} T_{reg}P cells and mature CD25$^+$FOXP3$^+$ T_{reg} cells. Consistent with previously published results[71,72,220], we found little overlap between the *Trav14* repertoire of conventional CD25$^-$FOXP3$^-$ thymocytes and mature thymic CD25$^+$FOXP3$^+$ T_{reg} cells (Figure 3.2 a). As reported[63], we found substantial overlap between the TRAV14 repertoire of CD25$^+$ T_{reg}P cells and that of mature CD25$^+$FOXP3$^+$ T_{reg} cells (Figure 3.2 a,b). Importantly, the TCR repertoire of FOXP3^{lo} T_{reg}P cells also overlapped substantially with that of mature CD25$^+$FOXP3$^+$ T_{reg} cells (Figure 3.2 a,b). However, TCR repertoires of the CD25$^+$ T_{reg}P and FOXP3^{lo} T_{reg}P cell populations showed very little overlap, despite their substantial

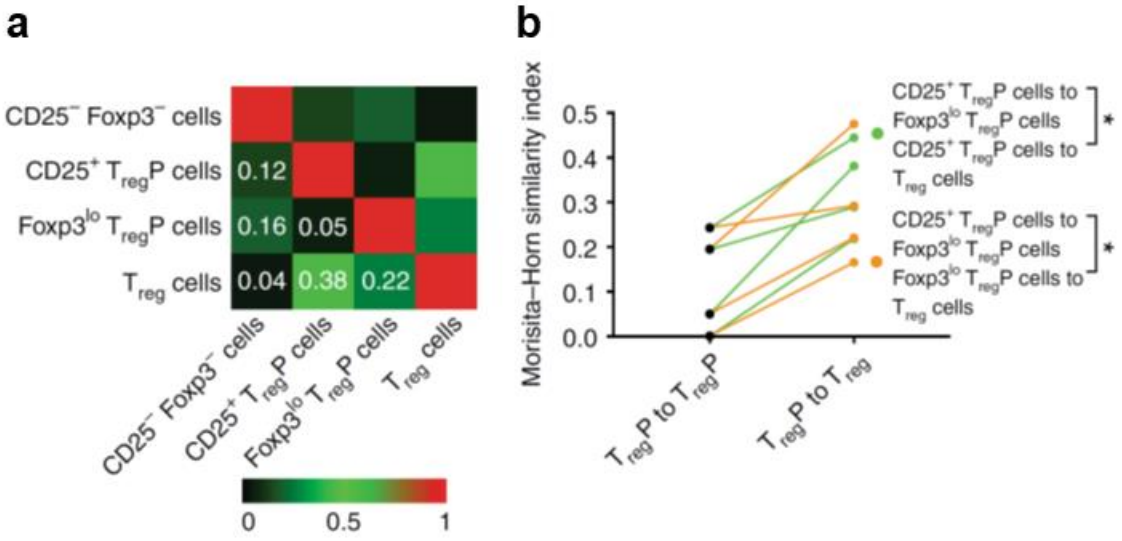

c

	Ratio of Morisita-Horn indices for all TCRs	Ratio of Morisita-Horn indices for T_{reg} restricted TCRs	p-value
$CD25^+T_{reg}P$:$Foxp3^{lo}T_{reg}P$ to $CD25^+$ $T_{reg}P$: T_{reg}	0.31±0.29	0.44±0.37	p>0.2
$CD25^+T_{reg}P$:$Foxp3^{lo}T_{reg}P$ to $Foxp3^{lo}$ $T_{reg}P$: T_{reg}	0.35±0.35	0.41±0.36	p>0.2

Figure 3.2. $CD25^+$ $T_{reg}P$ cells and $FOXP3^{lo}$ $T_{reg}P$ cells have distinct TCR repertoires. **a)** Morisita–Horn indices comparing the similarity of Vα2 CDR3 repertoires generated by TCR sequencing of CD4+$CD25^-$ $FOXP3^-$ cells, $CD4^+CD25^+Foxp3^-$ $T_{reg}P$ cells, $CD4^+CD25^-$ $FOXP3^{lo}$ $T_{reg}P$ cells and $CD4^+CD25^+Foxp3^+$ mature T_{reg} cells isolated from $Tcli\beta^+$ x *Tcra*$^{+/-}$ mice. **b)** Plot of Morisita–Horn similarity indices comparing TCRs between $CD25^+$ and $FOXP3^{lo}$ $T_{reg}P$ cell populations, and TCRs in $CD25^+$ $T_{reg}P$ cells and mature T_{reg} cells or $FOXP3^{lo}$ $T_{reg}P$ cells and mature T_{reg} cells. $CD25^+$ $T_{reg}P$ cell comparisons are shown in green and $FOXP3^{lo}$ $T_{reg}P$ cell comparisons in orange. Data represent two independent experiments, *n* = 4 mice. Data were analyzed by a two-sided paired *t*-test. **c)** Shown are the ratios of the Morisita –Horn indices for $CD25^+$ $T_{reg}P$:$FOXP3^{lo}T_{reg}P$ to $CD25^+$ $T_{reg}P$ cells:mature T_{reg} cells (top) or $FOXP3^{lo}$ $T_{reg}P$:mature T_{reg} cells (bottom) when analysis is based on all sequenced TCR sequences (left) or when restricting analysis to only TCRs

that were found in mature $CD25^{+}FOXP3^{+}$ T_{reg} cells (right). p-values calculated using two-sided t-test.

individual overlap with the repertoire of mature T_{reg} cells (Figure 3.2 a,b). To confine our analysis to TCRs that are known to be represented in the mature T_{reg} cell pool, we re-analyzed our TCR repertoire data but this time excluding all TCRs not detected in the thymic mature T_{reg} cell pool. The ratios of Morisita–Horn indices (T_{reg}P cell:T_{reg}P cell vs T_{reg}P cell:T_{reg} cell) calculated using TCRs detected only in mature CD25$^+$FOXP3$^+$ T_{reg} cells in the thymus are not significantly different from those obtained using all TCRs (Figure 3.2 c). Thus, CD25$^+$ T_{reg}P cells and FOXP3^{lo} T_{reg}P cells have distinct TCR repertoires and contribute unique TCR clones to the mature T_{reg} cell repertoire.

CD25$^+$ T_{reg}P cells and FOXP3^{lo} T_{reg}P cells have distinct affinity for self-antigen

Next, we examined the types of antigens with which CD25$^+$ T_{reg}P cells and FOXP3^{lo} T_{reg}P cells interacted. The relative abundance of either T_{reg}P cell subset germ-free mice was similar to that in specific-pathogen-free mice (Figure 3.3 a,b) or in C57Bl/6 mice co-housed with pet-store mice, which have a normalized microbial experience[221] compared with that of specific-pathogen-free mice (Figure 3.3 c), suggesting that interactions with self-antigens are the major driver of T_{reg} cell selection in the thymus. We used expression of the transcription factor NUR77, whose abundance is directly proportional to TCR signal strength, to assess the strength of the interaction of CD25$^+$ T_{reg}P cells and FOXP3^{lo} T_{reg}P cells with self-antigens in the thymus. In *Nur77-GFP* mice, in which green fluorescent protein (GFP) expression correlates with the strength of TCR stimulation[77], mature CD25$^+$FOXP3$^+$ T_{reg} cells show higher expression of NUR77-GFP than that of conventional CD4$^+$FOXP3$^-$ T cells[66,77], corresponding with the higher degree of self-reactivity attributed to T_{reg} cells[71]. In this system, expression of NUR77-GFP in CD25$^+$ T_{reg}P cells is significantly higher than that recorded in mature T_{reg} cells (Figure 3.4 a,b), while its expression in FOXP3^{lo} T_{reg}P cells was significantly lower than that of CD25$^+$ T_{reg}P cells (Figure 3.4 a,b). These findings indicate that

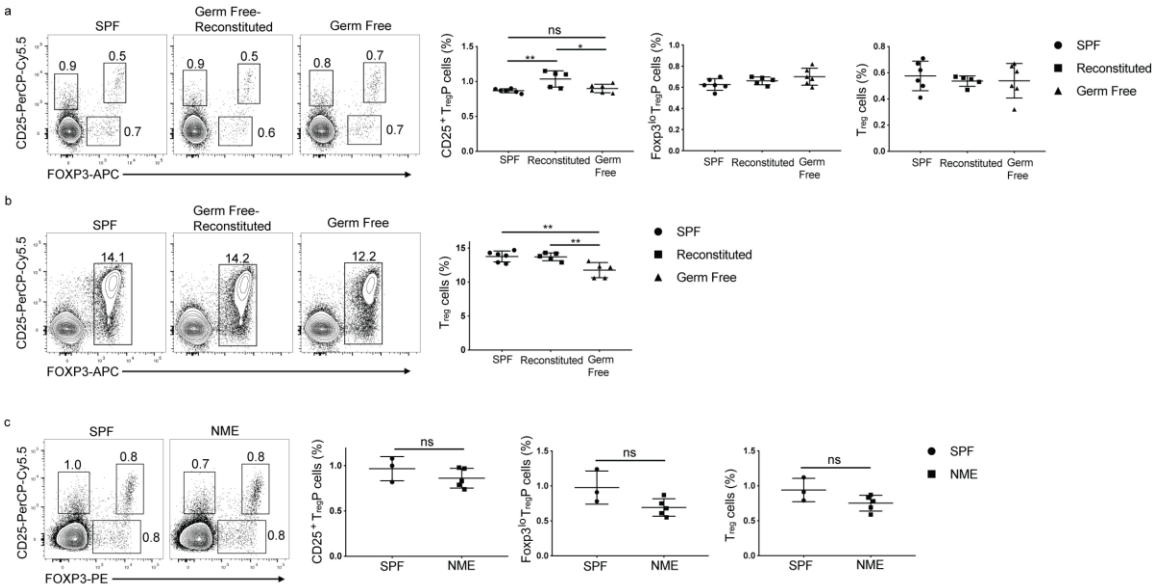

Figure 3.3. Germ-free and NME mice show no defect in either thymic $T_{reg}P$ cell pathway. **a)** Representative flow plots of SPF, germ-free reconstituted and germ-free mice thymi and quantification of the percent of each T_{reg} cell lineage subset within $CD4^+CD73^-$ thymocytes. **b)** Representative flow plots and quantification of SPF, germ-free reconstituted and germ-free mice spleens showing the percent of $CD4^+$ lymphocytes which are $FOXP3^+$. a,b) Data is representative of 1 experiment, *n* = 6 SPF mice, 5 germ-free reconstituted mice, and 6 germ-free mice. Data was analyzed by one-way ANOVA with Tukey's multiple comparisons test. **c)** Representative flow plots of $CD4^+CD73^-$ thymocytes from SPF mice or mice with normalized microbial experience (NME) and quantification of the percent within each T_{reg} cell lineage population. Data is representative of 2 experiments, *n* = 3 SPF mice and 5 NME mice. Data was analyzed by two-sided unpaired *t* test. All bars represent mean ± SD. *P<0.05, **P<0.005, ns- not significant.

$CD25^+$ $T_{reg}P$ cells and $FOXP3^{lo}$ $T_{reg}P$ cells have a distinct affinity for self-antigens in the thymus.

We next assessed transcriptomic differences between $T_{reg}P$ cell subsets using single-cell RNA sequencing (RNA-seq). $CD25^+$ $T_{reg}P$ cells, $FOXP3^{lo}$ $T_{reg}P$ cells and mature $CD25^+FOXP3^+$ T_{reg} cells, sorted from the thymus of *Foxp3*-GFP mice, in which an IRES–GFP construct was knocked into the 3' untranslated region of the *Foxp3* gene, were used to create individual single-cell RNA-seq libraries that were subjected to high-throughput sequencing. The transcriptomic data from these individual libraries were then combined for joint analysis. Individual cells were color-coded based on sort origin, and a combined dimensional reduction with a graph-based clustering approach followed by a shared nearest-neighbor modularity optimization-based clustering algorithm (Seurat R package) was then applied to this combined dataset to identify cell groups with distinct gene expression. This analysis generated clusters of cells that closely confirmed the original sorted populations (Figure 3.4 c) based on expression of *Il2ra* and *Foxp3* (Figure 3.5 a). The analysis also identified a small subset of contaminating thymocytes that expressed *Rag1*, *Cd8b1* and *Dntt* and therefore likely represented $CD4^+CD8^+$ double-positive thymocytes (Figure 3.4 c,d). Heatmaps based on the top ten most differentially expressed genes for each cell subset discriminated all four cell clusters (Figure 3.4 d). Analysis of differentially expressed genes indicated that there are ~180 reproducibly differentially expressed genes between $CD25^+$ and $FOXP3^{lo}$ $T_{reg}P$ cell subsets (Table 3.1). Similar results were obtained in an independent single-cell RNA-seq study with individually sorted $CD25^+$ $T_{reg}P$ cell, $FOXP3^{lo}$ $T_{reg}P$ cell and mature T_{reg} cell libraries (Figure 3.5 b). $CD25^+$ $T_{reg}P$ cells were enriched in pro-apoptotic genes and genes involved in negative selection (*Nr4a1* and *Bcl2l11*) (Figure 3.5 c), consistent with stronger TCR signaling in this subset. $FOXP3^{lo}$ $T_{reg}P$ cells showed increased expression

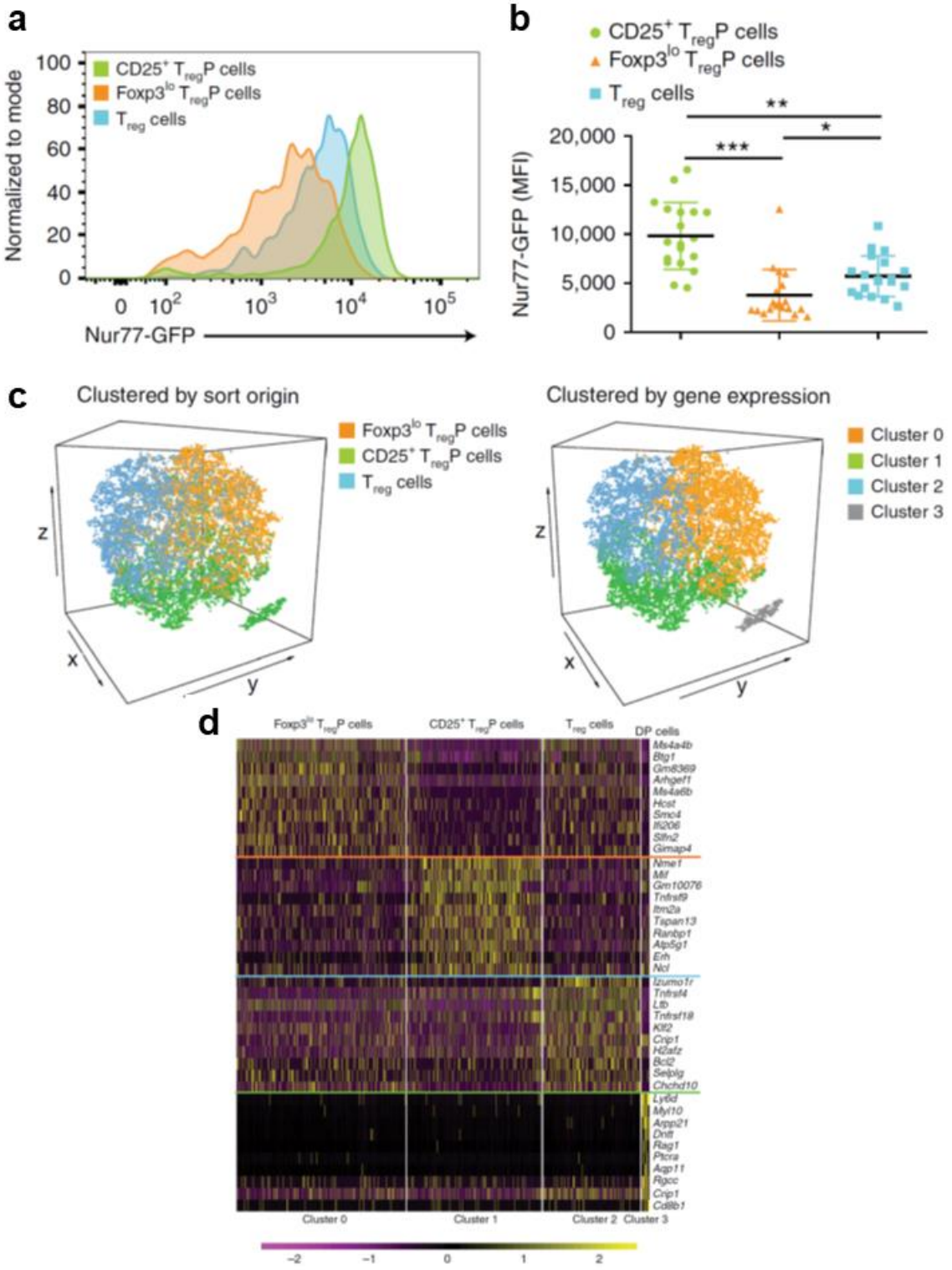

Figure 3.4. CD25^{+} T_{reg}P and FOXP3^{lo} T_{reg}P cells are distinct T_{reg}P populations. **a,b)** Flow cytometry analysis of NUR77-GFP MFI in CD25^{+}FOXP3^{-} T_{reg}P cells, CD25^{-}FOXP3^{lo} T_{reg}P

cells and $CD25^+FOXP3^+$ mature T_{reg} cells obtained from the thymus of NUR77-GFP reporter mice. Dots represent individual mice. Data are displayed as mean ± s.d. and represent seven independent experiments, *n* = 19 mice. Data were analyzed using a two-sided paired Friedman test with Dunn's multiple comparisons test. **c)** Left: Three-dimensional (3D) nonlinear dimensional reduction (tSNE) plots from 10X Genomics scRNA-seq dataset for sorted $CD25^+$ T_{reg}P cells, $FOXP3^{lo}$ T_{reg}P cells and $CD25^+FOXP3^+$ T_{reg} cells, displaying relationships between individual cells with color coding based on flow cytometry sort origin. Right: 3D tSNE plots of data identical to those at left but color-coded based on gene expression profiles. **d)** Heatmap of the top ten differentially regulated genes from each cluster derived from c. Each column represents gene expression for an individual cell; yellow is up and purple is down. Data from c,d are representative of three independent experiments, *n* = 3 mice. **P* < 0.05, ***P* < 0.0005, ****P* < 0.0001. DP, double-positive thymocyte; MFI, mean fluorescence intensity.

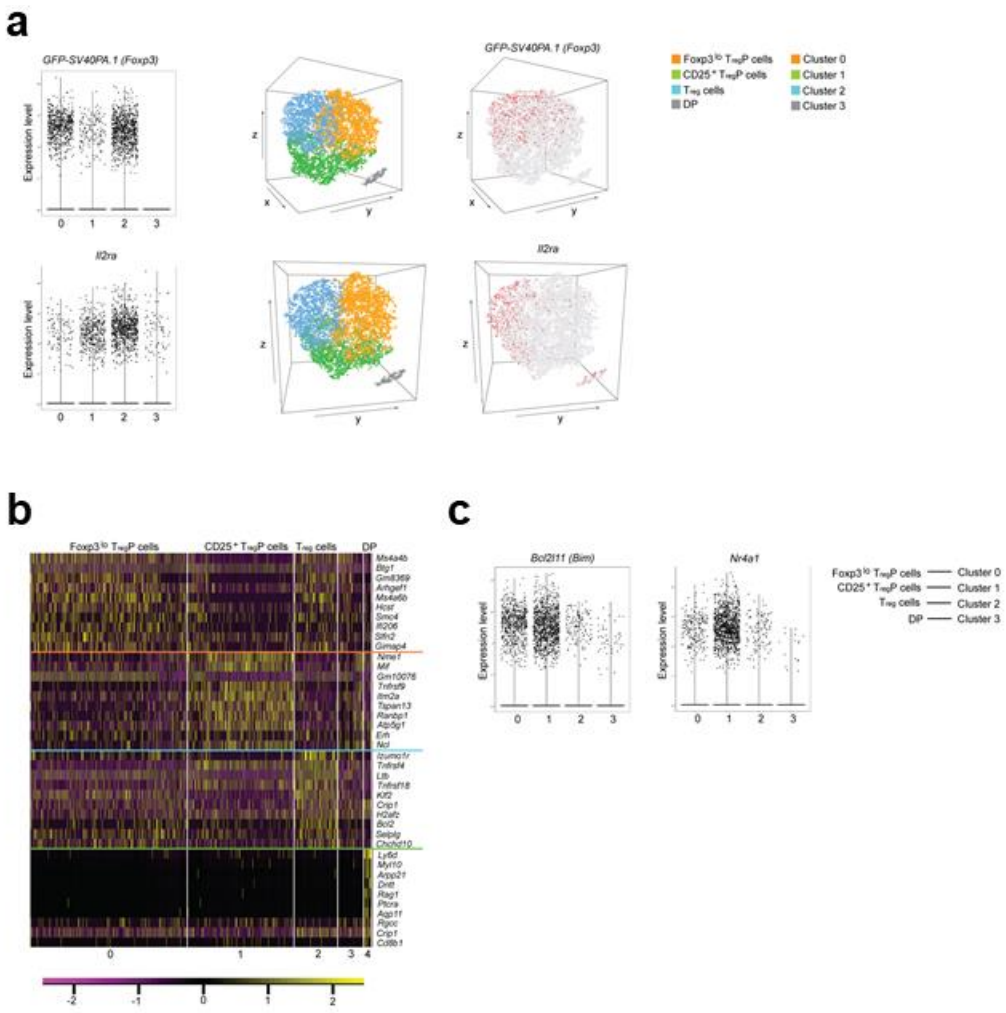

Figure 3.5. Single-cell RNA-seq of thymic T_{reg} cell lineage. **a)** Violin plots (left) or feature plots (right) displaying single-cell expression for either *Foxp3-GFP* reporter (top) or *Il2ra* (bottom) for each cluster from the scRNAseq data set presented in Fig. 3.4 c,d. **b)** Data from an independent repeat of 10X Genomics scRNAseq. Heatmap displays the top 10 differentially regulated genes in each cluster from the data set presented in Fig. 3.4 c,d. **c)** Violin plots displaying single-cell expression for *Bcl2l11* (left) and *Nr4a1* (right) for each cluster from the scRNAseq data set presented in Fig. 3.4 c,d. a-c) Data is representative from 3 independent experiments, *n* = 3 mice.

of *Ms4a4b* and *Ms4a6b* (Figure 3.4 d) encoding MS4A4B and MS4A6B, which bind to GITR and enhance signaling via TCR and GITR[222] and may facilitate differentiation of lower-affinity $CD4^+$ thymocytes into $FOXP3^{lo}$ $T_{reg}P$ cells and enhance the sensitivity of $FOXP3^{lo}$ $T_{reg}P$ cells to IL-2[66]. Thus, $CD25^+$ $T_{reg}P$ cells and $FOXP3^{lo}$ $T_{reg}P$ cells have distinct interactions with self-antigens present in the thymus and unique transcriptomes indicative of distinct modes of selection and differentiation.

$CD25^+$ $T_{reg}P$ cells and $FOXP3^{lo}$ $T_{reg}P$ cells are at distinct developmental stages

The cell surface markers CD24 and Qa2, or CD69 and MHCI, can be used as surrogates to analyze thymocyte age[223]. We found that $CD25^+$ $T_{reg}P$ cells were largely $CD24^{hi}Qa2^{lo}$ (87%) and $CD69^{hi}$ $MHC1^+$, and thus representative of immature $CD4^+$ thymocytes. In contrast, only 38% of $FOXP3^{lo}$ $T_{reg}P$ cells were found in the $CD24^{hi}Qa2^{lo}$ gate with the remainder being $CD24^{lo}Qa2^{hi}$, indicative of a more mature stage of thymocyte development (Figure 3.6 a,b). To examine this issue more precisely, we used *Rag2*-GFP transgenic mice, in which GFP expression is controlled by *Rag2* gene-regulatory elements, to determine the kinetics of differentiation for $CD25^+$ $T_{reg}P$ cells and $FOXP3^{lo}$ $T_{reg}P$ cells. The *Rag2*-GFP transgene turns off after positive selection in $CD4^+CD8^+$ thymocytes, after which the GFP protein decays with a relatively slow half-life, allowing GFP^+ recent thymic emigrants to be distinguished from older GFP^- T cells in peripheral blood and lymphoid organs[224]. We reasoned that the gradient of RAG2-GFP signal among $CD4^+$ single-positive (CD4SP) thymocytes could be used to distinguish thymocytes at different stages of development. For these studies, we took bins from RAG2-GFP^{bight} (youngest CD4SP) to RAG2-GFP^{dim} (oldest CD4SP) and examined expression of CD25 and FOXP3. RAG2-$GFP^{brightest}$ cells (bin 1) were all $CD25^-$ $FOXP3^-$ CD4SP thymocytes (Figure 3.7 a). $CD25^+$ $T_{reg}P$ cells, but not

Nme1	**Ptma**	**Nhp2**	**Cox5a**	**Bola2**	**Gimap6**	**Sumo2**	**Cyba**	**Llph**
Mif	**Ppia**	**Usmg5**	**Itm2b**	**Psmb6**	**Eif5b**	**Romo1**	**Psme2**	**Nfkbia**
Tnfrsf4	**Pfn1**	**Ndufa12**	**Atp5k**	**U2af1**	**Ptpn18**	**Atp5d**	**Aldoa**	**Cd200**
Gm10076	**Rps2**	**Ypel3**	**Rgs10**	**Timm13**	**2010107E04Rik**	**Ndufc1**	**Metap2**	**Cd53**
Tnfrsf9	**Rps14**	**mt-Nd1**	**Rbm3**	**Ndufa5**	**Klf2**	**Slfn2**	**Pomp**	**Psma2**
Ranbp1	**Rpl18a**	**Nop10**	**Cox7a2l**	**Hmgn1**	**Phb2**	**Serp1**	**Gm9493**	**Mrps24**
Tspan13	**Rps27**	**Rps27l**	**Atp5b**	**Npm3**	**Cox7b**	**Psmb3**	**Ndufs5**	**Atp5a1**
Atp5g1	**Rps15a**	**Eif4a1**	**Gapdh**	**Prdx2**	**Fxyd5**	**Gimap1**	**Psmb5**	**Cdk2ap2**
Itm2a	**Fau**	**Hnrnpa1**	**Psma7**	**Hcst**	**Mbnl1**	**Gm11808**	**Ndufb4**	**Arhgdib**
Eif5a	**Tmsb4x**	**Ndufa4**	**Set**	**Tuba1b**	**Cox6a1**	**Ldha**	**Pkm**	**Npc2**
Ran	**Ifi27l2a**	**Pebp1**	**Rac2**	**H2afz**	**Dad1**	**Ndufa1**	**Hnrnpa2b1**	**Psma3**
Prdx1	**Shisa5**	**Atpif1**	**Tubb5**	**Gimap4**	**Atp5o**	**Cox6b1**	**Cnbp**	**Ube2i**
Ybx1	**Arhgef1**	**Snrpf**	**Higd1a**	**H2-K1**	**Psmb2**	**Swi5**	**Serbp1**	**Cct5**
Hsp90ab1	**Ms4a4b**	**Lsm7**	**Anp32b**	**Limd2**	**Sem1**	**Cox7a2**	**Edf1**	**Rbm8a**
Hspe1	**Gm8369**	**Cycs**	**Tnfrsf18**	**Atp5g3**	**Minos1**	**Txn1**	**Nedd8**	**Sdhb**
Ikzf2	**Ncl**	**Uqcr10**	**Uqcr11**	**Snu13**	**Rpl13a**	**Snrpd3**	**Slc25a3**	**Emp3**
Npm1	**Rps11**	**Srsf3**	**Cox6c**	**Srsf2**	**Snrpe**	**Uqcrb**	**Gm2000**	**Id3**
Uqcrq	**Atp5e**	**H2-D1**	**Dynll1**	**St13**	**Park7**	**Gmfg**	**Ndufs6**	**Lef1**
Chchd2	**Gm9843**	**Hspa8**	**Snrpd2**	**Rbx1**	**Slc25a5**	**Ndufa11**	**Tomm20**	**Gpsm3**
Rpl35	**Ltb**	**B2m**	**Snrpb**	**Pdcd5**	**Ndufb2**	**Ndufc2**	**Ndufb8**	

Table 3.1. List of genes differentially regulated between $CD25^{+}$ $T_{reg}P$ and $FOXP3^{lo}$ $T_{reg}P$ in both scRNAseq data sets. This list represents 179 genes.

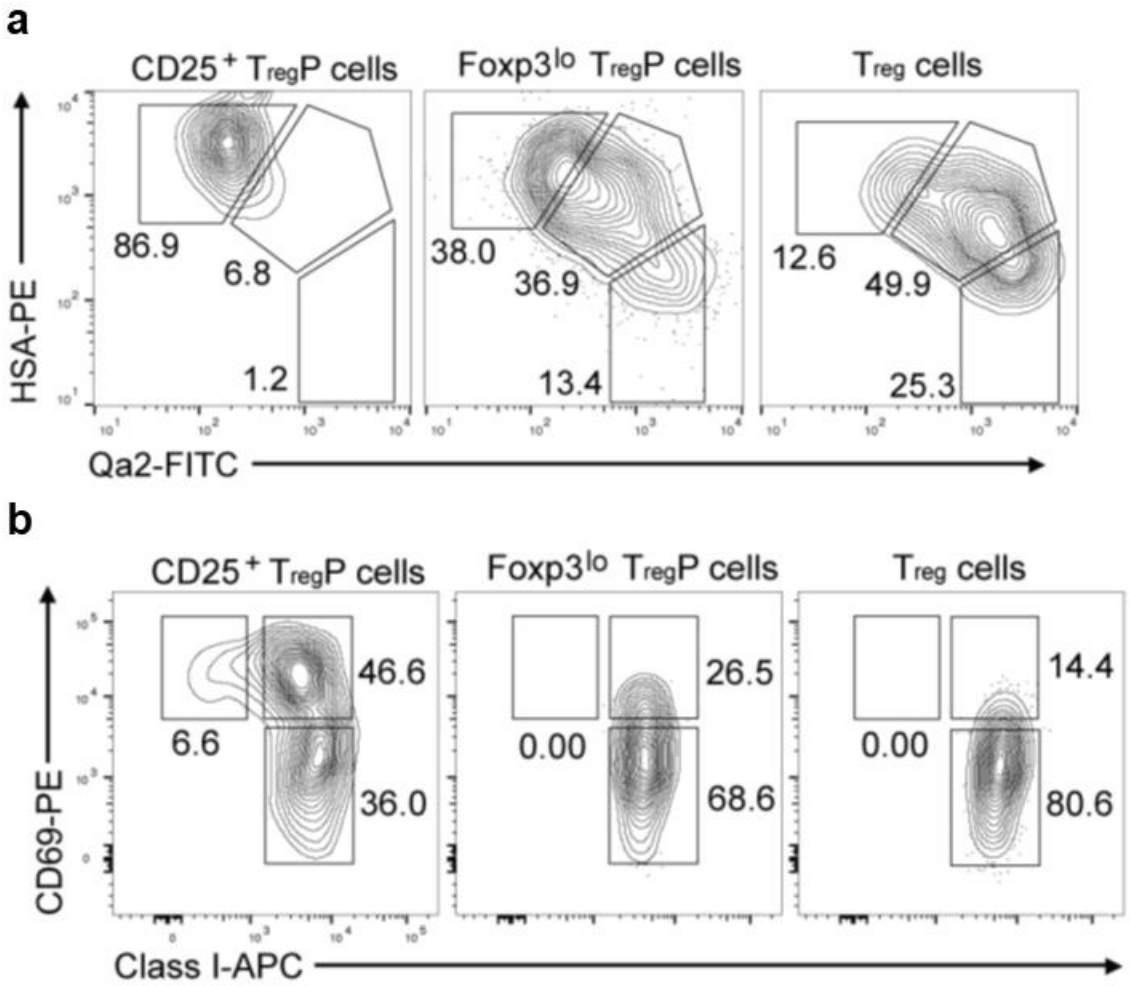

Figure 3.6. Maturation analysis of thymic T_{reg} cell populations. **a)** Thymocytes of the indicated subsets were analyzed for expression of HSA and Qa-2. Gates are drawn to demonstrate the frequency of cells within each maturation state. Data is representative of 1 experiment, *n* = 2 mice. **b)** Thymocytes of the indicated subsets were analyzed for CD69 and MHC-I expression. Gates are drawn to demonstrate the frequency of cells within each maturation state. Data is representative of 1 experiment, *n* = 3 mice.

FOXP3^{lo} T_{reg}P cells or mature CD25^{+}FOXP3^{+} T_{reg} cells, were detected in bin 2, while FOXP3^{lo} T_{reg}P cells and mature CD25^{+}FOXP3^{+} T_{reg} cells appeared in bin 3. CD25^{+} T_{reg}P cells, FOXP3^{lo} T_{reg}P cells and mature CD25^{+}FOXP3^{+} T_{reg} cells were all detected in bins 4–6, while CD25^{+} T_{reg}P cells were no longer detected in bin 7 because these cells differentiate, die or leave the thymus (Figure 3.7a). Bin 8 contained GFP^{-} cells (Figure 3.7 a), representing fully mature recirculating T cells. This analysis indicated that CD25^{+} T_{reg}P cells differentiate rapidly, while FOXP3^{lo} T_{reg}P cells take longer to develop.

About half of CD25^{+}FOXP3^{+} T_{reg} cells in the thymus represent mature recirculating cells[173,175]. Because 18% of FOXP3^{lo} T_{reg}P cells consisted of recirculating Rag2-GFP^{-} T cells (Figure 3.8), we looked for cell surface markers that could distinguish newly developed RAG2-GFP^{+} thymocytes from recirculating RAG2-GFP^{-} T cells. Over 99% of CD73^{-} cells were RAG2-GFP^{+}, while >85% of CD73^{+} cells were RAG2-GFP^{-} (Figure 3.7 b), suggesting that the expression of CD73 can distinguish between developing thymocytes and recirculating mature T cells in the thymus in the absence of the *Rag2-GFP* transgenic reporter. To assess whether FOXP3^{lo} T_{reg}P cells, which developed with slower kinetics and exhibited reduced TCR signal strength, were more dependent on adhesion molecules such as LFA-1, which help prolong T cell–antigen-presenting cell (APC) contacts and enhance TCR signaling[225], we examined T_{reg} cell development in *Itgal*$^{-/-}$ mice, which are LFA-1 deficient. CD73^{-} FOXP3^{lo} T_{reg}P cells, but not CD73^{-} CD25^{+} T_{reg}P cells, are decreased in the *Itgal*$^{-/-}$ thymus compared to their abundance in wild-type (WT) thymus (Figure 3.7 c). Thus, the development of FOXP3^{lo} T_{reg}P cells is more dependent on stable interactions between T cells and APCs or LFA-1-dependent co-stimulation than CD25^{+} T_{reg}P cells.

Based on FOXP3 overexpression studies, FOXP3^{lo} T_{reg}P cells were proposed to be very susceptible to apoptosis[65]. Because our scRNAseq analysis, based on *Bcl2l11* and

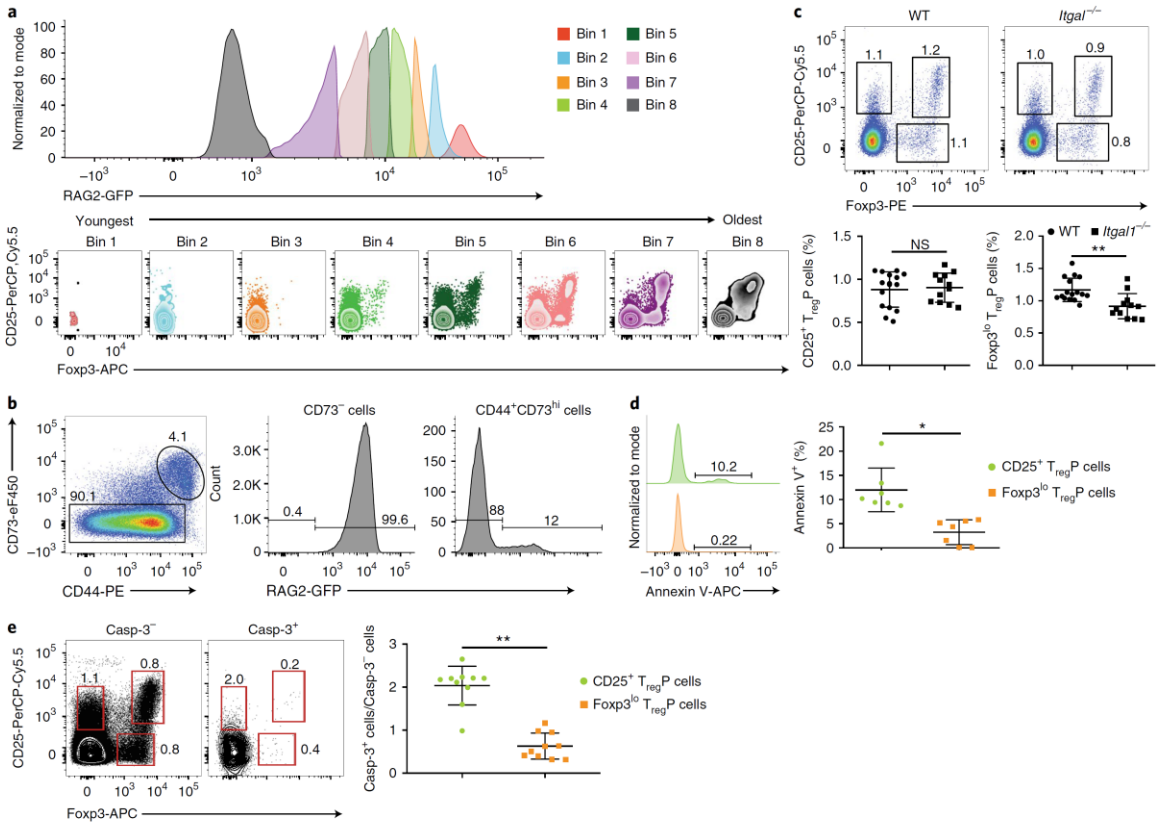

Figure 3.7. CD25^{+} and FOXP3^{lo} T_{reg}P cells are in discrete selection stages. **a)** Representative histograms of RAG2-GFP expression in CD4SP thymocytes obtained from the thymus of RAG2-GFP mice. Bins are displayed according to high (bin 1) to low (bin 8) RAG-GFP expression, and cells in each bin are plotted for CD25 versus FOXP3 expression. Data shown are concatenated results from three mice and are representative of seven independent experiments, *n* = 9 mice. **b)** Representative flow cytometry plots of CD73 staining in CD4SP thymocytes and RAG2-GFP expression in CD73^{-} and CD73^{+} compartments. Data are representative of five experiments, *n* = 5 mice. **c)** Representative flow cytometry plots (top) and quantification (below) of the percentage of CD4^{+}CD73^{-} thymocytes differentiating into each T_{reg}P cell population in WT vs *Itgal*$^{-/-}$ thymus. Data represent three independent experiments, *n* = 16 WT and *Itgal*$^{+/-}$ mice, *n* = 12 *Itgal*$^{-/-}$ mice. Data were analyzed by two-sided Mann–Whitney test. **d)** Left: representative example of annexin V staining on CD4^{+}CD73^{-}CD25^{+}FOXP3^{-} T_{reg}P cells (top green histogram) and

$CD4^+CD73^-CD25^-FOXP3^{lo}$ $T_{reg}P$ cells (bottom orange histogram) from *Foxp3-GFP* mice. Right: quantification of annexin V staining for $CD25^+$ $T_{reg}P$ cells and $FOXP3^{lo}$ $T_{reg}P$ cells. Data represent three independent experiments, n = 9 mice. Data were analyzed by two-sided Wilcoxon matched-pairs signed-rank test. e, Left and middle: representative examples of staining for CD25 and FOXP3 on $CD4^+CD73^-$ gated thymocytes from WT mice, either negative (left) or positive (middle) for cleaved casp-3. Right: quantification of the ratio of cleaved casp-3-positive to cleaved casp-3-negative $CD25^+$ $T_{reg}P$ cells (green circles) and $FOXP3^{lo}$ $T_{reg}P$ cells (orange squares); data represent four independent experiments, n = 10 mice. Data were analyzed by two-sided Wilcoxon matched-pairs signed-rank test. All data are displayed as mean ± s.d., $*P < 0.05$, $**P < 0.005$, NS not significant.

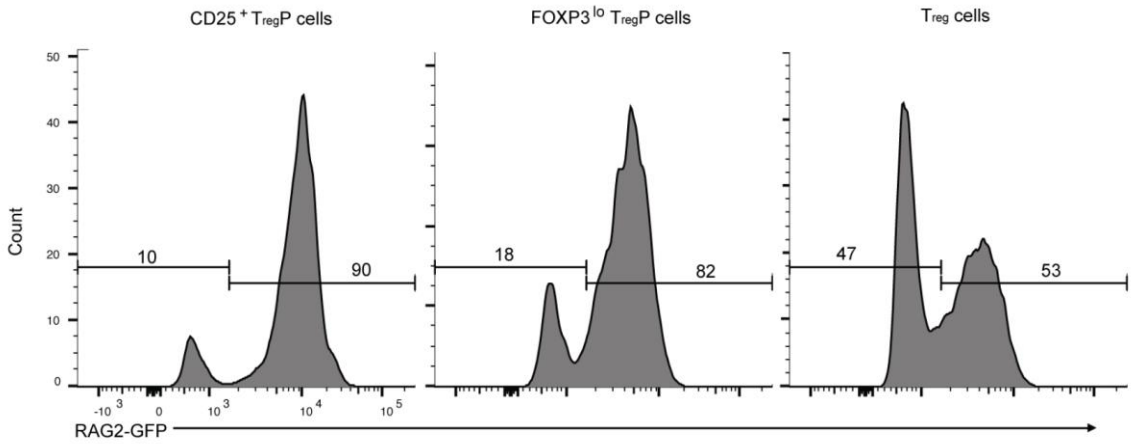

Figure 3.8. Frequency of contaminating recirculating cells in thymic Treg cell lineage subsets. Thymocytes of the indicated subsets were analyzed for RAG2-GFP expression. Gates were drawn to determine the frequency of RAG2-GFP$^-$ (recirculating/resident) and RAG2-GFP$^+$ (newly developing) fractions of cells within each subset. Displayed are concatenated data from 3 thymi. Results are representative of 7 experiments, *n* = 9 mice.

Nr4a1 expression, suggested that $CD25^+$ $T_{reg}P$ cells might be more apoptotic than $FOXP3^{lo}$ $T_{reg}P$ cells (Figure 3.5 c), we used annexin V staining to identify apoptotic cells in the thymus. Annexin V^+ cells were detected in both $T_{reg}P$ cell subsets, although there were substantially more among $CD73^-$ $CD25^+$ $T_{reg}P$ cells (12%) than among $CD73^-$ $FOXP3^{lo}$ $T_{reg}P$ cells (3.3%; Fiugre 3.7 d). We also stained thymocytes for cleaved caspase-3 (casp-3). $CD25^+$ $T_{reg}P$ cells were enriched fourfold for casp-3^+ cells compared to $FOXP3^{lo}$ $T_{reg}P$ cells (Figure 3.7 e). Thus, $CD25^+$ $T_{reg}P$ cells interacted most strongly with self-antigen in the thymus and contained a higher fraction of apoptotic cells, suggesting that they were undergoing negative selection.

We next examined the location of $FOXP3^{lo}$ $T_{reg}P$ cells within the thymus. Histocytometry[226] experiments in C57Bl/6 mouse thymus indicated that mature $CD25^+FOXP3^+$ T_{reg} cells were largely restricted to the thymic medulla (Figure 3.9 a,b), consistent with agonist-driven T_{reg} selection occurring in the thymic medulla. In contrast, while $FOXP3^{lo}$ $T_{reg}P$ cells were found in the thymic medulla, a substantial proportion (20%) were located in the thymic cortex (Figure 3.9 a,b), suggesting that at least some $FOXP3^{lo}$ $T_{reg}P$ cells are selected on cortical antigens. Thus, $CD25^+$ and $FOXP3^{lo}$ $T_{reg}P$ cell subsets differentiate with distinct kinetics and exhibit different rates of apoptosis; moreover, a fraction of the $FOXP3^{lo}$ $T_{reg}P$ cell subset shares features with conventional (that is, non-T_{reg}) T cells undergoing positive selection, which also occurs in the thymic cortex.

NF-kB is critical for the development of $FOXP3^{lo}$ $T_{reg}P$ cells

We next assessed the effect of co-stimulation and downstream signaling pathways on the development of $CD25^+$ $T_{reg}P$ cells and $FOXP3^{lo}$ $T_{reg}P$ cells. *Cd28*$^{-/-}$ thymi exhibited a decrease in abundance of 1.7-fold in $CD25^+$ $T_{reg}P$ cells but a larger decrease of 6.7-fold

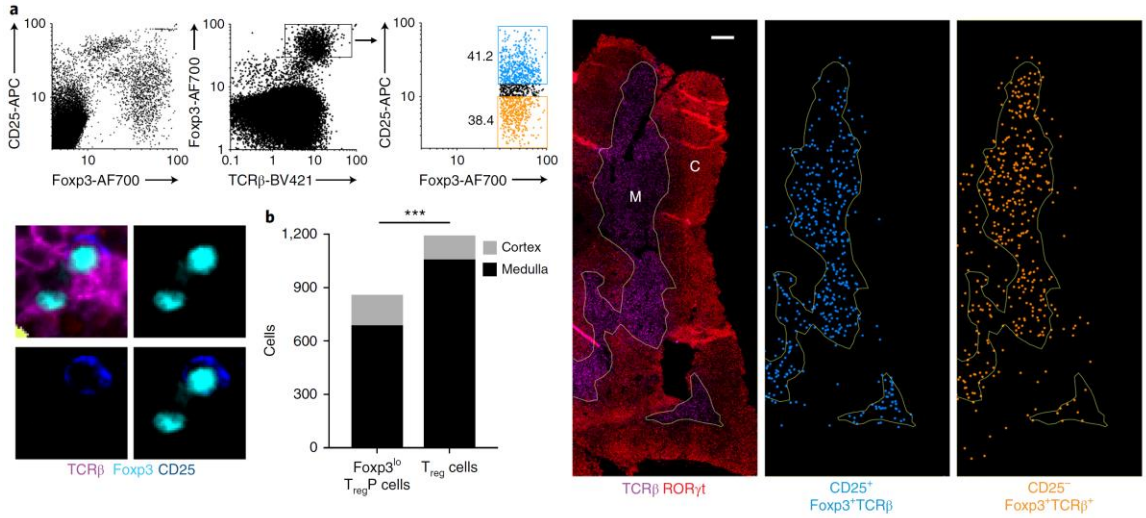

Figure 3.9. T_{reg} cells and FOXP3^{lo} T_{reg}P cells show different localization in the thymus. **a)** Top left: representative histocytometry dot plots of thymocytes stained with antibodies to CD25, FOXP3 and TCRβ, used to denote FOXP3^{lo} T_{reg}P cells (CD25^{-}Foxp3^{+}TCRβ^{+}) and T_{reg} cells (CD25^{+}FOXP3^{+}TCRβ^{+}) within stained thymic sections. Bottom left representative images of FOXP3^{lo} T_{reg}P cells and T_{reg} cells. Right: thymic sections stained with antibodies to TCRβ and RORγt, used to delineate the thymic medulla (M) and cortex (C). Distribution of CD25^{+}FOXP3^{+}TCRβ^{+} T_{reg} cells (blue) and CD25^{-}Foxp3^{+}TCRβ^{+} FOXP3^{lo} T_{reg}P cells (orange) within the thymic medulla and cortex (right). Scale bar, 200 μm. **b)** Distribution of FOXP3^{lo} T_{reg}P cells and T_{reg} cells between thymic cortex and medulla, *P* value determined by Fisher's exact test. Data represent one experiment, *n* = 2 mice. ****P* < 0.0001.

in FOXP3^{lo} T_{reg}P cells, compared to thymi from WT mice (Figure 3.10 a). Next, we examined the effect of the downstream transcription factor NF-κB1 on T_{reg} cell development. *Nfkb1*$^{-/-}$ mouse thymus show a 3.6-fold reduction in the abundance of CD73^{-}FOXP3^{lo} T_{reg}P cells compared to that from WT mice, while CD73^{-}CD25^{+} T_{reg}P cell abundance are unaffected (Figure 3.10 c). These results suggest that co-stimulation, and especially activation of NF-κB1, are selectively required for the formation of FOXP3^{lo} T_{reg}P cells.

CD25^{+} T_{reg}P cell and FOXP3^{lo} T_{reg}P cell development is regulated by distinct enhancers

To examine whether FOXP3 is required for the development of T_{reg} cells from both CD25^{+} T_{reg}P cells and FOXP3^{lo} T_{reg}P cells we used *Foxp3-GFP*^{KIN} mice, in which a GFP reporter construct is knocked into the *Foxp3* locus and generates a GFP-Foxp3 fusion protein[59]. These mice express normal amounts of GFP-Foxp3 protein but have been described as functional FOXP3 hypomorphs[227,228]. Following gating on CD4^{+}CD73^{-} thymocytes, a significant reduction in the frequency of FOXP3^{lo} T_{reg}P cells was found in the thymus of *Foxp3*-GFP^{KIN} mice compared with that of WT mice, while the abundance of CD25^{+} T_{reg}P cells is unaffected (Figure 3.11 a). To examine this in more detail, we analyzed *Foxp3*-GFP^{KIN} mice lacking the *Foxp3* regulatory element *Cns3* (called '*Cns3*$^{-/-}$ mice' here). *Cns3*$^{-/-}$ mice, which are known to have a ~40% reduction in the frequency of T_{reg} cells in the thymus[160], have selective defects in immune tolerance and a T_{reg} cell bias towards higher self-reactivity[163]. *Cns3*$^{-/-}$ mice lack FOXP3^{lo} T_{reg}P cells (Figure 3.11 a). Consistent with previous reports[160], mature CD25^{+}FOXP3^{+} T_{reg} cells are also substantially reduced in *Cns3*$^{-/-}$ mice compared to WT mice, and the defect is about twice as large (~85% reduction) when gating on CD73^{-} cells to eliminate mature recirculating T_{reg} cells (Figure 3.11 a). Importantly, mature CD25^{+}FOXP3^{+}CD73^{+}

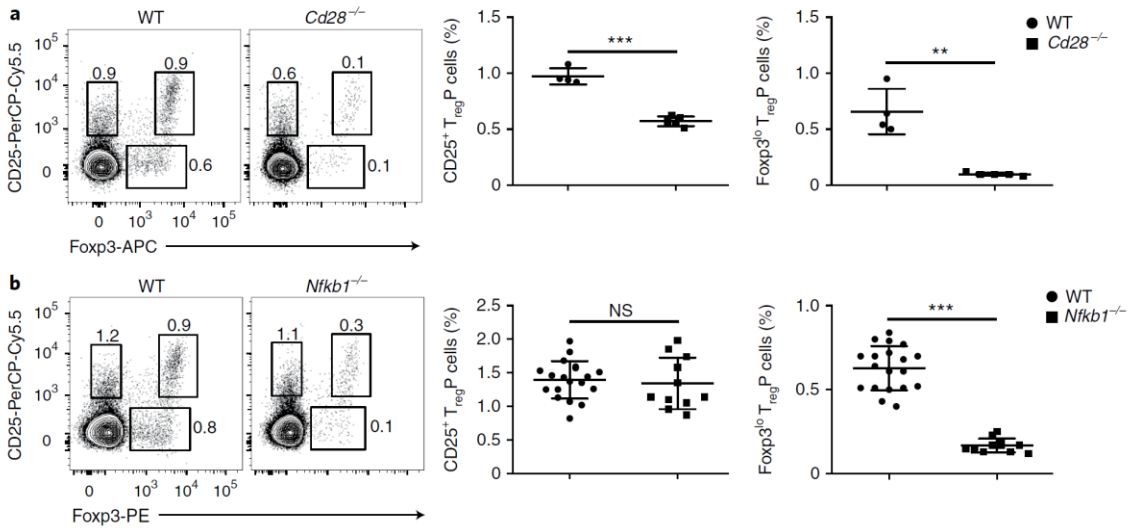

Figure 3.10. FOXP3^{lo} T_{reg}P cells are dependent on NFκB1 activation. **a)** Left: representative flow cytometry plots for CD4^{+}CD8$^{–}$CD73$^{–}$ gated thymocytes from WT and *Cd28*$^{–/–}$ mice stained with antibodies to CD25 and FOXP3 (one experiment, *n* = 4 WT and 5 *Cd28*$^{–/–}$ mice). Right: cumulative data for all mice, depicting the relative percentages of CD25^{+} T_{reg}P cells and FOXP3^{lo} T_{reg}P cells in CD4^{+}CD8$^{–}$CD73$^{–}$ thymocytes from WT and *Cd28*$^{–/–}$ mice. **b)** Flow cytometry **c)** Representative flow cytometry plots for CD4^{+}CD8$^{–}$CD73$^{–}$ gated thymocytes from WT and *Nfkb1*$^{–/–}$ mice stained with antibodies to CD25 and FOXP3 (three independent experiments, *n* = 19 WT and 11 *Nfkb1*$^{–/–}$ mice). Right: cumulative data for all mice depicting the relative percentages of CD25^{+} T_{reg}P cells and FOXP3^{lo} T_{reg}P cells among CD4^{+}CD8$^{–}$CD73$^{–}$ thymocytes from WT and *Nfkb1*$^{–/–}$ mice. a,b, Data were analyzed by two-sided unpaired *t*-test.

T_{reg} cells in *Cns3*$^{-/-}$ and WT mice expressed comparable amounts of FOXP3 (Figure 3.12 a), indicating that *Cns3* is not required for FOXP3 expression. CD25^{+} T_{reg}P cells isolated from *Foxp3*-GFP^{KIN} and *Cns3*$^{-/-}$ mice cultured *in vitro* upregulated FOXP3 and differentiated into mature CD25^{+}FOXP3^{+} T_{reg} cells with comparable efficiency when stimulated with IL-2 (Figure 3.11 b), suggesting that *Cns3* is not required for upregulation of FOXP3 in CD25^{+} T_{reg}P cells. These results indicate that the development of T_{reg} cells from FOXP3^{lo} T_{reg}P cells was blocked in the absence of *Cns3* and that mature T_{reg} cells developed primarily from CD25^{+} T_{reg}P cells in *Cns3*$^{-/-}$ mice.

A non-coding single-nucleotode polymorphism that contributes to an increased risk for autoimmunity in humans was previously described in the *Il2ra* locus[165–167], specifically in enhancer CaRE4, which is required for rapid induction of *Il2ra* following TCR activation[164]. Thus, we examined the role of this autoimmunity-associated *Il2ra* enhancer in T_{reg} cell development. Deletion of the CaRE4 *Il2ra* enhancer in a non-obese diabetic (NOD) mouse background led to a significant reduction in the percentages of thymic CD25^{+} T_{reg}P cells and mature T_{reg} cells compared with that of WT NOD mice (Figure 3.11 c). In contrast, the percentage of FOXP3^{lo} T_{reg}P cells is slightly increased, perhaps as a compensatory mechanism. This decrease in CD25^{+} T_{reg}P cells is not due to a lack of CD25 expression in general, as the expression of CD25 on mature T_{reg} cells, or on the remaining CD25^{+} T_{reg}P cells, is not reduced compared to WT controls (Figure 3.12 b). Collectively these data suggest that the development of T_{reg} cells from CD25^{+} T_{reg}P cells and FOXP3^{lo} T_{reg}P cells is controlled by distinct regulatory circuits.

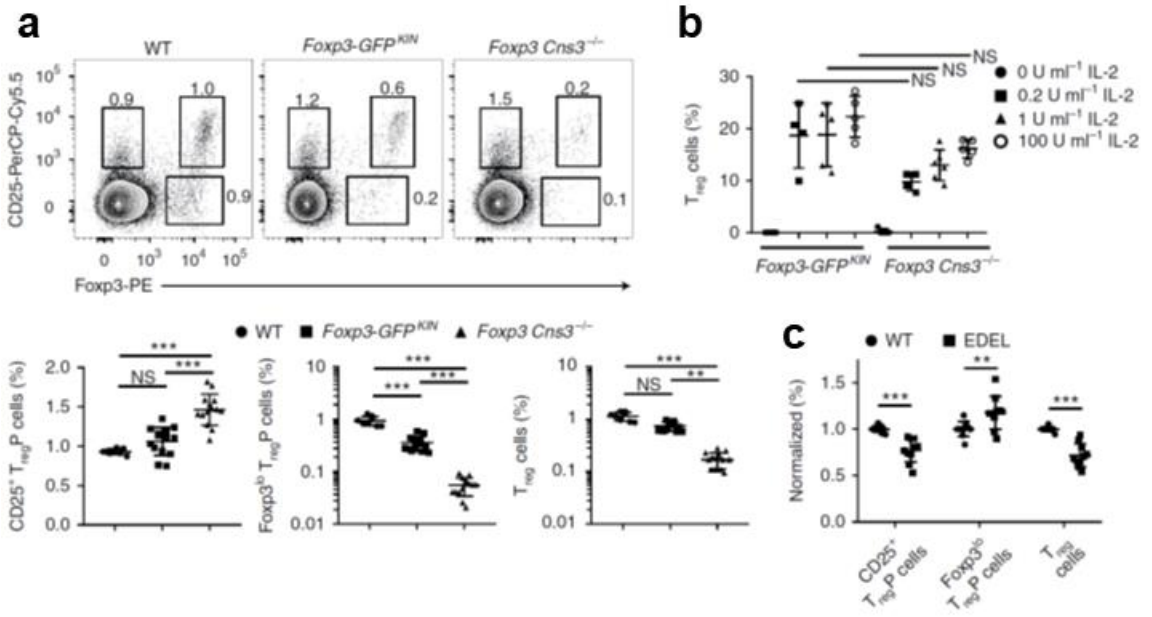

Figure 3.11. CD25$^+$ T_{reg}P cell and FOXP3^{lo} T_{reg}P cell development is regulated by distinct enhancers. **a)** Top: representative flow cytometry plots for CD4$^+$CD8$^-$CD73$^-$ gated thymocytes from WT, *Foxp3*-GFP^{KIN} and *Cns3*$^{-/-}$ mice stained with antibodies to CD25 and FOXP3 (four independent experiments, *n* = *8* WT, 14 *Foxp3*-GFPKIN and 14 *Cns3*$^{-/-}$ mice). Right panels: quantification of cumulative data for all mice, depicting relative percentages of CD25$^+$ T_{reg}P cells, FOXP3^{lo} T_{reg}P cells and mature CD25$^+$ FOXP3$^+$ T_{reg} cells in CD4$^+$CD8$^-$CD73$^-$ thymocytes from WT (black circles), *Foxp3*-GFPKIN (black squares) and *Cns3*$^{-/-}$ (black triangles) mice. **b**) Percentages of CD25$^+$FOXP3$^+$ mature T_{reg} cells generated after stimulating sorted CD4$^+$CD8$^-$CD73$^-$CD25$^+$ T_{reg}P cells from the thymus of *Foxp3*-GFPKIN and *Cns3*$^{-/-}$ mice for 3 days with 0 U ml–1 IL-2 (black circles, *n* = 5 *Foxp3*-GFPKIN and 5 *Cns3*$^{-/-}$ replicates), 0.2 U ml–1 IL-2 (black squares, *n* = 4 *Foxp3*-GFPKIN and 5 *Cns3*$^{-/-}$ replicates), 1 U ml–1 IL-2 (black triangles, *n* = 5 *Foxp3*-GFPKIN and 6 *Cns3*$^{-/-}$ replicates) and 100 U ml–1 IL-2 (open circles, *n* = 5 *Foxp3*-GFPKIN and 5 *Cns3*$^{-/-}$ replicates), derived from two independent experiments. **c)** Quantification of cumulative data from two independent experiments showing the relative percentages of CD25$^+$ T_{reg}P cells, FOXP3^{lo} T_{reg}P cells and mature CD25$^+$FOXP3$^+$ T_{reg} cells from

$CD4^+CD8^-CD73^-$ gated thymocytes from WT (black circles) or EDEL mice, which lack the CaRE4 enhancer (black squares). Data represent two independent experiments, *n*= 10 wild-type and 10 EDEL mice. a, $CD25^+$ $T_{reg}P$ cells (%) and $FOXP3^{lo}$ $T_{reg}P$ cells (%) were analyzed by one-way analysis of variance (ANOVA) with Tukey's multiple comparison test, and T_{reg} cells (%) were analyzed by Kruskal–Wallis test with Dunn's multiple comparison test; in b, data were analyzed by Kruskal–Wallis test with Dunn's multiple comparisons test; and in c, data were analyzed by two-way ANOVA with Sidak multiple comparisons test. All data are displayed as mean ± s.d. $^{**}P < 0.005$, $^{***}P < 0.0001$, NS not significant.

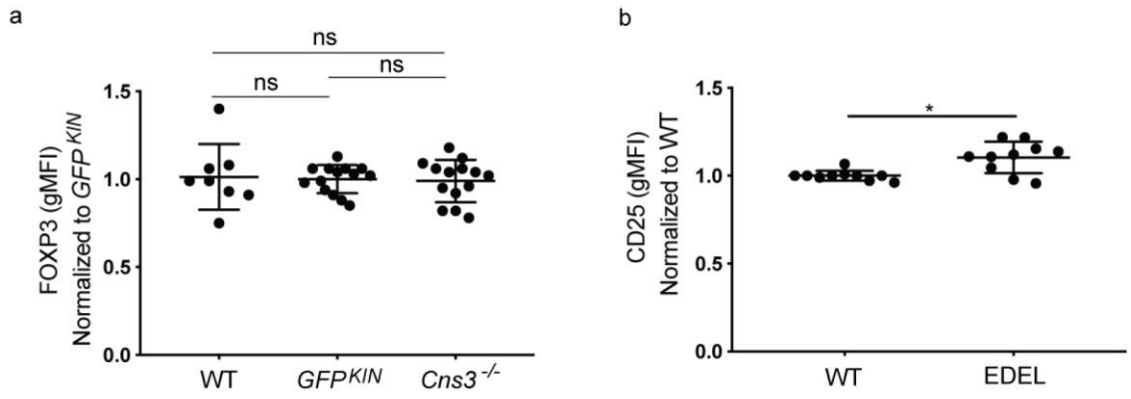

Figure 3.12. Enhancer deletions do not cause reduced levels of FOXP3 or CD25. **a)** Quantification of FOXP3-gMFI in mature, $CD73^{+}$ thymic T_{reg} cells in WT, *Foxp3*-GFPKIN or *Foxp3 Cns3*$^{-/-}$ mice. All data points are normalized to the *Foxp3*-GFPKIN average within each experiment. Data is representative of 4 experiments, n=8 wild-type mice, 14 *GFPKIN* mice and 14 *Cns3*$^{-/-}$ mice. Data was analyzed by a one-way ANOVA with Tukey's multiple comparisons test. b) Quantification of CD25-gMFI in $CD73^{-}$ thymic T_{reg} cells in WT or EDEL (*Il2ra CaRE4*$^{-/-}$) mice in the non-obese diabetic (NOD) background. Data is representative of 3 experiments, n=10 wild-type NOD mice and 10 EDEL NOD mice. Data was analyzed by a two-sided Mann-Whitney test. a,b) Bars represent mean ± SD. *P<0.05, ns- not significant.

Inhibition of negative selection pathways expand CD25$^+$ T_{reg}P cell generation

To further probe whether CD25$^+$ T_{reg}P cells are constrained by negative selection, we examined the development of T_{reg} cells in *Itk*$^{-/-}$ mice, as mice lacking the tyrosine kinase ITK have defects in negative selection[229]. The thymus of *Itk*$^{-/-}$ mice show higher frequencies of mature thymic CD25$^+$FOXP3$^+$ T_{reg} cells[230], as well as CD25$^+$ T_{reg}P cells and FOXP3^{lo} T_{reg}P cells (Figure 3.13 a). The adaptor ADAP, which is downstream of ITK, is also required for efficient negative selection[231]. Thymi from *Adap*$^{-/-}$ mice show an increase in the abundance CD25$^+$ T_{reg}P cells, but no change in FOXP3^{lo} T_{reg}P cells, compared to WT mice (Figure 3.13 b). The frequency of mature CD25$^+$FOXP3$^+$ T_{reg} cells in the thymus is also significantly increased in *Adap*$^{-/-}$ mice compared to WT mice (Figure 3.13 b). Thus, *Adap*$^{-/-}$ mice have a selective increase in CD25$^+$ T_{reg}P cells compared with that of WT mice. A potential explanation for the discrepancy between *Itk*$^{-/-}$ mice and *Adap*$^{-/-}$ mice is that ITK deficiency is known to induce increased production of IL-4 in invariant nature killer T cells (iNKT cells) in the thymus[232,233] , while ADAP deficiency does not. To determine whether the different phenotypes, in terms of T_{reg} cell development, in *Adap*$^{-/-}$ mice and *Itk*$^{-/-}$ mice are linked to IL-4 production, we examined T_{reg} cell development in *Itk*$^{-/-}$ and *Itk*$^{-/-}$ × *Il4ra*$^{-/-}$ mice. Compared to *Itk*$^{-/-}$ mouse thymus, no increase in abundance of FOXP3^{lo} T_{reg}P cells was seen in *Itk*$^{-/-}$ × *Il4ra*$^{-/-}$ mice (Figure 3.13 a,c), suggesting that the increase in FOXP3^{lo} T_{reg}P cells in the former is due to increased amounts of IL-4 present in the thymus. Thus, CD25$^+$ T_{reg}P cells are selectively pruned by the ITK–ADAP pathway required for negative selection.

CD25$^+$ T_{reg}P cells and FOXP3^{lo} T_{reg}P cells have distinct cytokine responsiveness

IL-2 and, to a lesser degree, IL-15 are the predominant cytokines driving the STAT5-dependent differentiation of CD25$^+$ T_{reg}P cells into mature T_{reg} cells[63,64,132,200,234]. Because

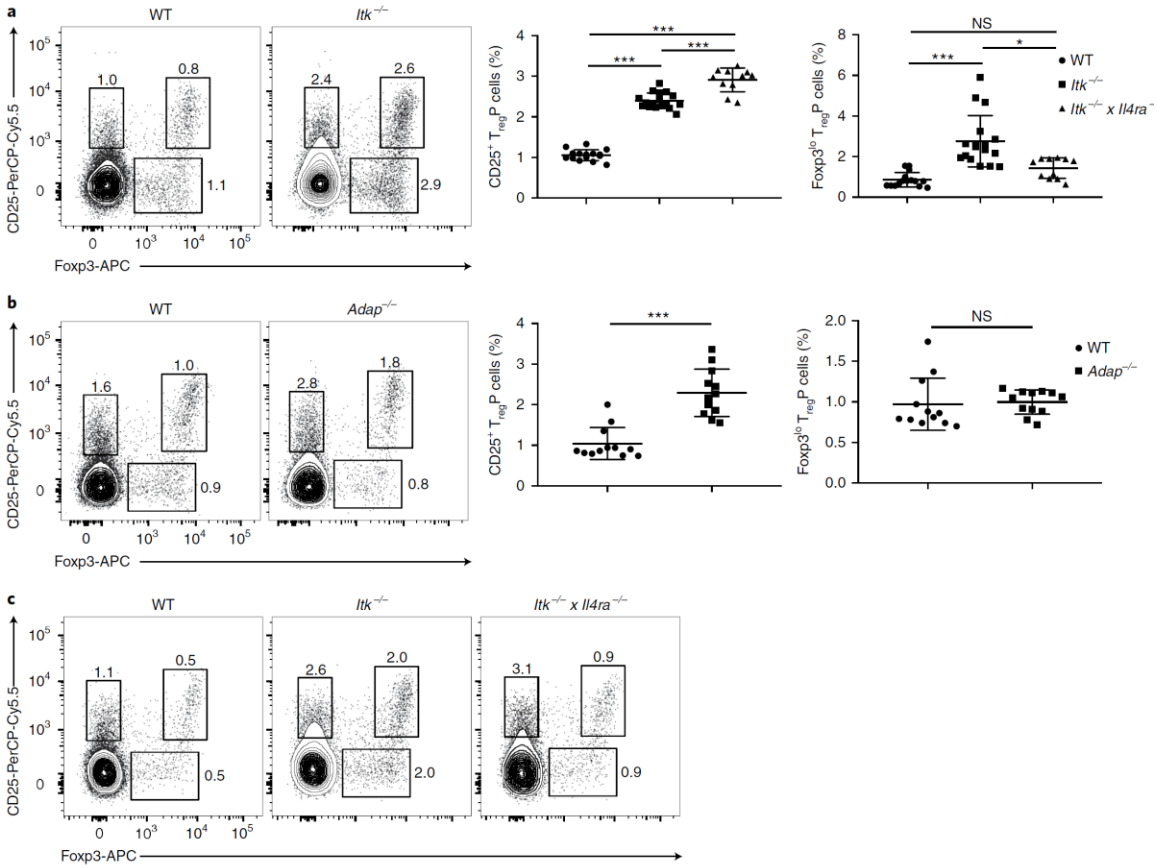

Figure 3.13. *Itk*$^{-/-}$ mice show increased T_{reg} cell production from both T_{reg}P cell pathways via distinct molecular mechanisms. **a)** Left: representative flow cytometry plots of CD4^{+}CD8^{-}CD73^{-} gated thymocytes from WT vs *Itk*$^{-/-}$ mice stained with antibodies to CD25 and FOXP3. Right: cumulative data for all mice depicting the relative percentages of CD25^{+} T_{reg}P cells and FOXP3^{lo} T_{reg}P cells in CD4^{+}CD8^{-}CD73^{-} thymocytes from WT, *Itk*$^{-/-}$ and *Itk*$^{-/-}$ × *Il4ra*$^{-/-}$ mice (three independent experiments, *n* = 15 WT, 17 *Itk*$^{-/-}$ and 11 *Itk*$^{-/-}$ × *Il4ra*$^{-/-}$ mice). **b)** Left: representative flow cytometry plots of CD4^{+}CD8^{-}CD73^{-} gated thymocytes from WT vs *Adap*$^{-/-}$ mice stained with antibodies to CD25 and FOXP3. Right: cumulative data for all mice, depicting the relative percentages of CD25^{+} T_{reg}P cells and FOXP3^{lo} T_{reg}P cells in CD4^{+}CD8^{-}CD73^{-} thymocytes from WT and *Adap*$^{-/-}$ mice (three independent experiments, *n* = 12 WT and 12 *Adap*$^{-/-}$ mice). **c)** Representative flow cytometry plots of CD4^{+}CD8^{-}CD73^{-} gated thymocytes from WT, *Itk*$^{-/-}$ and *Itk*$^{-/-}$ × *Il4ra*$^{-/-}$

mice stained with antibodies to CD25 and FOXP3. In a, $CD25^{+}$ $T_{reg}P$ cells (%) were analyzed by one-way ANOVA with Tukey's multiple comparisons test; $FOXP3^{lo}$ $T_{reg}P$ cells (%) were analyzed by Kruskal–Wallis test with Dunn's multiple comparisons test and in b, data were analyzed by two-sided Mann–Whitney test. All data are displayed as mean ± s.d. *P < 0.05, ***P < 0.0001, NS not significant.

the ability of FOXP3^{lo} T_{reg}P cells to differentiate into mature T_{reg} cells in response IL-4 has not been evaluated, we queried whether IL-4 could affect the differentiation of CD25^{+} T_{reg}P cell or FOXP3^{lo} T_{reg}P cell subsets into mature T_{reg} cells. As reported previously[63,200], IL-4 did not result in the robust conversion of thymically derived CD25^{+} T_{reg}P cells into mature T_{reg} cells but supported substantial conversion of thymus-derived FOXP3^{lo} T_{reg}P cells into mature CD25^{+}FOXP3^{+} T_{reg} cells in an *in vitro* assay (Figure 3.14 a). FOXP3^{lo} T_{reg}P cells show slightly higher expression of the IL-4 receptor (IL-4Ra) than CD25^{+} T_{reg}P cells (Figure 3.14b), which we consider unlikely to account for the difference in the differentiation of CD25^{+} T_{reg}P cells and FOXP3^{lo} T_{reg}P cells in response to IL-4. In addition, although IL-4 converted FOXP3^{lo} T_{reg}P cells into mature T_{reg} cells, these cells expressed less CD25 and FOXP3 than those stimulated with IL-2 alone (Figure 3.14 c-f).

It is unclear which cells drive the production of IL-4 in the thymus. In humans, Hassall's corpuscles, a distinct anatomical feature of the thymus containing cells that resemble tuft cells, are important for T_{reg} cell development[95]. Tuft cells were also reported in the murine thymus[93,94] and are major producers of IL-25, which induces IL-4 production in other cell types[235]. To test whether thymic tuft cells influence T_{reg}P cell differentiation, we examined T_{reg} cell development in *Pou2f3*$^{-/-}$ mice, which lack the transcription factor POU2F3 required for the development of tuft cells. We observed a decrease in frequency of ~30% for the development of FOXP3^{lo} T_{reg}P cells, but not for that of CD25^{+} T_{reg}P cells, in *Pou2f3*$^{-/-}$ thymus compared to WT thymus (Figure 3.15 a). To determine whether iNKT cells, the canonical producers of IL-4 in the thymus, selectively affect the development of FOXP3^{lo} T_{reg}P cells, we examined the frequency of T_{reg}P cells in *Cd1d*$^{-/-}$ mice, which lack NKT cells. There is a reduction of ~20% in the abundance of FOXP3^{lo} T_{reg}P cells in the *Cd1d*$^{-/-}$ thymus compared with that of WT BALB/c control

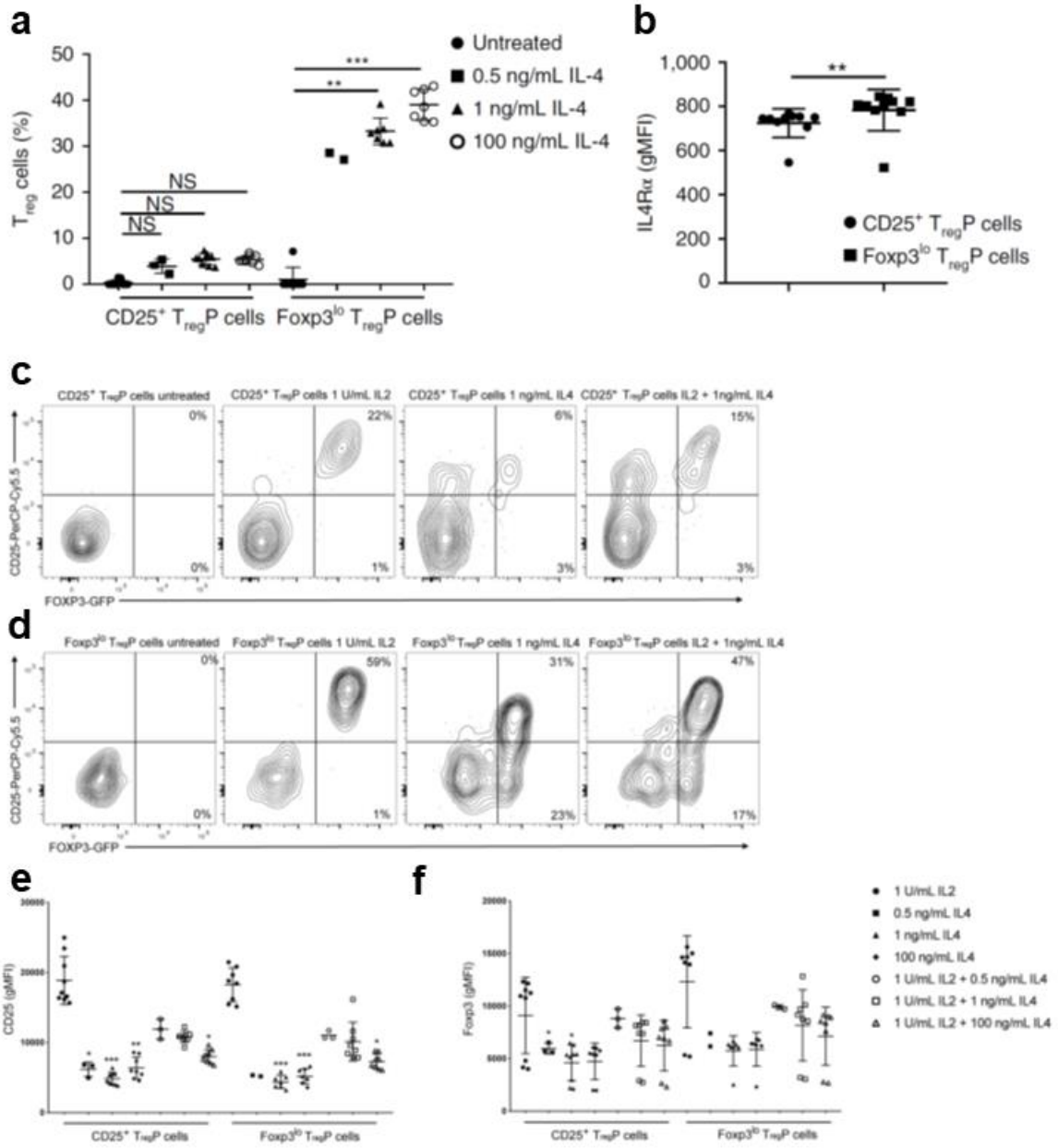

Figure 3.14. FOXP3^{lo} and CD25^{+} T_{reg}P respond distinctly to IL-4 stimulation. **a)** Percentage of T_{reg} cells generated from sorted CD4^{+}CD8^{-}CD73^{-}CD25^{+}FOXP3^{-} and CD4^{+}CD8^{-}CD73^{-}CD25^{+}FOXP3^{-} T_{reg}P cell subsets stimulated for 3 days with no cytokine (black circles, *n* = 9 CD25^{+} T_{reg}P cell cultures and 7 FOXP3^{lo} T_{reg}P cell cultures), 0.5 ng/mL IL-4 (black squares, *n* = 3 CD25^{+} T_{reg}P cell cultures and 2 FOXP3^{lo} T_{reg}P cell cultures), 1 ng/mL IL-4 (black triangles, *n* = 9 CD25^{+} T_{reg}P cell cultures and 7 FOXP3^{lo} T_{reg}P cell cultures) and 100 ng/mL IL-4 (open circles, *n* = 9 CD25^{+} T_{reg}P cell cultures and 7 FOXP3^{lo}

$T_{reg}P$ cell cultures). Data are representative of three independent experiments (excluding 0.5 ng/mL IL-4 stimulation, which is from one experiment) and were analyzed by Kruskal–Wallis test with Dunn's multiple comparisons test. **b)** IL4Ra gMFI in $CD25^+$ (black circles) and $FOXP3^{lo}$ (black squares) $T_{reg}P$ cells from thymus of WT mice. Data are representative of two independent experiments, *n* = 10 mice. Data were analyzed by two-sided Wilcoxon matched-pairs signed-rank test. **c,d)** Flow plots of the indicated $T_{reg}P$ cell subsets following 3 days of stimulation with the indicated cytokines. **e,f)** Quantification of the gMFI of CD25 or FOXP3 within mature T_{reg} cells ($CD25^+FOXP3^+$) generated from the indicated cytokine conditions. Data was analyzed by two-sided Kruskal-Wallis test. Data represents 3 experiments, *n* = 9 ($CD25^+$ $T_{reg}P$ cells- 1 U/mL IL-2, 1 ng/mL IL4), *n* = 8 ($CD25^+$ $T_{reg}P$ cells- 100 ng/mL IL4, 1 U/mL IL-2 + 1 ng/mL IL4, 1 U/mL IL-2 + 100 ng/mL IL4; $FOXP3^{lo}$ $T_{reg}P$ cells- 1 U/mL IL-2, 1 U/mL IL-2 + 1 ng/mL IL4, 1 U/mL IL-2 + 100 ng/mL IL4), *n* = 7 ($FOXP3^{lo}$ $T_{reg}P$ cells- 1 ng/mL IL4, 100 ng/mL IL4) or 1 experiment, *n* = 3 ($CD25^+$ $T_{reg}P$ cells- 0.5 ng/mL IL4, 1 U/mL IL-2 + 0.5 ng/mL IL4; $FOXP3^{lo}$ $T_{reg}P$ cells- 1 U/mL IL-2 + 0.5 ng/mL IL4), *n* = 2 ($FOXP3^{lo}$ $T_{reg}P$ cells- 0.5 ng/mL IL4) replicates. Bars represent mean ± SD. *P<0.05; **P<0.005; ***P<0.0001.

thymus (Figure 3.15 b). This effect was observed only in BALB/c mice, which produce abundant NKT cell–derived IL-4, not in C57Bl/6 mice, in which NKT cells produce very little IL-4 (Figure 3.15 c). Thus, the development of both $CD25^+$ $T_{reg}P$ cells and $FOXP3^{lo}$ $T_{reg}P$ cells clearly shows a degree of dependence on thymic tuft cells, and this is probably partially mediated via tuft cell induction of IL-4 production in iNKT cells.

$CD25^+$ and $FOXP3^{lo}$ $T_{reg}P$ cells exhibit distinct functions

Next we investigated whether the mature T_{reg} cells derived from $CD25^+$ $T_{reg}P$ cells or $FOXP3^{lo}$ $T_{reg}P$ cells are distinct in their ability to prevent distinct types of autoimmune disease driven by different auto-antigens. To test whether mature T_{reg} cells generated from $CD25^+$ $T_{reg}P$ cells differed in their ability to suppress autoimmunity in the central nervous system in comparison to $FOXP3^{lo}$ $T_{reg}P$ cell–generated T_{reg} cells, we isolated thymic $CD25^+$ $T_{reg}P$ cells and $FOXP3^{lo}$ $T_{reg}P$ cells, transferred them separately into individual C57Bl/6 host mice 1 day before immunization with the peptide $MOG_{35–55}$ and monitored the development of EAE signs. Transfer of mature T_{reg} cells is known to prevent or ameliorate signs of disease in this EAE model[236]. Mice receiving $FOXP3^{lo}$ $T_{reg}P$ cells show disease scores throughout the study similar to those of mice not receiving $T_{reg}P$ cell transfer (Figure 3.16 a,b). In contrast, disease progression and severity in mice that received $CD25^+$ $T_{reg}P$ cells is significantly ameliorated from days 14–19 after disease induction compared with that of mice receiving no $T_{reg}P$ cells or $FOXP3^{lo}$ $T_{reg}P$ cells (Figure 3.16 a,b). The number of congenically marked donor $FOXP3^+$ T_{reg} cells observed following transfer of $CD25^+$ or $FOXP3^{lo}$ $T_{reg}P$ cells was similar in the spleen at the endpoint of the experiment, 20 days after $T_{reg}P$ cell transfer (Figure 3.16 c), suggesting that conversion of $CD25^+$ $T_{reg}P$ cells and $FOXP3^{lo}$ $T_{reg}P$ cells into mature T_{reg} cells was similar. However, transferred $FOXP3^{lo}$ $T_{reg}P$ cells prevent weight loss in a T cell–transfer model of colitis (Figure 3.16 d), demonstrating that

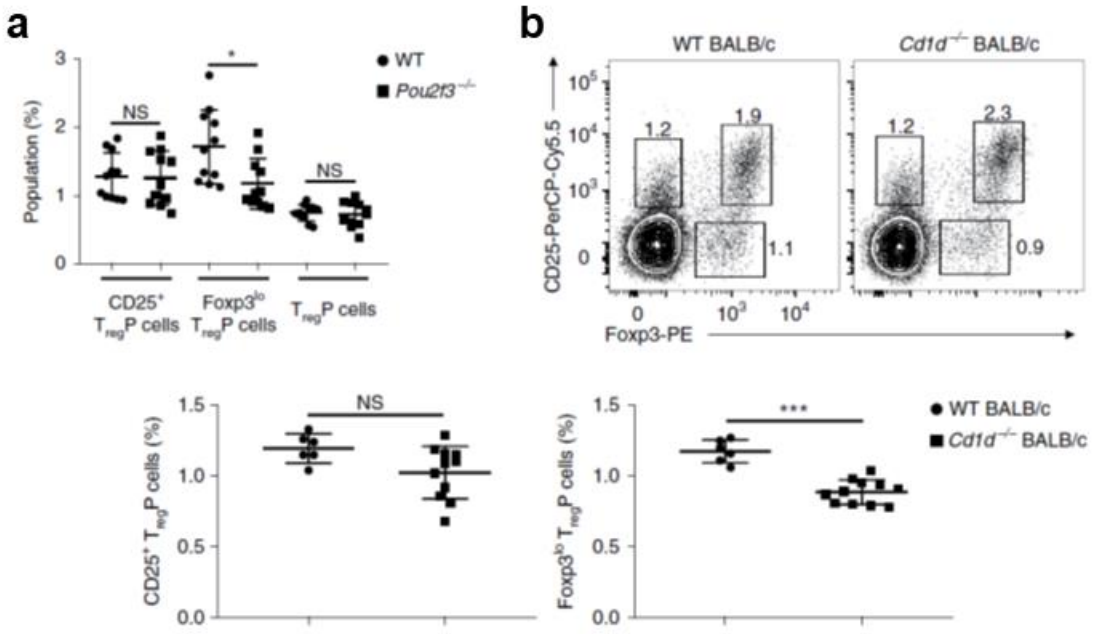

Figure 3.15. FOXP3^{lo} T_{reg}P cells depend on Tuft cells and iNKT cells. **a)** Percentages of CD4^{+}CD8$^{–}$CD73$^{–}$CD25^{+}FOXP3$^{–}$ T_{reg}P cells, CD4^{+}CD8$^{–}$CD73$^{–}$CD25$^{–}$FOXP3^{lo} T_{reg}P cells and CD4^{+}CD8$^{–}$CD73$^{–}$CD25^{+}FOXP3^{+} T_{reg} cells in thymus from WT mice (black circles, n = 11 mice) and *Pou2f3*$^{–/–}$ mice (black squares, n = 11 mice). Data are representative of two independent experiments and were analyzed by two-sided unpaired t-test. **b)** Top: representative flow cytometry plots of CD4^{+}CD8$^{–}$CD73$^{–}$ gated thymocytes from WT BALB/c and *Cd1d*$^{–/–}$ BALB/c mice, stained with antibodies to CD25 and FOXP3. Bottom: percentages of CD4^{+}CD8$^{–}$CD73$^{–}$CD25^{+}FOXP3$^{–}$ T_{reg}P cells (left) and CD4^{+}CD8$^{–}$CD73$^{–}$CD25$^{–}$FOXP3^{lo} T_{reg}P cells (right) in WT BALB/c (back circles) and *Cd1d*$^{–/–}$ BALB/c (black squares) mice. Data are representative of two independent experiments, n = 6 WT and 11 *Cd1d*$^{–/–}$ mice and were analyzed by two-sided unpaired t-test. All data are displayed as mean ± s.d. *P < 0.05, **P < 0.005, ***P < 0.0001; NS, not significant.

suppressor activity in FOXP3^{lo} T_{reg}P cell–derived T_{reg} cells is normal. Finally, we used MOG:I-A^{b} tetramers in combination with magnetic bead enrichment approaches to identify MOG:I-A^{b}-specific T_{reg} cells and T_{reg}P cells in the thymus of WT mice. We found MOG:I-A^{b}-specific T cells in the CD25^{+} T_{reg}P cell and mature T_{reg} cell subsets but observed only one MOG:I-A^{b}-specific T cell among FOXP3^{lo} T_{reg}P cells in the 15 mice examined (Figure 3.17 a,b), suggesting that MOG:I-A^{b}-specific T_{reg} cells are almost always generated from CD25^{+} T_{reg}P cells and are specifically required for protection against EAE.

3.3 Discussion

Here we found that both CD25^{+} T_{reg}P cells and FOXP3^{lo} T_{reg}P cells contribute to mature T_{reg} cell development in the thymus and that in our hands, they did so relatively equivalently. However, these two distinct T_{reg}P cell subsets differed in many important ways. They utilized different signaling pathways and enhancers for their differentiation, were affected in distinct ways by different stromal cells and cytokines and expressed distinct TCR repertoires and RNA transcriptomes. Most importantly, T_{reg} cells derived from the CD25^{+} T_{reg}P cell subset versus those derived from the FOXP3^{lo} T_{reg}P cell subset had distinct roles in protecting against autoimmunity. Thus, there are at least two different developmental pathways in the thymus that contribute substantially to the generation of the mature T_{reg} cell repertoire.

Several pieces of evidence support the notion that mature T_{reg} cells derived from both CD25^{+} T_{reg}P cells and FOXP3^{lo} T_{reg}P cells are required for full maintenance of immunotolerance. Both the *Foxp3*-GFP^{KIN} hypomorph and *Cns3*$^{-/-}$ mice showed defects in generating FOXP3^{lo} T_{reg}P cells and specific defects in immunotolerance. *Foxp3*-GFP^{KIN} mice have a relatively mild defect in immunotolerance that is revealed only on

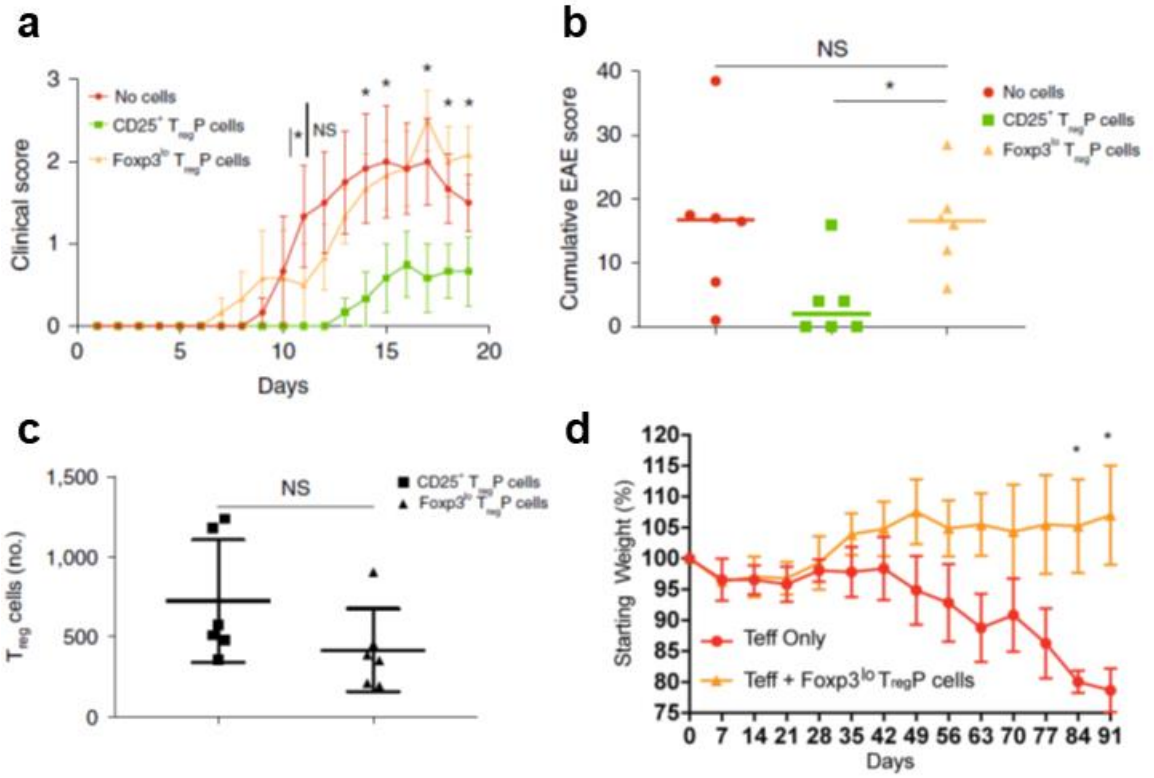

Figure 3.16. T_{reg} cells derived from $CD25^+$ and $FOXP3^{lo}$ $T_{reg}P$ cells are functionally distinct. **a)** Clinical score over 20-day time course of $MOG_{35–55}$ peptide–induced EAE in WT mic treated with no T_{reg} cells (red), $FOXP3^{lo}$ $T_{reg}P$ cells (orange) or $CD25^+$ $T_{reg}P$ cells (green). Data were analyzed by two-sided unpaired *t*-tests with Holm–Sidak multiple comparisons correction. Asterisks denote values with adjusted $P < 0.05$. Bars represent mean ± s.e.m. **b**, Cumulative EAE scores for control mice (no treatment, red) and mice injected with $CD25^+$ $T_{reg}P$ cells (green) or $FOXP3^{lo}$ $T_{reg}P$ cells (orange). Data were analyzed by Kruskal–Wallis test with Dunn's multiple comparisons test. Bar represents median. **c)** Number of donor T_{reg} cells recovered from the spleen of EAE-induced mice receiving $CD25^+$ $T_{reg}P$ cells (black squares) and $FOXP3^{lo}$ $T_{reg}P$ cells (black triangles). Data were analyzed by two-sided unpaired *t*-test. Bars represent mean ± s.d. In **a**–**c**, data represent two independent experiments, $n = 6$ mice per group. **d)** Data depicts % starting weight from $FOXP3^{lo}$ $T_{reg}P$ cell transfer over the time-course of transfer colitis experiment. Graph

represents 2 experiments, *n* = 4 mice per group. Data was analyzed by two-sided multiple *t* test with Holm-Sidak method. *adjusted p-value<0.05. Bars represent mean ± SEM.

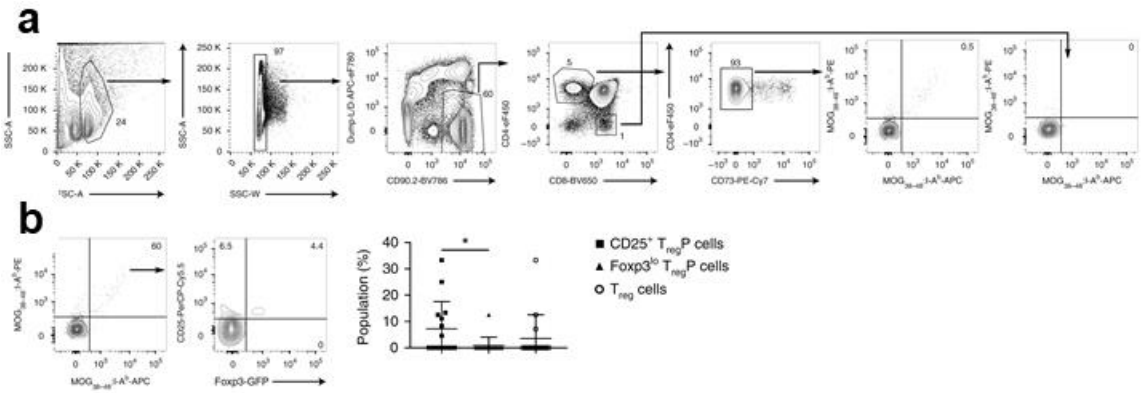

Figure 3.17. CD25^{+} but not FOXP3^{lo} T_{reg}P cells react with the self-antigen MOG. **a)** Representative gating strategy for thymic tetramer pulldowns. Dual-tetramer gates are drawn on CD8^{+} thymocytes such that ~0% of CD8^{+} thymocytes appear in the double-tetramer-positive gate. This gate was applied to CD4^{+}CD73^{-} thymocytes to identify bona fide $MOG_{38–48}$:I-Ab-specific thymocytes. **b)** Representative flow cytometry plots of MOG tetramer pulldowns, concatenated from six thymi from WT mice. Left: number of MOG:I-Ab dual-tetramer^{+} T cells within the CD4^{+}CD73^{-} thymocyte cell gate. Middle: percentage of MOG:I-Ab dual tetramer^{+} cells in CD25^{+} T_{reg}P cell, FOXP3^{lo} T_{reg}P cell and T_{reg} cell gates. Right: cumulative data showing percentages of CD25^{+} T_{reg}P cells (black squares), FOXP3^{lo} T_{reg}P cells (black triangles) and T_{reg} cells (open circles) in thymus from 15 WT mice. Data were analyzed by two-sided Wilcoxon matched-pairs signed-rank test, and represent three independent experiments. Bars represent mean ± s.d. *P < 0.05.

distinct genetic backgrounds[227,228]. In contrast, *Cns3*$^{-/-}$ mice have unique defects in immunotolerance, such as greater lung inflammation than that of WT mice[163]. In addition, *Cns3*$^{-/-}$ mice have increased titers of specific autoantibodies[163]. Because *Cns3*$^{-/-}$ mice selectively lack FOXP3^{lo} T_{reg}P cells but not CD25^{+} T_{reg}P cells, this suggests a unique role for FOXP3^{lo} T_{reg}P cell–derived mature T_{reg} cells in preventing autoimmunity.

Additional studies suggest a unique role for CD25^{+} T_{reg}P cells in promoting immune tolerance. The CaRE4 enhancer in the *Il2ra* locus harbors an autoimmunity risk variant that promotes susceptibility to inflammatory bowel disease but protection against diabetes[165–167]. Deletion of this enhancer resulted in a selective decrease in CD25^{+} T_{reg}P cells, suggesting that CD25^{+} T_{reg}P cell–derived T_{reg} cells have an important role in protecting against inflammatory bowel disease. Likewise, *Cns3*$^{-/-}$ mice exhibit increased protection against EAE[163]. Because T_{reg} cells in *Cns3*$^{-/-}$ mice are derived almost exclusively from CD25^{+} T_{reg}P cells, this suggests that CD25^{+} T_{reg}P cell–derived T_{reg} cells protect against EAE. We directly confirmed this idea by showing that CD25^{+} T_{reg}P cell–derived T_{reg} cells provide robust protection against EAE, while FOXP3^{lo} T_{reg}P cell–derived T_{reg} cells do not. Thus, modulating the frequency of CD25^{+} T_{reg}P cells results in differential protection against autoimmunity. This observation has important translational implications, as it indicates that it is possible to identify T_{reg} cells with selected TCRs that have uniquely potent efficacy against specific types of autoimmune disease.

The presence of more than one developmental pathway leading to mature T_{reg} cells raises the question of why such a system has evolved. T_{reg} cells are required to prevent responses to self-antigens and commensal antigens, as well as to dampen anti-pathogen immune responses once these agents have been cleared. Establishing such a diverse repertoire requires the generation of T_{reg} cells able to recognize thymic self-antigens with high affinity. Such a population could be generated by a process of agonist selection in

the thymus. However, agonist selection alone is unlikely to generate the broad repertoire of T_{reg} cells needed to prevent immune responses to commensal organisms, or to limit responses to foreign pathogens. In many ways this resembles the problem facing conventional thymocytes, which must generate a repertoire capable of recognizing a vast array of antigens that they never encounter in the thymus. Thus, establishing a broader, non-self-focused repertoire for T_{reg} cells may require a process that resembles positive selection for conventional thymocytes. We showed that T_{reg} cells developed through two distinct developmental programs that exhibit such characteristics. $CD25^{+}$ $T_{reg}P$ cells developed through a process of agonist selection that shares many similarities with the underlying process of negative selection and would result in mature T_{reg} cells focused on TCRs with high affinity for thymic self-antigens. $FOXP3^{lo}$ $T_{reg}P$ cells developed through a mechanism that may be akin to positive selection, resulting in a broader repertoire capable of reacting with both self-antigens and non-self-antigens. Thus, thymic T_{reg} cells derived from $FOXP3^{lo}$ $T_{reg}P$ cells could complement the function of induced peripheral T_{reg} cells. Our model also suggests that the *Cns3* regulatory element evolved, in part, to promote the development of mature T_{reg} cells through the $FOXP3^{lo}$ $T_{reg}P$ cell pathway. Finally, the genetic variability that altered the relative balance of these two developmental pathways also altered the T_{reg} cell repertoire and correlated with susceptibility to distinct forms of autoimmunity. Given the differences in signaling pathways and cytokines that control these two developmental pathways, specific targeting of each T_{reg} cell population could help patients with various autoimmune defects.

Chapter 4: Visualizing thymic T_{reg} cell differentiation using single-cell sequencing

4.1 Background

Canonical T_{reg} cells are derived from the $CD4^+$ T cell lineage. While some controversy exists in determining whether T_{reg} cell development is initiated from $CD4^+CD8^+$ or CD4SP thymocytes[237–239], most studies identify CD4SP as the origin of T_{reg} cell commitment[63,64,240]. T_{reg} cell development is defined as a two-step process- step one being driven by agonist stimulation of the TCR by self-antigens generating $T_{reg}P$ cells and step two being dependent on STAT5 activation in $T_{reg}P$ cells downstream of IL-2 or IL-15 stimulation[63,64]. However, whether heterogeneity or transitional cells exist within this paradigm remains unknown.

Flow cytometry has identified some heterogeneity within the $CD25^+$ $T_{reg}P$ cell population. $CD25^+$ thymocytes that express high amounts of GITR and CD122 are thought to be the direct progenitors of T_{reg} cells. This is likely due to the augmented sensitivity to IL-2 stimulation garnered from increased CD122, the IL-2 receptor β chain, and GITR expression[185,241]. However, $CD25^+$ $T_{reg}P$ cells that express lower amounts of these receptors are still capable of converting into mature T_{reg} cells[63]. Further, no such discrimination has been defined for the $FOXP3^{lo}$ $T_{reg}P$ cell pathway.

Single cell RNA-seq studies in the thymus have been used to understand early commitment to the T cell fate and to take a general census of cells in the thymus[242,243]. However, these latter studies, that do include cells of the T_{reg} cell lineage, lack sufficient cell numbers to effectively stratify small populations like thymic $T_{reg}P$ and T_{reg} cells, which comprise approximately 0.05-0.01% of total thymocytes. In order to address this issue, we performed single cell RNA-seq analysis of equal ratios of $CD25^+$ $T_{reg}P$, $FOXP3^{lo}$ $T_{reg}P$, mature T_{reg} cells, CD4SP and $CD4^+CD8^+$DP thymocytes. Analysis of the conventional

CD4SP population identified a number of markers up- or down-regulated throughout thymocytes maturation. Further, we identified an agonist selection signature cluster associated with both $CD25^+$ and $FOXP3^{lo}$ $T_{reg}P$ cell pathways. Finally, using the transcriptional changes we defined for CD4SP maturation, we describe the intermediate populations of T_{reg} cell development from each $T_{reg}P$ pathway. This data set can serve as an atlas for CD4SP maturation and T_{reg} cell development from agonist selection to mature T_{reg} cells. Further, we captured the recirculating and resident thymic T_{reg} cell subset which will be discussed in chapter 5.

4.2 Results

Maturation of CD4 single positive thymocytes

Following TCR V(D)J recombination and positive selection, $CD4^+CD8^+$ double positive (DP) thymocytes commit to the $CD4^+$ or $CD8^+$ lineage. For the $CD4^+$ T cell lineage this decision is orchestrated by the activation of transcription factors TOX, GATA3 and ThPOK and repression of $CD8^+$ T cell lineage transcription factors such as RUNX3[244]. In this data set, we focused on the $CD4^+$ T cell lineage as this is the source of thymically derived T_{reg} cells. For this experiment we sorted $CD73^-$- $CD4^+CD8^+$, $CD4^+CD25^-FOXP3^-$, $CD4^+CD25^+FOXP3^-$, $CD4^+CD25^-FOXP3^{lo}$ and $CD4^+CD25^+FOXP3^+$ and $CD73^+$ $CD4^+FOXP3^+$ from the thymi of *TCliβ* x *Tcra*$^{+/-}$ mice and performed combined scRNAseq and single cell TCR sequencing (scTCRseq) using the 10X Genomics 5' solution. Following sequencing, our collaborator at the University of Minnesota Supercomputing Institute, Rebecca LaRue, performed clustering analysis using Seurat[245]. At a resolution of 0.6, we identified 18 distinct clusters. Three clusters represented contaminating populations, B cells, dying cells and low-quality cells, which were excluded from further analysis. Within the remaining 15 clusters we identified 2 major clusters derived from

conventional CD4^{+} thymocytes as evidenced by detection of a population specific "hashtag" (Figure 4.1 a,b).

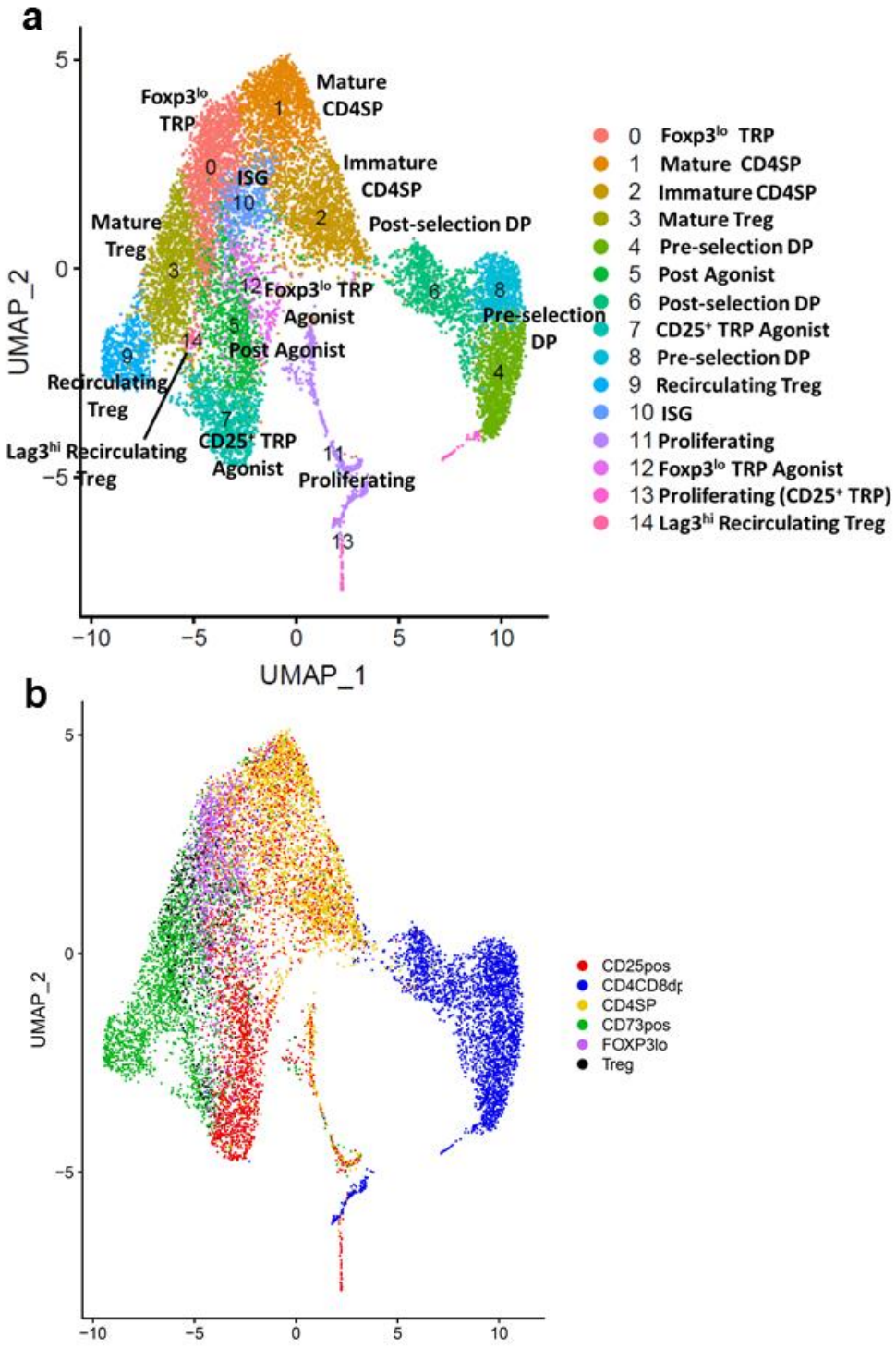

Figure 4.1. Identification of $CD4^+$ thymocyte and T_{reg} cell lineage developmental stages. **a)** UMAP dimension reduction projection and clusters identities from Seurat analysis at a resolution of 0.6. **b)** Each sorted population within the data set was stained with a unique 'hashtag" antibody. Color denotes the detection of the population specific hashtag in a cell. All data presented represents cells expressing a single hashtag to exclude doublets.

The conventional CD4SP thymocyte clusters were defined by differences in maturation status. Cluster 2, which resides closest to $CD4^+CD8^+$ thymocyte clusters within the UMAP plot, was identified as an immature CD4SP population while Cluster 1 was identified as more mature CD4SP (Figure 4.1 a,b). The immature CD4SP cluster maintained elevated expression of $CD4^+$ T cell lineage transcription factors that are upregulated in $CD4^+CD8^+$ thymocytes, such as *Tox*, *Gata3*, *Satb1* and *Zbtb7b* (ThPOK)[244], while the mature CD4SP cluster had downregulated these factors (Table 4.1). Additionally, the immature CD4SP cluster expresses more of the chemokine receptor *Ccr9*, associated with localization in the thymic cortex, while the mature CD4SP cluster expresses more *Ccr7*, the chemokine receptor required to transition to the thymic medulla where single-positive thymocytes undergo the final round of negative selection and complete maturation[246]. A type 1 interferon gene signature, found primarily in the thymic medulla, is associated with the maturation of single-positive thymocytes[223]. We indeed find that mature CD4SP upregulate canonical IFN target genes such as *Stat1*, *Irf7*, and *H2-K1* (Table 4.1). Further, mature CD4SP upregulate *Klf2*, and its downstream target *S1pr1* (Table 4.1), a migratory receptor required for T cells to exit the thymus and traffic within the lymphatics[247,248], supporting the idea that mature CD4SP have gained competence to leave the thymus. Many of the above markers have been associated with development through the CD4SP lineage previously. However, this data set also identified novel markers previously unappreciated in CD4SP development. The integrin *Itgb7*, previously associated with homing of T cells to the gut and inflamed tissues[249], is highly upregulated in mature CD4SP versus immature CD4SP (Table 4.1). Further, *Ms4a4b* and *Ms4a6b* exhibit very strong association with CD4SP maturation and are nearly ubiquitously expressed in the mature CD4SP cluster (Table 4.1). The understanding of the MS4A4B and MS4A6B proteins in T cell biology is limited.

p value	avg logFC	% cells+ C1	% cells+ C2	p value adj	Gene Name
7.19E-279	**-1.918297686**	0.573	0.942	1.06E-274	**Itm2a**
3.33E-216	**-1.65528493**	0.101	0.652	4.93E-212	**Ccr9**
4.35E-112	**-1.016189309**	0.262	0.619	6.44E-108	**Ckb**
2.47E-185	**-1.004182084**	0.627	0.914	3.66E-181	**Satb1**
1.58E-73	**-0.912742754**	0.083	0.354	2.34E-69	**Id2**
5.72E-77	**-0.811567767**	0.282	0.577	8.46E-73	**Tox**
3.82E-26	**-0.780630594**	0.131	0.288	5.66E-22	**Egr1**
8.85E-28	**-0.696258543**	0.129	0.285	1.31E-23	**Cd69**
1.56E-29	**-0.599272968**	0.26	0.425	2.31E-25	**Cd40lg**
4.59E-65	**-0.599038179**	0.514	0.744	6.79E-61	**Cd28**
9.45E-25	**-0.557093895**	0.384	0.529	1.40E-20	**Bcl2**
2.45E-24	**-0.550536203**	0.193	0.342	3.63E-20	**Gata3**
9.14E-21	**-0.528825998**	0.139	0.271	1.35E-16	**Ccr8**
1.31E-17	**-0.482717482**	0.238	0.362	1.94E-13	**Socs1**
2.23E-22	**-0.454197779**	0.48	0.603	3.30E-18	**Cd5**
1.37E-42	**-0.430615513**	0.613	0.77	2.03E-38	**Itgb2**
1.68E-07	**-0.426710903**	0.194	0.262	0.002488918	**Izumo1r**
2.88E-19	**-0.41739602**	0.435	0.556	4.26E-15	**Il7r**
2.06E-16	**-0.3501366**	0.197	0.318	3.04E-12	**Bach2**
5.33E-12	**-0.334315578**	0.79	0.817	7.88E-08	**Lef1**
3.22E-19	**-0.321236798**	0.723	0.785	4.76E-15	**Tcf7**
7.00E-16	**-0.311083385**	0.189	0.309	1.03E-11	**Itgal**
3.05E-08	**-0.307239336**	0.271	0.345	0.000451783	**Tnfrsf18**
7.65E-12	**-0.303230409**	0.199	0.302	1.13E-07	**Icos**
9.64E-11	**-0.298022164**	0.222	0.316	1.43E-06	**Zbtb7b**
1.01E-21	**-0.287625318**	0.773	0.824	1.49E-17	**Ybx1**
2.34E-11	**-0.268938313**	0.691	0.755	3.46E-07	**Cd4**
1.42E-28	**-0.256885861**	0.946	0.953	2.09E-24	**Il2rg**
6.10E-15	**0.284967586**	0.289	0.167	9.03E-11	**Il27ra**
7.44E-25	**0.288306922**	0.742	0.541	1.10E-20	**Slfn2**
2.88E-35	**0.352904619**	0.862	0.699	4.26E-31	**Ccr7**
7.43E-48	**0.376656538**	0.559	0.274	1.10E-43	**Id3**
8.03E-28	**0.383651155**	0.625	0.423	1.19E-23	**Stat1**
3.86E-39	**0.403108827**	0.758	0.558	5.71E-35	**Selplg**
2.00E-29	**0.406386208**	0.286	0.115	2.96E-25	**Ifi203**
1.40E-27	**0.410263205**	0.419	0.226	2.07E-23	**Tgfbr2**
1.36E-27	**0.451960265**	0.349	0.175	2.02E-23	**Irf7**
6.88E-33	**0.463298934**	0.369	0.17	1.02E-28	**Foxo1**
2.23E-108	**0.542496906**	0.971	0.812	3.30E-104	**B2m**
2.42E-63	**0.596778592**	0.263	0.035	3.59E-59	**S1pr4**
1.29E-126	**0.601036573**	0.981	0.772	1.91E-122	**H2-D1**
1.19E-68	**0.67586725**	0.516	0.208	1.76E-64	**Ass1**
1.65E-89	**0.693334937**	0.701	0.326	2.44E-85	**Gimap3**
4.09E-103	**0.824400619**	0.619	0.229	6.05E-99	**Itgb7**
7.57E-110	**0.888925926**	0.535	0.144	1.12E-105	**Sell**
1.13E-214	**0.915358788**	0.983	0.64	1.68E-210	**H2-K1**
4.58E-185	**1.119589058**	0.763	0.224	6.77E-181	**Ms4a6b**
3.23E-189	**1.317121042**	0.519	0.019	4.78E-185	**S1pr1**
2.44E-221	**1.351460132**	0.796	0.214	3.60E-217	**Klf2**
0	**1.667783522**	0.9	0.238	0	**Ms4a4b**

Table 4.1. Selected genes associated with immature or mature CD4SP clusters. Genes in light orange are upregulated in cluster 2 (immature CD4SP) versus cluster 1 (mature CD4SP) and genes in orange are upregulated in cluster 1 versus cluster 2.

Expression of MS4A4B is associated with Th1 responses and enhancement of GITR signaling to facilitate IL-2 production[222,250]. MS4A4B also heightens TCR sensitivity of conventional T cells and T_{reg} cells[222]. We find here that expression of *Ms4a4b* and *Ms4a6b* is a reliable identifier of mature thymocyte clusters.

Immature thymocytes also express genes associated with TCR signaling initiated during $CD4^+CD8^+$ thymocyte positive selection. The immature thymocyte cluster expresses more *Cd69*, *Cd5* and *Itm2a* (Table 4.1), all markers associated with thymocytes receiving the requisite TCR signaling for positive selection[251]. Interestingly, immature thymocytes also expressed more of the brain associated creatine kinase *Ckb* (Table 4.1). TCR signaling requires the activation of numerous protein kinases to facilitate signal transduction, all dependent on intracellular ATP to provide the phosphoyl group to phosphorylate target proteins. Creatine kinases act to bolster and stabilize the intracellular ATP pool and CKB protein is low in $CD4^+CD8^+$ thymocytes but upregulated in single-positive thymocytes[252]. Expression of *Ckb* may represent a mechanism to bolster TCR signaling in the later stages of CD4SP development to facilitate induction of immune tolerance, either by T_{reg} cell induction or negative selection. Indeed, ectopic expression of *Ckb* in $CD4^+CD8^+$ thymocytes causes upregulation of BIM and NUR77[253,254], two proteins involved in potentiating negative selection, and increases cell death in $CD4^+CD8^+$ thymocytes[252]. TCR signaling targets, as well as genes involved in potentiating that signal such as *Ckb*, correlate with less mature conventional CD4SP thymocytes. Analysis of all the markers discussed above allows for the placement of cells and populations within across the spectrum of maturity.

In addition to finding the expected populations representing distinct CD4SP maturation stages, we also identified a unique thymocyte cluster represented by high expression of interferon stimulated genes (ISG). The ISG signature is represented in cluster 10 and

contains cells from both conventional and T_{reg} cell lineage populations (Figure 4.1 a,b). The ISG cluster signature is distinct from the normal "tonic" interferon signature associated with thymocyte maturation (Table 4.2). The ISG signature population expresses some genes unique to this strong interferon stimulation, such as *Ifit1* and *Ifit3*, and elevated expression of genes associated with tonic interferon driven thymocyte maturation, such as *Stat1* and *Irf7* (Table 4.2). While interferon is known to be produced in the thymic medulla[255] we do not yet understand what these cells represent in the thymus. However, this population is observed in other scRNAseq T_{reg} experiments outside the thymus and ISG signature T_{reg} cells were recently found to be negatively correlated with the development of house dust mite allergy[256]. Altogether, scRNAseq analysis of CD4SP thymocytes provides novel insight into the molecular changes associated with maturation and identifies a previously undescribed population of CD4SP thymocytes.

Identification and characterization of agonist selection signature clusters

T_{reg} cell development is initiated by strong TCR stimulation of self-reactive thymocytes. scRNAseq analysis of T_{reg} cell lineage subsets and conventional thymocytes revealed two distinct clusters representing agonist selection, clusters 7 and 12 (Figure 4.1). Cluster 7 is comprised primarily of $CD25^{+}$ T_{reg}P cells while cluster 12 contains $FOXP3^{lo}$ T_{reg}P cells, conventional thymocytes as well as some $CD25^{+}$ T_{reg}P cells (Figure 4.1). $CD25^{+}$ and $FOXP3^{lo}$ T_{reg}P cell subsets receive different strengths of TCR stimulation and are at different maturation states[96]. Thus, these two distinct agonist selection signatures, one dominated by $CD25^{+}$ T_{reg}P cells and the other containing $FOXP3^{lo}$ T_{reg}P cells, may differ due differences in TCR signal strength and maturation state.

Some TCR responsive genes are shared between these two clusters while others are biased towards a single cluster. The $CD25^{+}$ and $FOXP3^{lo}$ T_{reg}P agonist selection clusters

p value	**avg logFC**	% cells+ C1	% cells+ C1(	p value adj	**Gene Name**
8.10E-173	-1.748163159	0.2	0.826	1.20E-168	Ifit1
4.31E-152	-1.74122292	0.309	0.852	6.38E-148	Isg15
1.56E-123	-1.668691546	0.07	0.524	2.31E-119	Ifit3
1.73E-98	-1.321885896	0.106	0.518	2.56E-94	Isg20
9.04E-90	-1.226708317	0.11	0.502	1.34E-85	Usp18
6.70E-102	-1.096323184	0.349	0.798	9.91E-98	Irf7
7.85E-62	-1.042333847	0.122	0.441	1.16E-57	Slfn5
3.00E-100	-1.039177356	0.625	0.921	4.44E-96	Stat1
5.29E-61	-1.001804917	0.027	0.265	7.82E-57	Foxp3
9.52E-62	-0.993422538	0.391	0.702	1.41E-57	Bst2
4.44E-74	-0.992725967	0.339	0.7	6.57E-70	Ifi209
1.92E-32	-0.955891514	0.165	0.385	2.84E-28	Tnfrsf4
2.34E-57	-0.926662532	0.034	0.271	3.46E-53	Ikzf2
7.77E-84	-0.866257365	0.856	0.955	1.15E-79	Ifi27l2a
3.10E-64	-0.83764841	0.617	0.852	4.58E-60	Ifi47
7.54E-31	-0.748864495	0.069	0.251	1.12E-26	Il2rb
7.32E-17	-0.672722029	0.238	0.389	1.08E-12	Socs1
9.68E-23	-0.647447554	0.271	0.455	1.43E-18	Tnfrsf18
1.50E-49	-0.580999902	0.9	0.943	2.22E-45	Ms4a4b
2.90E-07	-0.400004763	0.217	0.304	0.004290119	Ikzf3
1.62E-09	-0.382926739	0.394	0.482	2.39E-05	Foxn3
1.54E-08	-0.37082574	0.535	0.585	0.000228133	Sell
6.69E-10	-0.360710601	0.48	0.591	9.90E-06	Cd5
1.58E-07	-0.330659191	0.426	0.512	0.002343546	Nfkbia
0.000100962	-0.328590448	0.194	0.263	1	Izumo1r
1.74E-13	-0.325132939	0.763	0.806	2.58E-09	Ms4a6b
0.00016811	-0.286138492	0.282	0.34	1	Tox
7.73E-12	0.333328374	0.252	0.101	1.14E-07	Myc
1.57E-24	0.488282375	0.516	0.229	2.32E-20	Ass1
1.10E-25	0.57811808	0.435	0.164	1.62E-21	Il7r

Table 4.2. Selection gene associated with the “Interferon Signature” thymocyte subset. Genes upregulated in cluster 10 (ISG) versus cluster 1 (mature CD4SP) are in light blue while genes upregulated in cluster 1 versus cluster 10 are in orange.

both express increased *Nr4a1*, *Tnfrsf9*, *Ikzf2*, *Tagap*, *Tnfrsf18*, and *Tnfrsf4* (Table 4.3). However, *Nr4a1* is more highly expressed in the FOXP3^{lo} T_{reg}P agonist selection cluster while *Tnfrsf9* is more highly expressed in CD25^{+} T_{reg}P agonist selection cells (Table 4.3). Expression of *Tnfrsf9*, or 4-1BB, is used as a surrogate marker of T cells encountering an agonist TCR signal in effector T cells[257,258]. Increased detection of*Tnfrsf9* in CD25^{+} T_{reg}P agonist selection cells suggests that CD25^{+} T_{reg}P agonist selection cells have received strong TCR stimulation. Additionally, the TCR response genes *Egr 1* and *Egr2*, both early response targets of TCR signaling that promote positive selection[259,260], are both highly expressed in FOXP3^{lo} T_{reg}P agonist selection cells but not in the CD25^{+} T_{reg}P agonist selection cluster (Table 4.3). We previously postulated that FOXP3^{lo} T_{reg}P cells may arise via a process more similar to positive selection via repeated low-affinity TCR interactions while CD25^{+} T_{reg}P cells arise from acute strong TCR stimulation. Association of *Egr1* and *Egr2* with the FOXP3^{lo} T_{reg}P agonist selection cluster may support this hypothesis. Yet, *Nr4a1* is expressed in the majority of the FOXP3^{lo} T_{reg}P agonist selection cluster and only ~40% of the CD25^{+} T_{reg}P agonist selection cluster (Table 4.3). Nonetheless, this may be due to persistent low-level TCR activation maintaining *Nr4a1* expression in FOXP3^{lo} T_{reg}P agonist selection cluster while *Nr4a1* is lost following cessation of the acute TCR signal in CD25^{+} T_{reg}P agonist selection cells, thus not representing absolute TCR signal strength here.

Genes related to the maturation of CD4SP thymocytes are differentially expressed between these two agonist selection clusters. Indeed, FOXP3^{lo} T_{reg}P agonist selection cells express more *Itgb7*, *Sell*, *Klf2*, and *S1pr1* (Table 4.3). Expression of these genes, all related to trafficking out of the thymus, suggest these cells are gaining more competence to leave the thymus. Further, *Stat1* and *Irf7*, targets of maturation related tonic IFN signaling, are also more highly expressed in FOXP3^{lo} T_{reg}P agonist selection

p value	**avg logFC**	% cells+ C1	% cells+ C2	p value adj	**Gene Name**
1.60E-94	**-2.465301196**	0.079	0.605	2.37E-90	**Egr1**
1.25E-96	**-1.717864242**	0.394	0.914	1.85E-92	**Nr4a1**
1.28E-62	**-1.436507143**	0.058	0.442	1.89E-58	**Egr2**
1.72E-57	**-1.392703208**	0.234	0.657	2.55E-53	**Cd69**
3.01E-61	**-1.208463008**	0.471	0.829	4.45E-57	**Junb**
2.32E-36	**-1.059585363**	0.324	0.635	3.43E-32	**Nfkbid**
1.83E-76	**-1.053349771**	0.746	0.945	2.71E-72	**Btg1**
2.53E-34	**-1.040250618**	0.468	0.704	3.74E-30	**Ms4a4b**
2.07E-22	**-1.017199298**	0.371	0.583	3.05E-18	**Id3**
7.42E-40	**-1.014629888**	0.185	0.517	1.10E-35	**Nr4a3**
7.77E-29	**-0.983813897**	0.232	0.492	1.15E-24	**Ms4a6b**
1.21E-23	**-0.912920684**	0.238	0.472	1.79E-19	**Irf1**
9.63E-59	**-0.874275995**	0.905	0.959	1.42E-54	**Trbv19**
1.84E-28	**-0.870493129**	0.234	0.492	2.73E-24	**Itgb7**
2.14E-15	**-0.821986162**	0.141	0.309	3.16E-11	**S1pr1**
1.82E-28	**-0.808611831**	0.465	0.704	2.70E-24	**Vim**
3.98E-18	**-0.802923748**	0.198	0.39	5.88E-14	**Slfn1**
5.68E-20	**-0.794974549**	0.198	0.414	8.40E-16	**Sell**
4.86E-69	**-0.780908681**	0.883	0.981	7.18E-65	**Itm2b**
8.52E-17	**-0.760817769**	0.237	0.423	1.26E-12	**Bcl2**
5.26E-22	**-0.724521453**	0.831	0.829	7.78E-18	**Nfkbia**
4.54E-19	**-0.650633272**	0.538	0.646	6.72E-15	**Itk**
2.78E-29	**-0.642459989**	0.568	0.735	4.11E-25	**Skap1**
8.34E-14	**-0.631857366**	0.161	0.326	1.23E-09	**Ifi203**
1.72E-15	**-0.630108901**	0.22	0.392	2.55E-11	**Cdkn2d**
8.07E-17	**-0.620361009**	0.449	0.583	1.19E-12	**Satb1**
1.41E-07	**-0.611624674**	0.252	0.365	0.002082538	**Izumo1r**
7.70E-27	**-0.606787399**	0.764	0.843	1.14E-22	**Cd5**
7.25E-16	**-0.590332334**	0.584	0.68	1.07E-11	**Stat1**
6.81E-13	**-0.586529003**	0.167	0.323	1.01E-08	**Ifi209**
5.66E-17	**-0.582641792**	0.535	0.644	8.37E-13	**Lef1**
1.25E-16	**-0.559796412**	0.606	0.691	1.84E-12	**Tgfb1**
9.39E-37	**-0.558914601**	0.882	0.942	1.39E-32	**Lck**
1.65E-18	**-0.558642856**	0.442	0.624	2.44E-14	**Slfn2**
4.98E-11	**-0.554134352**	0.212	0.359	7.36E-07	**Irf7**
6.81E-40	**-0.546911716**	0.94	0.972	1.01E-35	**Cd3g**
1.73E-12	**-0.519023833**	0.493	0.575	2.55E-08	**Jak1**
1.26E-09	**-0.516681016**	0.274	0.401	1.87E-05	**Rel**
1.33E-08	**-0.478227816**	0.142	0.257	0.000196039	**Ift80**
0.000194039	**-0.473357731**	0.356	0.431	1	**Myc**

1.61E-05	**-0.468608132**	0.311	0.398	0.238427161	**Isg15**
5.57E-39	**-0.466700038**	0.981	0.981	8.24E-35	**Cd3e**
1.67E-31	**-0.46456292**	0.951	0.964	2.46E-27	**Cd3d**
1.95E-05	**-0.462534419**	0.227	0.32	0.287832569	**Foxp3**
1.68E-06	**-0.443974919**	0.457	0.533	0.024833455	**Klf2**
2.12E-05	**-0.442178537**	0.399	0.467	0.313778632	**Bcl2a1b**
0.002739833	**-0.441482264**	0.392	0.42	1	**Gata3**
2.08E-08	**-0.441229413**	0.327	0.428	0.000307059	**Tox**
2.36E-06	**-0.431477693**	0.659	0.657	0.03496302	**Ifi47**
1.54E-06	**-0.424685431**	0.44	0.486	0.022755272	**Ccnd3**
6.26E-06	**-0.418176374**	0.297	0.373	0.092603175	**Trac**
6.14E-08	**-0.40730112**	0.544	0.597	0.000907418	**Cd4**
3.24E-21	**-0.397630074**	0.943	0.95	4.80E-17	**B2m**
1.99E-08	**-0.39421496**	0.575	0.63	0.000294485	**Cd28**
4.80E-06	**-0.390920664**	0.259	0.376	0.070989377	**Cd40lg**
1.03E-14	**-0.383658802**	0.845	0.895	1.52E-10	**Lat**
0.00015489	**-0.369140665**	0.254	0.315	1	**Irf9**
2.56E-09	**-0.364789666**	0.673	0.685	3.79E-05	**Itgb2**
0.006405557	**-0.339173652**	0.24	0.276	1	**Igf2r**
0.00141213	**-0.335799634**	0.353	0.384	1	**Jund**
0.004419932	**-0.334265053**	0.285	0.329	1	**Traf1**
1.30E-05	**-0.314461658**	0.488	0.519	0.192423205	**Pak2**
0.013185725	**-0.306180614**	0.296	0.323	1	**Icos**
0.00133005	**-0.29750901**	0.311	0.359	1	**Stat3**
0.016297239	**-0.296365245**	0.433	0.423	1	**Foxp1**
0.051567166	**-0.278673307**	0.235	0.251	1	**Ifnar1**
9.44E-05	**-0.265991527**	0.602	0.641	1	**Ccnd2**
0.001292618	**-0.261035953**	0.359	0.401	1	**Irf2**
1.98E-11	**0.259252233**	0.287	0.094	2.93E-07	**Mcm7**
8.63E-11	**0.294613827**	0.617	0.34	1.28E-06	**Bax**
8.46E-19	**0.37799212**	0.339	0.077	1.25E-14	**Siva1**
1.36E-18	**0.408045267**	0.303	0.061	2.01E-14	**Nme1**
4.53E-22	**0.437918198**	0.72	0.345	6.70E-18	**Pdcd5**
6.56E-21	**0.450969719**	0.251	0.019	9.70E-17	**Serf1**
4.56E-17	**0.461398482**	0.341	0.094	6.74E-13	**Mcm6**
1.16E-18	**0.475075271**	0.804	0.528	1.72E-14	**Serp1**
4.53E-17	**0.556783137**	0.571	0.282	6.70E-13	**Bmyc**
7.01E-95	**0.579220383**	1	0.997	1.04E-90	**Ppia**
6.67E-56	**0.782343415**	0.959	0.481	9.86E-52	**Tnfrsf9**
6.36E-69	**0.789003278**	0.973	0.738	9.41E-65	**Ybx1**
3.10E-70	**1.232090997**	0.833	0.254	4.59E-66	**Lad1**
3.56E-125	**1.535813144**	0.995	0.552	5.27E-121	**Mif**

Table 4.3. Selected genes differentially regulated between $CD25^+$ $T_{reg}P$ and $FOXP3^{lo}$ $T_{reg}P$ agonist selection clusters. Genes upregulated in cluster 12 ($FOXP3^{lo}$ $T_{reg}P$ agonist selection) versus cluster 7 ($CD25^+$ $T_{reg}P$ agonist selection) are in purple and genes upregulated in cluster 7 versus cluster 12 are in teal.

cluster (Table 4.3). Based on the analysis in Figure 4.1, expression of *Ms4a4b* and *Ms4a6b* are closely associated with the maturation state of CD4SP thymocytes. While expression of *Ms4a4b* and *Ms4a6b* are lower in both agonist selection clusters than mature CD4SP, the FOXP3^{lo} T_{reg}P agonist selection cluster has significantly higher expression than the CD25^{+} T_{reg}P agonist selection cluster (Table 4.3). This data agrees with the previous observation that FOXP3^{lo} T_{reg}P cells are older, as evidenced by decreased RAG2-GFP signal, and more mature than CD25^{+} T_{reg}P cells[96]. This scRNAseq analysis of the starting points in T_{reg} cell development suggests that TCR selection of each T_{reg}P cell pathway is occurring at distinct maturation states in CD4SP development.

It is worth noting that the FOXP3^{lo} T_{reg}P agonist selection cluster contains what appears to be an intermediate population between immature CD4SP and the CD25^{+} T_{reg}P agonist selection cluster. This small group of cells is comprised of conventional CD4SP which transition to CD25^{+} T_{reg}P cells as the cells become closer to the CD25^{+} T_{reg}P agonist selection cluster (Figure 4.1). We were unable to resolve this population into a distinct cluster, but this group of cells may represent the transition of highly self-reactive conventional CD4SP upregulating CD25 and committing to the CD25^{+} T_{reg}P cell lineage.

Development and maturation of T_{reg} cells from CD25^{+} T_{reg}P cells

While T_{reg} cell development is described as a two-step process, it is unclear if major intermediate populations exist. Previous reports have suggested that CD25^{+} T_{reg}P cells contain a subpopulation of GITR^{hi}CD122^{hi} cells that are the most efficient in responding to IL-2 and differentiating into mature T_{reg} cells[185,241]. In this model, activation of c-Rel downstream of CD28 ligation caused upregulation of CD122 and the ability to efficiently respond to IL-2 to facilitate T_{reg} cell differentiation. However, beyond acquisition of cytokine responsiveness the developmental progression of T_{reg}P to mature T_{reg} cells is incompletely understood.

Within the CD25$^+$ T_{reg}P cell population we do indeed find two populations- cluster 7, or the CD25$^+$ T_{reg}P agonist selection cluster, and cluster 5, labelled as a “post-agonist” selection. The post-agonist cluster lies between the agonist selection cluster and the mature T_{reg} cell cluster, suggesting that this population is an intermediate in T_{reg} cell development in the CD25$^+$ T_{reg}P cell pathway (Figure 4.1). Compared to the CD25$^+$ T_{reg}P agonist selection cluster the post-agonist populations express less *CD24a* and more *Itgb7*, *Ms4a4b*, *Ms4a6b*, and genes associated with tonic IFN signaling during CD4SP maturation (Table 4.4). Post-agonist cells downregulate expression of TCR signaling targets, including *Nr4a1*, *Tnfrsf9*, and *Tnfrsf4* (Table 4.4). Upregulation of maturation genes and downregulation of TCR signaling genes suggests that post-agonist cells do represent an intermediate population in T_{reg} cell development from CD25$^+$ T_{reg}P. However, *Il2rb* and *Tnfrsf18*, which encode CD122 and GITR respectively, are unchanged between the CD25$^+$ T_{reg}P agonist selection and post-agonist clusters. In fact, it is the next transition, post-agonist cell to mature T_{reg} cells, when *Il2rb* and *Tnfrsf18* are upregulated (Table 4.5). Additionally, the STAT5 target genes, *Cish* and *Socs1*, are upregulated in mature T_{reg} cell versus post-agonist cells, suggesting that these post-agonist cells have not received γC cytokine stimulation to activate STAT5 (Table 4.5). A noteworthy anomaly in this data is the loss of *Il2ra*, or CD25, expression in post-agonist cells. CD25 expression is induced both by strong TCR signaling and STAT5 activation. The loss of *Il2ra* expression in post-agonist cells may represent the loss of TCR induced expression of *Il2ra* prior to cytokine driven reactivation upon the final, STAT5 dependent, step of T_{reg} cell development. Indeed, the post-agonist cluster is largely derived from cells that were sorted as expressing CD25 on their cell surface (Figure 4.1). Therefore, while these cells

p value	avg logFC	% cells+ C1	% cells+ C2	p value adj	Gene Name
1.18E-52	**-0.99551959**	0.067	0.356	1.75E-48	**Myc**
5.62E-42	**-0.802184229**	0.721	0.86	8.31E-38	**Tnfrsf4**
4.76E-45	**-0.743178466**	0.064	0.324	7.04E-41	**Nfkbid**
4.53E-18	**-0.741783708**	0.218	0.394	6.70E-14	**Nr4a1**
4.74E-50	**-0.725068417**	0.097	0.399	7.01E-46	**Il2ra**
1.20E-30	**-0.632954877**	0.178	0.42	1.78E-26	**Bcl2a1d**
1.10E-49	**-0.537729797**	0.767	0.959	1.62E-45	**Tnfrsf9**
7.25E-19	**-0.533767253**	0.722	0.827	1.07E-14	**Itm2a**
1.08E-05	**-0.467551663**	0.182	0.259	0.15947118	**Cd40lg**
4.87E-60	**-0.466416722**	0.834	0.957	7.20E-56	**Serbp1**
1.55E-18	**-0.414297084**	0.124	0.292	2.29E-14	**Bcl2l1**
1.64E-35	**-0.406628365**	0.097	0.348	2.42E-31	**Pdcd11**
7.16E-17	**-0.40219566**	0.23	0.422	1.06E-12	**Cd24a**
1.80E-40	**-0.369737307**	0.89	0.973	2.67E-36	**Ybx1**
6.42E-19	**-0.333109223**	0.238	0.453	9.50E-15	**Nfkb2**
1.82E-26	**-0.318153426**	0.116	0.339	2.69E-22	**Siva1**
1.27E-20	**-0.311159669**	0.47	0.72	1.88E-16	**Pdcd5**
3.81E-10	**-0.290822541**	0.699	0.831	5.64E-06	**Nfkbia**
1.57E-08	**-0.273093074**	0.332	0.471	0.000232697	**Junb**
4.28E-10	**-0.262715993**	0.248	0.403	6.33E-06	**Socs1**
1.51E-09	**0.256127354**	0.71	0.655	2.23E-05	**Cd27**
1.40E-06	**0.258033234**	0.33	0.254	0.020693477	**Irf9**
2.04E-05	**0.265106484**	0.321	0.268	0.301369737	**Ifnar2**
2.90E-07	**0.280475299**	0.626	0.584	0.004293206	**Stat1**
3.01E-10	**0.283916488**	0.556	0.442	4.45E-06	**Slfn2**
6.65E-11	**0.29101818**	0.657	0.575	9.83E-07	**Cd28**
1.44E-06	**0.311761789**	0.455	0.371	0.021364364	**Id3**
4.28E-10	**0.316024888**	0.558	0.493	6.34E-06	**Jak1**
8.92E-21	**0.330983555**	0.879	0.845	1.32E-16	**Lat**
1.36E-08	**0.337776247**	0.373	0.286	0.000200438	**Cd96**
8.43E-10	**0.340524524**	0.344	0.242	1.25E-05	**Pdcd4**
4.88E-09	**0.349857909**	0.363	0.276	7.22E-05	**Foxo1**
2.52E-08	**0.350216542**	0.457	0.372	0.000372334	**Lgals1**
6.20E-09	**0.3538594**	0.317	0.212	9.16E-05	**Irf7**
1.14E-09	**0.363141503**	0.422	0.327	1.68E-05	**Tox**

3.92E-12	**0.364443219**	0.479	0.359	5.80E-08	**Irf2**
2.79E-21	**0.369139421**	0.837	0.746	4.12E-17	**Btg1**
5.20E-13	**0.369664002**	0.301	0.174	7.69E-09	**Bcl11b**
1.68E-44	**0.379892335**	0.965	0.94	2.48E-40	**Cd3g**
1.66E-20	**0.387353467**	0.719	0.599	2.45E-16	**Lgals9**
7.36E-13	**0.387595248**	0.497	0.382	1.09E-08	**Ikzf3**
1.82E-52	**0.398122161**	0.971	0.951	2.69E-48	**Cd3d**
1.32E-21	**0.399520122**	0.681	0.568	1.95E-17	**Skap1**
1.87E-11	**0.40159087**	0.352	0.234	2.77E-07	**Itgb7**
4.03E-17	**0.402717431**	0.276	0.127	5.96E-13	**Ccng2**
1.25E-14	**0.405102485**	0.306	0.167	1.84E-10	**Ifi209**
8.95E-05	**0.408375362**	0.498	0.468	1	**Ms4a4b**
2.13E-23	**0.409988741**	0.726	0.585	3.15E-19	**Tcf7**
1.55E-08	**0.414314857**	0.355	0.257	0.000228857	**Ckb**
1.02E-17	**0.415373332**	0.642	0.535	1.51E-13	**Lef1**
1.03E-43	**0.416710466**	0.942	0.882	1.53E-39	**Lck**
1.05E-22	**0.416959993**	0.754	0.673	1.55E-18	**Itgb2**
2.10E-08	**0.421093266**	0.328	0.232	0.000310974	**Ms4a6b**
0.000229496	**0.423564557**	0.3	0.235	1	**Trav14-1**
1.47E-10	**0.436546366**	0.348	0.237	2.18E-06	**Bcl2**
6.07E-20	**0.437946511**	0.571	0.44	8.98E-16	**Ccnd3**
1.75E-19	**0.443459377**	0.701	0.595	2.59E-15	**Trbc2**
2.97E-14	**0.448323182**	0.373	0.24	4.40E-10	**Igf2r**
8.51E-21	**0.461568443**	0.664	0.544	1.26E-16	**Cd4**
5.00E-19	**0.465524522**	0.578	0.449	7.40E-15	**Satb1**
8.18E-13	**0.482313286**	0.324	0.198	1.21E-08	**Slfn1**
5.45E-20	**0.55260859**	0.612	0.457	8.06E-16	**Klf2**
1.76E-30	**0.55583654**	0.438	0.22	2.61E-26	**Cdkn2d**
1.72E-84	**0.606010974**	0.968	0.883	2.54E-80	**Itm2b**
8.67E-34	**0.645607594**	0.457	0.229	1.28E-29	**Btg2**
7.00E-86	**0.78227126**	0.948	0.905	1.04E-81	**Trbv19**
5.60E-67	**0.842736348**	0.712	0.41	8.28E-63	**Nsg2**
2.48E-68	**0.935832664**	0.779	0.465	3.67E-64	**Vim**

Table 4.4. Selected genes differentially regulated between $CD25^+$ $T_{reg}P$ agonist and post-agonist clusters. Genes upregulated in cluster 7 ($CD25^+$ $T_{reg}P$ agonist) versus cluster 5 (post-agonist) are in teal and those upregulated in cluster 5 versus cluster 7 are in green.

p value	avg logFC	% cells+ C1	% cells+ C2	p value adj	Gene Name
2.75E-81	**-0.888472391**	0.397	0.767	4.06E-77	**Tnfrsf9**
1.50E-101	**-0.866161173**	0.303	0.726	2.22E-97	**Tcf7**
3.20E-70	**-0.837231109**	0.066	0.355	4.73E-66	**Ckb**
1.49E-41	**-0.687181531**	0.472	0.722	2.20E-37	**Itm2a**
9.75E-69	**-0.618241631**	0.681	0.89	1.44E-64	**Ybx1**
4.20E-33	**-0.50820456**	0.324	0.578	6.21E-29	**Satb1**
1.06E-34	**-0.445419966**	0.522	0.754	1.56E-30	**Itgb2**
9.36E-34	**-0.442397844**	0.399	0.657	1.38E-29	**Cd28**
2.56E-15	**-0.317315849**	0.635	0.751	3.79E-11	**Ikzf2**
5.29E-17	**-0.283201346**	0.637	0.778	7.83E-13	**Cd5**
1.07E-14	**-0.270675604**	0.154	0.296	1.59E-10	**Hdac7**
3.61E-15	**-0.263087268**	0.372	0.564	5.35E-11	**Itk**
6.68E-13	**-0.252416897**	0.334	0.497	9.88E-09	**Ikzf3**
8.06E-07	**0.255296325**	0.281	0.201	0.011924736	**Ikzf4**
2.05E-10	**0.258997068**	0.501	0.39	3.03E-06	**Bmyc**
7.22E-08	**0.297941433**	0.419	0.337	0.001067481	**Gata3**
2.98E-10	**0.302971405**	0.735	0.699	4.41E-06	**Nfkbia**
8.39E-48	**0.33318624**	0.979	0.941	1.24E-43	**B2m**
3.90E-12	**0.366113156**	0.263	0.152	5.77E-08	**Rel**
6.13E-14	**0.437137796**	0.569	0.455	9.07E-10	**Id3**
3.19E-17	**0.464014979**	0.471	0.332	4.72E-13	**Junb**
6.37E-83	**0.477149382**	0.985	0.938	9.43E-79	**H2-D1**
1.92E-44	**0.508318761**	0.799	0.634	2.85E-40	**Ypel3**
1.02E-50	**0.510618687**	0.859	0.717	1.51E-46	**Tnfrsf18**
3.25E-33	**0.574679686**	0.557	0.348	4.81E-29	**Bcl2**
5.34E-63	**0.607008776**	0.884	0.721	7.90E-59	**Tnfrsf4**
1.95E-68	**0.627463043**	0.86	0.612	2.88E-64	**Klf2**
2.82E-53	**0.663143249**	0.625	0.352	4.17E-49	**Itgb7**
1.02E-28	**0.672635197**	0.278	0.101	1.51E-24	**Ass1**
6.74E-37	**0.683778055**	0.399	0.165	9.97E-33	**Cish**
5.21E-45	**0.802166298**	0.51	0.248	7.71E-41	**Socs1**
3.03E-65	**0.852852788**	0.491	0.154	4.48E-61	**Ctla4**
2.37E-124	**0.859480736**	0.919	0.498	3.51E-120	**Ms4a4b**
4.83E-79	**0.887625178**	0.608	0.228	7.14E-75	**S1pr1**
1.62E-101	**0.902022468**	0.75	0.328	2.40E-97	**Ms4a6b**
1.19E-85	**0.904608953**	0.727	0.396	1.75E-81	**Il2rb**
2.62E-93	**1.085161888**	0.637	0.246	3.87E-89	**Izumo1r**
1.26E-134	**1.151144412**	0.734	0.249	1.87E-130	**Sell**
1.73E-118	**1.354258163**	0.562	0.097	2.56E-114	**Il2ra**
1.19E-163	**1.369389623**	0.73	0.144	1.76E-159	**Foxp3**

Table 4.5. Selected genes differentially regulated between post-agonist and mature T_{reg} cell clusters. Genes upregulated in cluster 5 (post-agonist) versus cluster 3 (mature T_{reg}) are in teal and those upregulated in cluster 3 versus cluster 5 are in moss green.

have lost some expression of *Il2ra*, they retain CD25 protein and the ability to respond to IL-2 efficiently.

Development and maturation of T_{reg} cells from FOXP3^{lo} T_{reg}P cells

In contrast to CD25^{+} T_{reg}P cells, nothing is known about the heterogeneity of the FOXP3^{lo} T_{reg}P cell pathway. scRNAseq analysis of sorted FOXP3^{lo} T_{reg}P cells identifies two clusters where the majority FOXP3^{lo} T_{reg}P cells reside, cluster 0, of the "core" FOXP3^{lo} T_{reg}P cells and cluster 12, or the above described FOXP3^{lo} T_{reg}P agonist selection cluster (Figure 4.1). Comparing FOXP3^{lo} T_{reg}P cells to the FOXP3^{lo} T_{reg}P agonist cluster revealed almost total loss of TCR target genes in the FOXP3^{lo} T_{reg}P cluster, including *Nr4a1*, *Egr1*, *Cd69*, and *Tagap* (Table 4.6). Further, FOXP3^{lo} T_{reg}P cells upregulate the maturation related genes *Klf2*, *S1pr1*, *Ms4a4b* and *Ccr7*, suggesting FOXP3^{lo} T_{reg}P agonist selection cells precede the FOXP3^{lo} T_{reg}P cell population (Table 4.6). Interestingly, STAT5 target genes *Cish* and *Socs1* are more highly expressed in the FOXP3^{lo} T_{reg}P agonist cluster (Table 4.6), suggesting that this population may be receiving cytokine stimulation. IL-4 signaling, which can also turn on *Cish* and *Socs1*[261], augments the FOXP3^{lo} T_{reg}P cell pathway[96], thus perhaps IL-4 provides a survival signal for FOXP3^{lo} T_{reg}P cells receiving TCR stimulation. However, the mature T_{reg} cell cluster further increased expression of *Cish*, *Socs1* and *Il2ra* (Table 4.7), likely due to stimulation by IL-2 or IL-15. Additionally, mature T_{reg} cells further upregulate the core "T_{reg}" signature genes[262] including *Foxp3*, *Il2ra*, *Ctla4*, *Ikzf2* and *Tnfrsf18* (Table 4.7). Upregulation of T_{reg} cell core genes in the FOXP3^{lo} T_{reg}P to mature T_{reg} cell transition further supports previous observations that FOXP3^{lo} T_{reg}P cells are indeed progenitors and not fully functional and stabilized T_{reg} cells. Collectively, this data suggests that development of T_{reg} cells via the FOXP3^{lo} T_{reg}P cell pathway involves an initial TCR stimulation step followed by an intermediate that then receives IL-2 stimulation to

p value	avg logFC	% cells+ C0	% cells+ C12	p value adj	Gene Name
1.23E-251	**-2.888586803**	0.098	0.914	1.82E-247	**Nr4a1**
1.84E-126	**-2.201158968**	0.082	0.605	2.72E-122	**Egr1**
2.16E-173	**-1.80013383**	0.043	0.635	3.20E-169	**Nfkbid**
7.93E-136	**-1.795321254**	0.093	0.657	1.17E-131	**Cd69**
6.40E-117	**-1.556974214**	0.084	0.591	9.46E-113	**Tagap**
1.77E-145	**-1.549351282**	0.009	0.442	2.62E-141	**Egr2**
3.49E-173	**-1.496285386**	0.009	0.517	5.17E-169	**Nr4a3**
2.60E-109	**-1.429422653**	0.247	0.829	3.85E-105	**Junb**
3.04E-79	**-1.413747048**	0.062	0.431	4.50E-75	**Myc**
8.44E-69	**-1.153539842**	0.049	0.367	1.25E-64	**Ccr8**
2.12E-76	**-1.140199167**	0.08	0.467	3.13E-72	**Bcl2a1b**
2.94E-41	**-1.127743484**	0.404	0.71	4.35E-37	**Tnfrsf4**
5.30E-49	**-1.118604973**	0.326	0.691	7.84E-45	**Srgn**
3.11E-52	**-1.032868385**	0.523	0.829	4.60E-48	**Nfkbia**
2.98E-40	**-0.976094075**	0.099	0.376	4.40E-36	**Cd40lg**
1.23E-27	**-0.945161549**	0.214	0.481	1.82E-23	**Tnfrsf9**
1.84E-43	**-0.790084113**	0.042	0.271	2.73E-39	**Il2ra**
2.76E-17	**-0.745836977**	0.505	0.71	4.08E-13	**Itm2a**
2.91E-33	**-0.637242538**	0.122	0.401	4.30E-29	**Rel**
1.10E-35	**-0.59899079**	0.083	0.337	1.63E-31	**Nfkb2**
1.16E-28	**-0.588106857**	0.367	0.691	1.71E-24	**Tgfb1**
6.18E-23	**-0.516749112**	0.086	0.282	9.13E-19	**Cish**
3.87E-15	**-0.505220239**	0.514	0.727	5.73E-11	**Tnfrsf18**
1.17E-20	**-0.4822643**	0.282	0.555	1.73E-16	**Ikzf2**
3.75E-17	**-0.340584445**	0.822	0.936	5.55E-13	**Il2rg**
2.74E-14	**-0.336317784**	0.105	0.268	4.06E-10	**Nfkbib**
1.69E-09	**-0.328136978**	0.17	0.323	2.50E-05	**Icos**
2.32E-16	**-0.325322832**	0.095	0.265	3.44E-12	**Traf4**
9.12E-11	**-0.312087021**	0.192	0.367	1.35E-06	**Socs1**
6.71E-11	**-0.301488301**	0.67	0.843	9.92E-07	**Cd5**
1.11E-05	**-0.299516879**	0.242	0.365	0.164466603	**Izumo1r**
6.76E-11	**-0.278429953**	0.166	0.337	1.00E-06	**Fas**
1.40E-06	**-0.275139816**	0.489	0.646	0.020779029	**Itk**
5.24E-13	**-0.252697085**	0.143	0.326	7.75E-09	**Relb**
6.58E-06	**0.272149044**	0.51	0.414	0.097324608	**Sell**
0.004385552	**0.283829202**	0.28	0.229	1	**Pdcd4**
0.012063733	**0.285493252**	0.363	0.345	1	**Ikzf3**
5.67E-07	**0.317600864**	0.6	0.492	0.008383434	**Ms4a6b**
2.85E-12	**0.328509864**	0.852	0.704	4.21E-08	**Ms4a4b**
1.42E-15	**0.397650242**	0.716	0.539	2.10E-11	**Ccr7**
2.55E-05	**0.413733662**	0.342	0.257	0.377674753	**Foxo1**
8.00E-22	**0.599504866**	0.579	0.309	1.18E-17	**S1pr1**
2.88E-24	**0.658679079**	0.719	0.533	4.25E-20	**Klf2**

Table 4.6. Selected genes differentially regulated between FOXP3^{lo} T_{reg}P and FOXP3^{lo} T_{reg}P agonist clusters. Genes upregulated in cluster 12 (FOXP3^{lo} T_{reg}P agonist) versus cluster 0 (FOXP3^{lo} T_{reg}P) are in purple and those upregulated in cluster 0 versus cluster 12 are in salmon.

p value	**avg logFC**	% cells+ C0	% cells+ C3	p value adj	**Gene Name**
1.98E-200	**-1.417426116**	0.042	0.562	2.92E-196	**Il2ra**
1.79E-180	**-1.069989182**	0.404	0.884	2.65E-176	**Tnfrsf4**
6.49E-133	**-0.942167801**	0.26	0.727	9.60E-129	**Il2rb**
1.09E-83	**-0.802773503**	0.086	0.399	1.61E-79	**Cish**
1.40E-92	**-0.788941816**	0.242	0.637	2.07E-88	**Izumo1r**
1.35E-65	**-0.688830497**	0.248	0.575	2.00E-61	**Ifngr1**
7.87E-66	**-0.68603247**	0.192	0.51	1.16E-61	**Socs1**
5.57E-63	**-0.640577401**	0.179	0.491	8.25E-59	**Ctla4**
1.86E-80	**-0.627383322**	0.338	0.73	2.75E-76	**Foxp3**
1.26E-89	**-0.611241615**	0.514	0.859	1.86E-85	**Tnfrsf18**
1.52E-54	**-0.56348809**	0.203	0.501	2.25E-50	**Bmyc**
2.71E-59	**-0.463844217**	0.282	0.635	4.01E-55	**Ikzf2**
6.98E-29	**-0.41188155**	0.247	0.471	1.03E-24	**Junb**
3.41E-25	**-0.410666594**	0.118	0.278	5.05E-21	**Ass1**
1.16E-21	**-0.374696605**	0.326	0.53	1.71E-17	**Srgn**
2.26E-26	**-0.331587965**	0.183	0.38	3.35E-22	**Lgals1**
2.67E-21	**-0.327253207**	0.368	0.574	3.96E-17	**Mif**
1.12E-22	**-0.320495796**	0.523	0.735	1.65E-18	**Nfkbia**
6.09E-22	**-0.301302775**	0.214	0.397	9.01E-18	**Tnfrsf9**
3.66E-25	**-0.299904053**	0.51	0.734	5.42E-21	**Sell**
5.15E-19	**-0.289576865**	0.122	0.263	7.62E-15	**Rel**
1.40E-17	**-0.286595529**	0.127	0.26	2.07E-13	**Traf1**
1.18E-07	**0.266437305**	0.466	0.439	0.001748372	**Ccnd3**
6.04E-13	**0.267764984**	0.647	0.635	8.93E-09	**Skap1**
6.30E-13	**0.269511419**	0.695	0.7	9.32E-09	**Ptprc**
2.38E-05	**0.272228122**	0.363	0.334	0.352016913	**Ikzf3**
1.79E-10	**0.275361623**	0.574	0.566	2.65E-06	**Ets1**
2.72E-05	**0.288754109**	0.273	0.237	0.402578609	**Tgfbr2**
3.61E-09	**0.291033574**	0.535	0.522	5.34E-05	**Itgb2**
5.29E-30	**0.308074906**	0.89	0.885	7.83E-26	**Lck**
1.05E-19	**0.374093311**	0.67	0.637	1.55E-15	**Cd5**
3.59E-10	**0.385816989**	0.505	0.472	5.31E-06	**Itm2a**
3.29E-22	**0.435708171**	0.489	0.372	4.86E-18	**Itk**
1.84E-23	**0.451156184**	0.615	0.549	2.72E-19	**Lef1**
2.83E-35	**0.53650056**	0.559	0.399	4.19E-31	**Cd28**
1.12E-36	**0.616743775**	0.495	0.324	1.65E-32	**Satb1**
2.46E-70	**0.917905189**	0.554	0.303	3.64E-66	**Tcf7**

Table 4.7. Genes differentially regulated between mature T_{reg} cells and FOXP3^{lo} T_{reg}P. Genes upregulated in cluster 3 (mature T_{reg}) versus cluster 0 (FOXP3^{lo} T_{reg}P) are in moss green while those upregulated in cluster 0 versus cluster 3 are in salmon.

complete T_{reg} cell differentiation, a similar paradigm as we observed in the $CD25^+$ T_{reg}P cell pathway.

4.3 Discussion

In order to understand CD4 thymocyte maturation and T_{reg} cell development we generated a scRNAseq data set with $CD4^+CD8^+$ thymocytes, conventional CD4SP, $CD25^+$ and $FOXP3^{lo}$ T_{reg}P and mature T_{reg} cells. Analysis of conventional CD4SP clusters demonstrated downregulation of CD4 lineage defining transcription factors, such as *Tox*, *Gata3*, *Satb1* and *Zbtb7b* (ThPOK), from immature to mature CD4SP. Additionally, we used expression of *Ccr9*, the chemokine receptor associated with cortical localization, to mark immature CD4SP and *Ccr7*, the chemokine receptor required to traffic to the thymic medulla where maturation is completed, to denote more mature CD4SP. Mature CD4SP also acquire a tonic IFN signature, as evidenced by *Stat1*, *Irf7* and *H2-K1* expression. Tonic IFN signaling is important for thymocyte maturation and IFN is produced in the thymic medulla where single-positive thymocytes complete maturation[223]. Expression of the transcription factor KLF2 and downstream activation of the chemokine receptor S1PR1 is essential for T cell egress from the thymus[247,248]. The mature CD4SP cluster has increased expression of *Klf2* and *S1pr1* versus immature CD4SP, further evidence that this cluster is mature and competent to emigrate from the thymus. This scRNAseq data set recapitulates transcriptional phenomena previously associated with thymocytes maturation. However, we also identify new markers that show a strong correlation with thymocyte maturity. The integrin *Itgb7* and the transmembrane adaptor proteins *Ms4a4b* and *Ms4a6b* are positively corelated with the transition from immature to mature CD4SP while the brain associated creatine kinase *Ckb* is negatively corelated with maturation. Upregulation of *Ms4a4b* and *Ms4a6b* may represent a mechanism that allows mature T cells to become more sensitive to antigen receptor and cytokine stimulation[222], preparing

these cells to mount more robust immune responses. Collectively, these transcriptional changes that occur throughout development facilitate identification of the maturation state of a group of thymocytes.

Application of this group of transcriptional changes allowed for the step by step interrogation of the T_{reg} cell developmental pathway. For both the $CD25^{+}$ $T_{reg}P$ and $FOXP3^{lo}$ $T_{reg}P$ cell pathways we identified a cluster of cells undergoing agonist selection. While the signatures of these populations differ, both agonist selection clusters represent the most immature cells in each $T_{reg}P$ cell developmental pathway. For $CD25^{+}$ $T_{reg}P$ cells the agonist selection cluster is fairly large and represents a significant proportion of all $CD25^{+}$ $T_{reg}P$ cells. However, the $FOXP3^{lo}$ $T_{reg}P$ agonist selection cluster only represents a small amount of all $FOXP3^{lo}$ $T_{reg}P$ cells. Increased strength of TCR stimulation in $CD25^{+}$ $T_{reg}P$ cells could be why the agonist selection signature is proportionally larger than $FOXP3^{lo}$ $T_{reg}P$ cells. Both pathways also contained an intermediate population between agonist selection and mature T_{reg} cells. Intermediate, or “post-agonist”, $CD25^{+}$ $T_{reg}P$ cells downregulated TCR response genes, including *Il2ra* (CD25), and upregulated the maturation signature. However, despite what may be expected from previous reports[185,241], these cells did not express greater amounts of *Il2rb* (CD122) or *Tnfrsf18* (GITR). Thus, perhaps the $CD122^{hi}GITR^{hi}$ subset of $CD25^{+}$ $T_{reg}P$ cells previously observed doesn’t represent a more mature subset of $CD25^{+}$ $T_{reg}P$ cells but simply a more cytokine responsive subset. This may be due to greater TCR stimulation or strong costimulation via CD28, as NFκB family member activation downstream of these pathways is important for the differentiation of the $CD122^{hi}GITR^{hi}$ population[185,241]. The transition in the $FOXP3^{lo}$ $T_{reg}P$ cell pathway from agonist selection to intermediate population is similarly marked by the loss of TCR response gene expression and upregulation of maturation related genes. However, while *Il2rb* is not differentially expressed during this transition, *Tnfrsf18* is mildly

downregulated in the intermediate "FOXP3^{lo} T_{reg}P" population. Interestingly, two STAT5 target genes, *Cish* and *Socs1*, are both downregulated in the intermediate FOXP3^{lo} T_{reg}P cluster versus the agonist selection cluster. STAT5 activation is typically associated with the final step of T_{reg} cell development however FOXP3^{lo} T_{reg}P cells appear to be augmented by IL-4 stimulation (Figures 3.13a,c, 3.14 and 3.15b). Thus, activation of these genes in cells receiving TCR stimulation may represent the activity of IL-4 induced STAT activation. The transition between T_{reg}P cell intermediate and mature T_{reg} cells exhibited convergent transcriptional changes. The transition of both T_{reg}P cell pathways to mature T_{reg} cells exhibits upregulation of *Cish* and *Socs1*, suggesting the activation of STAT5 downstream of cytokine stimulation, the critical pathway required to complete T_{reg} cell development. Further, mature T_{reg} cells upregulate genes associated with maturation and T_{reg} functional competence such as *Il2ra, Foxp3*, *Ctla4* and *Izumo1r*. Together this data agrees with the general scheme proposed for T_{reg}P cell differentiation in Chapter 3, mainly that step one, or TCR stimulation, appears distinct between the two T_{reg}P pathways while step two appears convergent due to the shared dependence on STAT5 activation. Ultimately, we want to use this scRNAseq data set to develop a highly granular understanding of changes that occur throughout the course of T_{reg} cell development. To do this we would employ algorithms such as pseudotime[263], however we have currently been unable to properly align our data set within pseudotime.

scRNAseq analysis of CD4SP thymocytes also revealed a novel population of thymocytes defined by high expression of numerous interferon-stimulated genes. Interestingly, a similar population has been identified in T cells from the periphery[256]. In humans, this IFN signature population is negatively associated house dust mite allergies however no specific function of ISG signature T_{reg} cells has been directly tested in mice or humans. We have also observed this ISG signature population in scRNAseq data sets for splenic

T_{reg} cells in mice, but we lack sufficient ISG cluster cell numbers to perform rigorous TCR repertoire analysis to determine if any relation exists between this population in the periphery and thymus. We have speculated that the ISG thymocyte population represents thymocytes expressing ISG reactive TCRs that arrest near a source of IFN. CARTANA, a spatial transcriptomic sequencing method, is currently being optimized to understand if ISG signature thymocyte populations are found in a specific niche in the thymus. Further, larger TCR sequencing data sets can be generated to test if the ISG signature related TCRs in the thymus are related or not to those ISG signature T_{reg} cell populations in the periphery. TCR repertoire analysis and transfer studies will ultimately be required to understand if the ISG T_{reg} cell cluster represents a specific functional subset of T_{reg} cells or is simply a marker of T_{reg} cells entering IFN rich environments.

Chapter 5: Role of recirculating T_{reg} cells in thymus function

5.1 Background

The thymus is a dynamic environment that changes throughout life. A principle change that occurs as a function of age is the involution of the thymus which involves the deposition of adipose tissue in place of functional thymic stroma[264,265]. Nevertheless, the function of the thymus, after normalizing to the size of the $CD4^+CD8^+$ thymocyte compartment, is age-independent[266]. This suggests that the thymus remains grossly functional throughout life, up to ~100 weeks of age in mice, even though the size of the developing thymocyte compartment decreases dramatically. In contrast, the accumulation of recirculating mature T cells, defined as RAG2-GFP^-, in the thymus shows a strong age-dependency, where the single positive compartment of the thymus in mice greater than one year old is comprised of 20-30% recirculating mature T cells[266]. Further, it was suggested that the thymus may function as a reservoir for memory in the T cell compartment as these recirculating cells predominantly express an activated, $CD44^{hi}$ $CD62L^{lo}$, phenotype[224,266]. No functional consequences of this accumulation were identified.

Several previous studies indicate that the characteristics of central tolerance and T_{reg} cell selection change throughout ontogeny[177,178,181]. Specifically, the perinatal thymus exports T_{reg} cells distinct from those that develop in the adult thymus[178]. Similarly, thymocytes expressing a TCR capable of recognizing the self-antigen PADI4 commit to the T_{reg} cell lineage in young thymi and undergo negative selection in the adult thymus[78]. However, the mechanism underlying these shifts in the ability of the thymus to enforce central tolerance and T_{reg} development remain a mystery.

One parameter that changes throughout ontogeny is the accumulation of recirculating or resident thymic T_{reg} cells (RT-T_{reg}). RT-T_{reg} begin to accumulate fairly early in ontogeny and by ~5 weeks of age represent ~50% of the thymic T_{reg} cell compartment. By 1 year of age RT-T_{reg} cells comprise ~80% of thymic FOXP3$^+$ cells[174]. RAG-2-GFP$^+$ CD25$^+$ T_{reg}P cell abundance is unchanged while FOXP3$^+$ thymocytes decrease throughout ontogeny, suggesting that RT-T_{reg} cells might be limiting the availability of IL-2 to inhibit T_{reg} cell development[142,174]. This RT-T_{reg} cell depletion of IL-2 could be responsible for the shift from T_{reg} cell development to negative selection in older mice for PADI4 specific thymocytes[78]. Indeed, FOXP3 acts to induce apoptosis when not counterbalanced by γC cytokine stimulation, such as IL-2[65]. Thus, as RT-T_{reg} cells reduce IL-2 availability, these self-reactive thymocytes may be deleted rather than differentiating into T_{reg} cells. However, we have found that CD25$^+$ T_{reg}P cells can produce IL-2 (Figure 2.6). Autocrine IL-2, which would be unlikely to be depleted by RT-T_{reg} cells before binding the high-affinity IL-2R on CD25$^+$ T_{reg}P cells, could act to activate STAT5 and complete T_{reg} cell development even while RT-T_{reg} cells are highly abundant. Thus, RT-T_{reg} cells may alter central tolerance by other mechanisms outside of IL-2 competition.

Medullary thymic epithelial cells (mTEC) expressing the transcription factor AIRE can express over 80% of the genome[267]. Thus, AIRE$^+$ mTEC abundance represents an efficient mechanism to enforce central tolerance by purging the thymocyte repertoire of self-reactive TCRs[84,85,177] or polarizing cells expressing self-reactive TCRs to the T_{reg} cell lineage[86,90,178,268]. Indeed, given the high degree of cross-reactivity of the TCR[269], perfect central tolerance to the entire endogenous peptidome would eliminate many foreign reactive TCRs. A preliminary study recently found that AIRE$^+$ mTEC abundance peaks around 4 weeks of age before a significant and progressive decline throughout the remainder of ontology. Interestingly, TCR diversity in mature, non-T_{reg}, CD4SP thymocytes

shows a positive correlation with age[181]. These observations suggest that AIRE$^+$ mTEC abundance, and/or RT-T_{reg} cell accumulation, cause a shift in central tolerance leading to a more diverse effector T cell repertoire[181] and the selection of functionally distinct T_{reg} cells[178].

RT-T_{reg} cells exhibit an activated T_{reg} cell phenotype and express the cytolytic molecule GZMB[174]. Further, RT-T_{reg} cells begin to accumulate to high levels at the same time as AIRE$^+$ mTEC abundance peaks[174,181]. Given that RT-T_{reg} cells are activated, capable of cytolysis and AIRE$^+$ mTEC abundance decreases following RT-T_{reg} cell accumulation we hypothesized that RT-T_{reg} cells may be directly regulating the APC compartments within the thymus. First, phenotyping analysis revealed that RT-T_{reg} cells are a heterogeneous population that indeed includes a population that expresses TIM-3, a marker associated with cytolytic T_{reg} cells that express GZMB[270,271]. To test if RT-T_{reg} cells regulate stromal cell or APC abundance in the thymus we developed an intrathymic RT-T_{reg} depletion protocol which involves treating *Foxp3^{DTR}* mice with low-dose intrathymic DT. Strikingly, chronic depletion of RT-T_{reg} cells by intrathymic DT treatment led to a resurgence in AIRE$^+$ mTEC abundance. Currently, we hypothesize that RT-T_{reg} cell accumulation signals that peripheral T_{reg} cells have expanded and are enforcing peripheral tolerance. These RT-T_{reg} cells then act as rheostat to loosen the stringency of central tolerance by eliminating AIRE$^+$ mTEC. RT-T_{reg} cell accumulation favors the diversity of the effector compartment and inhibits the development of T_{reg} cells functionally convergent with those generated early in life. Thus, early in life while the organism is protected from local pathogens by maternal Ig, T_{reg} cell development in prioritized over effector cell diversity. However, after T_{reg} cells have established peripheral tolerance, T_{reg} cells migrate back to the thymus to decrease the stringency of central tolerance, thereby allowing a more diverse effector T cell

repertoire to be exported from the thymus facilitating more effective pathogen or tumor cell control.

5.2 Results

RT-T_{reg} cells are a heterogeneous population

Little is known about the phenotype of RT-T_{reg} cells. Bulk RNAseq analysis of RAG2-GFP^{+} versus RAG2-GFP^{-} thymic T_{reg} cells suggests that RT-T_{reg} cells contain activated or effector T_{reg} cells[174]. This phenotype agrees with previous studies on mature thymic effector T cells, as recirculating thymic effector T cells also possess an activated phenotype[224,266]. While these studies suggest that the RT-T_{reg} cell compartment contains eT_{reg} cells, questions remained about the heterogeneity of RT-T_{reg} cells. From bulk RNAseq it is uncertain if the RT-T_{reg} cell compartment is largely comprised of eT_{reg} cells or simply contains a larger proportion of eT_{reg} cells than *de novo* developing T_{reg} cells. Additionally, several subsets of eT_{reg} cell phenotypes have been identified with distinct functionality, thus it is unclear what types and proportions of eT_{reg} cells make up the RT-T_{reg} cell compartment.

To understand the phenotype and heterogeneity of RT-T_{reg} cells we first used flow cytometry analysis of thymic CD73^{hi} T_{reg} cells, which represent RT-T_{reg} cells[96]. CD73^{hi} thymic T_{reg} cells have a higher NUR77-GFP signal[77] than splenic CD73^{hi} T_{reg} cells, suggesting RT-T_{reg} cells are being activated via the TCR (Figure 5.1 a). Next, we analyzed several surface markers associated with eT_{reg} cells, and eT_{reg} cell subsets, and identified considerable heterogeneity within the RT-T_{reg} cell compartment. A large fraction, ~16%, of RT-T_{reg} cells express the eT_{reg} cell marker TIGIT[272] suggesting that at least some RT-T_{reg} cells are activated. Within the TIGIT^{+} fraction of RT-T_{reg} cells we found TIM3^{+}, LAG3^{+} and ST-2^{+} subsets of RT-T_{reg} cells (Figure 5.1 b,c). Expression of ST-2 and TIM3 on RT-T_{reg} cells appears to be mutually exclusive, thus the ST-2^{+} and

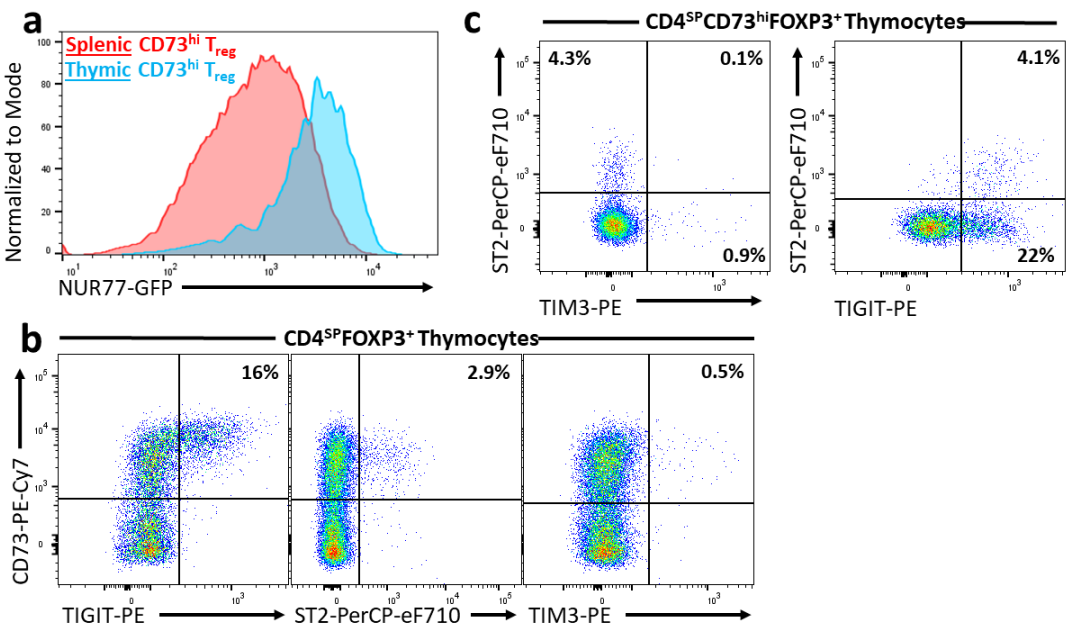

Figure 5.1. RT-T_{reg} cells are activated. **a)** *Foxp3-RFP* x *Nur77-GFP* splenocytes and thymocytes evaluated directly ex vivo for NUR77-GFP signal intensity. Blue histogram represents CD4SP FOXP3^{+} CD73^{hi} thymocytes and red histogram represents CD4^{+}FOXP3^{+}CD73^{hi} splenocytes. **b)** Staining for TIGIT (left), ST-2 (middle) and TIM3 (right) in CD4SP FOXP3^{+} thymocytes. **c)** Staining for ST-2 (to denote tissue-like phenotype T_{reg}) versus TIM3 (left) and TIGIT (right) in CD4SP CD73^{hi}FOXP3^{+} thymocytes.

TIM3$^+$ cell populations are likely unique RT-T$_{reg}$ cell subsets. TIM3$^+$ eT$_{reg}$ cells express GZMB and are capable of direct cytolysis[270,271]. TIM3$^+$ RT-T$_{reg}$ cells may be regulating the abundance of thymic APC expressing their cognate antigen. ST-2 expression is associated with a "non-lymphoid tissue" phenotype[273] of eT$_{reg}$ cells and is also constitutively expressed on T$_{reg}$ cells found in visceral adipose tissue[22,23]. ST-2$^+$ RT-T$_{reg}$ cells could represent "tissue-like" T$_{reg}$ cells responsible for maintaining thymic homeostasis and/or T$_{reg}$ cells associated with thymic adipose deposits in the aging thymus. Collectively, this data supports the presence of at least 4 functional subsets of RT-T$_{reg}$ cells: a partially activated subset expressing CD73 but not TIGIT and a fully activated TIGIT$^+$ compartment that contains distinct ST-2$^+$ and TIM3$^+$ RT-T$_{reg}$ cell subsets.

To further define the signature of different RT-T$_{reg}$ cell subset we performed scRNAseq analysis of CD73$^+$ FOXP3-GFP$^+$ CD4$^+$ T cells from *TCliβ* x *Tcra*$^{+/-}$ thymi using 10X Genomics. Analysis of CD73$^+$ thymic FOXP3$^+$ RT-T$_{reg}$ cells at a resolution of 0.6 identified 6 clusters representing distinct RT-T$_{reg}$ cell states and 1 contaminating cluster of immature, non-T$_{reg}$ cells (Figure 5.2 a). The largest cluster, cluster 0, within the CD73$^+$ T$_{reg}$ cell fraction is a population with similarity to cT$_{reg}$ cells, or T$_{reg}$ cells which recently developed, as indicated by expression of *Klf2*, *S1pr1*, *Sell*, and *Ccr7* (Figure 5.2 a, Table 5.1). This agrees with the observation of some RAG2-GFP$^+$ T$_{reg}$ cells within the thymic CD73$^+$ fraction which may represent recently developed T$_{reg}$ cells that have not yet emigrated from the thymus (Figure 3.7 b). All 5 other T$_{reg}$ cell clusters appeared to exhibit an eT$_{reg}$ cell phenotype indicating that RT-T$_{reg}$ cells are more differentiated and have received TCR stimulation. Cluster 1 is an RT-T$_{reg}$ cell subset defined by high expression of *Tigit* (Figure 5.2 a,b). This population also exhibits upregulation of *Icos*, *Batf* and *Itgae* (CD103) and downregulation *Sell* and *Ccr7* (Table 5.1). Thus, this population likely represents terminally differentiated eT$_{reg}$ cells that are adopting a

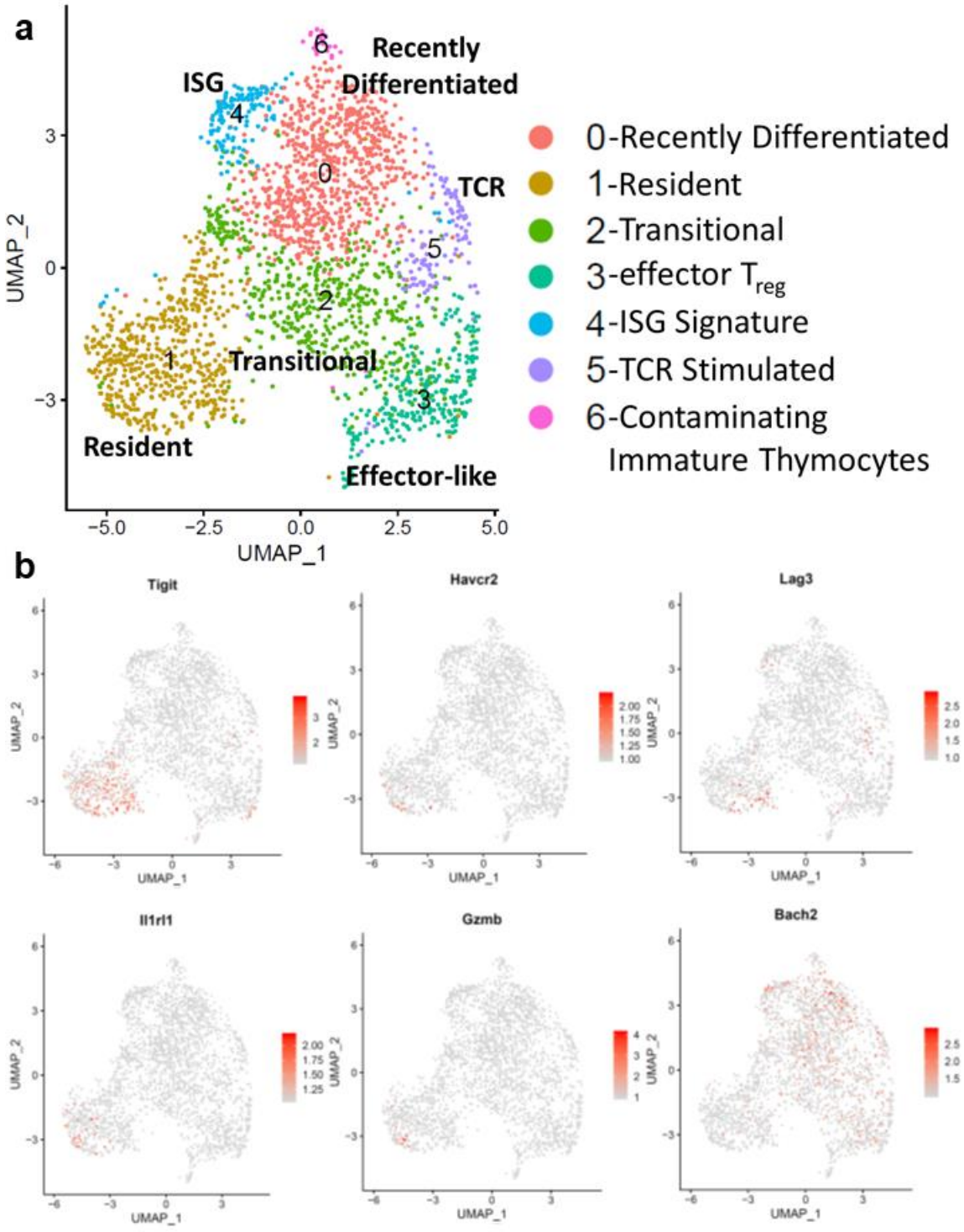

Figure 5.2. scRNAseq identification of RT-T_{reg} cell subsets. **a)** UMAP analysis and Seurat cluster identification, at a resolution of 0.6, of thymic $CD73^{+}$ T_{reg} cells from 8-9 week old

mice. **b)** Feature plots denoting cells expressing *Tigit*, *Havcr2* (TIM3), *Lag3*, *Il1rl1* (ST-2), *Gzmb* and *Bach2* by intensity of red coloring.

"non-lymphoid tissue" phenotype (Table 5.1). Cluster 2 appears to be a transitional population with upregulation of ribosomal components. A strong TCR stimulation signature is found in cluster 3, identified by upregulation of *Tnfrsf9, Nr4a1* and *Bmyc*. These cells also appeared more mature and likely represent T_{reg} cells being restimulated by local antigens. The signature of cluster 4 is dominated by IFN stimulated genes, such as *Ifit3, Bst2* and *Isg20*, and represents an RT-T_{reg} cell cluster analogous to the IFN stimulated cluster found previously in *de novo* developing thymocytes (Figure 4.1). Finally, the smallest population of RT-T_{reg} cells, cluster 5, expresses *Egr1/2*, *Nr4a1-3*, *Tagap* and *Cd69*, genes that all act as early activation markers in T cells (Figure 5.2 a, Table 5.1). Cluster 5 likely signifies a subset of RT-T_{reg} cells that is actively receiving TCR stimulation. This scRNAseq analysis of RT-T_{reg} cells currently points to 2 branches of RT-T_{reg} cell differentiation. One branch is represented by cluster 1 and likely contains terminally differentiated and tissue T_{reg} cells, as evidenced by T_{reg} cells expressing markers of terminal eT_{reg} differentiation, *Tigit*, *Lag3*, *Havcr2* (TIM3) and *Il1rl1* (ST-2) (Figure 5.2 a,b), and non-lyphoid T_{reg} markers such as *Itgae* (CD103) and *Icos* (Table 5.1). Indeed, this cluster contains cells expressing *Gzmb*, suggesting there is a subset of cytotoxic T_{reg} cells within this cluster (Figure 5.2 b). The second branch is dominated by TCR signaling and may represent a short-lived effector-like subset of RT-T_{reg} cells. Downregulation of *Bach2* is required to facilitate the induction of eT_{reg} cell phenotype in T_{reg} cells receiving TCR stimulation[274]. We observe that *Bach2* is most highly expressed by cluster 0 (cT_{reg}) cells and is downregulated in all other clusters (Figure 5.2 b), supporting the idea that RT-T_{reg} cells are competent to become more differentiated eT_{reg} cell subsets. Follow-up studies involving proteomic analysis, via CITEseq, and functional characterization of these subsets will be necessary to fully understand the properties of these RT-T_{reg} cell subsets.

p value	log fold change	pct.1	pct.2	p value adj	cluster	gene
1.22E-41	0.512866306	0.817	0.662	1.81E-37	0	Klf2
7.40E-38	0.608673134	0.626	0.43	1.09E-33	0	S1pr1
1.49E-18	0.337952261	0.713	0.597	2.21E-14	0	Ccr7
4.56E-16	0.359483595	0.648	0.55	6.75E-12	0	Sell
4.35E-132	1.34717086	0.4	0.029	6.43E-128	1	Tigit
7.26E-87	1.293267546	0.583	0.208	1.07E-82	1	Icos
9.45E-66	-0.927554977	0.313	0.73	1.40E-61	1	Ccr7
1.50E-59	-0.858864852	0.286	0.67	2.22E-55	1	Sell
4.62E-50	0.966939617	0.268	0.056	6.83E-46	1	Itgae
3.50E-12	0.52176463	0.261	0.148	5.18E-08	1	Batf
4.13E-10	-0.271367338	0.15	0.292	6.11E-06	1	Fas
4.76E-58	0.288619221	1	0.997	7.04E-54	2	Rplp0
9.46E-56	0.274280175	1	0.993	1.40E-51	2	Rpl32
3.88E-54	0.322379549	0.998	0.982	5.74E-50	2	Rpl10a
3.47E-69	1.127621159	0.859	0.372	5.13E-65	3	Tnfrsf9
1.99E-36	0.372151116	0.354	0.083	2.94E-32	3	Siva1
9.03E-36	0.560518664	0.942	0.675	1.34E-31	3	Ybx1
9.94E-24	0.524640371	0.787	0.441	1.47E-19	3	Bmyc
4.76E-13	0.253851599	0.477	0.231	7.04E-09	3	Fas
7.87E-13	0.478260218	0.285	0.121	1.16E-08	3	Nr4a1
7.49E-06	-0.463211116	0.347	0.418	0.110770754	3	Ctla4
1.59E-05	-0.410203786	0.65	0.613	0.23572741	3	Il2rb
0.000928153	-0.351543126	0.592	0.588	1	3	Izumo1r
0.000988197	-0.542399408	0.242	0.301	1	3	Icos
2.40E-104	1.827572533	0.694	0.09	3.56E-100	4	Ifit3
1.84E-52	1.180879173	0.679	0.177	2.72E-48	4	Isg20
1.24E-27	1.075093689	0.724	0.36	1.83E-23	4	Bst2
2.14E-05	-0.431395192	0.149	0.33	0.316491065	4	Cish
0.001777757	0.309274468	0.403	0.287	1	4	Satb1
6.47E-114	1.355007548	0.491	0.027	9.57E-110	5	Egr2
2.42E-89	2.568705109	0.733	0.11	3.58E-85	5	Nr4a1
2.13E-65	2.023687552	0.578	0.088	3.15E-61	5	Egr1
1.42E-51	1.194216776	0.353	0.037	2.10E-47	5	Nr4a3
9.50E-44	1.306584013	0.267	0.024	1.40E-39	5	Nr4a2
1.39E-24	1.204752427	0.56	0.201	2.06E-20	5	Tagap
3.69E-23	1.13697983	0.552	0.2	5.46E-19	5	Cd69
7.83E-21	0.9852495	0.526	0.199	1.16E-16	5	Pdcd1
4.68E-09	0.731646606	0.716	0.501	6.92E-05	5	Junb
8.80E-06	0.325864875	0.552	0.352	0.130200307	5	Tox
5.58E-05	0.279217077	0.284	0.143	0.825363374	5	Il6st
6.06E-05	-0.57306397	0.181	0.352	0.895755943	5	Ass1
0.000115839	-0.462787525	0.25	0.418	1	5	Ctla4
0.000274991	0.34195834	0.345	0.211	1	5	Cblb
1.59E-37	1.583813696	0.556	0.041	2.35E-33	6	Ccr9
2.01E-34	1.3751859	0.667	0.066	2.98E-30	6	Ckb
3.65E-12	1.013261477	0.407	0.068	5.40E-08	6	Cd40lg
6.05E-09	-1.772845689	0	0.633	8.94E-05	6	Foxp3
3.05E-05	-1.419560374	0	0.416	0.450628941	6	Il2ra
0.000142551	-1.079433864	0.037	0.414	1	6	Ctla4
0.000171751	0.755767092	0.778	0.466	1	6	Cd4
0.000477511	-1.019258295	0	0.323	1	6	Cish
0.000481475	0.65034	0.667	0.358	1	6	Tox

Table 5.1. Table of selected differentially regulated genes in clusters from thymic CD73^{+} T_{reg} cell scRNAseq analysis. Differential genes were identified for each cluster by

comparing expressing of genes in that cluster versus all other cells in the data set. Table is color coded to match the respective clusters in the UMAP analysis and Seurat clustering in Figure 5.2 a.

Depletion of RT-T_{reg} cells drives resurgence of AIRE$^+$ mTEC

mTEC in the thymus are a major enforcer of central tolerance to self-antigens via negative selection and T_{reg} cell selection. Specifically, mTEC that express the transcription factor AIRE, a key driver of tissue-restricted antigen (TRA) expression, are crucial to prevent autoimmunity[83–85]. Indeed, AIRE$^+$ mTEC represent an efficient population of cells to deplete the effector T cell repertoire of self-reactive TCRs as AIRE$^+$ mTEC can express ~85% of the entire genome[267]. However, AIRE$^+$ mTEC abundance peaks early in life, ~4 weeks of age in mice[181], before a significant reduction later in life. AIRE expression and T_{reg} cell generation in this same window, from birth to 3-4 weeks of age, is essential to prevent autoimmune reactions to TRA[177,178]. Further, ~3-4 weeks of age is when RT-T_{reg} cells begin to appreciably accumulate[174]. Given the temporal overlap in AIRE$^+$ mTEC abundance and RT-T_{reg} cell accumulation, we wanted to understand if RT-T_{reg} cells were responsible for the decrease in AIRE$^+$ mTEC. To answer this question, we developed a system to preferentially delete RT-T_{reg} cells, sparing *de novo* T_{reg} cell development and preserving peripheral T_{reg} cell abundance. Treatment of *Foxp3-DTR* mice bi-weekly, via i.t. injection, with low-dose DT caused a significant reduction in CD73^{hi} thymic T_{reg} cells while CD73$^-$ *de novo* developing T_{reg} cells were not strongly affected (Figure 5.3 a,b). In fact, *de novo* T_{reg} cell development is significantly increased following RT-T_{reg} cell depletion with DT, confirming previous suggestions that RT-T_{reg} cells are repressing T_{reg} cell development[142,174]. Similarly, splenic T_{reg} cell abundance is also not reduced in i.t. DT treated mice (Figure 5.3 c). Thus, this dosage scheme efficiently reduces RT-T_{reg} cell abundance while leaving other T_{reg} cell populations and T_{reg} cell development largely intact.

We first performed analysis of thymic stromal cell populations over a 1-4 week time course of RT-T_{reg} depletion following the above protocol. AIRE$^+$ mTEC abundance

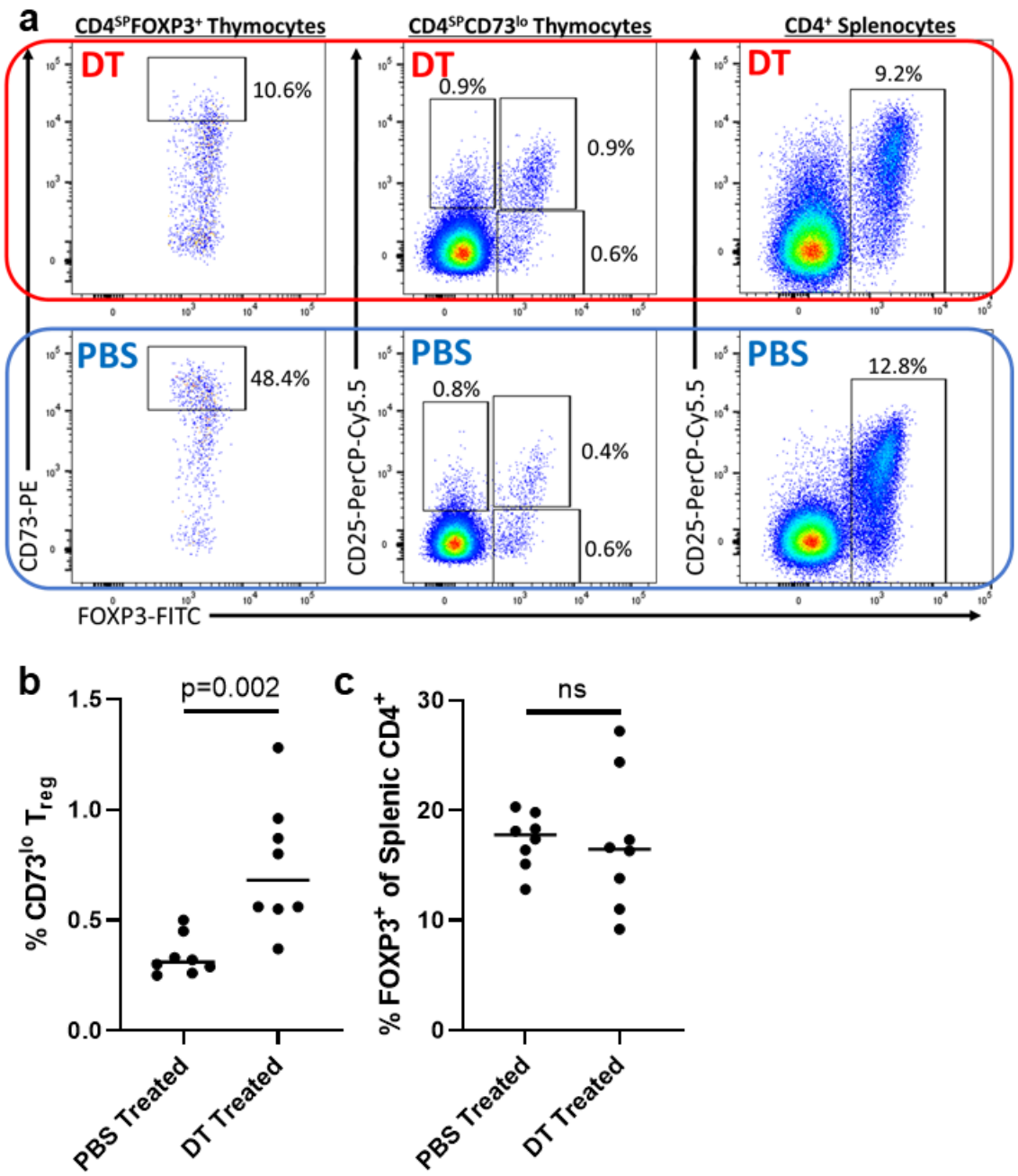

Figure 5.3. Low dose intrathymic DT treatment in *Foxp3*^{DTR} mice preferentially depletes RT-T_{reg} cells. **a)** *Foxp3*^{DTR} mice were treated bi-weekly for 3 weeks with either 0.05µg DT or 1xPBS. Mice were harvested 72 hours after final i.t. DT treatment to quantify the depletion of T_{reg} subsets. Left, RT-T_{reg} cell (CD73^{hi}FOXP3^{+}) abundance in CD4SP thymocytes, middle, CD25^{+} T_{reg}P, FOXP3^{lo} T_{reg}P and mature T_{reg} in *de novo* developing

(CD73^{lo}) CD4SP thymocytes, right, T_{reg} cell (FOXP3^{+}) abundance in CD4^{+} splenocytes in DT treated (red) versus 1xPBS treated controls (blue). **b)** Quantification of thymic CD73^{lo} T_{reg} cells in the CD4SP compartment in 1xPBS vs DT treated mice. **c)** Quantification of splenic T_{reg} cell abundance in 1xPBS vs DT treated mice. **b,c)** Data is representative of 2 experiments, n=8 mice (1xPBS treatment) and n=8 mice (DT treatment). Data was analyzed by unpaired *t*-test.

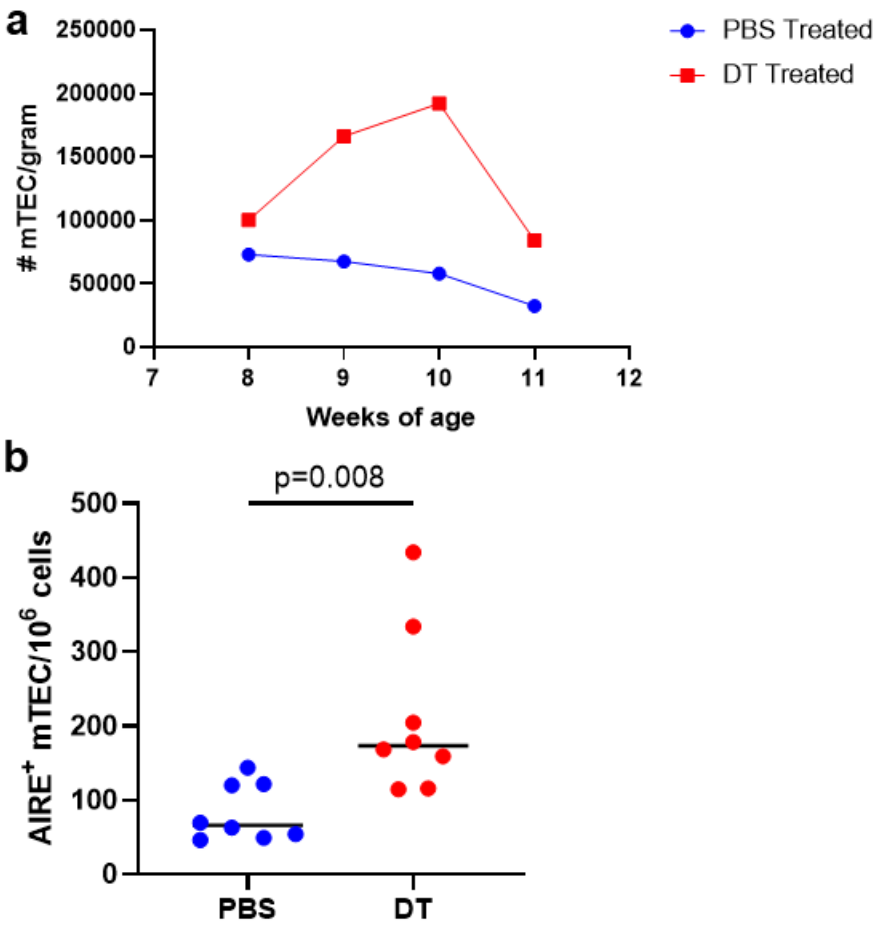

Figure 5.4. RT-T_{reg} cell depletion causes an increase in $AIRE^+$ mTEC density. **a)** Mice were treated for 1.5 (8 weeks of age), 2.5 (9 weeks of age), 3.5 (10 weeks of age) or 4.5 weeks (11 weeks of age) with i.t. DT (red) or 1xPBS (blue) and # mTEC/gram was quantified once/week. **b)** Mice were treated with 0.05µg DT (red), or 1xPBS (blue) as a control, bi-weekly for 1.5-4.5 weeks. $AIRE^+$ mTEC were quantified as $EPCAM^+UEA1^+MHCII^{hi}AIRE^+$. Data was analyzed by unpaired *t*-test.

decreased throughout the time course in control mice, treated with i.t. injection of 1xPBS. However, DT mediated RT-T_{reg} cell depletion led to an increase in $AIRE^+$ mTEC abundance that peaked 3 weeks after initiating DT treatment (Figure 5.4 a). $AIRE^+$ mTEC abundance at the four-week time point approached the control group. However, this was likely due to ineffective RT-T_{reg} cell depletion at these timepoints due to the development of anti-DT neutralizing antibodies after 4 weeks of DT treatment[275]. Given that the difference in $AIRE^+$ mTEC cell abundance peaked following three weeks of DT treatment, we setup a cohort of mice that were all analyzed after three weeks of DT treatment. DT treated mice had significantly higher $AIRE^+$ mTEC cell abundance than control mice (Figure 5.4 b). Together, this data suggests that $AIRE^+$ mTEC progressively decline during aging and that RT-T_{reg} cells control the density of $AIRE^+$ mTEC.

5.3 Discussion

The presence of RT-T_{reg} cells has been appreciated for more than a decade however little is known about their functional importance in immunity or immune homeostasis. Earlier studies noted that RT-T_{reg} cells accumulate with age and are associated with a decrease in *de novo* T_{reg} cell differentiation without an accompanying block in $CD25^+$ T_{reg}P cell development[174]. Further, depletion of CCR6, a chemokine receptor thought to be important for mature T_{reg} cell trafficking to the thymus, results in a reduction in RT-T_{reg} cells along with an increase in RAG2-GFP^+ T_{reg} cell abundance[276]. Along with the observation that excess T_{reg} cells inhibit T_{reg} cell development[142], the field suggested a model whereby RT-T_{reg} cell accumulation functioned largely to block *de novo* T_{reg} cell development, perhaps via IL-2 competition. Such as effect could be due to T_{reg} cell consumption of IL-2, mediated by robust expression of the high affinity IL-2 receptor, a trimer of CD25-CD122-CD132. This mechanism indeed accounts for one strategy by which T_{reg} cells suppress effector T cell responses in the periphery[210].

Several observations disagree with the assumption that RT-T_{reg} cells inhibit *de novo* T_{reg} cell development broadly. First, *Aire*$^{-/-}$ mice have defects in recirculation of T_{reg} cells back to the thymus without an accompanying increase in *de novo* T_{reg} cell development[276], although the defect downstream of AIRE deficiency may counteract any pro-T_{reg} development effect of reduced RT-T_{reg} cell accumulation. A more recent study found that IL18R marks a population of RT-T_{reg} cells and is important for trafficking of mature T_{reg} cells back to the thymus. *Il18r1*$^{-/-}$ mice exhibit a defect in RT-T_{reg} cell accumulation but no rise in *de novo* T_{reg} cell differentiation[277]. Finally, some RT-T_{reg} cells express the decoy IL-1 receptor, IL1R2. Increases in IL-1, as might be found during inflammation, were found to reduce T_{reg} cell development but the addition of IL1R2^{+} RT-T_{reg} cells to IL-1 treated fetal thymic organ cultures rescues this defect[278]. These results all suggest that RT-T_{reg} cell accumulation is either neutral or beneficial to *de novo* T_{reg} cell development.

A potential shortcoming of all the studies presented is the lack of a specific way to target RT-T_{reg} cell accumulation to understand the effect of RT-T_{reg} cells on T_{reg} cell development. In order to better understand how RT-T_{reg} cells effect the biology of the thymus we developed a targeted RT-T_{reg} cell depletion strategy using low-dose DT delivered intrathymically to *Foxp3*^{DTR} mice. We observed a significant increase in *de novo*, CD73^{-}, T_{reg} cell development following RT-T_{reg} cell depletion (Figure 5.3 b). This result agrees with the former studies that hypothesized RT-T_{reg} cells inhibit T_{reg} cell development. Indeed, *Ccr6*$^{-/-}$ mice, mice lacking the chemokine receptor thought to be important for mature T_{reg} cell trafficking to the thymus, have a reduction in RT-T_{reg} cells along with an increase in RAG2-GFP^{+} T_{reg} cell abundance[276]. Thus, based on our experiments, RT-T_{reg} cell accumulation in the thymus does indeed block *de novo* T_{reg} cell differentiation. However, it is still unclear if this is a general feature of all RT-T_{reg} cell subsets and what mechanism RT-T_{reg} cells utilize to block *de novo* T_{reg} cell development.

While we provide convincing evidence that RT-T_{reg} cells do antagonize T_{reg} cell development, the evolutionary benefit of reducing T_{reg} cell output remains enigmatic. It is true that the size of the thymus decreases with age although it continues to function and produce T cells throughout life[266]. Thus, no matter the mechanism by which RT-T_{reg} cells function, the presence of RT-T_{reg} cell would likely redirect TCRs destined for the T_{reg} cell lineage towards the effector T cell fate. The field has suggested that deprivation from γC cytokines, such as IL-2 or IL-15, would simply result in death of self-reactive thymocytes[65,279]. However, we provide data that self-reactive thymocytes, as represented by T_{reg}P cell populations, persist in *Il2*$^{-/-}$ x *Il15*$^{-/-}$ mice (Figure 2.4 a,b). Thus, RT-T_{reg} cell antagonization of T_{reg} cell development would increase the autoimmune hazard of the thymus continuing to function after RT-T_{reg} cell accumulation. Perhaps peripheral tolerance mechanisms[280,281] could be utilized to control these pathogenic T cells. However, the net result of exporting pathogenic effectors in this scenario would at best be neutral, as these cells would be rendered non-functional or deleted entirely.

RT-T_{reg} cell accumulation likely evolved due to some benefit of restricting or changing *de novo* T_{reg} cell development. Interestingly, AIRE^{+} mTEC cell density peaks as RT-T_{reg} cells are starting to accumulate. Since AIRE^{+} mTEC express the majority of the proteins found within the genome, loss of AIRE^{+} mTEC would dramatically reduce the diversity of peptides developing thymocytes are tolerized to. We hypothesize that the net effect of RT-T_{reg} cell accumulation, which inhibit T_{reg} cell development and reduce AIRE^{+} mTEC abundance, would be increased output of self-reactive thymocytes. Increasing the output of self-reactive effector T cells would produce greater diversity in the anti-pathogen or anti-tumor immune responses, perhaps providing a benefit to detect a broader array of antigens from potential hazards. We provide evidence that RT-T_{reg} cell accumulation and AIRE^{+} mTEC loss may be linked, as depletion of RT-T_{reg} cells causes an increase in the

abundance of AIRE^{+} mTEC (Figure 5.4). This suggests that RT-T_{reg} cell accumulation is a major mechanism to reduce the stringency of central tolerance resulting in the export of a more diverse effector T cell TCR repertoire. We hypothesize that RT-T_{reg} cell accrual signals the development of a competent peripheral T_{reg} cell repertoire capable of maintaining immune homeostasis. Thus, RT-T_{reg} cells act as a rheostat to safely loosen central tolerance after ensuring peripheral tolerance is established.

Chapter 6. Summary and Future Directions

6.1 Summary of Research

Cellular sources of IL-2 in T_{reg} cell development and homeostasis

Development of T_{reg} cells in the thymus is crucial to maintaining immune homeostasis. The developmental scheme involves two steps- first self-reactive thymocytes receive TCR stimulation, generating T_{reg}P cells, and second these T_{reg}P cells obtain cytokine stimulation to activate STAT5 completing T_{reg} cell development. The major cytokine important for this second step is IL-2, along with IL-15 which plays a minor or compensatory role. To understand the cellular source of IL-2 that is important for T_{reg} cell development, and peripheral homeostasis, we crossed *Cd4*^{Cre}, *Cd11c*^{Cre} and *Cd79a*^{Cre} to *Il2*$^{fl/fl}$ x *Il15*$^{-/-}$ mice. In chapter 2 we demonstrate that T cell derived IL-2 is necessary and sufficient for T_{reg} cell development in the thymus. The source of T cell derived IL-2 was refined to CD25^{+} T_{reg}P cells undergoing agonist selection using a combination of bulk and scRNAseq analysis. Further, using mixed bone marrow chimeras, we found that paracrine IL-2 is sufficient for T_{reg} cell development with autocrine IL-2 being dispensable. Thus, the second, cytokine and STAT5 dependent, step of T_{reg} cell development is governed by the availability of IL-2 produced from self-reactive thymocytes engaging cognate antigens during development.

Homeostasis of peripheral T_{reg} cells is similarly dependent on T cell derived IL-2. While we could not refine our analysis of the potential source of IL-2 in peripheral organs, IL-2 is known to be produced by activated effector T cells which acts in trans to facilitate T_{reg} cell homeostasis and function[214]. However, deletion of *Il2* with *Cd11c*^{Cre}, which largely targets dendritic cells, did cause a further reduction in T_{reg} cell proportions in the mesenteric lymph nodes when combined with IL-2 deletion in T cells. This data suggests that other cellular sources of IL-2 are important in different contexts. Indeed, ILC derived

IL-2 is important for maintaining T_{reg} cells in the intestine and ILC production of IL-2 is negatively correlated with Crohn's disease[215]. Collectively, these observations suggest that maintaining T_{reg} cell homeostasis in peripheral lymphoid organs is largely dependent on T cell derived IL-2 but T_{reg} maintenance in specific tissues is governed by different cellular producers of IL-2.

Contributions of CD25$^+$ T_{reg}P and FOXP3^{lo} T_{reg}P cell pathways to mature T_{reg} cells

Step one of T_{reg} cell development, and negative selection, is driven by TCR stimulation. This ensures that the autoimmune hazard of self-reactive thymocytes is nullified by polarization to the T_{reg} cell phenotype or removal from the effector T cell repertoire. However, two populations of T_{reg}P cells have been described, each expressing either CD25 or FOXP3[63–65]. In order to understand the evolutionary rationale of two pathways that produce the same end product we characterized the differences between each T_{reg}P cell population in chapter 3.

The introduction of FOXP3^{lo} T_{reg}P cells[65], coming 5 years after the identification of CD25$^+$ T_{reg}P cells[63,64], stimulated debate on the contributions of each pathway to mature T_{reg} cells. Indeed, it was suggested that FOXP3^{lo} T_{reg}P cells were the major contributor to the mature T_{reg} cell compartment with CD25$^+$ T_{reg}P cells only being a minor contributor[282]. We find that each T_{reg}P cell population contributes relatively equivalently to mature T_{reg} cells in competitive intrathymic development experiments. Further, each T_{reg}P cell TCR repertoire overlaps with mature T_{reg} cells to a similar degree. These results suggest that both T_{reg}P cell populations contribute equally, at least quantitatively, to the mature T_{reg} cell compartment. However, the TCR repertoires between the two T_{reg}P cell populations do diverge, suggesting that T_{reg}P subsets are contributing distinctly to the mature T_{reg} cell repertoire. Supporting this idea, CD25$^+$, but not FOXP3^{lo} T_{reg}P cells contained TCRs specific for the AIRE driven self-antigen MOG and protected mice from MOG immunization

induced EAE. FOXP3^{lo} T_{reg}P cells failed to protect mice from EAE but were competent to suppress the development of a transfer model of colitis. Thus, T_{reg} cells derived from either T_{reg}P cell subset have distinct functions in maintaining immune homeostasis.

The evolutionary rationale for two T_{reg}P cell pathways is likely to broaden the functional capacity of stable T_{reg} cells that develop in the thymus. We wanted to understand how thymocytes commit to either T_{reg}P cell pathway. Analysis of NUR77-GFP expression suggests that CD25^{+} T_{reg}P cells interact more strongly with self-antigens in the thymus than FOXP3^{lo} T_{reg}P cells, likely placing CD25^{+} T_{reg}P cell closer to negative selection and FOXP3^{lo} T_{reg}P cells closer to positive selection from a TCR signaling perspective. Indeed, CD25^{+} T_{reg}P cells are more apoptotic than FOXP3^{lo} T_{reg}P cells. Deficiency of proteins involved in transducing negative selection, *Itk* and *Adap*, results in expanded CD25^{+}, but not FOXP3^{lo}, T_{reg}P cell proportions. However, FOXP3^{lo} T_{reg}P cells are expanded in *Itk*$^{-/-}$ but not *Adap*$^{-/-}$ thymi. The increase of FOXP3^{lo} T_{reg}P cells in *Itk*$^{-/-}$ thymi is due to increased IL-4 production, as *Itk*$^{-/-}$ x *Il4ra*$^{-/-}$ thymi have no increase in FOXP3^{lo} T_{reg}P cells. Interestingly, T_{reg} cells from mice deficient in the *Foxp3* enhancer *Cns3* are more self-reactive, as evidenced by increased expression of NUR77[163]. *Cns3* is a pioneer regulatory element in *Foxp3,* which is targeted by TCR stimulation and downstream c-REL activation, to poise the *Foxp3* locus for expression[160]. FOXP3^{lo} T_{reg}P cells are nearly absent in *Cns3*$^{-/-}$ mice while the CD25^{+} T_{reg}P cell pathway remains operative. In *Cns3*$^{-/-}$ mice, we propose that CD25^{+} T_{reg}P cell TCR signal strength is sufficient to activate the *Foxp3* locus but thymocytes normally destined for the FOXP3^{lo} T_{reg}P pathway fail to receive sufficient TCR stimulation to express FOXP3. Collectively, these data suggest that increased TCR signal strength constrains the CD25^{+} T_{reg}P cell pathway while FOXP3^{lo} T_{reg}P cell development requires sensitization to TCR signaling. Therefore, we hypothesize that differences in TCR

signaling are a key driver in thymocytes committing to the T_{reg} cell lineage via $CD25^{+}$ or $FOXP3^{lo}$ $T_{reg}P$ cell pathways.

Understanding CD4SP maturation and T_{reg} cell development with scRNAseq

In order to develop a more granular understanding of T_{reg} cell development in the thymus we performed scRNAseq analysis of conventional and T_{reg} cell lineage thymocytes. Using previously identified schemes of transcriptional changes in thymocyte maturation, including chemokine receptors, transcription factors and tonic IFN signatures, we were able to identify two major populations of conventional CD4SP thymocytes, an immature and mature cluster. However, in addition to recapitulating the known transcription changes of maturation we found several new markers associated with maturation state. The integrin *Itgb7* is highly upregulated in mature versus immature CD4SP. *Itgb7* has previously been associated with peripheral T cell homing, particularly to the gut[249], but the expression pattern during thymocyte maturation was unappreciated. *Ms4a4b* and *Ms4a6b* are also highly upregulated in mature thymocytes and serve as accurate markers of CD4SP maturity. These membrane spanning proteins are not well studied in T cell biology but are associated with increased sensitivity to TCR stimulation and cytokine production in mature T cells as well as the Th1 subset of $CD4^{+}$ T cells[222,250]. We can speculate that these proteins are repressed during thymic selection to prevent over-induction of negative selection which may narrow the T cell repertoire considerably. However, following maturation MS4A4B and MS4A6B are expressed to poise T cells for peripheral stimulation. Interestingly, the brain related creatine kinase *Ckb* is upregulated in immature CD4SP thymocytes. Previous work has suggested that CKB is important for positive selection. This is likely due to creatine kinases maintaining intracellular ATP concentrations which facilitate TCR signaling cascades[252]. Altogether, these

transcriptional changes that occur during maturation can be used to grade the maturity of different thymocyte populations.

Using the above identified maturation related transcriptional changes as a guide we were able to further understand T_{reg} cell development. We could find an agonist selection signature cluster in both $T_{reg}P$ cell populations and this agonist selection signature is the most immature subset within each $T_{reg}P$ cell pathway. Given that step one of T_{reg} development is initiated by TCR signaling, it is unsurprising that the most immature cluster in each $T_{reg}P$ pathway contains the cells receiving TCR stimulation. However, one interesting difference between the two agonist selection clusters is the expression of STAT target genes, *Cish* and *Socs1*, in the FOXP3^{lo} $T_{reg}P$ agonist selection cluster. FOXP3 is thought to drive apoptosis in FOXP3^{lo} $T_{reg}P$ cells if unbalanced by γC cytokine stimulation[65], a pathway which activates STAT proteins. While we find the FOXP3^{lo} $T_{reg}P$ cells are not highly apoptotic *in vivo*, expression of *Cish* and *Socs1* suggests that FOXP3^{lo} $T_{reg}P$ are receiving cytokine stimulation. FOXP3^{lo} $T_{reg}P$ cells can be bolstered by increased expression of IL-4. Thus, the expression of these STAT target genes in the FOXP3^{lo} $T_{reg}P$ agonist selection cluster may be further evidence that FOXP3^{lo} $T_{reg}P$ are protected from FOXP3 and/or TCR induced apoptosis by cytokine stimulation, perhaps from IL-4. Without scRNAseq analysis, it would be difficult to uncover these changes as we have been unable to isolate “agonist selection” cells by flow cytometry for either $T_{reg}P$ cell population.

In contrast to the “tonic” IFN signature associated with normal thymocyte development, our scRNAseq analysis also identified a cluster of cells whose transcriptome is dominated by ISGs. The ISG cluster is comprised of a mix of CD4SP, $T_{reg}P$ and mature T_{reg} cells but the major contributors are conventional CD4SP and FOXP3^{lo} $T_{reg}P$ cells. A similar population has been identified in peripheral tissues, by us and others[256], but no function has been defined. Indeed, we still do not know why this ISG subset exists in the thymus.

However, type I IFN is known to be produced in the thymic medulla, primarily by AIRE$^+$ mTEC[255]. Thus, these ISG cells could represent a population of thymocytes residing in an IFN rich niche. That AIRE$^+$ mTEC are major producers of IFN may suggest that ISG signature thymocytes are arrested by the antigens displayed on IFN producing AIRE$^+$ mTEC. We are currently interested in understanding the TCR repertoire and specificity of ISG thymocytes. We also want to understand if the ISG signature in the thymus is stable and is related to the ISG T_{reg} cells that exist in peripheral tissues.

Regulation of central tolerance by recirculating and resident thymic T_{reg} cells

FOXP3$^+$ cells in the thymus not only include *de novo* developing T_{reg}P and T_{reg} cells but also a high proportion of fully differentiated recirculating and resident thymic T_{reg} cells (RT-T_{reg}). RT-T_{reg} accumulate throughout ontogeny reaching ~50% of thymic T_{reg} cells by 5-6 weeks of age and ~80% by one year of age. Previous work suggested that RT-T_{reg} cells are activated and transcriptionally similar to effector T_{reg} (eT_{reg}) cells[174]. eT_{reg} cells are not homogeneous and can take on more specific functional phenotypes including a “tissue-like” or adipose related subset (ST-2$^+$)[22,23,273] and a cytotoxic (TIM-3$^+$) subset[270,271]. Using flow cytometry, we found a large fraction of eT_{reg} phenotype cells within the RT-T_{reg} cell compartment. eT_{reg} phenotype cells in the thymus are comprised of at least three eT_{reg} cell subsets including TIM-3$^+$, ST-2$^+$ and TIGIT$^+$. Similarly, scRNAseq analysis found a large TIGIT$^+$ population which contains cells expressing *Havcr2* (TIM-3) and *Il1rl1* (ST-2). Another eT_{reg} cell population distinct from the *Tigit* expressing population is also present along with a cluster defined by a strong TCR signaling signature. TIM-3$^+$ RT-T_{reg} cells could represent a cytotoxic subset of T_{reg} cells in the thymus while ST-2$^+$ RT-T_{reg} cells may be a thymic resident or adipose associated T_{reg} cell population. RT-T_{reg} cells are a phenotypically, and likely functionally, diverse population of T_{reg} cells in the thymus.

Previous work associated RT-T_{reg} cell abundance with alterations in *de novo* T_{reg} cell development, either promoting[278] or inhibiting[142,174] T_{reg} cell differentiation. However, these studies lack the ability to specifically modulate the RT-T_{reg} cell compartment, relying instead on correlations or genetic alterations of T_{reg} cells to understand the function of RT-T_{reg} cells. To directly test the function of RT-T_{reg} cells we developed a protocol to specifically delete RT-T_{reg} cells by low dose, repeated intrathymic (i.t.) DT treatments in *Foxp3*^{DTR} mice. This protocol effectively reduces RT-T_{reg} cell abundance without marked changes in T_{reg} cell abundance in the spleen. Following depletion of RT-T_{reg} cells, we observed an increase in *de novo* T_{reg} cell development, suggesting that RT-T_{reg} cells do broadly inhibit T_{reg} cell development. This effect is likely proportional to the abundance of RT-T_{reg} cells in relation to T_{reg}P cells or self-reactive CD4SP. IL-2 competition is assumed to be the primary function by which RT-T_{reg} cells inhibit T_{reg} cell development, preventing the IL-2 dependent conversion of T_{reg}P to mature T_{reg} cells. However, CD25^{+} T_{reg}P cells are capable of IL-2 production, which is unlikely to be depleted by RT-T_{reg} cells prior to autocrine signaling. Additionally, IL-15 would still function as a compensatory source of STAT5 activating cytokine, as shown in chapter 2, if RT-T_{reg} cells do meaningfully compete for IL-2. Further, the field has assumed that lack of cytokine stimulation, via IL-2 or IL-15, would cause these self-reactive thymocytes to simply undergo apoptosis. However, we found that T_{reg}P cells persisted in the absence of both IL-2 and IL-15, suggesting that these undifferentiated T_{reg}P cells could still represent an autoimmune hazard. Thus, while IL-2 competition could represent a mechanism to limit T_{reg} cell development, it is unlikely to account for broad reductions in thymic T_{reg} cell output.

AIRE^{+} mTEC abundance peaks early in life before significantly decreasing. The peak of AIRE^{+} mTEC coincides with the accumulation of RT-T_{reg} cells. Given that RT-T_{reg} cells are activated, experiencing antigen, express *Gzmb*[174] and contain a cytotoxic T_{reg} cell subset

(TIM-3$^+$) we reasoned that RT-T_{reg} cell accumulation limits AIRE$^+$ mTEC abundance. Indeed, depletion of RT-T_{reg} cells, for 1-4 weeks, caused a resurgence in AIRE$^+$ mTEC abundance. This suggests that RT-T_{reg} cells are directly modulating AIRE$^+$ mTEC, therefore TRA, abundance in the thymus. Interestingly, both AIRE expression and T_{reg} cell development during the perinatal window (~1-4 weeks of age) is crucial to enforce immune tolerance to TRA in the periphery[177,178]. Thus, it is possible that the accumulation of RT-T_{reg} cells represents a negative feedback loop to prevent the development of functionally overlapping T_{reg} cells. Reduction of AIRE$^+$ mTEC may also narrow the peptidome presented to developing thymocytes to facilitate output of more diverse effector T cells. Combined with existing studies, the data presented here in chapter 5 confirm that RT-T_{reg} cells inhibit T_{reg} cell development. The inability to efficiently convert self-reactive thymocytes to stable T_{reg} cells would represent a significant autoimmune hazard. Thus, RT-T_{reg} cell accumulation must provide some benefit to the organism to outweigh this detriment- I will discuss potential advantages below in the future directions of RT-T_{reg} cell research.

6.2 Future Directions

Cytokines in T_{reg} cell development

Activation of STAT5 is essential for T_{reg} cell development and homeostasis. However, there are a number of cytokines, and cellular sources of such cytokines, that can activate STAT5.

<u>IL-2</u>

We found that T cell derived IL-2 is necessary and sufficient for bulk T_{reg} cell development. This result contradicted a previous study that identified DC derived IL-2 as the critical source of IL-2 using an *in vitro* thymic slice model[142]. However, we found no deficit in T_{reg} cell development in *Cd11c*^{Cre} x *Il2*$^{fl/f}$, and no additional defect comparing *Cd4*^{Cre} x *Il2*$^{fl/fl}$ to

Cd4^{Cre} x *Cd11c*^{Cre} x *Il2*$^{fl/f}$ mice. We found similar results studying B cell derived IL-2, despite B cells being in the thymus and activated B cells being capable of producing IL-2. Thus, it is possible that B cell and/or DC derived IL-2 still plays a role on in T_{reg} cell development for some T_{reg} cell specificities, perhaps those only found on DC or B cells. Future studies could interrogate this further by analyzing T_{reg} cell TCR repertoires in mice depleted of IL-2 on DC or B cells. Mice lacking B cell or DC derived IL-2 could also be aged to see if signs of autoimmunity develop in these mice.

RT-T_{reg} cells represent another mechanism to reduce IL-2 availability. However, it is still unclear if RT-T_{reg} cells use IL-2 competition to limit T_{reg} cell differentiation. Outside of *Ccr6*$^{-/-}$ mice[276], which only have a mild RT-T_{reg} cell accumulation defect, there are no genetic models that modulate RT-T_{reg} cell abundance without disrupting peripheral T cell homeostasis. Using our model of RT-T_{reg} cell depletion we can perform TCR sequencing experiments with or without short term RT-T_{reg} cell depletion. If RT-T_{reg} cells do primarily regulate the transition from T_{reg}P to mature T_{reg} cell via IL-2 depletion, we should observe that TCRs once biased to the T_{reg}P compartment are found in mature T_{reg} cells after RT-T_{reg} cell depletion.

IL-2 is not only important for thymic T_{reg} cell development but also for T_{reg} cell homeostasis and function in the periphery of the organism. While T cell derived IL-2 is principally important for maintaining T_{reg} cell homeostasis in the spleen, DC derived IL-2 contributed to T_{reg} cell abundance in the mesenteric lymph nodes. Additionally, ILC derived IL-2 is important for maintaining T_{reg} cells in the intestine[215]. Thus, while T_{reg} cells certainly rely on T cell production of IL-2, it is again possible that there are contexts where IL-2 from other cellular sources is important for T_{reg} homeostasis. Given that T cell derived IL-2 is critical for thymic T cell development, and the likely source is developing self-reactive thymocytes, it will be important to test the contribution of T cell derived IL-2 in models

where *Il2* can be deleted in mature T cells, such as the distal Lck^{Cre} [283]. Further, these mice could be a setting to test the relative importance of other cellular sources of IL-2 against T cell derived IL-2.

IL-15 and IL-7

While IL-2 seems to be the dominant cytokine that drives T_{reg} cell development, both IL-15 and IL-7 are potent STAT5 inducers as well. IL-15 deficient mice have mild defects in T_{reg} cell development while T_{reg} cell development in mice lacking the IL-7 receptor is largely preserved[200]. However, IL-7 and IL-15 are both produced in the medulla and thus could activate STAT5 in T_{reg}P cells to complete differentiation. Similar to the caveats discussed above for the cellular sources of IL-2, TCR sequencing experiments could reveal if there are any T_{reg} cell TCRs that fail to develop when thymocytes cannot respond to either of these cytokines.

IL-4

Contrary to previous reports, we found in chapter 3 that IL-4 could augment T_{reg} cell development through the $FOXP3^{lo}$ T_{reg}P pathway. We also found that $FOXP3^{lo}$ T_{reg}P cells are maintained in the absence of IL-2 and IL-15 and immature $FOXP3^{lo}$ T_{reg}P receiving TCR stimulation also appear to be receiving cytokine stimulation. From this data we hypothesize that IL-4 is an important survival factor for $FOXP3^{lo}$ T_{reg}P cells. We also found that IL-4 is sufficient to partially upregulate CD25 and maintain FOXP3 expression in $FOXP3^{lo}$ T_{reg}P cells. IL-4 stimulation *in vivo* may drive some CD25 expression which then allows these cells to compete for the limited IL-2 in the thymus. However, we currently do not know when IL-4 is acting in T_{reg} cell development. Mixed bone marrow chimera mice could confirm that IL-4 does influence the efficiency of $FOXP3^{lo}$ T_{reg}P cell generation. We

could also quantify apoptosis in these mice to understand if IL-4 is acting as a survival factor for FOXP3^{lo} T_{reg}P cells.

Contributions of CD25^{+} and FOXP3^{lo} T_{reg}P cells to immune tolerance

In chapter 3 we tested the functional capacity of T_{reg} cells derived from either CD25^{+} T_{reg}P or FOXP3^{lo} T_{reg}P cells. We found that CD25^{+}, but not FOXP3^{lo}, T_{reg}P derived T_{reg} cells suppressed the development of experimental autoimmune encephalomyelitis. However, T_{reg} cells derived from FOXP3^{lo} T_{reg}P cells reduce the severity of colitis. Thus, in these two experimental systems each T_{reg}P cell pathway contributes distinct functions to the mature T_{reg} cell compartment. However, we would like to develop a holistic understanding of how each T_{reg}P pathway controls immune homeostasis. In order to do test this our collaborator, Dr. Calvin Williams at the Medical College of Wisconsin, is rescuing *Foxp3*$^{-/-}$ mice with an infusion of T_{reg} cells. This will allow *Foxp3*$^{-/-}$ mice to be bred together and produce litters of 100% *Foxp3*$^{-/-}$ offspring. Mice deficient in *Foxp3* develop rapid onset of a myriad of autoimmune manifestations which, left uncontrolled, are uniformly fatal[8]. We can transfer purified populations of either CD25^{+} or FOXP3^{lo} T_{reg}P cells to these *Foxp3*$^{-/-}$ mice to determine what aspects of autoimmunity each subset controls. Based on our previous results, we speculate that CD25^{+} T_{reg}P are more important for suppressing autoimmunity to TRA during sterile autoimmunity while FOXP3^{lo} T_{reg}P cells are required to control autoimmunity at mucosal sites. Rescue of *Foxp3*$^{-/-}$ mice with T_{reg}P subsets should allow for unbiased determination of the function of each T_{reg}P cell population.

We found that mice lacking *Cns3*, an enhancer of *Foxp3*, are deficient in FOXP3^{lo} T_{reg}P cells. Interestingly, *Cns3*$^{-/-}$ mice develop spontaneous lung inflammation[163]. Mice deficient in an *Il2ra* enhancer, CaRE4[164], have a mild block in CD25^{+} T_{reg}P cell development. SNPs found within the CaRE4 region in humans are known to increase susceptibility to inflammatory bowel disease but protect against diabetes[165,167]. To better understand what

genomic elements are important for each T_{reg}P pathway we performed **A**ssay for **T**ransposase-**A**ccessible **C**hromatin using **seq**uencing (ATACseq) to identify enhancer regions preferentially open in each T_{reg}P cell population. While preliminary analysis of this data failed to produce clear differences at hallmark genes, such as *Il2ra* and *Foxp3*, other genes may be important in facilitating development of either T_{reg}P cell. Recent advances in single-cell technology allow for ATACseq to be performed in single cells, analogous to scRNAseq. Given that we observed some heterogeneity within T_{reg}P cell populations, scATACseq could identify regulatory elements unique to each cluster of cells. For example, *Il2* is expressed in the immature $CD25^+$ T_{reg}P cells undergoing agonist selection however *Il2* is repressed in mature T_{reg} cells[212]. Thus, perhaps the *Il2* locus is repressed in more mature T_{reg}P cells and only readily accessible in these immature $CD25^+$ T_{reg}P cells receiving TCR stimulation. Understanding the regulatory elements required for each T_{reg}P cell pathway could reveal previously unappreciated connections of disease associated non-coding polymorphisms and thymic T_{reg} cell development.

Understanding thymocyte and T_{reg} cell development with single-cell approaches

Our scRNAseq analysis of CD4 lineage thymocytes and T_{reg} cells revealed new markers for thymocyte maturation, defined the agonist selection signature for each T_{reg}P population and revealed a novel subset of CD4SP thymocytes. These results can be extended though to better understand the thymocyte development and T_{reg} cell differentiation in several ways. First, a caveat of RNAseq analysis of any kind is that a transcript for a particular gene being up- or down-regulated does not deterministically predict the status of that gene's protein product. scProteomics (CITEseq) can be combined with scRNAseq, at least for surface markers, by using oligo tagged antibodies. We have recently initiated a combined scRNAseq and CITEseq experiment to better understand the dynamics of CD4SP maturation and T_{reg} cell development. Second, while we have found numerous

clusters within CD4SP and T_{reg} cell development, we do not know if they share unique localizations within the thymus. This may be of particular interest for the ISG subset which we hypothesize is defined by close proximity to a source of IFN. Nonetheless, studies of B cell development in bone marrow have revealed clear trafficking patterns that occur at different stages[284]. To better understand where the subsets found in the scRNAseq data set reside, we have started to optimize a method of *in situ* sequencing previously used to map neurons in the central nervous system. This method, termed CARTANA[285], relies on RNA-hybridization with a unique barcode then fluorescence-based sequencing within a tissue section. Our pilot experiment successfully identified some transcripts while others had obvious issues. We are now working with CARTANA to optimize strategies for spatial transcriptomics in lymphoid tissues. Finally, although the data discussed in chapter 4 is robust, we failed to recover a significant amount of $CD73^-$ *de novo* developing T_{reg} cells. While some $CD73^+$ T_{reg} cells do overlap with the *de novo* T_{reg} cell phenotype, they are certainly more mature than the $CD73^-$ T_{reg} cells. We hope that our most recent experiment, with CITEseq, will fill this gap. If so, this will allow more robust analysis of the changes that occur between T_{reg}P cells and mature T_{reg} cells. This is one area lacking in the data presented in chapter 4 as we could not properly piece together the T_{reg}P to mature T_{reg} cell trajectories using pseudotime[263]. Proper execution and analysis of the above experiments should provide a holistic picture of CD4SP thymocyte maturation and T_{reg} cell development in the thymus.

Determining the function of RT-T_{reg} cells in thymus biology

The RT-T_{reg} cell analysis presented in chapter 5 is preliminary but does provide evidence for phenotypic and functional heterogeneity. There are still many unanswered questions regarding RT-T_{reg} cell functions and their mechanistic drivers. First, the phenotypic heterogeneity of RT-T_{reg} cells can be further probed with scRNAseq with combined

CITEseq. We recently initiated this experiment and should have the data to analyze shortly. This experiment will hopefully provide a holistic analysis of the phenotypic diversity in RT-T_{reg} cells as well as the underlying signaling signature that defines each cluster. This data should provide enough information to accurately isolate each distinct subset of RT-T_{reg} cells, as well as perform transfer experiments to understand how each population functions. Such experiments could be performed in mice that genetically have reduced RT-T_{reg} cells, such as *Ccr6*$^{-/-}$[276], *GK transgenic* mice[173] or mice receiving the i.t. DT RT-T_{reg} cell depletion protocol discussed in chapter 5, to increase our sensitivity to detect the function of each subset. As discussed above, we do not understand where each RT-T_{reg} cell subset is located and/or what cells it is interacting with. To address this, we hope to use CARTANA to identify each subset and characterize their localization and potential cellular partners. However, once a holistic signature is formed by scRNAseq and CITEseq analysis, we could also use any subset defining markers in IHC experiments to obtain similar information to what CARTANA will provide.

Nevertheless, the mystery of why RT-T_{reg} cells exist and accumulate throughout life remains entirely unanswered. The RT-T_{reg} cell depletion experiments presented in chapter 5 confirm that RT-T_{reg} cells indeed inhibit *de novo* T_{reg} cell development. How and why RT-T_{reg} cells perform this function is unknown. We also found that RT-T_{reg} cell depletion caused a resurgence in AIRE^{+} mTEC abundance. Similarly, how RT-T_{reg} cells control AIRE^{+} mTEC cell density is unknown as well as the benefit this would provide to the organism. Previous work has shown that AIRE expression and T_{reg} cell development during the first few weeks of life is sufficient to protect against the autoimmunity related to AIRE deficiency[177,178]. Interestingly, the first few weeks of life also represent the window when AIRE^{+} mTEC are highly abundant and RT-T_{reg} cells have not appreciably accumulated. Together, we speculate that RT-T_{reg} cells are the driver of the shifts in central

tolerance that occur throughout ontogeny. The function of T_{reg} cells generated outside of early life remains unknown. Thus, perhaps a function of RT-T_{reg} cell accumulation is to alter the repertoire of TCRs committing to the T_{reg} cell lineage, allowing for greater T_{reg} cell functional diversity. An additional consequence of inhibiting T_{reg} cell development and $AIRE^+$ mTEC cell abundance could be increased effector T cell TCR diversity. The TCR is a highly cross-reactive antigen receptor, a single TCR being estimated to recognize over one million peptide ligands[269]. If this amount of cross-reactivity is generalizable, many foreign reactive TCRs would also recognize self-peptides. $AIRE^+$ mTEC can express over 80% of the genome, meaning that it is possible that a group of $AIRE^+$ mTEC could present the majority of endogenous peptides to developing thymocytes. Thus, perhaps reduction of $AIRE^+$ mTEC by RT-T_{reg} cells allows central tolerance to loosen by lowering the abundance of many peptides expressed only in $AIRE^+$ mTEC. We seek to test this hypothesis by performing TCR sequencing on young mice, before RT-T_{reg} cell accumulation, and older mice. We will perform parallel TCR sequencing experiments in *Aire*$^{-/-}$ mice as well as mice depleted of RT-T_{reg} cells. Comparisons of conventional, T_{reg}P and mature T_{reg} cell TCR repertoires can define the changes in TCR repertoires that occur which are dependent on age, RT-T_{reg} cell accumulation, AIRE or combinations of those factors. Additionally, we will analyze the diversity of conventional and T_{reg} cell lineages. We hypothesize that older thymi export less diverse T_{reg} cell repertoires and that this effect is due to RT-T_{reg} cells reducing $AIRE^+$ mTEC that produce diverse endogenous antigens required to positively select thymocytes into the T_{reg} lineage. Similarly, we expect that older thymi will generate a more diverse effector T cell repertoire, also due to decreased thymic antigen diversity. Overall, our model predicts that young organisms are protected from endemic pathogens via transfer of maternal Ig, allowing the thymus to prioritize central tolerance and T_{reg} cell development. In older animals, central tolerance can be loosened

to facilitate a more diverse effector T cell TCR repertoire capable of better detecting and responding to pathogens or mutated self-proteins in cancer cells. This system evolved to temporally regulate the characteristics of central tolerance to ensure that peripheral tolerance is enforced by T_{reg} cells, which nullify the autoimmune hazard of increased effector T cell diversity following the relaxation of central tolerance stringency.

6.3 Concluding Remarks

Why must T_{reg} cells exist?

The preceding ~150 pages are devoted to the study and discussion of the development of the T_{reg} cell, a small population within the $CD4^+$ subset of T cells. Yet these same pages are deficient in existential discussion of T_{reg} cells. Perhaps the final paragraph presented here represents this philosophical discussion, required to holistically understand the evolutionary motivations shaping the regulation of T_{reg} cell development and function.

The COVID-19 pandemic we are currently experiencing might seem surreal, as it indeed does for me as I write this dissertation in isolation from my apartment couch instead of my lab desk, but throughout evolution pathogens have shaped human existence. A simplistic view may be that the cellular immune system could use all the power one could offer it to protect from infection. However, the war the immune system wages against pathogens is subject to the same basic rule of conventional warfare- powerful weapons are of no use without the capacity to discriminate between allies and the enemy. Further, in a closed system, like the human body, a weapon can only be so powerful before ensuring collateral damage. The etiology of mortality in the current COVID-19 pandemic, often caused by the collateral damage of an overexuberant immune response[286], is a reminder that the intensity of the immune response must be tightly regulated to facilitate pathogen clearance while preventing self-destruction. Indeed, T_{reg} cell therapies have recently been employed

to combat the destructive effect of the immune response during SARS-CoV-2 infection[287,288]. But, why do T_{reg} cells exist?

One can imagine that TCR selection systems could have evolved to prevent any opportunity for self-reactivity. Altering selection to completely limit self-reactivity would also limit the diversity of the TCR repertoire. Similarly, the TCR could be highly specific for a single antigen, instead of highly cross-reactive, to limit autoimmune hazard- another change that would greatly reduce the diversity of ligands to which T cells can recognize. However, it seems that evolution favored a system that is built on diversity. Invasion of the early jawed vertebrate genome by the RAG recombinases allowed for the random recombination on RSS flanked TCR segments to generate antigen receptor diversity[4,289,290], a mechanism that has been maintained for millions of years despite producing many non-functional and self-reactive antigen receptors. Further, the presence of self-reactive effector T cells, recognizing peptide from MOG or INS[291], in healthy organisms is empirical evidence that central tolerance is in fact leaky. Peripheral tolerance mechanisms evolved to mitigate the autoimmune potential of such cells, mechanisms that are nonetheless insufficient to maintain immune homeostasis on their own[280,281]. T_{reg} cells allow the organism to take risks, which would otherwise cause autoimmunity and immunopathology, to prioritize the elimination of pathogens- perhaps a mechanism that also underlies immunosurveillance for transformed self-proteins in cancer cells. Furthermore, numerous studies, some discussed in chapter 1, point to a role for T_{reg} cells potentiating, not simply suppressing, the effector T cell response. Thus, instead of purely representing a roadblock to the effector immune response, T_{reg} cells likely evolved as a strategy to hedge against the autoimmune hazard inherent to a system with both incredible power and diversity. Interestingly, T_{reg} cells were initially described as “suppressor” T cells[55], a term that was later demonized by immunologists[292] during the fall of suppressor

T cells. Nonetheless, immunologists often view the function of the T_{reg} cell, resurrected from the fall of suppressor T cells, as purely “suppressive”. Unless T_{reg} cells are instead studied as their namesake suggests, “regulatory”, the diversity of T_{reg} cell function and their role in immune responses will remain enigmatic. A greater appreciation of T_{reg} cell function is essential to understand how the thymus shapes T_{reg} cell development to achieve immune homeostasis.

Chapter 7. Materials and methods

Mice.

Mice were housed in specific pathogen-free facilities at the University of Minnesota, Cornell University, Salk Institute or University of California San Francisco, and experiments were conducted in accordance with protocols approved by the Institutional Animal Care and Use Committees of these respective institutions. Exceptions were germ-free mice housed in germ-free facilities at the University of Chicago, and mice with a normalized microbial experience which were housed in the University of Minnesota's mouse vivarium. Pet store mice were purchased from various pet stores in the greater Minneapolis-St. Paul metropolitan area. Information about the age of the pet store mice was not available from the vendor. Co-housing of specific-pathogen-free mice with sex-matched pet store partner was performed as described[221] within the University of Minnesota BSL-3 facility. Conversion efficiency was confirmed by assessing the conversion of naïve $CD8^+$ T cells into $CD8^+$ memory T cells; effective conversion correlated with ~30–60% $CD8^+CD44^{hi}$ T cells. All relevant ethical guidelines were followed. Mice were generally 5–8 weeks old at time of analysis but ranged between 4–16 weeks. Mice were randomly selected for experiments in age-matched cohorts. The investigators were not 'blinded' to genotype during data acquisition.

The mice used for the experiments presented have all been described previously: *Cd4^{Cre}(C57Bl/6)*[207], *Il2$^{fl/fl}$(C57Bl/6)*[205], *Cd11c^{Cre}(C57Bl/6)*[206], *Cd79a^{Cre}(C57Bl/6)*[209], *Il15$^{-/-}$(C57Bl/6)*[293], *Foxp3^{GFP}(C57Bl/6)*[61], *Rag2$^{-/-}$(C57Bl/6)*[4], *Il2$^{-/-}$(C57Bl/6)*[294], *TCliβ (C57Bl/6)*[71], *Tcra$^{-/-}$(C57Bl/6)*[295], *Foxp3^{RFP}(C57Bl/6)*[60], *Nur77^{GFP}(C57Bl/6)*[77], *Rag2^{GFP}(C57Bl/6)*[224], *Itgal$^{-/-}$(C57Bl/6)*[296], *Cd28$^{-/-}$(C57Bl/6)*[297], *Nfkb1$^{-/-}$(C57Bl/6)*[298], *Foxp3$^{GFP\text{-}KIN}$(C57Bl/6)*[59], *Cns3$^{-/-}$(C57Bl/6)*[160], *CaRE4$^{-/-}$ (NOD)*[164], *Itk$^{-/-}$(C57Bl/6)*[299], *Adap$^{-/-}$(C57Bl/6)*[300], *Il4ra$^{-/-}$(C57Bl/6)*[301], *Pou2f3$^{-/-}$(C57Bl/6)*[235,302], *Cd1d$^{-/-}$ (Balb/c, C57Bl/6)*[303] and *Foxp3^{DTR} (C57Bl/6)*[10].

Tissue Preparation and Cell Isolation.

For analysis of thymocyte and T_{reg} development, thymi and peripheral lymphoid organs were mechanically dissociated into 1× PBS with 2% FBS and 2 mM EDTA (pH 7.4), with or without 0.05% NaN_3, using frosted glass slides. Cell suspensions were passed through 70-μm filters and washed prior to staining. DCs were isolated via cutting thymi or spleen into pieces, followed by collagenase D (120 U/mL) digestion in cRPMI at 37°C for 1 hour and mechanical dissociation. mTEC digestions were performed in RPMI + 0.005% w/v Liberase TH and 100 U/mL DNase I for ~ 1 hour at 37°C, as described previously[304]. When thymi were split for mTEC and DC/T cell analysis, each thymus was weighed and cut such that each cell isolation contained thymic tissue from each lobe.

Flow cytometry, Antibodies and Tetramer Staining.

All flow cytometry analysis was conducted in the University of Minnesota Flow Cytometry Core Facility using BD LSR II and Fortessa cytometers (BD Biosciences). For surface staining, cells were stained for 20 min with fluorochrome-conjugated antibodies before washing and analysis or intracellular staining. Intracellular detection of FOXP3, cleaved casp-3 and GFP was performed as previously described[64] using the eBioscience Transcription Factor staining kit. When staining for GFP, *Rag2*-GFP thymi were fixed for 10 min at room temperature in 1.6% paraformaldehyde before intracellular staining of GFP and FOXP3 using the eBioscience Transcription Factor staining kit. For apoptosis assays, thymi were harvested and mechanically dissociated into 1× phosphate buffered saline (PBS) on ice. Following surface staining, cells were washed into Annexin V binding buffer (eBioscience) and stained with annexin V. Antibodies used: anti-mouse CD4 (GK1.5, RM4-5), anti-mouse CD8α (53-6.7), anti-mouse CD25 (PC61.5), anti-mouse FOXP3 (FJK-16s), anti-mouse CD45.1 (A20), anti-mouse CD45.2 (104), anti-mouse CD90.1 (HIS51), anti-mouse CD90.2 (53-2.1 or 30-H12), anti-mouse CD73 (TY/11.8), anti-mouse TCRβ

(H57-597), anti-mouse Ter119, anti-mouse CD44 (IM7), anti-mouse CD45RB (C363.16A), anti-mouse CD11c (N418), anti-mouse CD11b (M1/70), anti-mouse NK1.1 (PK136), anti-mouse F4/80 (BM8), anti-mouse B220 (RA3-6B22), anti-mouse Qa2 (69H1-9-9), anti-mouse HSA (M1/69), anti-mouse CD69 (H1.2F3), anti-mouse RORγT (Q31-378), anti-mouse MHC-I H-2K^{b} (AF6-88.5.5.3), anti-mouse IL-2 (JES6-5H4), anti-mouse CD19 (1D3), anti-mouse EpCAM (G8.8), anti-mouse CD172a (P84), anti-mouse CD62L (MEL14), anti-mouse CD45RA (14.8), anti-mouse CD3 (17A2 or 145-2C11), anti-mouse AIRE (5H12), anti-mouse CD80 (16-10A1), anti-mouse I-A^{b} (M5/114.15.2), anti-mouse Ly51 (6C3), anti-mouse ST-2 (RMST2-33), anti-mouse TIGIT (GIGD7), anti-mouse TIM-3 (RMT3-23), anti-mouse LAG-3 (C9B7W), anti-mouse BST2 (927), Rat IgG1 (HPRN), UEA1, anti-cleaved caspase 3 Asp 175 (D3E9), anti-GFP (polyclonal), and Ghost Dye Red 780.

For tetramer staining, single-cell thymocyte suspensions were treated with Dasatinib (Axon Medchem) at 50 nM in complete Roswell Park Memorial Institute medium (RPMI) for 20 min at 37 °C, followed by dual (allophycocyanin (APC)- and phycoerythrin (PE)-conjugated) $MOG_{38–48}$ tetramer[305] staining at 10 nM for an additional 45 min in complete RPMI (10% FBS, 1% glutamine, 1% penicillin-streptomycin, 1% nonessential amino acids, 10 mM N-2-hydroxyethylpiperazine-N'-2-ethanesulfonic acid (HEPES), 50 uM β -mercaptoethanol) at 37 °C. Tetramer-stained cells were washed and incubated with anti-APC and anti-PE microbeads (Miltenyi Biotec) for 30 min on ice. Cells were washed and run over a LS column, then unbound and bound fractions were collected, stained and analyzed as described above.

Bone Marrow Chimeras.

Il2$^{-/-}$ x *Il15*$^{-/-}$ x *Rag2*$^{-/-}$ recipients were sublethally irradiated with 500 rad and rested for 18-24 hours before i.v. injection of a 50:50 mixture of bone marrow of the indicated origin.

Chimeric mice were analyzed 8–10 weeks following donor cell transfer. Donor bone marrow was magnetically depleted of mature lymphocytes by staining bone marrow with anti-CD3, anti-CD4, anti-CD8, anti-CD19 and anti-B220 biotinylated antibodies followed by streptavidin microbead binding and passing through a Miltenyi LS column. The flow through was collected then counted prior to transfer.

In Vitro Stimulation of DC and T cells

Isolated T cells or DCs were stimulated with 100 ng/ml PMA and 1 mM ionomycin for 1 h followed by GolgiPlug treatment for 7 h.

T_{reg} Progenitor Conversion Assays.

$T_{reg}P$ cells were isolated as previously described[216]. Briefly, *Foxp3-GFP* thymi were dissected and dissociated, and pooled CD4SP cells were enriched by magnetic depletion with biotinylated anti-CD8 and anti-Ter119 (eBioscience) followed by secondary labeling with streptavidin conjugated microbeads (Miltenyi Biotec). Enriched CD4SP cells were stained with fluorchrome-conjugated anti-CD4, anti-CD25, anti-CD73 and streptavidin prior to sorting $CD4^+CD73^-CD25^+GFP^-$, $CD4^+CD73^-CD25^-GFP^+$ or $CD4^+CD73^-CD25^+GFP^+$ cells using a BD FACSAria sorter (BD Biosciences). Purified $T_{reg}P$ or T_{reg} cells were incubated in complete RPMI and supplemented with human IL-2 (R&D Systems) or mouse IL-4 from Tonbo Biosciences. After 72 h, cells were harvested, stained with anti-CD4, anti-CD8 and anti-CD25 and were analyzed by flow cytometry for the percentage or number of cells expressing CD25 and GFP after incubation.

Ultrasound Guided Intrathymic Injections.

Injections were performed as described previously[217]. Briefly, mice were anesthetized with 2–4% isofluorane in medical gas (21% oxygen, 79% nitrogen) in an acrylic chamber, then transferred to a warmed ultrasound platform, face upwards, and the snout secured in a

facemask delivering 2–4% isofluorane and medical gas. Depilatory cream was used to remove hair from the mid-upper ventral thoracic region before applying ultrasound gel. Using the Vevo 2100 ultrasound unit, the MS550D probe was lowered parallel to the left or right side of the sternum. The ultrasound image generated was used to guide an insulin syringe (27 G) into the thymus and visualize injection of the 10–20 ul cell suspension.

Immunofluorescence and Histo-cytometry.

Immunofluorescence analysis of thymus was performed as previously described[306]. Thymi were washed, fixed with 4% paraformaldehyde for 1 hour and snap-frozen. Sections (5 μm) were blocked with PBS containing 5% bovine serum albumin and goat serum (Jackson Laboratory) before staining. The sections were then covered with Prolong anti-fade mounting medium (Life Technologies) and images were obtained 1–3 days later with a Leica DM6000B Epi-Fluorescent microscope.

Histo-cytometry analysis was performed as described previously[226].

TCR Sequencing.

CD4SP thymocytes were enriched by magnetic depletion using biotinylated anti-CD8/Ter119 antibodies, followed by secondary labeling with streptavidin-conjugated microbeads (Miltenyi Biotec). Enriched cells were labeled with fluorchrome-conjugated anti-CD4, CD25 and streptavidin, while FOXP3 was marked with a RFP reporter, before sorting on a BD FACSAria sorter (BD Biosciences). TCR sequencing was performed as described previously[71,106]. Briefly, $CD4^+CD25^-FOXP3^-$, $CD4^+CD25^+FOXP3^-$, $CD4^+CD25^-FOXP3^{lo}$ and $CD4^+CD25^+FOXP3^+$ populations were sorted into lysis buffer (Buffer RLT plus β -mercaptoethanol). Complementary DNA was generated from these samples using the RNeasy kit (Qiagen). CDR3 Vα2 TCRs were sequenced using an Ion Torrent as previously described. TCRs representing > 20% of the reads in the T_{reg} cell compartment,

which influence distribution disproportionally, were excluded from analysis as described[106].

Bulk RNA Sequencing.

CD4SP thymocytes were enriched by magnetic depletion using biotinylated anti-CD8, anti-CD11c, anti-B220, and anti-Ter119 antibodies, followed by secondary labeling with streptavidin-conjugated microbeads (Miltenyi Biotec). Enriched cells were labeled with fluorchrome-conjugated anti-CD4, anti-CD25, anti-CD73, anti-BST2 and Ghost Red Live-Dead eF780 and streptavidin-APC-eF780 to stain depletion cocktail. Dump (depletion cocktail and Live-Dead) negative, $CD73^{lo}$ $CD4^{+}CD25^{-}FOXP3^{-}$, $CD4^{+}CD25^{+}FOXP3^{-}$, $CD4^{+}CD25^{-}FOXP3^{lo}$ and $CD4^{+}CD25^{+}FOXP3^{+}$ populations were sorted into lysis buffer (Buffer RLT plus β -mercaptoethanol). Samples were placed on dry ice immediately after sorting and stored at -80 °C prior to RNA isolation. RNA was isolated using RNAeasy Micro Spin Kit and RNA was eluted in 20 µL. Samples were submitted to UMGC for library prep, using SMARTer Stranded Total RNA-Seq Kit v2 - Pico Input Mammalian kit, and sequencing by 2 x 150bp on a NovaSeq S4 lane to ~25 million reads/sample.

Single Cell RNA Sequencing.

$CD4^{+}CD73^{-}CD25^{+}FOXP3^{-}$, $CD4^{+}CD73^{-}CD25^{-}FOXP3^{lo}$ and $CD4^{+}CD73^{-}CD25^{+}FOXP3^{+}$ cells were isolated from a single *Foxp3-GFP* thymus for 3' sequencing presented in chapter 3. 5' sequencing data presented in chapters 2, 4 and 5 was from $CD4^{+}CD8^{+}$TCR $V\alpha2^{+}$, $CD4^{+}CD73^{-}CD25^{-}FOXP3^{-}$TCR $V\alpha2^{+}$, $CD4^{+}CD73^{-}CD25^{+}FOXP3^{-}$ TCR $V\alpha2^{+}$, $CD4^{+}CD73^{-}CD25^{-}FOXP3^{lo}$TCR $V\alpha2^{+}$, $CD4^{+}CD73^{-}CD25^{+}FOXP3^{+}$TCR $V\alpha2^{+}$, $CD4^{+}CD73^{+}FOXP3^{+}$TCR $V\alpha2^{+}$ from thymocytes pooled from TCliβ x $Tcra^{+/-}$ mice. Sorts were performed on a BD FACSAria sorter. Cells were resuspended at 1-3 million cells/mL in 5% (5') or 50% (3') FBS in 1× PBS before being counted and captured using 10x Genomics Single Cell 3' or 5' Solution.

For 3' sequencing, a custom genome was created by adding the sequence for the FoxP3-GFP construct as a new chromosome to the Ensembl GRCm38 reference and general feature format file (version 89). The gene annotation file was then filtered further till it contained only protein-coding genes. The 10x Genomic Cellranger pipeline (version 2.2.0; https://support.10xgenomics.com/single-cell-gene-expression/software/overview/welcome) was used to align reads and generate counts for each sorted population (or library). Sorted populations were then combined using depth normalization mode.

The Seurat R Package (version 1.4.0.12) was used to analyze the mapped single-cell reads. The data were filtered to include cells that contained 100–2,500 unique gene counts and expressed more than five genes. Global-scaling normalization was applied to the filtered data as described in the default settings in the Seurat package. The data were then scaled to regress out sequencing depth. Linear dimensional reduction was performed on the most variable genes. Heatmap analysis of different principal components and an elbow plot were created to determine the optimum number of principal components for cluster analysis using the Seurat function 'FindCluster'. To visualize the clusters, nonlinear dimensional reduction was performed using principal components. Clusters were assigned to a specific population by comparing cells labeled for the original sorted population and cellular markers. R package plot3D (version 1.1.1) and threejs (version 0.3.1) were used to create 3D visualization of the nonlinear dimensional reduction data. Differential expression ('bimod')[307] was calculated for each cluster against all other clusters to identify potential markers for each individual cluster. Differential expression was also calculated between individual clusters using the same method.

Hashtagging sorted populations, for 5' sequencing experiments, was performed by incubating each sorted population with either 0.25-0.5 µg/hashtag antibody (TotalSeq C,

Biolegend) for 30 minutes on ice. Cells were washed twice in sort buffer prior to mixing populations at final proportions and concentration in capture buffer (1xPBS + 5% FBS) for capture on the 10X Chromium instrument.

Experimental Induction of Autoimmune Encephalomyelitis.

The condition EAE was induced in mice as described previously[308]. Briefly, on day –1, sorted $T_{reg}P$ cell populations (4×10^5−5×10^5) were transferred intravenously into CD45.1$^+$ congenic mice. On day 0, mice were immunized with 200 ug of $MOG_{35–55}$ emulsified in complete Freund's adjuvant (CFA) with 4 mg/mL heat-killed tuberculosis (Tb). Immunization was performed with two subcutaneous injections (50 ul) of emulsion in the left or right flank of the lower back. Mice were treated with 200 ng Pertussis Toxin on days 0 and 2 via intraperitoneal injection in 1× PBS. Mice were monitored for disease progression and were treated with normal saline (subcutaneously) or were given wet food on the cage floor, as described previously[308].

Transfer Colitis.

Colitis was induced as previously described[309]. Briefly, 5×10^5 CD4$^+$CD45RB^{hi} cells were transferred by intravenous or intraperitoneal injection into *Rag*$^{-/-}$ recipient mice. Sorted $T_{reg}P$ cells were transferred by intraperitoneal injection in either a split dose (2.5×10^5 on days 1 and 7) or a single dose (5×10^5 on day 21). Mice were weighed weekly to monitor disease progress.

Statistics.

Statistical tests used to analyze data are included within the figure legends. Briefly, comparisons of two groups were done by either paired *t*-test (paired, normal data), Wilcoxon matched-pairs test (paired, non-normal data), *t*-test (non-paired, normal data) or Mann–Whitney (non-paired, non-normal data); tests were always two-sided. Comparison

of three or more groups was done by one-way ANOVA (non-paired, normal data), Kruskal–Wallis (non-paired, non-normal data) or Friedman test (paired, non-normal data). $P < 0.05$ was considered significant. Statistics were calculated using Prism (GraphPad Software).

References

1. Owen, D. L., Sjaastad, L. E. & Farrar, M. A. Regulatory T Cell Development in the Thymus. *J. Immunol.* **203**, 2031–2041 (2019).

2. Burnet, F. M. A Modification of Jerne's Theory of Antibody Production using the Concept of Clonal Selection. *Austrailian J. Sci.* **20**, 67–69 (1957).

3. Mombaerts, P., Iacomini, J., Johnson, R. S., Herrup, K., Tonegawa, S., Papaioannou, V. E. RAG-1-Deficient Mice Have No Mature B and T Lymphocytes. *Cell* **68**, 869–877 (1992).

4. Shinkai, Y. *et al.* RAG-2-deficient mice lack mature lymphocytes owing to inability to initiate V(D)J rearrangement. *Cell* **68**, 855–867 (1992).

5. Sakaguchi, S., Sakaguchi, N., Asano, M., Itoh, M., and Toda, M. Immunologic self-tolerance maintained by activated T cells expressing IL-2 receptor alpha-chains (CD25). Breakdown of a single mechanism of self-tolerance causes various autoimmune diseases. *J. Immunol.* **155**, 1151–1164 (1995).

6. Takahashi, T. *et al.* Immunologic self-tolerance maintained by CD25(+)CD4(+) regulatory T cells constitutively expressing cytotoxic T lymphocyte-associated antigen 4. *J. Exp. Med.* **192**, 303–310 (2000).

7. Wildin, R. S. *et al.* X-linked neonatal diabetes mellitus, enteropathy and endocrinopathy syndrome is the human equivalent of mouse scurfy. *Nat. Genet.* **27**, 18–20 (2001).

8. Brunkow, M. E. *et al.* Disruption of a new forkhead/winged-helix protein, scurfin, results in the fatal lymphoproliferative disorder of the scurfy mouse. *Nat. Genet.* **27**, 68–73 (2001).

9. Malek, T. R., Yu, A., Vincek, V., Scibelli, P. & Kong, L. CD4 regulatory T cells prevent lethal autoimmunity in IL-2Rβ-deficient mice: Implications for the nonredundant function of IL-2. *Immunity* **17**, 167–178 (2002).

10. Kim, J. M., Rasmussen, J. P. & Rudensky, A. Y. Regulatory T cells prevent catastrophic autoimmunity throughout the lifespan of mice. *Nat. Immunol.* **8**, 191–197 (2007).

11. Samstein, R. M., Josefowicz, S. Z., Arvey, A., Treuting, P. M. & Rudensky, A. Y. Extrathymic generation of regulatory T cells in placental mammals mitigates maternal-fetal conflict. *Cell* **150**, 29–38 (2012).

12. Aluvihare, V. R., Kallikourdis, M. & Betz, A. G. Regulatory T cells mediate maternal tolerance to the fetus. *Nat. Immunol.* **5**, 266–271 (2004).

13. Jasper, M. J., Tremellen, K. P. & Robertson, S. A. Primary unexplained infertility is associated with reduced expression of the T-regulatory cell transcription factor Foxp3 in endometrial tissue. *Mol. Hum. Reprod.* **12**, 301–308 (2006).

14. Rowe, J. H., Ertelt, J. M., Aguilera, M. N., Farrar, M. A. & Way, S. S. Foxp3 + regulatory T cell expansion required for sustaining pregnancy compromises host defense against prenatal bacterial pathogens. *Cell Host Microbe* **10**, 54–64 (2011).

15. Kahn, D. A. & Baltimore, D. Pregnancy induces a fetal antigen-specific maternal T regulatory cell response that contributes to tolerance. *Proc. Natl. Acad. Sci.* **107**, 9299–9304 (2010).

16. Shima, T. *et al.* Regulatory T cells are necessary for implantation and maintenance of early pregnancy but not late pregnancy in allogeneic mice. *J. Reprod. Immunol.* **85**, 121–129 (2010).

17. Teles, A. *et al.* Origin of Foxp3+ cells during pregnancy. *Am J Clin Exp Immunol* **2**, 222–233 (2013).

18. Rowe, J. H., Ertelt, J. M., Xin, L. & Way, S. S. Pregnancy imprints regulatory memory that sustains anergy to fetal antigen. *Nature* **490**, 102–106 (2012).

19. Tung, K. S. K. *et al.* Egress of sperm autoantigen from seminiferous tubules maintains systemic tolerance. *J. Clin. Invest.* **127**, 1046–1060 (2017).

20. Ali, N. *et al.* Regulatory T Cells in Skin Facilitate Epithelial Stem Cell Differentiation. *Cell* **169**, 1119-1129.e11 (2017).

21. Burzyn, D. *et al.* A Special Population of Regulatory T Cells Potentiates Muscle Repair. *Cell* **155**, 1282–1295 (2013).

22. Cipolletta, D. *et al.* PPAR-γ is a major driver of the accumulation and phenotype of adipose tissue T reg cells. *Nature* **486**, 549–553 (2012).

23. Feuerer, M. *et al.* Lean, but not obese, fat is enriched for a unique population of regulatory T cells that affect metabolic parameters. *Nat. Med.* **15**, 930–939 (2009).

24. Kolodin, D. *et al.* Antigen- and Cytokine-Driven Accumulation of Regulatory T Cells in Visceral Adipose Tissue of Lean Mice. *Cell Metab.* **21**, 543–557 (2015).

25. Bapat, S. P. *et al.* Depletion of fat-resident Treg cells prevents age-associated insulin resistance. *Nature* **528**, 137–141 (2015).

26. Li, C. *et al.* TCR Transgenic Mice Reveal Stepwise, Multi-site Acquisition of the Distinctive Fat-Treg Phenotype. *Cell* **174**, 285-299.e12 (2018).

27. Deliyanti, D. *et al.* Foxp3+ Tregs are recruited to the retina to repair pathological angiogenesis. *Nat. Commun.* **8**, 1–12 (2017).

28. Chung, Y. *et al.* Follicular regulatory T cells expressing Foxp3 and Bcl-6 suppress germinal center reactions. *Nat. Med.* **17**, 983–988 (2011).

29. Linterman, M. A. *et al.* Foxp3+ follicular regulatory T cells control the germinal center response. *Nat. Med.* **17**, 975–982 (2011).

30. Lanteri, M. C. *et al.* Tregs control the development of symptomatic West Nile virus infection in humans and mice. *J. Clin. Invest.* **119**, 3266–3277 (2009).

31. Schmitz, I. *et al.* IL-21 Restricts Virus-driven Treg Cell Expansion in Chronic LCMV Infection. *PLoS Pathog.* **9**, (2013).

32. Suvas, S., Kumaraguru, U., Pack, C. D., Lee, S. & Rouse, B. T. CD4 + CD25 + T Cells Regulate Virus-specific Primary and Memory CD8 + T Cell Responses. *J. Exp. Med.* **198**, 889–901 (2003).

33. Arpaia, N. *et al.* A Distinct Function of Regulatory T Cells in Tissue Protection. *Cell* **162**, 1078–1089 (2015).

34. Suvas, S., Azkur, A. K., Kim, B. S., Kumaraguru, U. & Rouse, B. T. CD4+CD25+ Regulatory T Cells Control the Severity of Viral Immunoinflammatory Lesions. *J. Immunol.* **172**, 4123–4132 (2004).

35. Oldenhove, G. *et al.* Decrease of Foxp3+ Treg Cell Number and Acquisition of Effector Cell Phenotype during Lethal Infection. *Immunity* **31**, 772–786 (2009).

36. Pandiyan, P. *et al.* CD4+CD25+Foxp3+ Regulatory T Cells Promote Th17 Cells In Vitro and Enhance Host Resistance in Mouse Candida albicans Th17 Cell Infection Model. *Immunity* **34**, 422–434 (2011).

37. Chen, Y. *et al.* Foxp3+ Regulatory T Cells Promote T Helper 17 Cell Development In Vivo through Regulation of Interleukin-2. *Immunity* **34**, 409–421 (2011).

38. Laidlaw, B. J. *et al.* Production of IL-10 by CD4+regulatory T cells during the resolution of infection promotes the maturation of memory CD8+T cells. *Nat. Immunol.* **16**, 871–879 (2015).

39. Shrikant, P., Khoruts, A. & Mescher, M. F. CTLA-4 blockade reverses CD8+T cell tolerance to tumor by a CD4+T cell- and IL-2-dependent mechanism. *Immunity* **11**, 483–493 (1999).

40. Shimizu, J., Yamazaki, S. & Sakaguchi, S. Induction of tumor immunity by removing CD25+CD4+ T cells: a common basis between tumor immunity and autoimmunity. *J. Immunol.* **163**, 5211–8 (1999).

41. Sefik, E. *et al.* Individual intestinal symbionts induce a distinct population of ROR + regulatory T cells. *Science (80-.).* **349**, 993–997 (2015).

42. Kim, K. S. *et al.* Dietary antigens limit mucosal immunity by inducing regulatory T cells in the small intestine. *Science (80-.).* **351**, 858–863 (2016).

43. Harrison, O. J. *et al.* Commensal-specific T cell plasticity promotes rapid tissue adaptation to injury. *Science (80-.).* **363**, (2019).

44. Maclean, L. D., Zak, S. J., Varco, R. L. & Good, R. A. The role of the thymus in antibody production; an experimental study of the immune response in thymectomized rabbits. *Transpl. Bull* **4**, 21–2 (1957).

45. Jankovic, B. D., Waksman, B. H. & Arnason, B. G. Role of the Thymus in Immune Reactions in Rate. *J. Exp. Med.* **116**, 159–177 (1962).

46. Miller, J. F. A. P. Immunological Function of the Thymus. *Lancet* **278**, 748–749 (1961).

47. Good, R. A. *et al.* The role of the Thymus in Development of Immunologic Capacity in Rabbits and Mice. *J. Exp. Med.* **116**, 773–796 (1962).

48. Miller, J. F. A. P. Effect of Neonatal Thymectomy on the Immunological Responsiveness of the Mouse. *Proc. R. Soc. B Biol. Sci.* **156**, 415–428 (1962).

49. Nishizuka, Y. & Sakakura, T. Thymus and Reproduction : Sex-Linked Dysgenesia of the Gonad after Neonatal Thymectomy in Mice. *Science (80-.).* **166**, 753–755

(1969).

50. Gershon, R. K. & Kondo, K. Cell interactions in the induction of tolerance: the role of thymic lymphocytes. *Immunology* **18**, 723–737 (1970).

51. Gershon, R. K. & Kondo, K. Infectious immunological tolerance. *Immunology* **21**, 903–14 (1971).

52. Gershon, R. K., Cohen, P., Hencin, R. & Liebhaber, S. A. Suppressor T Cells. *J. Immunol.* **108**, 586–590 (1972).

53. Benacerraf, B. & Germain, R. N. A single major pathway of T-lymphocyte interactions in antigen-specific immune suppression. *Scand. J. Immunol.* **13**, 1–10 (1981).

54. Kronenberg, M. *et al.* RNA transcripts for I-J polypeptides are apparently not encoded between the I-A and I-E subregions of the murine major histocompatibility complex. *Proc. Natl. Acad. Sci.* **80**, 5704–5708 (1983).

55. Möller, G. Do suppressor T cells exist? *Scand. J. Immunol.* **27**, 247–250 (1988).

56. Sakaguchi, S., Takahashi, T. & Nishizuka, Y. Study on cellular events in post-thymectomy autoimmune oophoitis in mice. *J. Exp. Med.* **156**, 1577–1586 (1982).

57. Asano, M., Toda, M., Sakaguchi, N., and Sakaguchi, S. Autoimmune disease as a consequence of developmental abnormality of a T cell subpopulation. *J. Exp. Med.* **184**, 387–396 (1996).

58. Bennett, C. L. *et al.* The immune dysregulation, polyendocrinopathy, enteropathy, X-linked syndrome (IPEX) is caused by mutations of FOXP3. *Nat. Genet.* **27**, 20–1 (2001).

59. Fontenot, J. D. *et al.* Regulatory T cell lineage specification by the forkhead transcription factor Foxp3. *Immunity* **22**, 329–341 (2005).

60. Wan, Y. Y. & Flavell, R. A. Identifying Foxp3-expressing suppressor T cells with a bicistronic reporter. *Proc. Natl. Acad. Sci.* **102**, 5126–5131 (2005).

61. Haribhai, D. *et al.* Regulatory T Cells Dynamically Control the Primary Immune Response to Foreign Antigen. *J. Immunol.* **178**, 2961–2972 (2007).

62. Roncador, G. *et al.* Analysis of FOXP3 protein expression in human CD4+CD25+ regulatory T cells at the single-cell level. *Eur. J. Immunol.* **35**, 1681–1691 (2005).

63. Lio, C. W. J. & Hsieh, C. S. A Two-Step Process for Thymic Regulatory T Cell Development. *Immunity* **28**, 100–111 (2008).

64. Burchill, M. A. *et al.* Linked T Cell Receptor and Cytokine Signaling Govern the Development of the Regulatory T Cell Repertoire. *Immunity* **28**, 112–121 (2008).

65. Tai, X. *et al.* Foxp3 Transcription Factor Is Proapoptotic and Lethal to Developing Regulatory T Cells unless Counterbalanced by Cytokine Survival Signals. *Immunity* **38**, 1116–1128 (2013).

66. Mahmud, S. A. *et al.* Costimulation via the tumor-necrosis factor receptor superfamily couples TCR signal strength to the thymic differentiation of regulatory T cells. *Nat. Immunol.* **15**, 473–481 (2014).

67. Pacholczyk, R. *et al.* Nonself-Antigens Are the Cognate Specificities of Foxp3 + Regulatory T Cells. *Immunity* **27**, 493–504 (2007).

68. van Santen, H.-M., Benoist, C. & Mathis, D. Number of T Reg Cells That Differentiate Does Not Increase upon Encounter of Agonist Ligand on Thymic Epithelial Cells. *J. Exp. Med.* **200**, 1221–1230 (2004).

69. Itoh, M., Takahashi, T., Sakaguchi, N., Kuniyasu, Y., Shimizu, J., Otsuka, F., Sakaguchi, S. CD25 +CD4+ Naturally Anergic and Thymus and Autoimmunity: Production of Suppressive T Cells as a Key Function of the Thymus in Maintaining Immunologic Self-Tolerance. *J. Immunol.* **162**, 5317–5326 (1999).

70. Martha S. Jordan *et al.* Thymic selection of CD4+CD25+ regulatory T cells induced by an agonist self-peptide. *Nat. Immunol.* **2**, 301–6 (2001).

71. Hsieh, C. *et al.* Recognition of the Peripheral Self by Naturally Arising CD25. *Immunity* **21**, 267–277 (2004).

72. Pacholczyk, R., Ignatowicz, H., Kraj, P. & Ignatowicz, L. Origin and T Cell Receptor Diversity of Foxp3+CD4+CD25+ T Cells. *Immunity* **25**, 249–259 (2006).

73. Hsieh, C. S., Zheng, Y., Liang, Y., Fontenot, J. D. & Rudensky, A. Y. An intersection between the self-reactive regulatory and nonregulatory T cell receptor repertoires. *Nat. Immunol.* **7**, 401–410 (2006).

74. Leung, M. W. L., Shen, S. & Lafaille, J. J. TCR-dependent differentiation of thymic Foxp3 + cells is limited to small clonal sizes . *J. Exp. Med.* **206**, 2121–2130 (2009).

75. Bautista, J. L. *et al.* Intraclonal competition limits the fate determination of regulatory T cells in the thymus. *Nat. Immunol.* **10**, 610–617 (2009).

76. Lee, H. M., Bautista, J. L., Scott-Browne, J., Mohan, J. F. & Hsieh, C. S. A Broad Range of Self-Reactivity Drives Thymic Regulatory T Cell Selection to Limit Responses to Self. *Immunity* **37**, 475–486 (2012).

77. Moran, A. E. *et al.* T cell receptor signal strength in Treg and iNKT cell development demonstrated by a novel fluorescent reporter mouse. *J. Exp. Med.* **208**, 1279–1289 (2011).

78. Stadinski, B. D. *et al.* A temporal thymic selection switch and ligand binding kinetics constrain neonatal Foxp3+ Treg cell development. *Nat. Immunol.* (2019). doi:10.1038/s41590-019-0414-1

79. Pugliese, A. *et al.* The insulin gene is transcribed in the human thymus and transcription levels correlate with allelic variation at the INS VNTR-IDDM2 susceptibility locus for type 1 diabetes. *Nat. gen* **15**, 293–297 (1997).

80. Vafiadis, P. *et al.* Insulin expression in human thymus is modulated by INS VNTR alleles at the IDDM2 locus. *Nat. Genet.* **15**, 289–292 (1997).

81. Derbinski, J., Schulte, A., Kyewski, B. & Klein, L. Promiscuous gene expression in medullary thymic epithelial cells mirrors the peripheral self. *Nat. Immunol.* **2**, 1032–1039 (2001).

82. Stenbit, A. E. *et al.* An autoimmune disease, APECED, caused by mutations in a

novel gene featuring two PHD-type zinc-finger domains. *Nat. Genet.* **17**, 399–403 (1997).

83. Nagamine, K. *et al.* Positional cloning of the APECED gene. *Nat. Genet.* **17**, 393–398 (1997).

84. Anderson, M. S. *et al.* Projection of an Immunological Self Shadow Within the Thymus by the Aire Protein. *Science (80-.).* **298**, 1395–1401 (2002).

85. Liston, A., Lesage, S., Wilson, J., Peltonen, L. & Goodnow, C. C. Aire regulates negative selection of organ-specific T cells. *Nat. Immunol.* **4**, 350–354 (2003).

86. Kekalainen, E. *et al.* A Defect of Regulatory T Cells in Patients with Autoimmune Polyendocrinopathy-Candidiasis-Ectodermal Dystrophy. *J. Immunol.* **178**, 1208–1215 (2007).

87. Aschenbrenner, K. *et al.* Selection of Foxp3+ regulatory T cells specific for self antigen expressed and presented by Aire+ medullary thymic epithelial cells. *Nat. Immunol.* **8**, 351–358 (2007).

88. Hinterberger, M. *et al.* Autonomous role of medullary thymic epithelial cells in central CD4 + T cell tolerance. *Nat. Immunol.* **11**, 512–519 (2010).

89. Malchow, S. *et al.* Aire-Dependent Thymic Development of Tumor-Associated Regulatory T Cells. *Science (80-.).* **339**, 1219–1224 (2013).

90. Malchow, S. *et al.* Aire Enforces Immune Tolerance by Directing Autoreactive T Cells into the Regulatory T Cell Lineage. *Immunity* **44**, 1102–1113 (2016).

91. Sng, J. *et al.* AIRE expression controls the peripheral selection of autoreactive B cells. *Sci. Immunol.* **4**, eaav6778 (2019).

92. Takaba, H. *et al.* Fezf2 Orchestrates a Thymic Program of Self-Antigen Expression for Immune Tolerance. *Cell* **163**, 975–987 (2015).

93. Bornstein, C. *et al.* Single-cell mapping of the thymic stroma identifies IL-25-producing tuft epithelial cells. *Nature* **559**, 622–626 (2018).

94. Miller, C. N. *et al.* Thymic tuft cells promote an IL-4-enriched medulla and shape thymocyte development. *Nature* **559**, 627–631 (2018).

95. Watanabe, N. *et al.* Hassall's corpuscles instruct dendritic cells to induce CD4 +CD25+ regulatory T cells in human thymus. *Nature* **436**, 1181–1185 (2005).

96. Owen, D. L. *et al.* Thymic regulatory T cells arise via two distinct developmental programs. *Nat. Immunol.* **20**, 195–205 (2019).

97. Li, J., Park, J., Foss, D. & Goldschneider, I. Thymus-homing peripheral dendritic cells constitute two of the three major subsets of dendritic cells in the steady-state thymus. *J. Exp. Med.* **206**, 607–622 (2009).

98. Liston, A. *et al.* Differentiation of regulatory Foxp3+ T cells in the thymic cortex. *Proc. Natl. Acad. Sci.* **105**, 11903–11908 (2008).

99. Proietto, A. I. *et al.* Dendritic cells in the thymus contribute to T-regulatory cell induction. *Proc. Natl. Acad. Sci.* **105**, 19869–19874 (2008).

100. Guerri, L. *et al.* Analysis of APC Types Involved in CD4 Tolerance and Regulatory T Cell Generation Using Reaggregated Thymic Organ Cultures. *J. Immunol.* **190**, 2102–2110 (2013).

101. Wirnsberger, G., Mair, F. & Klein, L. Regulatory T cell differentiation of thymocytes does not require a dedicated antigen-presenting cell but is under T cell-intrinsic developmental control. *Proc. Natl. Acad. Sci.* **106**, 10278–10283 (2009).

102. Gallegos, A. M. & Bevan, M. J. Central Tolerance to Tissue-specific Antigens Mediated by Direct and Indirect Antigen Presentation. *J. Exp. Med.* **200**, 1039–1049 (2004).

103. Koble, C. & Kyewski, B. The thymic medulla: a unique microenvironment for intercellular self-antigen transfer. *J. Exp. Med.* **206**, 1505–1513 (2009).

104. Hubery, F., Kinkel, S. A., Davey, G. M., Phipson, B., Mueller, S. N., Liston, A., Proietto, A. I., Cannon, P. Z. F., Forehan, S., Smyth, G. K., Wu, L., Goodnow, C. C., Carbone, F. R., Scott, H. S., Heath, W. R. Aire regulates the transfer of antigen from mTECs to dendritic cells for induction of thymic tolerance. *Blood* **118**, 2462–2472 (2011).

105. Lei, Y. *et al.* Aire-dependent production of XCL1 mediates medullary accumulation of thymic dendritic cells and contributes to regulatory T cell development. *J. Exp. Med.* **208**, 383–394 (2011).

106. Perry, J. S. A. *et al.* Distinct contributions of Aire and antigen-presenting-cell subsets to the generation of self-tolerance in the thymus. *Immunity* **41**, 414–426 (2014).

107. Leventhal, D. S. *et al.* Dendritic Cells Coordinate the Development and Homeostasis of Organ-Specific Regulatory T Cells. *Immunity* **44**, 847–859 (2016).

108. Atibalentja, D. F., Byersdorfer, C. A. & Unanue, E. R. Thymus-Blood Protein Interactions Are Highly Effective in Negative Selection and Regulatory T Cell Induction. *J. Immunol.* **183**, 7909–7918 (2009).

109. Atibalentja, D. F., Murphy, K. M. & Unanue, E. R. Functional Redundancy between Thymic CD8 + and Sirp + Conventional Dendritic Cells in Presentation of Blood-Derived Lysozyme by MHC Class II Proteins. *J. Immunol.* **186**, 1421–1431 (2011).

110. Wendland, M. *et al.* CCR9 is a homing receptor for plasmacytoid dendritic cells to the small intestine. *Proc. Natl. Acad. Sci.* **104**, 6347–6352 (2007).

111. Hadeiba, H. *et al.* Plasmacytoid Dendritic Cells Transport Peripheral Antigens to the Thymus to Promote Central Tolerance. *Immunity* **36**, 438–450 (2012).

112. Isaacson, P. G., Norton, A. J. & Addis, B. J. The Human Thymus Contains a Novel Population of B Lymphocytes. *Lancet* **330**, 1488–1491 (1987).

113. Gollob, K. J. & Palmer, E. Aberrant induction of T cell tolerance in B cell suppressed mice. *J. Immunol.* **150**, 3705–12 (1993).

114. Ferrero, I. *et al.* Functional and phenotypic analysis of thymic B cells: Role in the induction of T cell negative selection. *Eur. J. Immunol.* **29**, 1598–1609 (1999).

115. Fujihara, C. *et al.* T Cell–B Cell Thymic Cross-Talk: Maintenance and Function of Thymic B Cells Requires Cognate CD40–CD40 Ligand Interaction. *J. Immunol.* **193**, 5534–5544 (2014).

116. Frommer, F. & Waisman, A. B cells participate in thymic negative selection of murine auto-reactive CD4+ T cells. *PLoS One* **5**, (2010).

117. Perera, J., Meng, L., Meng, F. & Huang, H. Autoreactive thymic B cells are efficient antigen-presenting cells of cognate self-antigens for T cell negative selection. *Proc. Natl. Acad. Sci.* **110**, 17011–17016 (2013).

118. Walters, S. N., Webster, K. E., Daley, S. & Grey, S. T. A Role for Intrathymic B Cells in the Generation of Natural Regulatory T Cells. *J. Immunol.* **193**, 170–176 (2014).

119. Lu, F. T. *et al.* Thymic B cells promote thymus-derived regulatory T cell development and proliferation. *J. Autoimmun.* **61**, 62–72 (2015).

120. Rudensky, A. Y., Mazel, S. M. & Yurin, V. L. Presentation of endogenous immunoglobulin determinant to immunoglobulin-recognizing T cell clones by the thymic cells. *Eur. J. Immunol.* **20**, 2235–2239 (1990).

121. Detanico, T., Heiser, R. A., Aviszus, K., Bonorino, C. & Wysocki, L. J. Self-Tolerance Checkpoints in CD4 T Cells Specific for a Peptide Derived from the B Cell Antigen Receptor. *J. Immunol.* **187**, 82–91 (2011).

122. Munthe, L. A., Corthay, A., Os, A., Zangani, M. & Bogen, B. Systemic Autoimmune Disease Caused by Autoreactive B Cells That Receive Chronic Help from Ig V Region-Specific T Cells. *J. Immunol.* **175**, 2391–2400 (2014).

123. Meyers, G. *et al.* Activation-induced cytidine deaminase (AID) is required for B-cell tolerance in humans. *Proc. Natl. Acad. Sci.* **108**, 11554–11559 (2011).

124. Perera, J. *et al.* Self-Antigen-Driven Thymic B Cell Class Switching Promotes T Cell Central Tolerance. *Cell Rep.* **17**, 387–398 (2016).

125. Yamano, T. *et al.* Thymic B Cells Are Licensed to Present Self Antigens for Central T Cell Tolerance Induction. *Immunity* **42**, 1048–1061 (2015).

126. Sadlack, B. *et al.* Ulcerative Colitis-like Disease in Mice with a Disrupted Interleukin-2 Gene. *Cell* **75**, 253–261 (1993).

127. Suzuki, H. *et al.* Deregulated T Cell Activation and Autoimmunity in Mice Lacking Interleukin- 2 Receptor β Published by : American Association for the Advancement of Science Stable. *Science (80-.).* **268**, 1472–1476 (1995).

128. Willerford, D. M., Chen, J., Ferry, J. A., Davidson, L., Ma, A., Alt, F. W. Interleukin-2 Recptor a Chain Regulates the size and content of the peripheral lymphoid compartment. *Immunity* **3**, 521–530 (1995).

129. Malek, T. R., Porter, B. O., Codias, E. K., Scibelli, P. & Yu, A. Normal Lymphoid Homeostasis and Lack of Lethal Autoimmunity in Mice Containing Mature T Cells with Severely Impaired IL-2 Receptors. *J. Immunol.* **164**, 2905–2914 (2000).

130. D'Cruz, L. M. & Klein, L. Development and function of agonist-induced CD25+Foxp3+ regulatory T cells in the absence of interleukin 2 signaling. *Nat.*

Immunol. **6**, 1152–1159 (2005).

131. Fontenot, J. D., Rasmussen, J. P., Gavin, M. A. & Rudensky, A. Y. A function for interleukin 2 in Foxp3-expressing regulatory T cells. *Nat. Immunol.* **6**, 1142–1151 (2005).

132. Burchill, M. A., Yang, J., Vogtenhuber, C., Blazar, B. R. & Farrar, M. A. IL-2 receptor beta-dependent STAT5 activation is required for the development of Foxp3+ regulatory T cells. *J. Immunol.* **178**, 280–90 (2007).

133. Furtado, G. C., Curotto de Lafaille, M. A., Kutchukhidze, N. & Lafaille, J. J. Interleukin 2 signaling is required for CD4(+) regulatory T cell function. *J. Exp. Med.* **196**, 851–7 (2002).

134. Soper, D. M., Kasprowicz, D. J. & Ziegler, S. F. IL-2Rβ links IL-2R signaling with Foxp3 expression. *Eur. J. Immunol.* **37**, 1817–1826 (2007).

135. Vang, K. B. *et al.* IL-2, -7, and -15, but Not Thymic Stromal Lymphopoeitin, Redundantly Govern CD4+Foxp3+ Regulatory T Cell Development. *J. Immunol.* **181**, 3285–3290 (2008).

136. Bayer, A. L., Lee, J. Y., de la Barrera, A., Surh, C. D. & Malek, T. R. A Function for IL-7R for CD4+CD25+Foxp3+ T Regulatory Cells. *J. Immunol.* **181**, 225–234 (2008).

137. Yao Z *et al.* Nonredundant roles for Stat5a/b in directly regulating Foxp3. *Blood* **109**, 4368–75 (2007).

138. Burchill, M. A. *et al.* Distinct Effects of STAT5 Activation on CD4+ and CD8+ T Cell Homeostasis: Development of CD4+CD25+ Regulatory T Cells versus CD8+ Memory T Cells. *J. Immunol.* **171**, 5853–5864 (2003).

139. Wei, J. *et al.* Antagonistic nature of T helper 1/2 developmental programs in opposing peripheral induction of Foxp3+ regulatory T cells. *Proc. Natl. Acad. Sci.* **104**, 18169–18174 (2007).

140. Lai, D. *et al.* KLF13 sustains thymic memory-like CD8 + T cells in BALB/c mice by regulating IL-4–generating invariant natural killer T cells . *J. Exp. Med.* **208**, 1093–1103 (2011).

141. Lee, Y. J., Holzapfel, K. L., Zhu, J., Jameson, S. C. & Hogquist, K. A. Steady-state production of IL-4 modulates immunity in mouse strains and is determined by lineage diversity of iNKT cells. *Nat. Immunol.* **14**, 1146–1154 (2013).

142. Weist, B. M., Kurd, N., Boussier, J., Chan, S. W. & Robey, E. A. Thymic regulatory T cell niche size is dictated by limiting IL-2 from antigen-bearing dendritic cells and feedback competition. *Nat. Immunol.* **16**, 635–641 (2015).

143. Owen, D. L. *et al.* Identification of Cellular Sources of IL-2 Needed for Regulatory T Cell Development and Homeostasis. *J. Immunol.* **200**, 3926–3933 (2018).

144. Hori, S., Nomura, T. & Sakaguchi, S. Control of regulatory T cell development by the transcription factor Foxp3.[see comment]. *Science.* **299**, 1057–1061 (2003).

145. Hemmers, S. *et al.* IL-2 production by self-reactive CD4 thymocytes scales regulatory T cell generation in the thymus. *J. Exp. Med.* **216**, 2466–2478 (2019).

146. Hara, T. *et al.* Identification of IL-7-Producing Cells in Primary and Secondary Lymphoid Organs Using IL-7-GFP Knock-In Mice. *J. Immunol.* **189**, 1577–1584 (2012).

147. Cui, G. *et al.* Characterization of the IL-15 niche in primary and secondary lymphoid organs in vivo. *Proc. Natl. Acad. Sci.* **111**, 1915–1920 (2014).

148. Fu, W. *et al.* A multiply redundant genetic switch 'locks in' the transcriptional signature of regulatory T cells. *Nat. Immunol.* **13**, 972–980 (2012).

149. Rieder, S. A. *et al.* Eos Is Redundant for Regulatory T Cell Function but Plays an Important Role in IL-2 and Th17 Production by CD4+ Conventional T Cells. *J. Immunol.* **195**, 553–563 (2015).

150. Yang, B. H. *et al.* TCF1 and LEF1 Control Treg Competitive Survival and Tfr Development to Prevent Autoimmune Diseases. *Cell Rep.* **27**, 3629-3645.e6 (2019).

151. Kitagawa, Y. *et al.* Guidance of regulatory T cell development by Satb1-dependent super-enhancer establishment. *Nat. Immunol.* **18**, 173–183 (2017).

152. Josefowicz, S. Z., Wilson, C. B. & Rudensky, A. Y. Cutting Edge: TCR Stimulation Is Sufficient for Induction of Foxp3 Expression in the Absence of DNA Methyltransferase 1. *J. Immunol.* **182**, 6648–6652 (2009).

153. Ohkura, N. *et al.* T Cell Receptor Stimulation-Induced Epigenetic Changes and Foxp3 Expression Are Independent and Complementary Events Required for Treg Cell Development. *Immunity* **37**, 785–799 (2012).

154. Chorro, L. *et al.* Interleukin 2 modulates thymic-derived regulatory T cell epigenetic landscape. *Nat. Commun.* **9**, 1–17 (2018).

155. Sekiya, T. *et al.* The nuclear orphan receptor Nr4a2 induces Foxp3 and regulates differentiation of CD4+ T cells. *Nat. Commun.* **2**, 269 (2011).

156. Sekiya, T. *et al.* Nr4a Receptors Regulate Development and Death of Labile Treg Precursors to Prevent Generation of Pathogenic Self-Reactive Cells. *Cell Rep.* **24**, 1627-1638.e6 (2018).

157. Isomura, I. *et al.* c-Rel is required for the development of thymic Foxp3 + CD4 regulatory T cells. *J. Exp. Med.* **206**, 3001–3014 (2009).

158. Vang, K. B. *et al.* Cutting edge: CD28 and c-Rel-dependent pathways initiate regulatory T cell development. *J. Immunol.* **184**, 4074–4077 (2010).

159. Long, M., Park, S. G., Strickland, I., Hayden, M. S. & Ghosh, S. Nuclear Factor-κB Modulates Regulatory T Cell Development by Directly Regulating Expression of Foxp3 Transcription Factor. *Immunity* **31**, 921–931 (2009).

160. Zheng, Y. *et al.* Role of conserved non-coding DNA elements in the Foxp3 gene in regulatory T-cell fate. *Nature* **463**, 808–812 (2010).

161. Oh, H. *et al.* An NF-κB Transcription-Factor-Dependent Lineage-Specific Transcriptional Program Promotes Regulatory T Cell Identity and Function. *Immunity* **47**, 450-465.e5 (2017).

162. Ruan, Q. *et al.* Development of Foxp3+ Regulatory T Cells Is Driven by the c-Rel Enhanceosome. *Immunity* **31**, 932–940 (2009).

163. Feng, Y. *et al.* A mechanism for expansion of regulatory T-cell repertoire and its role in self-tolerance. *Nature* **528**, 132–136 (2015).

164. Dimitre R. Simeonov, Benjamin G. Gowen, Mandy Boontanrart, Theodore L. Roth, John D. Gagnon, Maxwell R. Mumbach, Ansuman T. Satpathy, Youjin Lee, Nicolas L. Bray, Alice Y. Chan, Dmytro S. Lituiev, Michelle L. Nguyen, Rachel E. Gate, Meena Subramaniam, Zho, A. M. Discovery of stimulation-responsive immune enhancers with CRISPR activation. *Nature* **549**, 111–115 (2017).

165. Huang, J., Ellinghaus, D., Franke, A., Howie, B. & Li, Y. 1000 Genomes-based imputation identifies novel and refined associations for the Wellcome Trust Case Control Consortium phase 1 Data. *Eur. J. Hum. Genet.* **20**, 801–805 (2012).

166. Huang, H. *et al.* Fine-mapping inflammatory bowel disease loci to single-variant resolution. *Nature* **547**, 173–178 (2017).

167. Onengut-Gumuscu, S. *et al.* Fine mapping of type 1 diabetes susceptibility loci and evidence for colocalization of causal variants with lymphoid gene enhancers. *Nat. Genet.* **47**, 381–386 (2015).

168. Herppich, S. *et al.* Dynamic Imprinting of the Treg Cell-Specific Epigenetic Signature in Developing Thymic Regulatory T Cells. *Front. Immunol.* **10**, 1–9 (2019).

169. Fontenot, J. D., Dooley, J. L., Farr, A. G. & Rudensky, A. Y. Developmental regulation of Foxp3 expression during ontogeny. *J. Exp. Med.* **202**, 901–906 (2005).

170. Tai, X. *et al.* Foxp3 Transcription Factor Is Proapoptotic and Lethal to Developing Regulatory T Cells unless Counterbalanced by Cytokine Survival Signals. *Immunity* **38**, 1116–1128 (2013).

171. Marshall, D. *et al.* Differential Requirement for IL-2 and IL-15 during Bifurcated Development of Thymic Regulatory T Cells. (2014). doi:10.4049/jimmunol.1402144

172. Yang, E., Zou, T., Leichner, T. M., Zhang, S. L. & Kambayashi, T. Both retention and recirculation contribute to long-lived regulatory T-cell accumulation in the thymus. *Eur. J. Immunol.* 1–9 (2014). doi:10.1002/eji.201444529

173. Zhan, Y., Bourges, D., Dromey, J. A., Harrison, L. C. & Lew, A. M. The origin of thymic CD4+CD25+ regulatory T cells and their co-stimulatory requirements are determined after elimination of recirculating peripheral CD4+ cells. *Int. Immunol.* **19**, 455–463 (2007).

174. Thiault, N. *et al.* Peripheral regulatory T lymphocytes recirculating to the thymus suppress the development of their precursors. *Nat. Immunol.* **16**, 628–634 (2015).

175. McCaughtry, T. M., Wilken, M. S. & Hogquist, K. A. Thymic emigration revisited. *J. Exp. Med.* **204**, 2513–2520 (2007).

176. Cowan, J. E., McCarthy, N. I. & Anderson, G. CCR7 Controls Thymus Recirculation, but Not Production and Emigration, of Foxp3+ T Cells. *Cell Rep.*

14, 1041–1048 (2016).

177. Guerau-de-Arellano, M., Martinic, M., Benoist, C. & Mathis, D. Neonatal tolerance revisited: A perinatal window for Aire control of autoimmunity. *J. Exp. Med.* **206**, 1245–1252 (2009).

178. Yang, S., Fujikado, N., Kolodin, D., Benoist, C. & Mathis, D. Regulatory T cells generated early in life play a distinct role in maintaining self-tolerance. *Science (80-.).* **348**, 589–594 (2015).

179. Scharschmidt, T. C. *et al.* A Wave of Regulatory T Cells into Neonatal Skin Mediates Tolerance to Commensal Microbes. *Immunity* **43**, 1011–1021 (2015).

180. Scharschmidt, T. C. *et al.* Commensal Microbes and Hair Follicle Morphogenesis Coordinately Drive Treg Migration into Neonatal Skin. *Cell Host Microbe* **21**, 467-477.e5 (2017).

181. Baran-Gale, J., Morgan, MD., Maio, S., Dhalla, F., Calvo-Asensio, I., Deadman, ME., Handel, AE., Maynard, A., Chen, S., Green, F., Sit, RV., Neff, NF., Darmanis, S., Tan, W., May, AP., Marioni, JC., Ponting, CP., Hollander, G. Ageing compromises mouse thymus function and remodels epithelial cell differentiation 2. *BioRX* (2020).

182. Dong, M. *et al.* Alterations in the Thymic Selection Threshold Skew the Self-Reactivity of the TCR Repertoire in Neonates. *J. Immunol.* **199**, 965–973 (2017).

183. Wissink, E. M., Smith, N. L., Spektor, R., Rudd, B. D. & Grimson, A. MicroRNAs and their targets are differentially regulated in adult and neonatal mouse CD8+ T Cells. *Genetics* **201**, 1017–1030 (2015).

184. Palin, A. C., Ramachandran, V., Acharya, S. & Lewis, D. B. Human Neonatal Naive CD4 + T Cells Have Enhanced Activation-Dependent Signaling Regulated by the MicroRNA miR-181a . *J. Immunol.* **190**, 2682–2691 (2013).

185. Schuster, M. *et al.* c-REL and IκB Govern Common and Independent Steps of Regulatory T Cell Development from Novel CD122-Expressing Pre-Precursors. *J. Immunol.* **199**, 920–930 (2017).

186. Wuest, S. C. *et al.* A role for interleukin-2 trans-presentation in dendritic cell-mediated T cell activation in humans, as revealed by daclizumab therapy. *Nat. Med.* **17**, 604–609 (2011).

187. Zhu, M., Bakhru, P., Conley, B., Nelson, J. S., Free, M., Martin, A., Starmer, J., Wilson, E. M., Su, M. A. Sex bias in CNS autoimmune disease mediated by androgen control of autoimmune regulator. *Nat. Commun.* **7**, 11350 (2016).

188. Ostatníková, D. *et al.* Salivary testosterone levels in preadolescent children. *BMC Pediatr.* **2**, 1–5 (2002).

189. Josefowicz, S. Z. *et al.* Extrathymically generated regulatory T cells control mucosal TH2 inflammation. *Nature* **482**, 395–399 (2012).

190. Samstein, R. M., Josefowicz, S. Z., Arvey, A., Treuting, P. M. & Rudensky, A. Y. Extrathymic Generation of Regulatory T Cells in Placental Mammals Mitigates Maternal-Fetal Conflict. *Cell* **150**, 29–38 (2012).

191. Cebula, A. *et al.* Thymus-derived regulatory T cells contribute to tolerance to commensal microbiota. *Nature* **497**, 258–62 (2013).

192. Nedjic, J., Aichinger, M., Emmerich, J., Mizushima, N. & Klein, L. Autophagy in thymic epithelium shapes the T-cell repertoire and is essential for tolerance. *Nature* **455**, 396–400 (2008).

193. Glabraith, R. F., Summerskill, W. H., Murray, J. Systemic lupus erythematosus, cirrhosis and ulcerative colitis after thymectomy for myasthenia gravis. *N. Engl. J. Med.* **270**, 229–232 (1964).

194. Haribhai, D. *et al.* A Central Role for Induced Regulatory T Cells in Tolerance Induction in Experimental Colitis. *J. Immunol.* **182**, 3461–3468 (2009).

195. Haribhai, D. *et al.* A requisite role for induced regulatory T cells in tolerance based on expanding antigen receptor diversity. *Immunity* **35**, 109–122 (2011).

196. Lathrop, S. K., Bloom, S. M., Rao, S. M., Nutsch, K., Lio, C., Santacruz, N., Peterson, D. A., Stappenbeck, T. S., Hsieh, C. Peripheral education of the immune system by the colonic microbiota. *Nature* **478**, 250–255 (2011).

197. Arpaia, N. *et al.* Metabolites produced by commensal bacteria promote peripheral regulatory T-cell generation. *Nature* **504**, 451–5 (2013).

198. Wyss, L. *et al.* Affinity for self antigen selects Treg cells with distinct functional properties. *Nat. Immunol.* **17**, 1093–1101 (2016).

199. Setoguchi, R., Hori, S., Takahashi, T. & Sakaguchi, S. Homeostatic maintenance of natural Foxp3(+) CD25(+) CD4(+) regulatory T cells by interleukin (IL)-2 and induction of autoimmune disease by IL-2 neutralization. *J. Exp. Med.* **201**, 723–735 (2005).

200. Vang, K. B. *et al.* IL-2, -7, and -15, but not thymic stromal lymphopoeitin, redundantly govern CD4+Foxp3+ regulatory T cell development. *J. Immunol.* **181**, 3285–3290 (2008).

201. Yang-Snyder, J. A. & Rothenberg, E. V. Developmental and Anatomical Patterns of IL-2 Gene Expression In Vivo in the Murine Thymus. *Dev. Immunol.* **3**, 85–102 (1993).

202. Yang-Snyder, J. A. & Rothenberg, E. V. Spontaneous expression of interleukin-2 in vivo in specific tissues of young mice. *Dev. Immunol.* **5**, 223–245 (1998).

203. Granucci, F. *et al.* Inducible IL-2 production by dendritic cells revealed by global gene expression analysis. *Nat. Immunol.* **2**, 882–888 (2001).

204. Wojciechowski, W. *et al.* Cytokine-Producing Effector B Cells Regulate Type 2 Immunity to H. polygyrus. *Immunity* **30**, 421–433 (2009).

205. Popmihajlov, Z., Xu, D., Morgan, H., Milligan, Z. & Smith, K. A. Conditional IL-2 gene deletion: Consequences for T cell proliferation. *Front. Immunol.* **3**, 1–12 (2012).

206. Caton, M. L., Smith-Raska, M. R. & Reizis, B. Notch-RBP-J signaling controls the homeostasis of CD8- dendritic cells in the spleen. *J. Exp. Med.* **204**, 1653–1664 (2007).

207. Sawada, S., Scarborough, J. D., Killeen, N. & Littman, D. R. A lineage-specific transcriptional silencer regulates CD4 gene expression during T lymphocyte development. *Cell* **77**, 917–929 (1994).

208. Lee, P. P. *et al.* A critical role for Dnmt1 and DNA methylation in T cell development, function, and survival. *Immunity* **15**, 763–774 (2001).

209. Pelanda, R. *et al.* Cre recombinase-controlled expression of the mb-1 allele. *Genesis* **32**, 154–157 (2002).

210. Chinen, T. *et al.* An essential role for the IL-2 receptor in T reg cell function. *Nat. Immunol.* **17**, 1322–1333 (2016).

211. Marshall, D. *et al.* Differential Requirement for IL-2 and IL-15 during Bifurcated Development of Thymic Regulatory T Cells. *J. Immunol.* **193**, 5525–5533 (2014).

212. Hori, S., Nomura, T. & Sakaguchi, S. Control of regulatory T cell development by the transcription factor Foxp3. *Science* **299**, 1057–1061 (2003).

213. Smigiel, K. S. *et al.* CCR7 provides localized access to IL-2 and defines homeostatically distinct regulatory T cell subsets. *J. Exp. Med.* **211**, 121–36 (2014).

214. Liu, Z. *et al.* Immune homeostasis enforced by co-localized effector and regulatory T cells. *Nature* **528**, 225–230 (2015).

215. Zhou, L. *et al.* Innate lymphoid cells support regulatory T cells in the intestine through interleukin-2. *Nature* **568**, 405–409 (2019).

216. Owen, D. & Farrar, M. In vitro Differentiation of Thymic Treg Cell Progenitors to Mature Thymic Treg Cells. *Bio-Protocol* **9**, 1–9 (2019).

217. Wang, Haiguang, Owen, D. L., Qian, L. J., Chopp, L. B., Farrar, M. A., Hogquist, K. A. Ultrasound Guided Intra-thymic Injection to Track Recent Thymic Emigrants and Investigate T Cell Development. *Bio-Protocol* **8**, 1–9 (2018).

218. Fenton, R. G., Marrack, P., Kappler, J. W., Kanagawa. O. & Seidman, J. G. Isotypic Exclusion of gamma delta T Cell Receptors in Transgenic Mice Bearing a Rearranged beta-Chain Gene. **241**, 1089–1092 (1988).

219. Jorgensen, J. L., Esser, U., Fazekas de St. Groth, B., Reay, P. A. & Davis, M. M. Mapping T-cell receptor-peptide contacts by variant peptide immunization of single-chain transgenics. *Nature* **355**, 224–230 (1992).

220. Wong, J. *et al.* Adaptation of TCR Repertoires to Self-Peptides in Regulatory and Nonregulatory CD4 + T Cells. *J. Immunol.* **178**, 7032–7041 (2007).

221. Beura, L. K. *et al.* Normalizing the environment recapitulates adult human immune traits in laboratory mice. *Nature* **532**, 512–516 (2016).

222. Howie, D. *et al.* MS4A4B Is a GITR-Associated Membrane Adapter, Expressed by Regulatory T Cells, Which Modulates T Cell Activation. *J. Immunol.* **183**, 4197–4204 (2009).

223. Xing, Y., Wang, X., Jameson, S. C. & Hogquist, K. A. Late stages of T cell maturation in the thymus involve NF-κB and tonic type i interferon signaling. *Nat.*

Immunol. **17**, 565–573 (2016).

224. Boursalian, T. E., Golob, J., Soper, D. M., Cooper, C. J. & Fink, P. J. Continued maturation of thymic emigrants in the periphery. *Nat. Immunol.* **5**, 418–425 (2004).

225. Paessens, L. C., Singh, S. K., Fernandes, R. J. & van Kooyk, Y. Vascular cell adhesion molecule-1 (VCAM-1) and intercellular adhesion molecule-1 (ICAM-1) provide co-stimulation in positive selection along with survival of selected thymocytes. *Mol. Immunol.* **45**, 42–48 (2008).

226. Gerner, M. Y., Kastenmuller, W., Ifrim, I., Kabat, J. & Germain, R. N. Histo-cytometry: A method for highly multiplex quantitative tissue imaging analysis applied to dendritic cell subset microanatomy in lymph nodes. *Immunity* **37**, 364–376 (2012).

227. Darce, J. *et al.* An N-Terminal Mutation of the Foxp3 Transcription Factor Alleviates Arthritis but Exacerbates Diabetes. *Immunity* **36**, 731–741 (2012).

228. Bettini, M. L. *et al.* Loss of Epigenetic Modification Driven by the Foxp3 Transcription Factor Leads to Regulatory T Cell Insufficiency. *Immunity* **36**, 717–730 (2012).

229. Schaeffer, E. M. *et al.* Tec family kinases modulate thresholds for thymocyte development and selection. *J. Exp. Med.* **192**, 987–1000 (2000).

230. Huang, W., Jeong, A.-R., Kannan, A. K., Huang, L. & August, A. IL-2–Inducible T Cell Kinase Tunes T Regulatory Cell Development and Is Required for Suppressive Function. *J. Immunol.* **193**, 2267–2272 (2014).

231. Wu, J. N. *et al.* Adhesion- and Degranulation-Promoting Adapter Protein Is Required for Efficient Thymocyte Development and Selection. *J. Immunol.* **176**, 6681–6689 (2006).

232. Weinreich, M. A., Odumade, O. A., Jameson, S. C. & Hogquist, K. A. T cells expressing the transcription factor PLZF regulate the development of memory-like CD8+ T cells. *Nat. Immunol.* **11**, 709–716 (2010).

233. Huang, W., Huang, F., Kannan, A. K., Hu, J. & August, A. ITK tunes IL-4-induced development of innate memory CD8 + T cells in a γδ T and invariant NKT cell-independent manner. *J. Leukoc. Biol.* **96**, 55–63 (2014).

234. Matthew A. Burchill, Jianying Yang, Kieng B. Vang, and M. A. F. Interleukin-2 Receptor Signaling in Regulatory T Cell. *Immunol. Lett.* **114**, 1–8 (2007).

235. Gerbe, F. *et al.* Intestinal epithelial tuft cells initiate type 2 mucosal immunity to helminth parasites. *Nature* **529**, 226–230 (2016).

236. McGeachy, M. J., Stephens, L. A. & Anderton, S. M. Natural Recovery and Protection from Autoimmune Encephalomyelitis: Contribution of CD4 + CD25 + Regulatory Cells within the Central Nervous System. *J. Immunol.* **175**, 3025–3032 (2005).

237. Cabarrocas, J. *et al.* Foxp3+ CD25+ regulatory T cells specific for a neo-self-antigen develop at the double-positive thymic stage. *Proc. Natl. Acad. Sci. U. S. A.* **103**, 8453–8458 (2006).

238. Kumar, P. *et al.* Critical role of OX40 signaling in the TCR-independent phase of human and murine thymic Treg generation. *Cell. Mol. Immunol.* **16**, 138–153 (2019).

239. Nunes-Cabaço, H., Caramalho, Í., Sepúlveda, N. & Sousa, A. E. Differentiation of human thymic regulatory T cells at the double positive stage. *Eur. J. Immunol.* **41**, 3604–3614 (2011).

240. Lee, Hyang-Mi, Hsieh, C.-S. Rare Development of Foxp3+ Thymocytes in the CD4+ CD8+ Subset. *J. Immunol.* **183**, 2261–2266 (2009).

241. Vang, K. B. *et al.* Cutting Edge: CD28 and c-Rel-Dependent Pathways Initiate Regulatory T Cell Development. *J. Immunol.* **184**, 4074–4077 (2010).

242. Kernfeld, E. M. *et al.* A Single-Cell Transcriptomic Atlas of Thymus Organogenesis Resolves Cell Types and Developmental Maturation. *Immunity* **48**, 1258-1270.e6 (2018).

243. Park, J. E. *et al.* A cell atlas of human thymic development defines T cell repertoire formation. *Science (80-.).* **367**, (2020).

244. Xiong, Y. & Bosselut, R. The enigma of CD4-lineage specification. *Eur. J. Immunol.* **41**, 568–574 (2011).

245. Satija, R., Farrell, J. A., Gennert, D., Schier, A. F. & Regev, A. Spatial reconstruction of single-cell gene expression data. *Nat. Biotechnol.* **33**, 495–502 (2015).

246. Takahama, Y. Journey through the thymus: stromal guides for T-cell development and selection. *Nat. Rev. Immunol.* **6**, 127–135 (2006).

247. Carlson, C. M. *et al.* Kruppel-like factor 2 regulates thymocyte and T-cell migration. *Nature* **442**, 299–302 (2006).

248. Mandala, S. *et al.* Alteration of lymphocyte trafficking by sphingosine-1-phosphate receptor agonists. *Science (80-.).* **296**, 346–349 (2002).

249. Mora, J. R. *et al.* Selective imprinting of gut-homing T cells by Peyer's patch dendritic cells. *Nature* **424**, 88–93 (2003).

250. Xu, H., Williams, M. S. & Spain, L. M. Patterns of expression, membrane localization, and effects of ectopic expression suggest a function for MS4a4B, a CD20 homolog in Th1 T cells. *Blood* **107**, 2400–2408 (2006).

251. Hogquist, K. A., Xing, Y., Hsu, F.-C. & Shapiro, V. S. T Cell Adolescence: Maturation Events Beyond Positive Selection. *J. Immunol.* **195**, 1351–1357 (2015).

252. Zhang, Y., Li, H., Wang, X., Gao, X. & Liu, X. Regulation of T cell development and activation by creatine kinase B. *PLoS One* **4**, (2009).

253. Hu, Q. N. & Baldwin, T. A. Differential Roles for Bim and Nur77 in Thymocyte Clonal Deletion Induced by Ubiquitous Self-Antigen. *J. Immunol.* **194**, 2643–2653 (2015).

254. Baldwin, T. A. & Hogquist, K. A. Transcriptional Analysis of Clonal Deletion In

Vivo. *J. Immunol.* **179**, 837–844 (2007).

255. Otero, D. C., Baker, D. P. & David, M. IRF7-Dependent IFN-β Production in Response to RANKL Promotes Medullary Thymic Epithelial Cell Development. *J. Immunol.* **190**, 3289–3298 (2013).

256. Seumois, G. *et al.* Single-cell transcriptomic analysis of allergen-specific T cells in allergy and asthma. *Sci. Immunol.* **5**, (2020).

257. Wolfl, M. *et al.* Activation-induced expression of CD137 permits detection, isolation, and expansion of the full repertoire of CD8+ T cells responding to antigen without requiring knowledge of epitope specificities. *Blood* **110**, 201–210 (2007).

258. Kniemeyer, O., Brakhage, A. A., Ferreira, F., Wallner, M. & Sawitzki, B. Regulatory T Cell Specificity Directs Tolerance versus Allergy against Aeroantigens in Humans. *Cell* **167**, 1067-1078.e16 (2016).

259. Lauritsen, J.-P. H. *et al.* Egr2 Is Required for Bcl-2 Induction during Positive Selection. *J. Immunol.* **181**, 7778–7785 (2008).

260. Bettini, M., Xi, H., Milbrandt, J. & Kersh, G. J. Thymocyte Development in Early Growth Response Gene 1-Deficient Mice. *J. Immunol.* **169**, 1713–1720 (2002).

261. Zhang, W. J. *et al.* IL-4-induced Stat6 activities affect apoptosis and gene expression in breast cancer cells. *Cytokine* **42**, 39–47 (2008).

262. Morikawa, H. & Sakaguchi, S. Genetic and epigenetic basis of Treg cell development and function: From a FoxP3-centered view to an epigenome-defined view of natural Treg cells. *Immunol. Rev.* **259**, 192–205 (2014).

263. Trapnell, C. *et al.* The dynamics and regulators of cell fate decisions are revealed by pseudotemporal ordering of single cells. *Nat. Biotechnol.* **32**, 381–386 (2014).

264. Linton, P. J. & Dorshkind, K. Age-related changes in lymphocyte development and function. *Nat. Immunol.* **5**, 133–139 (2004).

265. Palmer, D. B. The effect of age on thymic function. *Front. Immunol.* **4**, 1–6 (2013).

266. Hale, J. S., Boursalian, T. E., Turk, G. L. & Fink, P. J. Thymic output in aged mice. *Proc. Natl. Acad. Sci. U. S. A.* **103**, 8447–8452 (2006).

267. Sansom, S. N. *et al.* Population and single-cell genomics reveal the Aire dependency, relief from Polycomb silencing, and distribution of self-antigen expression in thymic epithelia. *Genome Res.* **24**, 1918–1931 (2014).

268. Savage, P. a, Leventhal, D. S. & Malchow, S. Shaping the repertoire of tumor-infiltrating effector and regulatory T cells. *Immunol. Rev.* 245–258 (2014).

269. Wooldridge, L. *et al.* A single autoimmune T cell receptor recognizes more than a million different peptides. *J. Biol. Chem.* **287**, 1168–1177 (2012).

270. Sun, B., Liu, M., Cui, M. & Li, T. Granzyme B-expressing treg cells are enriched in colorectal cancer and present the potential to eliminate autologous T conventional cells. *Immunol. Lett.* **217**, 7–14 (2020).

271. Liu, Z. *et al.* Novel effector phenotype of TIM-3þ Regulatory T cells leads to

enhanced suppressive function in head and neck cancer patients. *Clin. Cancer Res.* **24**, 4529–4538 (2018).

272. Joller, N. *et al.* Treg cells expressing the coinhibitory molecule TIGIT selectively inhibit proinflammatory Th1 and Th17 cell responses. *Immunity* **40**, 569–581 (2014).

273. Miragaia, R. J. *et al.* Single-Cell Transcriptomics of Regulatory T Cells Reveals Trajectories of Tissue Adaptation. *Immunity* **50**, 493-504.e7 (2019).

274. Sidwell, T. *et al.* Attenuation of TCR-induced transcription by Bach2 controls regulatory T cell differentiation and homeostasis. *Nat. Commun.* **11**, 1–17 (2020).

275. Wang, J., Siffert, M., Spiliotis, M. & Gottstein, B. Repeated long-term DT application in the DEREG mouse induces a neutralizing anti-DT antibody response. *J. Immunol. Res.* (2016). doi:10.1155/2016/1450398

276. Cowan, J. E. *et al.* Aire controls the recirculation of murine Foxp3+ regulatory T-cells back to the thymus. *Eur. J. Immunol.* **48**, 844–854 (2018).

277. Peligero-Cruz, C. *et al.* IL18 signaling promotes homing of mature Tregs into the thymus. *Elife* **9**, (2020).

278. Nikolouli, E. *et al.* Recirculating IL-1R2+ Tregs fine-tune intrathymic Treg development under inflammatory conditions. *Cell. Mol. Immunol.* (2020). doi:10.1038/s41423-019-0352-8

279. Klein, L., Robey, E. A. & Hsieh, C. S. Central CD4 + T cell tolerance: deletion versus regulatory T cell differentiation. *Nat. Rev. Immunol.* **19**, 7–18 (2019).

280. Kalekar, L. A. *et al.* CD4+ T cell anergy prevents autoimmunity and generates regulatory T cell precursors. *Nat. Immunol.* **17**, 304–314 (2016).

281. Kalekar, Lokesh A., Mueller, D. L. Relationship between CD4 Tregs and anergy in vivo. *J. Immunol.* **198**, 2527–2533 (2017).

282. Tai, X. & Singer, A. Basis of Treg development in the thymus. *Cell Cycle* **13**, 501–502 (2014).

283. Wang, Q., Strong, J. & Killeen, N. Homeostatic competition among T cells revealed by conditional inactivation of the mouse Cd4 gene. *J. Exp. Med.* **194**, 1721–1730 (2001).

284. Fistonich, C. *et al.* Cell circuits between B cell progenitors and IL-7+ mesenchymal progenitor cells control B cell development. *J. Exp. Med.* **215**, 2586–2599 (2018).

285. Ke, R. *et al.* In situ sequencing for RNA analysis in preserved tissue and cells. *Nat. Methods* **10**, 857–860 (2013).

286. Blanco-Melo, D. *et al.* Imbalanced Host Response to SARS-CoV-2 Drives Development of COVID-19. *Cell* **181**, 1036-1045.e9 (2020).

287. Liu, Y., Qi, G. & Bellanti, J. A. Regulatory T cells : A potential weapon to combat COVID-19 ? *MedComm* 1–8 (2020). doi:10.1002/mco2.12

288. Gladstone, D. E., Kim, B. S., Mooney, K., Karaba, A. H. & D'Alessio, F. R.

Regulatory T Cells for Treating Patients With COVID-19 and Acute Respiratory Distress Syndrome: Two Case Reports. *Ann. Intern. Med.* 1–2 (2020). doi:10.7326/l20-0681

289. Fugmann, S. D. The origins of the Rag genes-From transposition to V(D)J recombination. *Semin. Immunol.* **22**, 10–16 (2010).

290. Hozumi, N. & Tonegawa, S. Evidence for somatic rearrangement of immunoglobulin genes coding for variable and constant regions. *Proc. Natl. Acad. Sci. U. S. A.* **73**, 3628–3632 (1976).

291. Spanier, J. A. *et al.* Increased effector memory insulin-specific CD4+ T cells correlate with insulin autoantibodies in patients with recent-onset type 1 diabetes. *Diabetes* **66**, 3051–3060 (2017).

292. Shevach, E. M. The Resurrection of T Cell-Mediated Suppression. *J. Immunol.* **186**, 3805–3807 (2011).

293. Kennedy, M. K. *et al.* Reversible defects in natural killer and memory CD8 T cell lineages in interleukin 15-deficient mice. *J. Exp. Med.* **191**, 771–780 (2000).

294. Schorle, H., Holtschke, T., Hiinig, T., Schimpl, A. & Horak, I. Development and function of T cells in mice rendered interleukin-2 deficient by gene targeting. *Nature* **352**, 621–624 (1991).

295. Mombaerts, P. *et al.* Mutations in T-cell antigen receptor genes α and β block thymocyte development at different stages. *Nature* **360**, 225–231 (1992).

296. Rudolf Schmits, Thomas M. Kiindig, Dianne M. Bakerfl Grace Shumakerfl John J.L. Simard, Gordon Duncan, Andrew Wakeham, Arda Shahinian, Annette van der Heiden, Martin E Bachmann, Pamela S. Ohashi, Tak W. Mak, and D. D. H. LFA-l-deficient Mice Show Normal CTL Responses to Virus but Fail to Reject Immunogenic Tumor. *J. Exp. Med.* **183**, 1415–1426 (1996).

297. Shahinian, A. *et al.* Differential T Cell Costimulatory Requirements in CD28-Deficient Mice. *Science (80-.).* **261**, 609–612 (1993).

298. Sha, W. C., Liou, H. C., Tuomanen, E. I. & Baltimore, D. Targeted disruption of the p50 subunit of NF-κB leads to multifocal defects in immune responses. *Cell* **80**, 321–330 (1995).

299. Liao, X. C. & Littman, D. R. Altered T cell receptor signaling and disrupted T cell development in mice lacking Itk. *Immunity* **3**, 757–769 (1995).

300. Peterson, E. J. *et al.* Coupling of the TCR to integrin activation by SLAP-130/Fyb. *Science (80-.).* **293**, 2263–2265 (2001).

301. Noben-Trauth, N. *et al.* An interleukin 4 (IL-4)-independent pathway for CD4+ T cell IL-4 production is revealed in IL-4 receptor-deficient mice. *Proc. Natl. Acad. Sci. U. S. A.* **94**, 10838–10843 (1997).

302. Matsumoto, I., Ohmoto, M., Narukawa, M., Yoshihara, Y. & Abe, K. Skn-1a (Pou2f3) specifies taste receptor cell lineage. *Nat. Neurosci.* **14**, 685–687 (2011).

303. Sonoda, K. H., Exley, M., Snapper, S., Balk, S. P. & Stein-Streilein, J. CD1-reactive natural killer T cells are required for development of systemic tolerance

through an immune-privileged site. *J. Exp. Med.* **190**, 1215–1225 (1999).

304. Xing, Y. & Hogquist, K. A. Isolation, identification, and purification of murine thymic epithelial cells. *J. Vis. Exp.* 1–8 (2014). doi:10.3791/51780

305. Nelson, R. W. *et al.* T Cell Receptor Cross-Reactivity between Similar Foreign and Self Peptides Influences Naive Cell Population Size and Autoimmunity. *Immunity* **42**, 95–107 (2015).

306. Ruscher, R., Kummer, R. L., Lee, Y. J., Jameson, S. C. & Hogquist, K. A. CD8αα intraepithelial lymphocytes arise from two main thymic precursors. *Nat. Immunol.* **18**, 771–779 (2017).

307. McDavid, A. *et al.* Data exploration, quality control and testing in single-cell qPCR-based gene expression experiments. *Bioinformatics* **29**, 461–467 (2013).

308. Miller, S. Encephalomyelitis in the Mouse. *Immunology* 1–18 (2007).

309. Mottet, C., Uhlig, H. H. & Powrie, F. Cutting Edge: Cure of Colitis by CD4 + CD25 + Regulatory T Cells . *J. Immunol.* **170**, 3939–3943 (2003).